UNIVERSITY OF SOUTHAMPTON

FACULTY OF ENGINEERING, SCIENCE AND MATHEMATICS

School of Chemistry

New Hydrogen Bonding Motifs For Anion and Neutral Guest Complexation

by

Matthew George Fisher

Thesis for the degree of Doctor of Philosophy

March 2009

UNIVERSITY OF SOUTHAMPTON

ABSTRACT

FACULTY OF ENGINEERING, SCIENCE AND MATHEMATICS

SCHOOL OF CHEMISTRY

Doctor of Philosophy

NEW HYDROGEN BONDING MOTIFS FOR ANION AND NEUTRAL GUEST COMPLEXATION

by Matthew George Fisher

This thesis presents three different areas of anion or neutral molecule recognition chemistry. There is an extensive study of homoleptic and heteroleptic platinum(II) based receptors for anion recognition. The homoleptic receptor study revealed that urea ligands are more effective than amido-pyrrole based ligands for binding anions in DMSO solution. Also, isoquinoline based ligands form more stable complexes than pyridine based ligands and their extra rigidity preorganises the receptor for increased anion affinities. The heteroleptic receptor (*trans*-[Pt(isoquinoline-urea)$_2$(pyridine)$_2$](BF$_4$)$_2$) exhibited either an *up-down* or *up-up* conformation in DMSO solution and the solid state, depending on the type and concentration of anion. Two different crystal structures with sulfate revealed formation of both the conformations.

The properties of a simple benzimidazole cleft receptor for barbiturates and ureas are reported. Compared to various control analogues, the receptor binds barbital or urea in highly competitive DMSO/MeNO$_2$ solutions. A crystal structure with barbital revealed binding through six hydrogen bonds. The synthesis of a more soluble version of the receptor was attempted. The synthesis of a neutral guest templated catenane was also attempted in an effort to expand on the simple cleft work.

Finally, a new triazole strapped calix[4]pyrrole synthesised by 'click' chemistry is reported. The receptor shows a high affinity for chloride and bicarbonate in MeCN and DCM solutions. It also exhibits strong lipid bilayer chloride transport properties when compared to the parent *meso*-octamethylcalix[4]pyrrole. A brief investigation into the use of triptycenes as potential scaffolds for appending hydrogen bond donor groups for anion recognition is also reported.

DECLARATION OF AUTHORSHIP

I, ……., declare that the thesis

entitled……..……

……

and the work presented in this thesis is my own, and has been generated by me as the result of my own original research. I confirm that:

- this work was done wholly or mainly while in candidature for a research degree at this University;
- where any part of this thesis has previously been submitted for a degree or any other qualification at this University or any other institution, this has been clearly stated;
- where I have consulted the published work of others, this is always clearly attributed;
- where I have quoted from the work of others, the source is always given. With the exception of such quotations, this thesis is entirely my own work;
- I have acknowledged all main sources of help;
- where the thesis is based on work done by myself jointly with others, I have made clear exactly what was done by others and what I have contributed myself;
- parts of this work have been published as:

  M. G. Fisher, P. A. Gale and M. E. Light, *New J. Chem.,* **2007**, 31, 1583-1584.

  M. G. Fisher, P. A. Gale, M. E. Light and S. J. Loeb, *Chem. Commun.,* **2008**, 5695-5697.

  A. J. Wilson, *Annu. Rep. Prog. Chem. Sect. B,* **2008**, 104, 164-183.

  M. G. Fisher, P. A. Gale, J. R. Hiscock, M. B. Hursthouse, M. E. Light, F. P. Schmidtchen and C. C. Tong, *Chem. Commun.*, **2009**, 3017-3019.

  C. R. Bondy, M. G. Fisher, P. A. Gale and S. J. Loeb, *Inorg. Chem.,* **2010**, *in preparation*.

Signed: ……..

Date:…….

Abbreviations

Å	Ångström
Anal.	Analysis
Bipy	2, 2'-Bipyridine
BOC	*t*-Butoxycarbonyl
br	Broad (NMR)
Bu	Butyl
^{o}C	Degrees Celsius
Calcd.	Calculated
cat.	Catalytic amount
CD_2Cl_2	Dichloromethane-d_2
$CDCl_3$	Chloroform-d_1
CD_3CN	Acetonitrile-d_3
CFTR	Cistic fibrosis transmembrane conductance regulator
CI	Chemical ionisation
Cp	Cyclopentadienyl
d	Doublet (NMR)
D	Debye
DCE	Dichloroethane
DCM	Dichloromethane
decomp.	Decomposed
DMA	Dimethylacetamide
DMAP	4-Dimethylaminopyridine
DMF	Dimethylformamide
DMSO	Dimethylsulfoxide
DNA	Deoxyribonucleic acid
EDCI	1-Ethyl-3-(3-dimethylaminopropyl)carbodiimide hydrochloride

equiv. or eqv.	Equivalent
ESI	Electrospray Ionisation
ES	Electrospray
fig.	Figure
HR-MS	High resolution mass spectrum
hrs	Hours
ITC	Isothermal titration calorimetry
L	Ligand
LR-MS	Low resolution mass spectrum
MHz	Megahertz
K_a	Association constant
K	Kelvin
m	Multiplet
M	Molarity per dm^3
Me	Methyl
mmol	Millimoles
mol	Moles
mM	Millimolarity per dm^3
M.p.	Melting point
m/z	Mass to charge ratio (mass spectrometry)
mV	Millivolts
NMR	Nuclear magnetic resonance
POPC	1-palmitoyl-2-oleoyl-*sn*-glycero-3-phosphocholine
ppm	Parts per million
q	Quartet (NMR)
R_f	Retention factor
RT	Room temperature
sch.	Scheme
s	Singlet (NMR)
t	Triplet (NMR)

TBA	Tetrabutylammonium
tbl.	Table
TEA	Tetraethylammonium or triethylamine depending on context
tert	Tertiary
TFA	Trifluoroacetic acid
THF	Tetrahydrofuran
Tren	Tris(2-aminoethyl)amine
UV-vis	Ultraviolet – visible spectroscopy
wt.	Weight
Δ	Delta
$\{^1H\}$	Proton decoupled (carbon NMR)

Contents

Chapter 4: Triazoles in Anion Receptor Chemistry

Chapter 5: Experimental Methods

Acknowledgements

Firstly, I would like to thank my supervisor Prof. Phil Gale for giving me the opportunity to do a PhD and for all his support and encouragement during my research. I would also like to thank all members of the Gale group, both past (Simon, Gareth, Gavin, Jo, Claudia, Sergio, Bob) and present (Pete, Jenny, Christine, Cally, Steve, Sam) for the great times in the lab and their help and advice. My particular thanks go to Gareth and Christine, who have helped me the most during my PhD through their advice, encouragement and chats to discuss new ideas. I also express my thanks to the visitors to the group (Marta, Tomas, Luis-Miguel). I would also like to thank my project student Becky for her hard work and contributions to my work.

I would like to thank my collaborators. Prof. Steve Loeb (University of Windsor, Canada) for his advice and Prof. Franz Schmidtchen (Technical University of Munich, Germany) for applying his expertise to my work.

I thank the University of Southampton and the EPSRC for funding my PhD. I also thank the vital analytical departments, mass-spec and NMR for providing a great service. My particular thanks go to Dr. Mark Light and the EPSRC crystallographic services for their valuable time and expertise solving the X-ray crystal structures outlined in this thesis.

My special thanks go to my family for encouraging and helping me and providing me with everything I need to get this far with my education.

Chapter 1 – Introduction

1.1 Supramolecular Chemistry

Supramolecular chemistry is often referred to as 'chemistry beyond the molecule'.[1] This neatly summarising statement can be deciphered as chemistry that solely focuses on the study of non-covalent interactions between molecules. Thus, a supermolecule can be thought of as an assembly of two or more chemical species held together by reversible intermolecular forces that are much weaker than a covalent bond. These ideas were first formally described by Jean-Marie Lehn (who previously coined the term 'Supramolecular Chemistry') in his Nobel Prize in Chemistry lecture in 1987.[2] He concluded that 'supermolecules are to molecules and the intermolecular bond what molecules are to atoms and the covalent bond'.[2]

There are a range of intermolecular forces at hand to a supramolecular chemist and some of the most important ones are as follows:-

- Hydrogen bonds – classically defined as an interaction wherein a hydrogen atom is attracted to two atoms, X and A to result in a bridge, X–H···A. The interaction is a complex conglomerate of electrostatic, Van der Waals and charge transfer characteristics.[3] They can span energies between 4 and 120 kJ mol^{-1}. In fact the strength of a hydrogen bond can be determined by how electronegative the atoms either side of the hydrogen bridge are. So the strongest hydrogen bond is F–H···F. More conventional strong hydrogen bonds include; N–H···O, O–H···O, N–H···N and O–H···N bonds. Weak hydrogen bonds include; C–H···O, C–H···π and O–H···Metal.[3]

- Van der Waals forces – these are attractive or repulsion forces between molecules and are the result of induced-dipole-induced-dipole (London Dispersions), permanent-dipole-permanent-dipole and permanent-dipole-induced-dipole interactions.[4] They are very weak compared to hydrogen bonds (<5 kJ mol^{-1})

but as a collective, they can considerably contribute to the stability of a supramolecular complex.

- Electrostatic forces – these are Coulombic attractions or repulsions between charges or partial charges on molecules.[4] They include ion pairs (100-350 kJ mol^{-1}), salt bridges, ion-dipole (50-200 kJ mol^{-1}) and dipole-dipole (5-50 kJ mol^{-1}) interactions (*fig*. 1.1).[5]

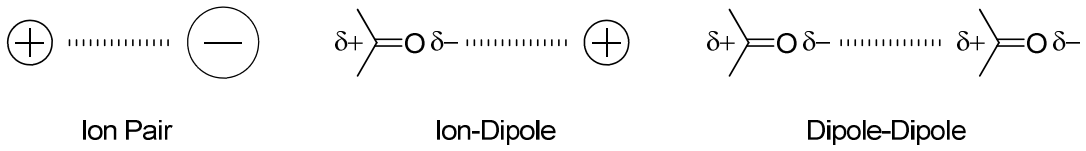

Figure 1.1 - Types of electrostatic interactions.

- Charge transfers – these are donor-acceptor interactions between two molecules; one with low energy orbitals (acceptors) and one with high energy filled orbitals (donors). When these two orbitals are aligned properly, some extent of charge transfer can occur from the donor to the acceptor.[4]

- π-π Stacking – these are interactions between the π systems on aromatic molecules and have energies between 0-50 kJ mol^{-1}. There are two different types of this interaction, face to face and edge to face (*fig*. 1.2).[4, 5]

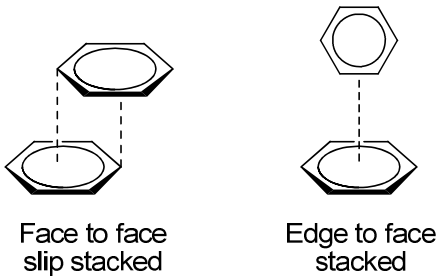

Figure 1.2 - Types of π-π interactions.

Supramolecular chemistry is a multidisciplinary field that exploits these interactions and fundamental concepts such as self-organisation, self-assembly and host-guest chemistry. Host-guest chemistry can further be broken down into the following areas; anion recognition, cation recognition, simultaneous cation/anion recognition (dual host systems) and neutral molecule recognition.

1.2 Anion Recognition

The development of receptors for the binding of anions is an increasingly vigorous area of research but in fact, it is only in the last two decades that this expansion has really started to gather momentum. The hither to slow growth of this area is surprising considering how ubiquitous anions are in nature. For example, there are many anions present in the oceans including chloride and carbonates, and nitrate and sulfate are present in acid rain.[6] Anions are also critical to the maintenance of life as they are involved in a vast array of biological processes. The most important anion in life is the poly-anionic species DNA, but anions are also critical in ion transport processes in cells, enzyme-substrate interactions and a multitude of other protein interactions. Sadly, the failure of certain anion transport mechanisms can be seriously detrimental to our health. For instance, the malfunctioning of the CFTR chloride transport channel, the cause of cystic fibrosis, is one of the most commonly inherited diseases amongst Caucasians.[6]

There are also many anthropogenic anions that can have deleterious effects such as; phosphates and nitrates from agriculture, radioactive anions such as pertechnetate from nuclear fuel reprocessing, and many other anions from chemical processes, which can cause serious pollution hazards.[6] So with the realisation of the importance anions in our world, the field of anion recognition chemistry has now significantly developed into various areas, from simple anion receptors, to fluorescent or colorimetric sensors, to anion templated assembly, to anion transporters. A key feature desired in all these areas of anion recognition is selectivity. Achieving selectivity has been a difficult challenge due to some unique features of anions:

- They are much larger when compared to iso-electronic cations (e.g. Na^+ = 1.02 Å, F^- = 1.33 Å) which means they have a lower charge to radius ratio. This means electrostatic binding interactions are much less effective than they would be for the smaller cation.[7]

- Unlike simple metal cations, most anions only exist over a limited pH range; becoming protonated and losing their negative charge at lower pH.[5]

- Solvent effects are crucial in anion binding strength and selectivity. This means that any anion receptor must effectively compete with the solvent environment in which the anion binding event takes place.[7]

- Anions have a diverse range of geometries which must be accounted for in the design of an anion receptor (*fig.* 1.3):

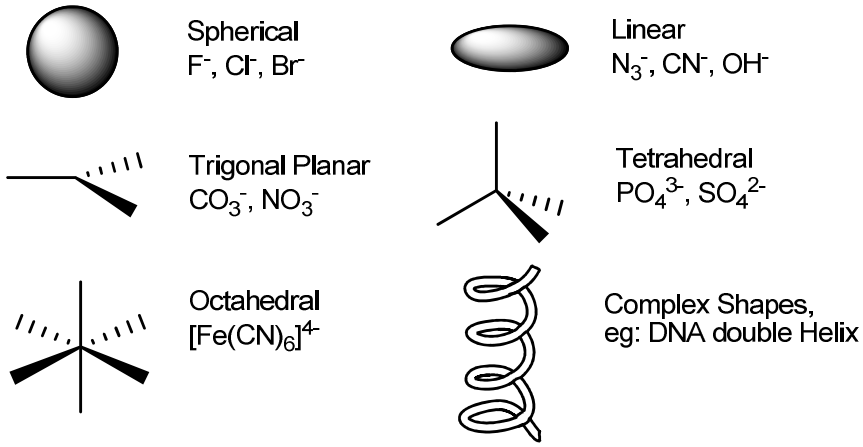

Figure 1.3 – Examples of the geometry of different anions.

Ion-ion interactions are very strong but they lack directionality which, given the diverse nature of anion geometry, is fundamental to achieving selectivity in anion receptors. So the most exploited molecular interaction for anion binding is the highly directional hydrogen bond. This allows design of precise geometry clefts for the binding of specific anions. Another vital design challenge is to develop systems which do not self-associate, as this competes with anion complexation and hence lowers their effectiveness. These last two points have been the key principles in most research towards anion receptor design in the last two decades and are still proving exciting challenges in this emerging area of supramolecular chemistry.

1.3 Neutral Non-Metallic Amide-, Urea- and Pyrrole- Based Anion Receptors

1.3.1 Amides

There is an ever expanding arsenal of hydrogen-bond donor groups that one can use in the design of an anion receptor but perhaps the most fundamental ones are amides and ureas.

The first anion receptor to incorporate amide hydrogen-bond donor groups was the tricyclic compound **1** in 1986 by Pascal Jr. and co-workers (*fig.* 1.4).[8] It was synthesised from an acid chloride condensation reaction between the corresponding triamine and tris-acid chloride in 11% yield. The C_3-symmetric receptor consists of 3 amide groups which were predicted to point into the cavity to accommodate small anions such as fluoride. The crystal structure of the receptor did not show the NH groups pointing into the cavity but preliminary ^{1}H-NMR and ^{19}F-NMR studies in highly competitive DMSO-d_6 solutions did show an interaction with fluoride.[8]

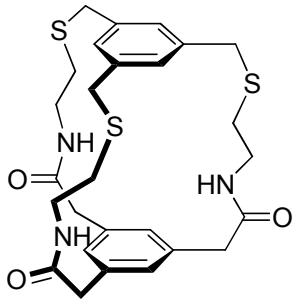

1

Figure 1.4 - The first amide receptor by Pascal and co-workers.

Other early work included the tris-amide receptors based on the tris(2-aminoethyl)amine (known as *tren*) framework of Reinhoudt and co-workers (*fig.* 1.5).[9] Again, the receptors were C_3-symmetric and their designs were inspired by phosphate binding proteins seen in nature. Receptors **2**-**5** were synthesised from the corresponding triamine and the appropriate acid chloride in the presence of triethylamine in yields of 70-90%. Proton-NMR binding studies with the tetrabutylammonium (TBA) salts of $H_2PO_4^-$, HSO_4^- and Cl^- provided binding constants (K_a) via curve fitting procedures, which showed selectivity for $H_2PO_4^-$. For example, compound **2** gave a binding constant of 4700 M^{-1} with $H_2PO_4^-$ compared to 36 and 96 M^{-1} for HSO_4^- and Cl^- respectively.[9]

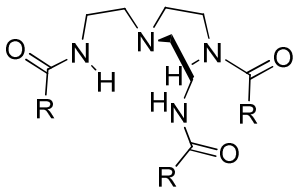

2 R = CH_2Cl
3 R = $(CH_2)_4CH_3$
4 R = C_6H_5
5 R = 4-$MeOC_6H_4$

Figure 1.5 - Reinhoudt's early tris-amide receptors.

In 1997 came the now famous work of Crabtree *et al.* with the first of a set of wonderfully simple isophthalamide cleft receptors (*fig.* 1.6).[10]

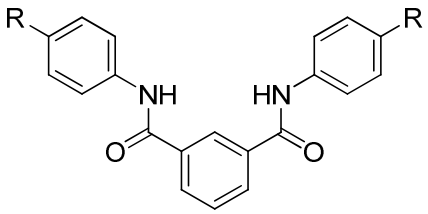

6 R = H
7 R = *para*-$^{n}BuC_6H_4$

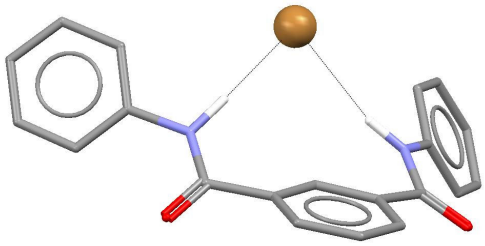

Figure 1.6 - Crabtree's isophthalamide cleft receptors 6 & 7 (left) and the crystal structure of 6 with bromide (right).

Initially, the bis-amide receptor **6** was synthesised and a crystal structure was obtained with bromide, which reveals (*fig.* 1.6) the presence of two hydrogen bond interactions between the two amide groups and a single bromide anion (N···Br 3.42 and 3.71 Å). The structure also shows that the bromide is positioned above the plane of the central aryl ring with the amide groups twisted out of plane.

In order for solution studies to be carried out, the more soluble receptor **7** was synthesised which allowed ^{1}H-NMR binding studies to be carried out in CD_2Cl_2. These studies revealed that the receptor exhibits a high affinity for halides with a 1:1 binding stoichiometry and a general trend Cl^- (K_a = 61000 M^{-1}) > F^- (K_a = 30000 M^{-1}) > Br^- (K_a = 7100 M^{-1}) > I^- (K_a = 460 M^{-1}).[10, 11] Later work included a pyridinyl version of **6** which interestingly exhibited an increased selectivity in favour of the smaller halide anions (K_a = 24000, 1500 and 57 M^{-1} for F^-, Cl^- and Br^- respectively).[11] This was thought[12-14] to be the result of favourable electrostatic interactions between the amide groups (see *fig.* 1.7) and the pyridine nitrogen which pre-organises the structure and does not allow twisting out of plane to accommodate the larger anions.

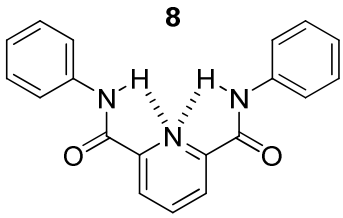

Figure 1.7 - Crabtree's pre-organised version of 6 using a pyridinyl core.

This work highlights how simplicity in design can still lead to highly efficient and selective anion receptors.

Gale and Quesada *et al.* have recently explored other ways in which pre-organisation could be incorporated into these isophthalamide cleft type receptors.[15] They achieved this by appending hydroxyl groups at the 4- and 6-positions on the aryl ring (**9**) and compared its behaviour to some control analogues (**10** & **11**). It is now well known[12, 14] that **10** predominantly prefers to adopt the *syn-anti* conformation seen in Figure 1.8. It was hoped that the addition of these hydroxyl groups would lead to the predominantly *syn-syn* conformation for **9** and hence enhance its binding properties (see *fig*. 1.8).

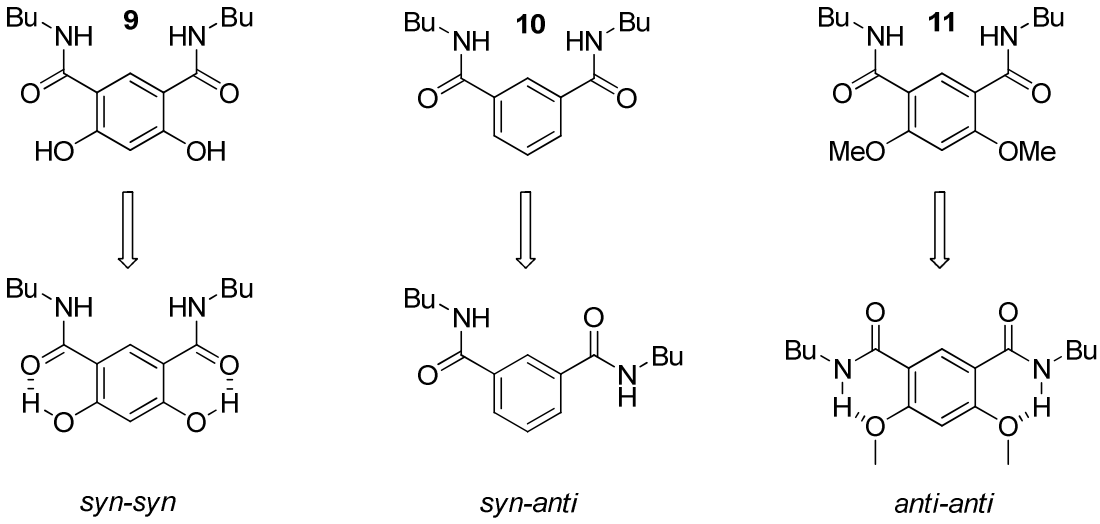

Figure 1.8 - Ways of 'fine tuning' pre-organisation by Gale and co-workers.

X-ray crystal structures of **9** and **11** did indeed show that these species adopted their predicted conformations with hydrogen bonds between the hydroxyls and carbonyls on **9** (O···O 2.55-2.57 Å) and between the amide NH and methoxy-groups on **11** (N···O 2.67-2.68 Å).[15]

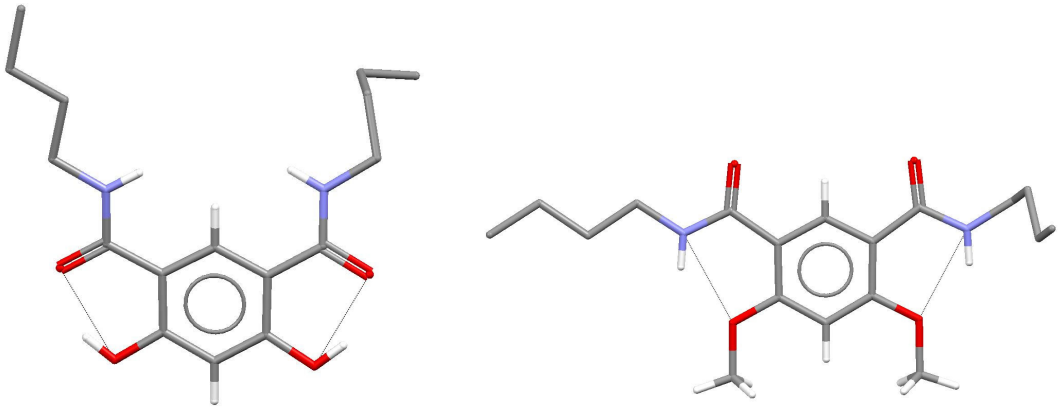

Figure 1.9 – X-ray crystal structures of 9 & 11 showing the *syn-syn* and *anti-anti* structures as predicted.

Subsequently, the same behaviour was observed in solution with far downfield shifts for the OH protons (δ = 13.5) in the ^{1}H-NMR spectrum of **9** in CD_3CN, which is indicative of the strong hydrogen bonding expected. Proton-NMR binding studies in CD_3CN also revealed much higher binding constants for **9** compared to the control **10**, especially with chloride (K_a = 5230 and 195 M^{-1} for **9** and **10** respectively). Addition of anion solutions to a solution of **11** caused no changes in the ^{1}H-NMR spectrum indicating no anion binding. This was thought to be due to the hydrogen bond donor groups being involved in intramolecular hydrogen bonding.[15]

Macrocyclic receptors present a more efficient way of binding anions as they allow for more stable anion-receptor complexes due to the macrocyclic effect. This refers to the increased thermodynamic stability of macrocyclic systems compared to their acyclic analogues. They can also have more selectivity than their acyclic analogues by excluding specific anions according to size and/or shape.

In 2001, Hamilton and Choi provided a fine example that demonstrates the macrocyclic effect with a study of a macrocyclic amide receptor and its acyclic analogue.[16, 17] The macrocycles (**12** & **13**) were designed (with the aid of energy minimisation calculations) to have rigidly organised, convergent hydrogen bond donor groups (three amide and six aryl) to accommodate tetrahedral oxyanions such as *p*-tosylate (*fig*. 1.10).

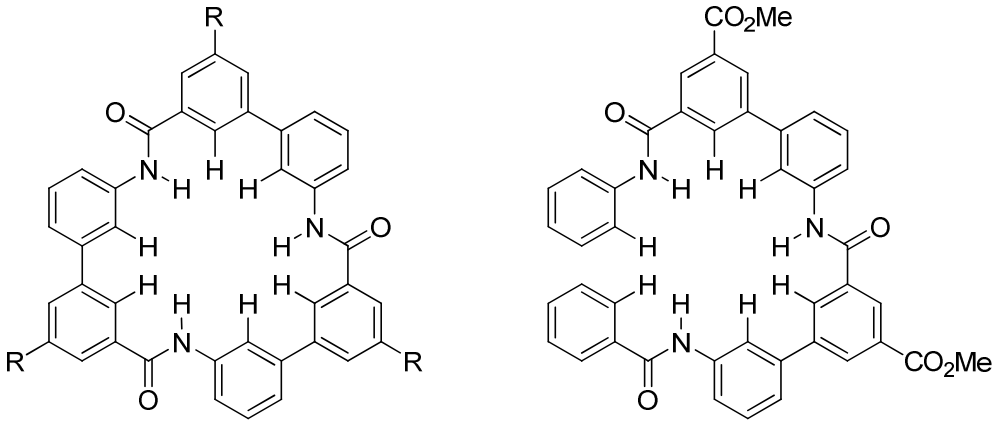

12 R = CO_2Et
13 R = NHBoc

14

Figure 1.10 - Hamilton and Choi's amide macrocycles (12&13) and acyclic test analogue (14).

Binding constants were determined by ^{1}H-NMR titrations in 2% DMSO-d_6/$CDCl_3$ solutions. As expected, the binding constants were much lower for **14** than **12** and **13** with some unsual binding stoichiometries observed. For example, at low concentrations of iodide with **13** the authors believed a 1:2 anion/receptor complex was formed with π-stacking between the macrocycles to form a 'sandwich'. After 0.5 equivalents of iodide was added, the receptor adopted a simple 1:1 binding stoichiometry as inferred by the NMR shift binding profile. In general, the binding affinities were similar for **12** and **13** with the highest binding constants observed with the tetrahedral anions, NO_3^- and *p*-tosylate. With HSO_4^- and $H_2PO_4^-$ a slow exchange of anion/receptor was observed on the NMR timescale meaning binding constants could not be obtained. This is indicative of very strong binding and even changing to the more polar 100% DMSO-d_6 still showed a slow exchange for $H_2PO_4^-$ and a high binding constant for HSO_4^- (K_a = 1700 M^{-1}).[16]

1.3.2 Ureas and Thioureas

Ureas and thioureas are widely employed in anion receptor chemistry due to their usually facile synthesis. They are commonly generated in high yields by a simple reaction of the corresponding amine with a usually highly reactive isocyanate (in the case of ureas) or thioisocyanate (in the case of thioureas). Symmetric ureas/thioureas can also be generated from condensation of an amine in the presence of triphosgene or thiophosgene accordingly.

They have two parallel NH hydrogen bond donor groups which naturally means they often (but not exclusively) have high affinities for 'Y' shaped anions such as carboxylates or nitrates due their complimentary shapes. This principle can be exemplified by a simple urea system looked at by Fabbrizzi *et al.*[18] They synthesised a *para*-nitro substituted bis-phenylurea receptor (**15**) and studied its interaction with a selection of various 'Y' shaped oxyanions, both in the solid state and in solution. An X-ray crystal structure of **15** was obtained with acetate which showed the expected complementary binding between the two species (*fig.* 1.11).

Stability constants were determined by UV-vis titrations in acetonitrile since bright colour changes were noted upon addition of the various oxyanions. The results showed a 1:1 binding stoichiometry for all the anions tested with an order of selectivity; $CH_3CO_2^-$ (*log* K 6.61) > $C_6H_5CO_2^-$ (*log* K 6.42) > $H_2PO_4^-$ (*log* K 5.37) > NO_2^- (*log* K 4.33) > HSO_4^- (*log* K 4.26) > NO_3^- (*log* K 3.65). Interestingly with fluoride, a 1:1 complex was stable at low concentrations, but at higher concentrations the receptor became deprotonated generating HF_2^- (confirmed by ^{1}H-NMR and a new UV-vis band during titrations).[18]

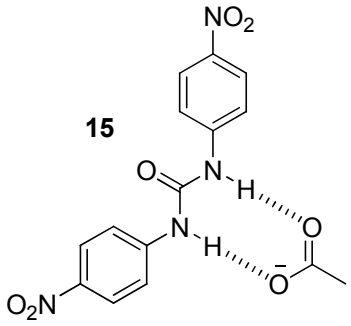

Figure 1.11 - Fabbrizzi's bis-phenylurea anion receptor.

Also, Gunnlaugsson and co-workers have shown how a simple thiourea based system can fluorescently detect anions in solution (*fig.* 1.12).[19]

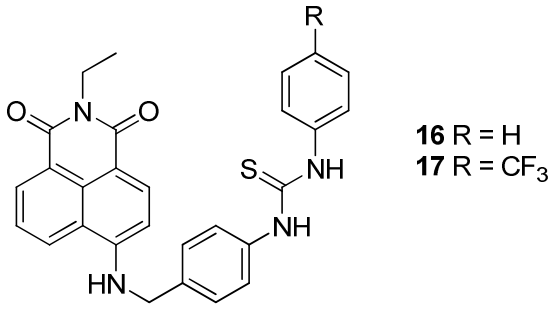

Figure 1.12 - Gunnlaugsson's urea based anion receptor.

The receptors utilise the bisphenyl-thiourea core in a classic fluorophore-spacer-receptor design with one of them containing an electron-withdrawing CF_3- group. The fluorescence of the fluorophore (a naphthalimide) is quenched upon binding of anions to the receptor part. Stability constants were calculated by fluorescence spectrometry titrations in DMSO which showed a 1:1 binding stoichiometry and a trend, $F^- > CH_3CO_2^- > H_2PO_4^-$, with slightly higher binding constants for **17**. Interestingly, large changes in the UV-vis spectra for the receptors with F^- were also observed which was thought to be because of the deprotonation of the amine spacer unit next to the fluorophore. This demonstrates that this system can be used as a dual sensor where at low anion concentrations the fluorescence is quenched and at higher concentrations the absorption spectrum is modulated.[19]

Recently, Ghosh and co-workers have revisited the familiar theme of using tren-type scaffolds to organise ureas for anion recognition (*fig.* 1.13).[20] They synthesised a small series of these receptors with different appends to the urea groups, the most interesting of which was the pentafluorophenyl version (**18**).

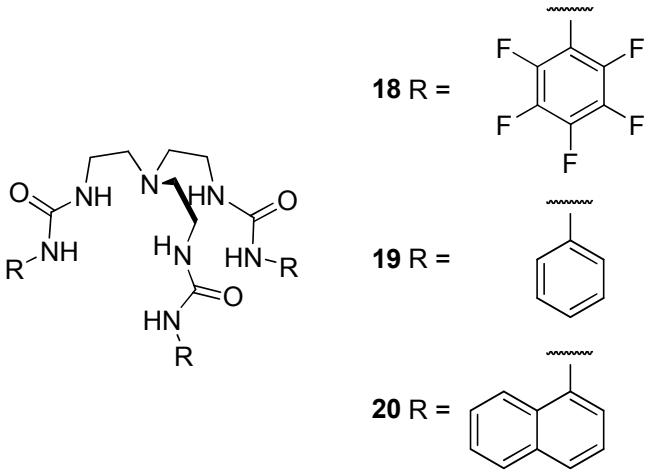

Figure 1.13 - Ghosh and co-worker's pentafluorophenyl tripodal urea based receptors.

Proton-NMR titrations in DMSO-d_6 showed a 1:1 binding stoichiometry of **18** with $H_2PO_4^-$ and $CH_3CO_2^-$ with binding constants (*log* K_a) of 5.52 and 4.45 M^{-1} respectively. Most interestingly, compound **18** formed a phosphate dimer complex in the solid state, with the dimer encapsulated in a pseudodimeric cage of the receptor (see *fig.* 1.14).[20]

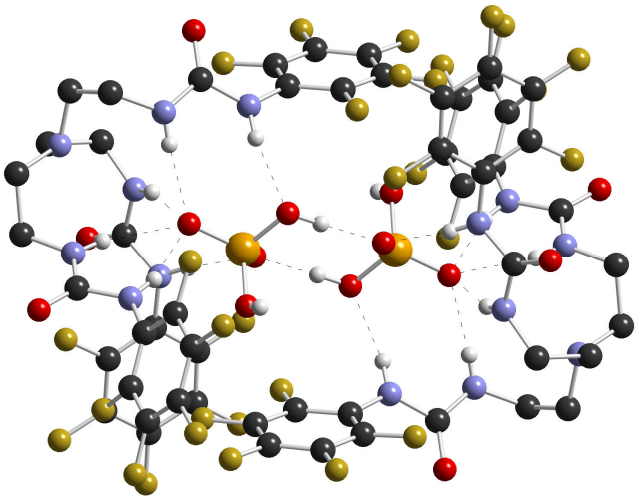

Figure 1.14 - A $H_2PO_4^-$ dimer inside the pseudo cage formed by receptor 18 in the solid state.[21]
Reproduced by permission of The Royal Society of Chemistry.

Remarkably, the crystal structure shows the phosphate dimer binding through a total of eighteen hydrogen bonds and anion···π interactions.

Often anion receptors are designed with no specific anion to target for selective binding. They are simply synthesised and tested with a chosen range of anions to find selectivity and interesting phenomena. Recently, Meshcheryakov *et al*. have tried a more

calculated and rational approach to anion receptor design, by carrying out preliminary molecular modelling studies in order to evaluate the best structure required for binding the nitrate anion. They wished to further investigate oligoureas and so designed and synthesised receptor **21** as part of a series of test analogues (the other analogues are not detailed here).[22]

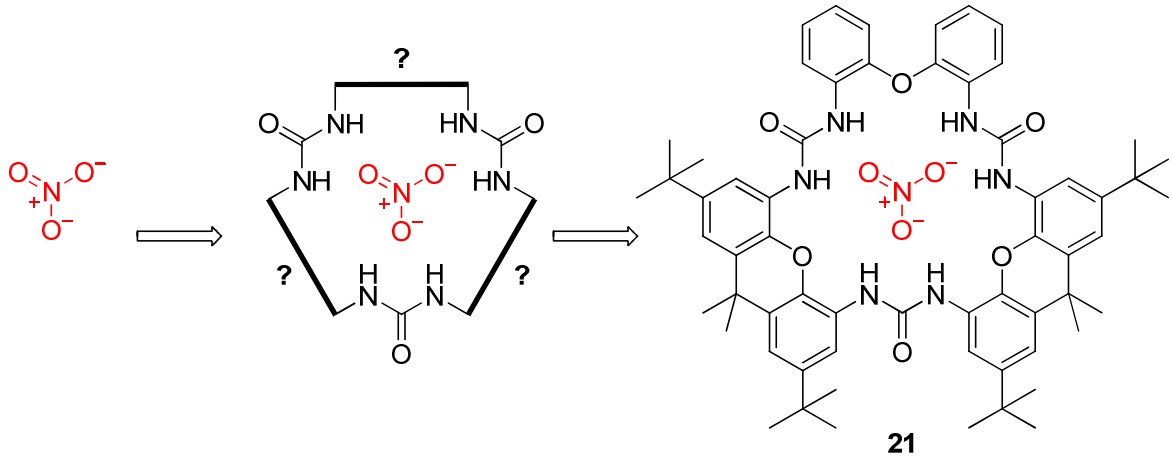

Figure 1.15 - The rational design of a nitrate receptor by Meshcheryakov *et al*.

X-ray suitable crystals were obtained by slow evaporation of a solution of **21** in a mixture of chloroform/DCM/ethanol to give an unexpected structure (*fig*. 1.16). The structure showed the urea groups linking the diphenylether unit and the two xanthene units adopting a *trans*-conformation. In addition, the ureas are intramolecularly hydrogen bonding to the third urea which is *cis*-orientated (N···O distances 2.48-2.60 Å).

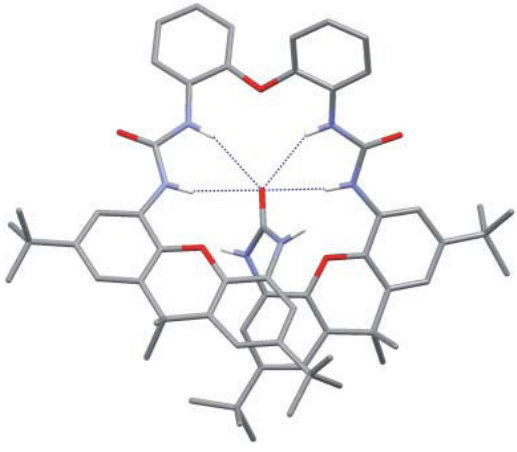

Figure 1.16 - Crystal structure of 21 showing an unexpected twisted conformation.[22]

This result was surprising given that the structure was designed to be rigid and pre-organised for optimum binding. They were unable to obtain a crystal structure of **21** (or any of the analogues) with nitrate.

In solution, ^{1}H-NMR studies were not possible due to the very broad peaks observed which they were unable to follow, so UV-vis titrations were carried out in acetonitrile. These showed no interaction with nitrate but strong interactions with chloride (*log* K_a = 11.7) and acetate (*log* K_a = 5.7) in a mixture of binding stoichiometries. This example clearly shows how rational design, backed by advanced computer modelling does not always lead to expected results.[22]

1.3.3 Pyrrole Based Systems

The use of pyrrole in anion receptor systems has its origins in a serendipitous discovery by Sessler and co-workers in 1990. At the time, the workers were trying to find a more efficient synthesis of the pentapyrrolic sapphyrin **22** (*fig.* 1.17).[23, 24]

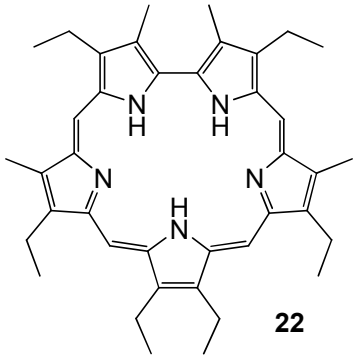

22

Figure 1.17 – The Sapphyrin studied by Sessler and co-workers.

During their studies they thought they had obtained X-ray quality crystals of the HPF_6^- salt of sapphyrin **22**. However, the crystal structure revealed that they had actually made the diprotonated version of the macrocycle which was binding a fluoride in the cavity through five hydrogen bonds. A PF_6^- counter-anion was also located in the lattice, but it was not proximate to the sapphyrin structure. Other structures were also later solved, such as the 2HCl solvate of **22** which showed the sapphyrin binding two chloride anions.

These initial studies paved the way for development into a significantly large area of research with an ever increasing number of varieties of extended sapphyrins, each with unique anion binding properties and selectivity.[23, 25, 26]

In 2001 a crystal structure of pyrrole with tetramethylammonium (TMA) chloride was reported by Gale and co-workers.[27] It was remarkable because it was the first time a single ring pyrrole/anion complex had been reported (*fig.* 1.18).

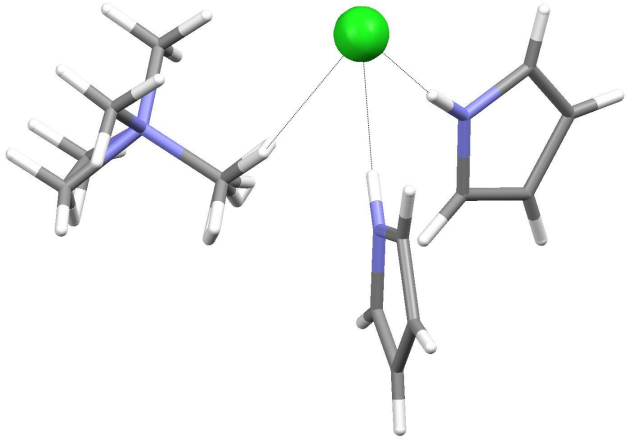

Figure 1.18 - X-ray crystal structure of the coordination environment of pyrrole with TMA^+ chloride.[27]

The structure shows the chloride bound by two pyrroles via the NH groups (N···Cl 3.24 Å) and a slightly weaker interaction through the methyl proton of the TMA^+ (C···Cl 3.66 Å). NH···π and CH···π interactions were also observed between the pyrroles to form a 'honeycomb' network of pyrrole, TMA^+ and Cl^-.

Most significantly, the binding of chloride to the pyrrole shows very similar geometry to the binding of chloride to the first ever *neutral* pyrrole based anion receptor reported; *meso*-octamethylcalix[4]pyrrole (**23**, *fig.* 1.19). The compound was in fact first synthesised by Baeyer[28] in 1886, but it wasn't until 1996 that it was put forward as an anion receptor by Gale and Sessler *et al.*[29]

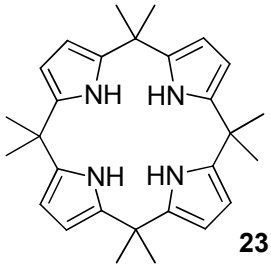

23

Figure 1.19 - The first neutral pyrrole based receptor by Gale and Sessler *et al.*

Solution studies (^{1}H-NMR titrations in CD_2Cl_2) revealed that **23** was highly selective for fluoride with a binding constant of 17200 M^{-1} when compared to chloride (K_a=350 M^{-1}), bromide (K_a=10 M^{-1}) and dihydrogen phosphate (K_a=100 M^{-1}).

In the solid state they found that the macrocycle adopts a dramatically different structure upon anion complexation; *viz.*, the free calixpyrrole adopts a 1,3-alternate conformation wherein the rings are orientated in opposite directions. However, when the macrocycle is bound to an anion such as fluoride or chloride, it adopts a cone conformation with the four pyrrole NH groups forming hydrogen bonds to the central anion (*fig.* 1.20). It is particularly interesting to see how the larger chloride anion sits slightly out of the cleft compared to the 'snug fit' of the much smaller fluoride anion.

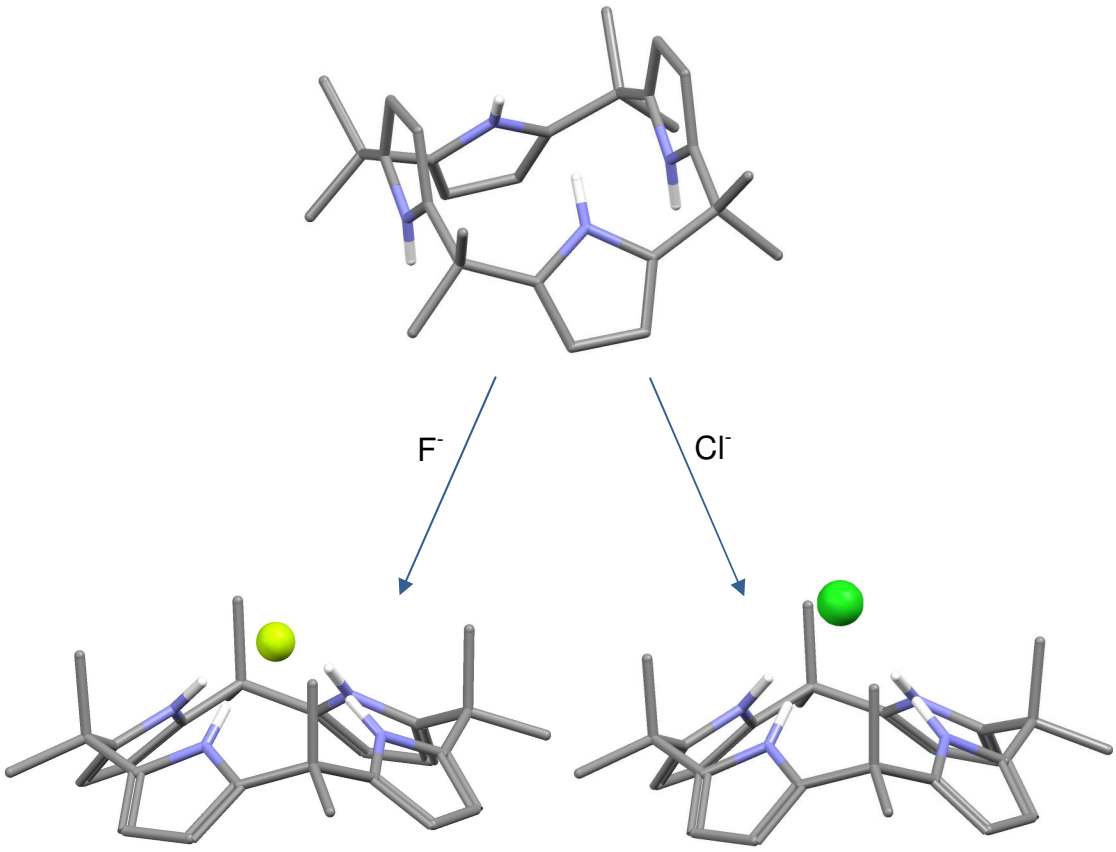

Figure 1.20 - X-ray crystal structure of 23 showing it unbound in the 1,3 alternate conformation (top) and bound with fluoride (left) and chloride (right) in the cone conformation.

Recent studies by Sessler, Schmidtchen and Gale *et al.*[30-33] have shed some new light on the anion binding behaviour of calix[4]pyrroles in solution and the solid state. These intriguing studies on **23** have shown that:

1. The anion selectivity in solution is very reliant on the nature of the solvent the studies are conducted in, i.e. the more polar the solvent the less selective the receptor is for fluoride.[30, 32]

2. By testing a variety of chloride salts with different counter-cations by isothermal calorimetry (ITC) and ^{1}H-NMR titrations, the authors have shown that the binding constants are not reliant on which method is used.[30]

3. Compound **23** can act as a ditopic ion pair receptor. In particular, it has been shown to bind caesium chloride in the solid state, with the caesium bound in the vacant cup formed by the calixpyrrole upon anion binding. Likewise, it can bind organic counter-ions such as triethylammonium and *N*-ethylpyridinium cations (see *fig*.1.21).[30, 31, 33, 34]

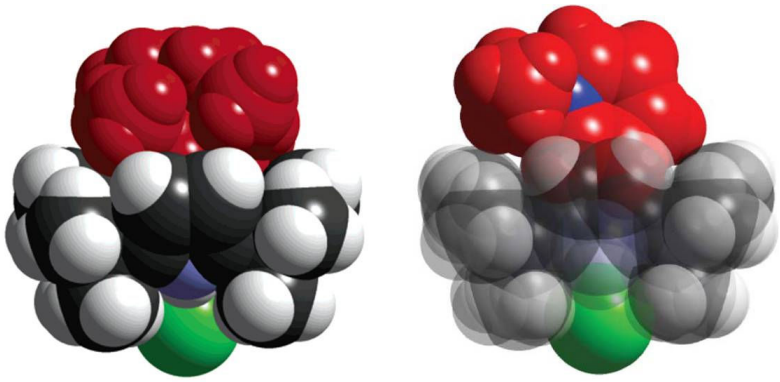

Figure 1.21 - Crystal structures of 23 with $TEA^{+}Cl^{-}$ (left) and *N*-ethylpyridinium chloride (right) in a space-filling representation.

As a consequence of the last point, it was also discovered that when dichloromethane was used in solution studies, there was a strong influence of the countercation on the stability constants observed. This puts forward a strong antithesis to the assumption that when anions are used as TBA salts in solution studies, the anion behaves as a free species.[30]

This class of receptor has sparked a continuingly growing area of anion receptor chemistry, as they are remarkably easy to prepare and fine tune to alter their affinities and selectivity for various anions. The synthetic scheme below demonstrates just two of the many ways in which this tuning can be achieved (*fig*.1.22).

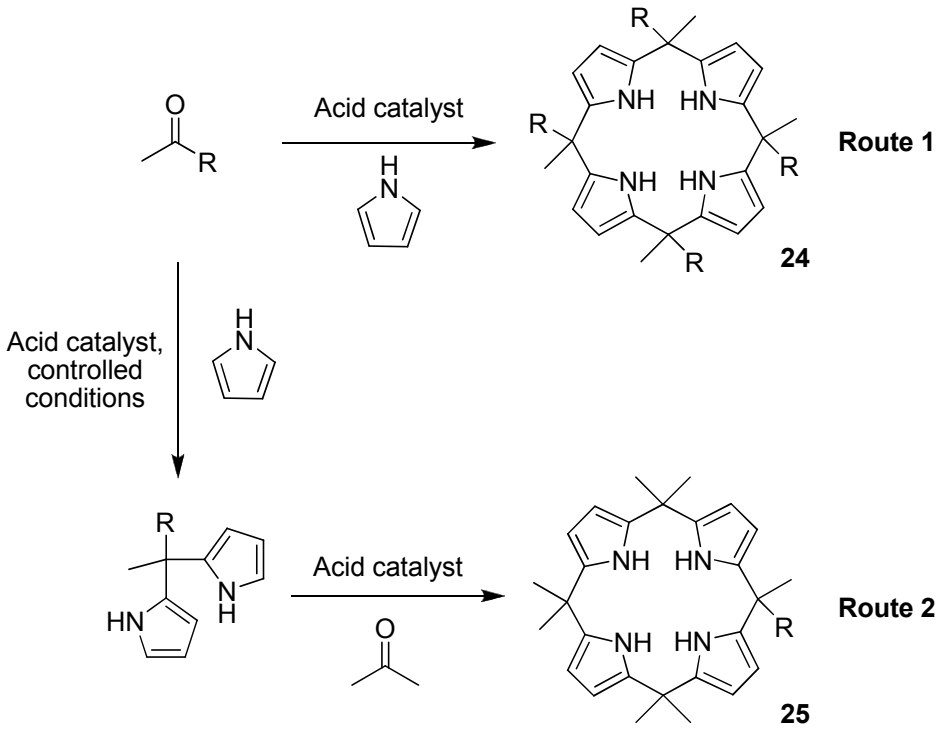

Figure 1.22 - Two ways of adding functionality to calixpyrroles.

Receptor **23** is made simply with acetone via **Route 1**. However, any number of ketones can be used with varying R groups to add enhanced functionality to the basic calixpyrrole unit. One such example is that of Gale and Warriner *et al.* who used **Route 2** (see *fig.* 1.22) to generate the calixpyrrole, **26**.[35]

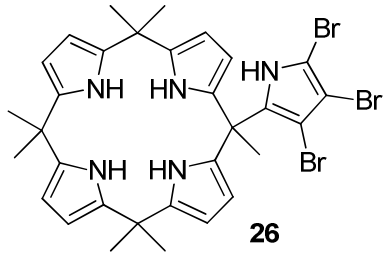

Figure 1.23 - Gale and Warriner's modified calix[4]pyrrole.

Proton-NMR titrations in CD_2Cl_2 showed much higher binding constants as expected, for example, the binding constant (K_a) for **26** with chloride was 1042 M^{-1} compared with 350 M^{-1} for **23**. Surprisingly however, **26** also showed high selectivity for carboxylates which was not displayed by **23**. The authors attributed this to the ability of **26** being able to coordinate to both oxygen atoms on the carboxylate simultaneously.

The first pyrrole based receptor was cyclic but there have also been significant advances in the study of acyclic pyrrole based systems, most notably by Gale and co-

workers. Most this work focused around 2,5-bisamidopyrroles which were inspired by the work of Crabtree and his isophthalamide receptors (see earlier). Receptors **27** and **28** were made from the reaction of the appropriate amine with the pyrrole-bisacid chloride in yields of 18 and 47% respectively (*fig*. 1.24).[36]

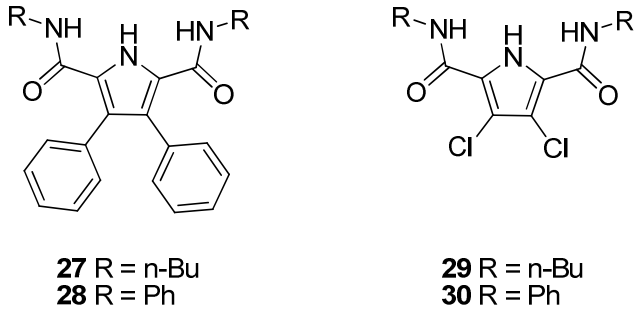

27 R = n-Bu
28 R = Ph

29 R = n-Bu
30 R = Ph

Figure 1.24 - Bisamidopyrrole receptors by Gale and co-workers.

One of the advantages of *exclusively* pyrrole based receptors is that they usually cannot undergo self-association to form dimers since they lack a hydrogen bond acceptor group. However, with these receptors (**27**-**30**), the introduction of an amide group detrimentally allows dimerisation to occur as seen in the crystal structure of **28** shown below (*fig*. 1.25).

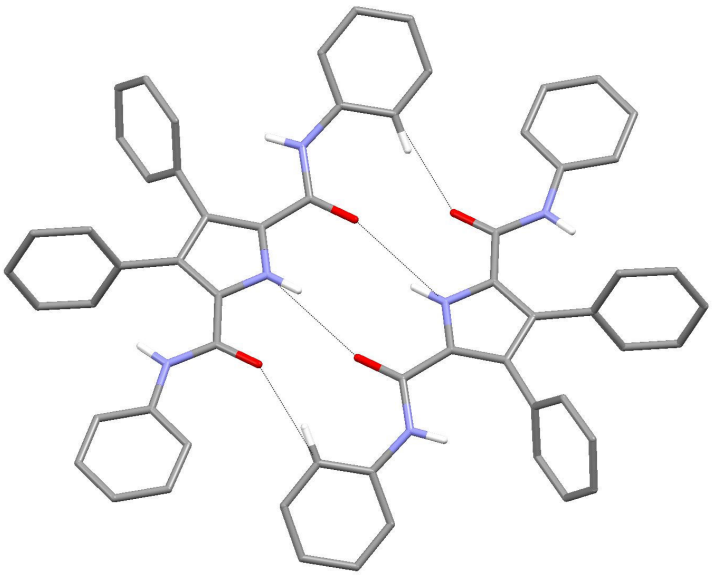

Figure 1.25 - X-ray crystal structure of 27 showing the dimer ($N_{py}\cdots H$ 3.238 Å).

A similar structure was observed for **30** which makes the solvation of these receptors problematic. As a consequence of this, ^{1}H-NMR binding studies were carried out in polar solvent systems such as DMSO-d_6/0.5% water or acetonitrile-d_3. Receptor **27**

showed a high selectivity for benzoate in acetonitrile-d_3, whilst **28** showed selectivity for dihydrogen phosphate in DMSO-d_6/0.5% water.

Introduction of chloride groups to the pyrrole skeleton were effected (**29** and **30**) to make the pyrrole NH more acidic and hence enhance anion binding. However, one of the undesirable effects of this was witnessed with the addition of TBA fluoride to an acetonitrile-d_3 solution of **30**, which resulted in an unusual titration profile whereby the pyrrole NH signal completely vanished. This is indicative of deprotonation which was supported by the crystal structure of **30** with fluoride which showed the receptor forming a so-called 'narcissistic' dimer of itself with NH···N$^-$ hydrogen bonds (*fig.* 1.26).[36]

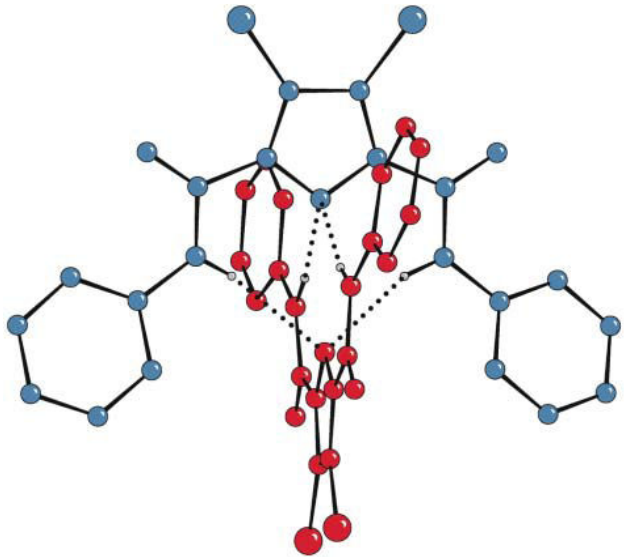

Figure 1.26 - X-ray crystal structure of the dimer formed by 30 when deprotonated by fluoride anions.[36] ***Reproduced by permission of The Royal Society of Chemistry.***

This work shows the challenge involved in trying to strike a fine balance between providing the most optimum hydrogen bond donors that at the same time, are not going to be prone to deprotonation.

1.4 Metal-Organic Anion Receptors

The hydrogen bond is arguably the most fundamental molecular interaction employed in the design of an anion receptor. As has been seen, this is mostly because it is a strong and highly directional interaction, with cumulative effects that can lead to very high selectivity and binding constants. A key challenge however, is how to arrange and position these interactions for optimum effect, and in particular, create binding sites for anions of specific geometry.

One such tool at disposal for arranging hydrogen donors in space is to employ a metal centre, to which can be attached organic ligands appended with hydrogen bond donor groups. The metal centre or centres can restrict the conformations available to the receptor leading to more rigidity and pre-organisation for anion binding. In addition, these metal centres can potentially contribute electrostatic binding interactions for even more enhanced binding affinities (see *fig.*1.27).

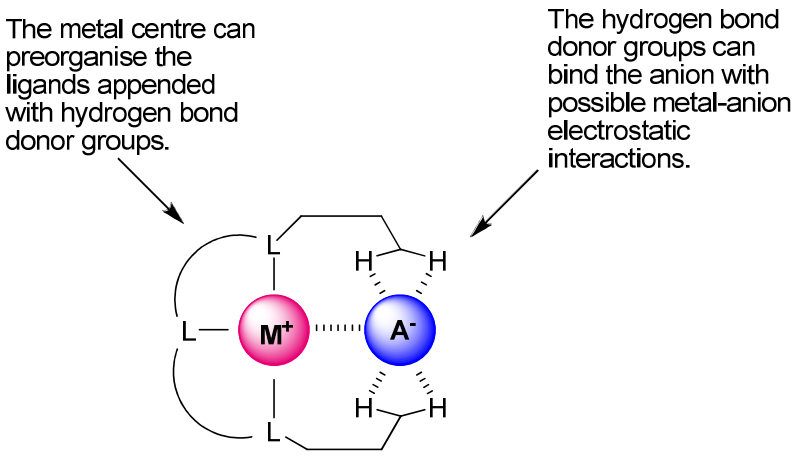

Figure 1.27 - Pictorial representation of how a metal-organic anion receptor can function.

Other advantages of metal centres include their potential for use as electrochemical, luminescent or colorimetric reporter units whereby they are 'switched on' or 'off' in the presence of anions.

Despite these perceived benefits, the use of metal ions to assemble anion receptors has been and remains quite a small growth area in the field of anion recognition. Perhaps some of the reasons for this are the inherent difficulties of:

a) Finding a metal with a suitable coordination number and preferable coordination geometry.

b) Finding ligands that can coordinate to the metal without being subject to substitution in the presence of anions or strong donor solvents.

c) Finding a metal complex which is stable under standard conditions, *i.e.* not light, air or solvent sensitive.

d) Choosing a suitable counter-anion for the complex, such that it does not interact with either the hydrogen-bond donor groups or interact electrostatically to the metal centre.

The significance of points (b) and (d) can by highlighted by referring to the work of Halcrow and co-workers from 2002.[37, 38] This work involved exploring some novel 3(5)-*tert*-butylpyrazole (Bupz) zinc complexes **31**-**33** (see *fig*. 1.28 below).

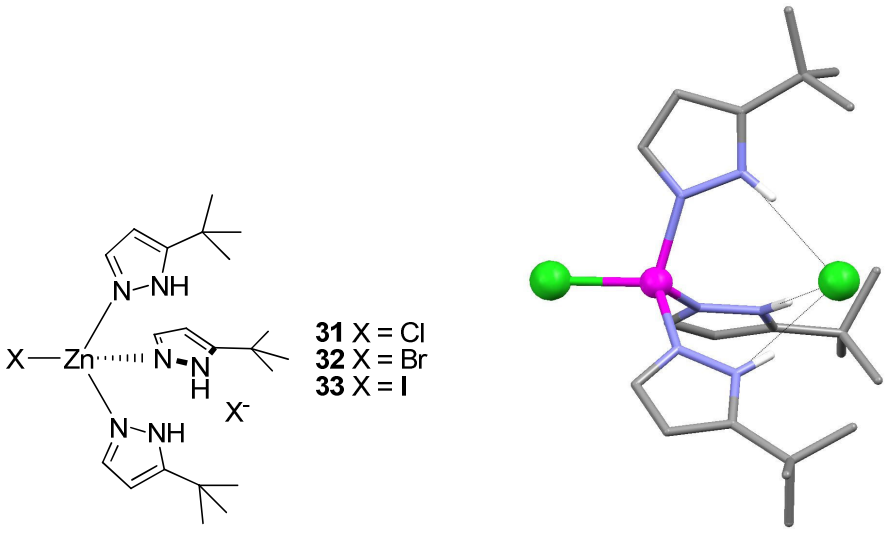

Figure 1.28 - Zinc pyrazole complexes by Halcrow and co-workers (left), x-ray crystal structure of 31 (right).

The crystal structure of **31** showed the ligands orientated such that they form a convergent array of the three NH hydrogen bond donors to the central non-coordinated chloride anion (*fig*. 1.28). To address point (d) they exchanged the halides with large counter-anions with delocalised charges such as BF_4^-, PF_6^- or $CF_3SO_3^-$, with which they also obtained crystal structures. However in solution, when they added TBA salts of halides to these compounds, ligand exchange was observed due to the nucleophilic effect of the halides attacking the zinc centre. Perez and Riera *et al.* have recently tried to address this problem by studying analogues of **31** with different metal centres such as molybdenum and different counter-anions.[39, 40]

Of course, much of the inspiration behind metal-organic receptors has come from nature's fundamental biological processes involving metalloenzymes and other metalloproteins. In particular, Paul Beer and his group used this inspiration to initiate a pioneering research program in the 1990s which involved studying a large range of transition metal based, organometallic receptors for anions.[41] Some of this early work focused on ferrocene and cobaltocene based receptors which were unexplored at the time. It was hoped that the cobaltocene units would be able to electrochemically recognise anions (observable by cyclic voltammetry) and preorganise the hydrogen bonding units for anion binding. Receptors **34** and **35** (see *fig.* 1.29) are highlights of the early range of this class of receptor. In CD_3CN solution, ^{1}H-NMR titrations with TBA salts of anions revealed strong perturbations of the amide NH protons. Cyclic voltammetric studies (in dry acetonitrile) demonstrated electrochemical sensing; with the redox potential of the reducible cobaltocenium moiety cathodically perturbed (ΔE = 240 mV with $H_2PO_4^-$). Essentially, the complexed anion stabilises the positive charge, making the cobaltocenium unit more difficult to reduce during the voltammetry.[41]

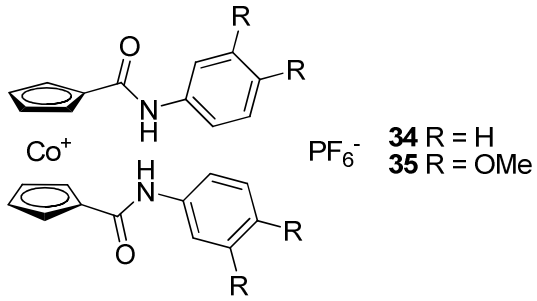

Figure 1.29 - An example of two of Beer's original cobaltocene based anion receptors.

An X-ray crystal structure of **34** with bromide revealed two equivalents of bromide binding to one receptor through not only each amide NH but also through interactions with the Cp and aryl protons (*fig.* 1.30).

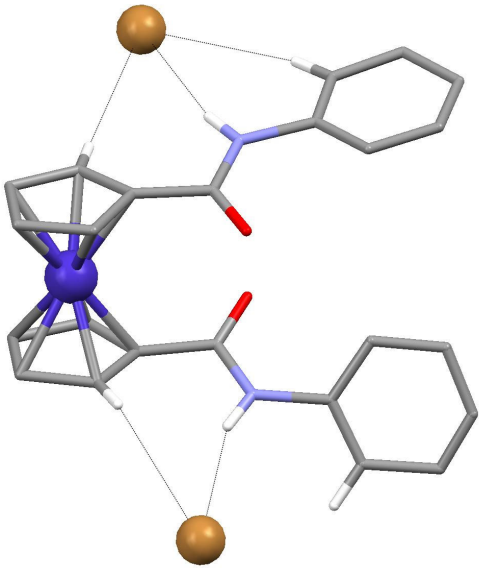

Figure 1.30 - X-ray crystal structure of 34 with bromide showing the anions interacting with the NHs, Cp and aryl protons.

This work was further developed over the years with more selective and stable cobaltocenium and ferrocene compounds (including ditopic and macrocyclic versions) reported.

Also included in this seminal research effort by Beer and co-workers were some ruthenium bipyridyl (Ru-bipy) based receptors which have the potential to be both electrochemically and optically active. The first one to be synthesised in this series was receptor **36** which consists of a ruthenium centre complexed with three bipyridyl units, one of which is functionalised with a bis-amide for hydrogen bonding to anions (*fig.* 1.31).[42]

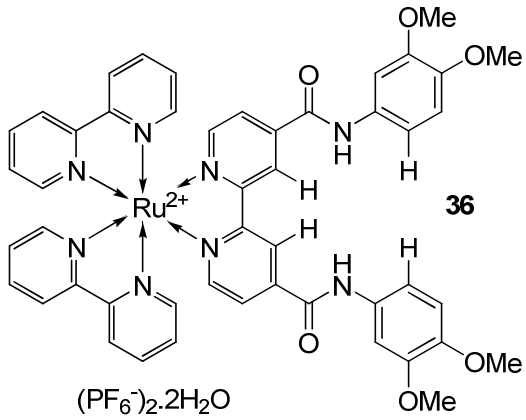

36

Figure 1.31 - Beer and co-worker's original Ru-bipy receptor.

The ruthenium ion is dipositive which means that electrostatic interactions with anions are particularly favourable. Proton-NMR titrations in DMSO-d_6 (a highly competitive solvent) showed strong interactions with chloride and dihydrogen phosphate (K_a = 500 and 8000 M^{-1} respectively).[41, 42]

Slow evaporation of an acetonitrile solution of **36** with an excess of TBA^+Cl^- provided single crystals suitable for an X-ray crystal structure determination (*fig.* 1.32). Remarkably the structure revealed the receptor-anion complex is stabilised by 6 hydrogen bonds (two amide NHs and four aryl CHs, distances = 2.006-2.033 Å).[41, 42]

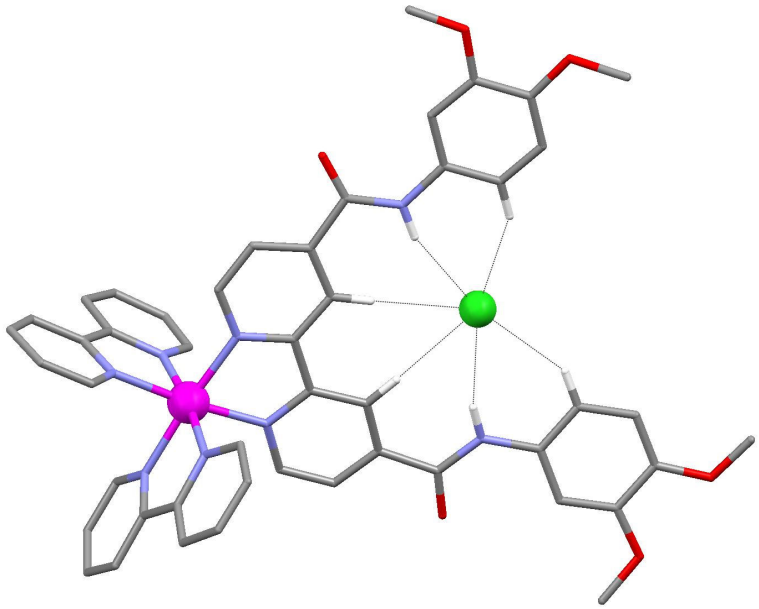

Figure 1.32 - X-ray crystal structure of 36 with chloride.

Other work followed which includeded new ditopic and macrocyclic versions of these ruthenium complexes for improved binding and selectivity. A highlight of these very extensive studies includes the homo-dinuclear twenty six membered macrocycle, **37** (*fig.* 1.33). This was found to be particularly effective for acetate and dihydrogen phosphate in DMSO solution (both association constants > 10^5) as determined by ^{1}H-NMR titrations.[43]

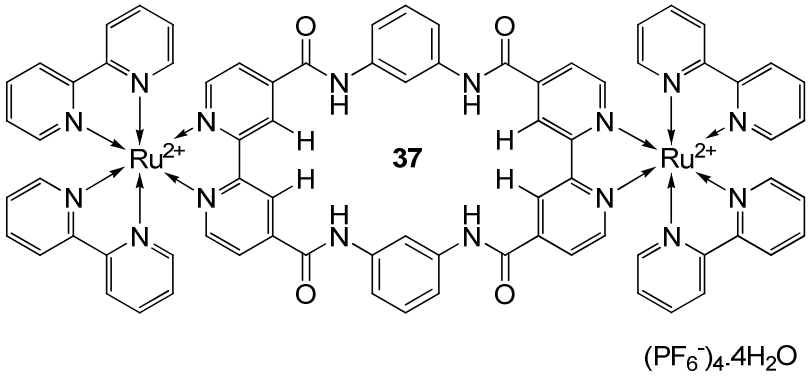

Figure 1.33 - One of Beer and co-worker's dinuclear ruthenium based macrocycles.

Slow evaporation of an acetonitrile solution of **37** in the presence of acetate gave single crystals suitable for an X-ray crystal structure (*fig.* 1.34).

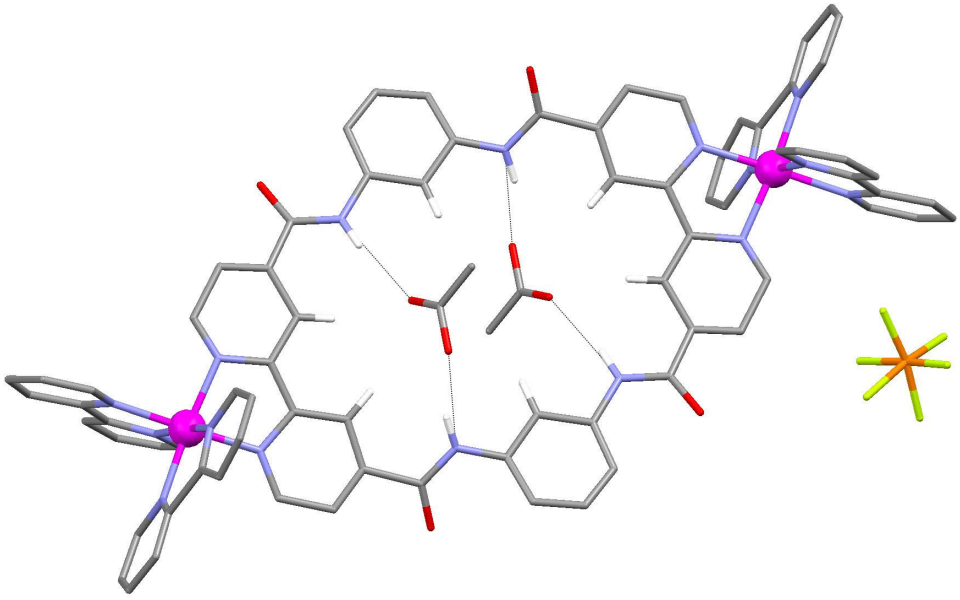

Figure 1.34 - X-ray crystal structure of 37 with acetate.

The structure showed the two octahedral metal centres linked together through the substituted bipyridyl units to form a planar macrocycle. The macrocycle accommodates two acetate anions without distortion, binding through two strong hydrogen bonds to the amide NH groups (2.781 – 2.894 Å) and weaker CH···O hydrogen bonds (3.022 – 3.408 Å).[43]

One of the most challenging goals in anion receptor chemistry is to design systems that can bind anions in water. The main challenge is that water is a very competitive solvent for hydrogen bond binding sites. The other problem is designing a receptor that is sufficiently water soluble. The anion receptors thus far have been studied

only in organic solvents but all natural processes (e.g. enzymatic or antibody functioning) take place in the aqueous media of living organisms. As is a reoccurring theme now, it naturally follows that inspiration can be taken from nature in the design of receptors for anions in water.[44]

Some elegant examples of metal-organic systems that can recognise phosphate in water were put forward by Anslyn and co-workers in 2003.[45] The designs both feature C_{3v} symmetric cavities with copper(II) ions on the C_3 axis and encapsulating hydrogen bond donor groups (**38** and **39**, *fig.* 1.35).

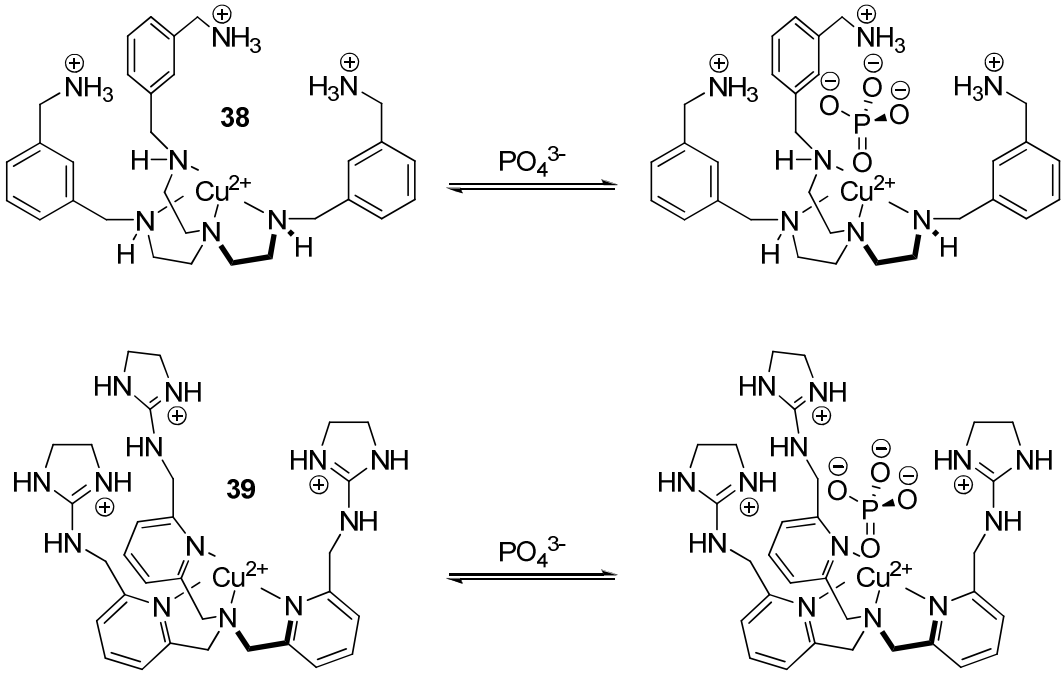

Figure 1.35 - Anslyn and co-worker's copper (II) C_{3v} symmetric receptors.

Figure 1.35 shows how the designs of the cavities provide excellent shape, size and charge complimentarity to the phosphate anion. Accordingly, binding studies (conducted in water at neutral pH and measured by UV-vis spectroscopy methods) showed a particularly high affinity for HPO_4^{2-} with compounds **38** and **39** (K_a = 25000 and 15000 M^{-1} respectively). It was also interesting that one of the controls (**40**) studied bound HPO_4^{2-} with K_a = 900 M^{-1} despite lacking the hydrogen bond donor groups of **38** and **39** (*fig.* 1.36).[45]

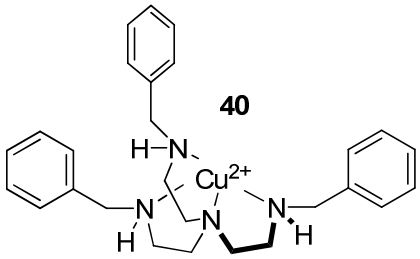

Figure 1.36 - One of the control analogues tested against 38 and 39.

This result suggests that the copper (II) metal centre plays a key role in the binding of phosphate to **38** and **39**, which proves how metals can be utilised to complement hydrogen bond donor groups with electrostatic interactions to bind anions.

Moyer and co-workers have previously had success binding sulfate with a phenyl derivative of receptor **41** (*fig.* 1.37). This phenyl version bound the anion through twelve hydrogen bonds in the crystalline state.[46] However, their goal was to selectively and efficiently separate sulfate from aqueous solutions and this crystalline framework proved ineffective because of its low stability and high solubility in water. They reasoned that replacing the phenyl groups with stronger coordinating groups such as pyridines, would facilitate the formation of more robust crystalline frameworks, with superior sulfate separation abilities. This led to the synthesis of compound **41**.[47]

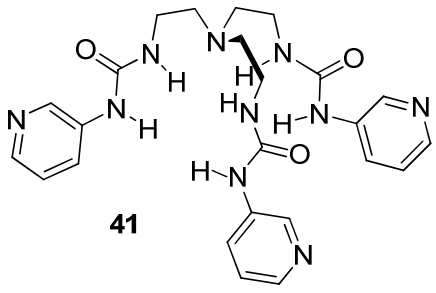

Figure 1.37 – Moyer and co-worker's tripodal sulfate receptor.

X-ray suitable crystals of $MgSO_4$(**41**)$_2$(H_2O)$_6$ composition were obtained from a 1:1 H_2O/MeOH solution of **41** in the presence of $MgSO_4$. The structure showed the sulfate bound by six ureas through twelve hydrogen bonds. The complex is incorporated in a hydrogen bonded capsule from twelve additional hydrogen bonds from six water molecules. These capsules are linked by 2+ magnesium cations to form a three dimensional framework with distorted NaCl topology (*fig.* 1.38).

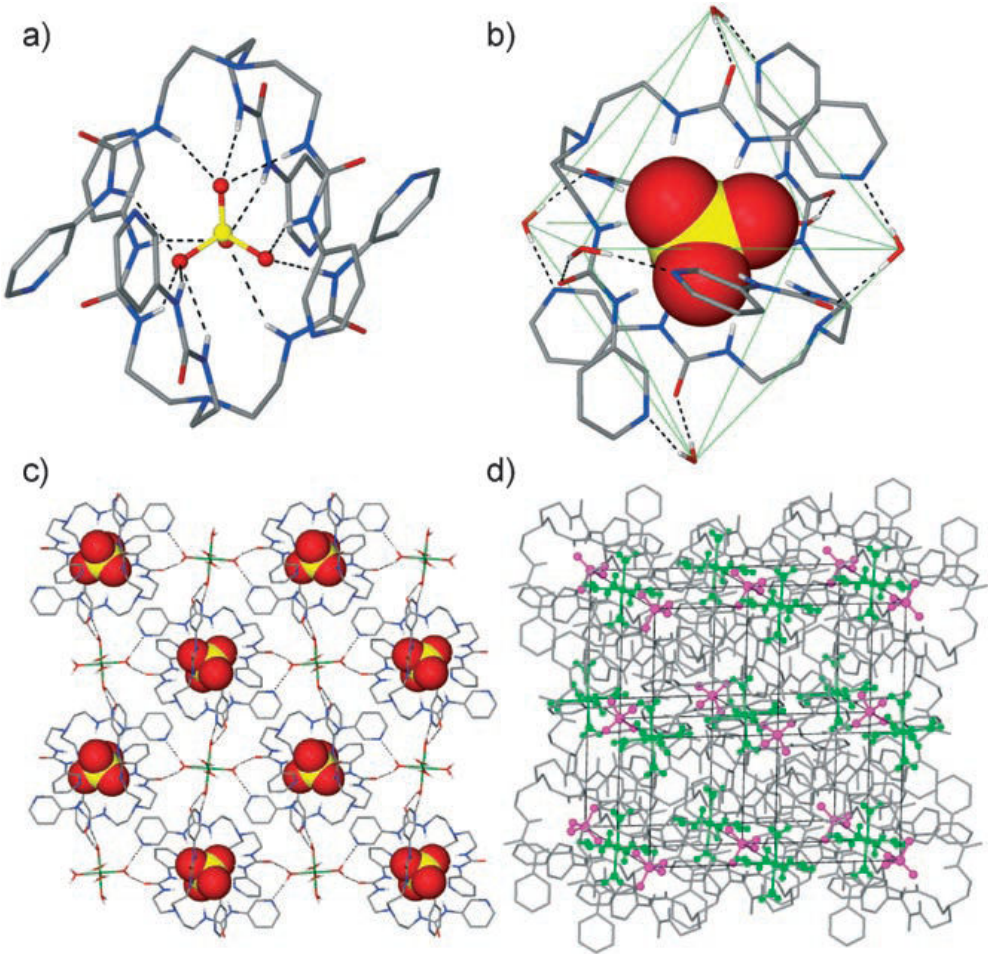

Figure 1.38 – Crystal structure of 41 a) Sulfate encapsulation by the six urea groups. b) Hydrogen bonded capsule showing two 41 ligands, one sulfate and six water bridging molecules. c) The hydrogen bonded framework from self-assembly of the anionic capsules with Mg^{2+} ions. d) 3D representation of the octahedral framework.[47] ***Copyright Wiley-VCH Verlag GmbH & Co. KGaA. Reproduced with permission.***

One of the useful aspects of employing metals (particularly transition metals) in anion receptor design is the wide range of geometries that can be accessed according to which metal and oxidation state is chosen. For example, palladium (II) has preferential geometry to be square planar due its d^8 electron configuration. Recently, Vilar and co-workers have utilised this metal in the construction of a bis-palladium urea complex for anion recognition.[48, 49]

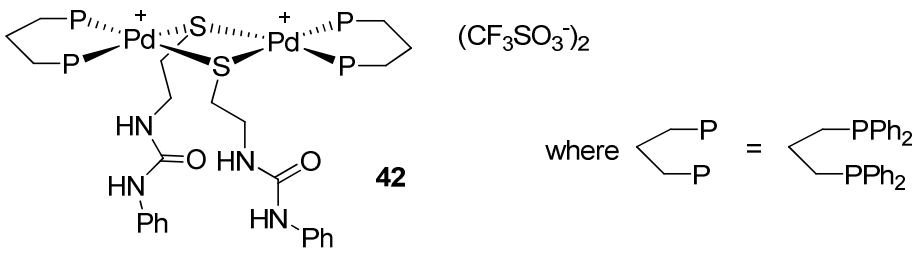

Figure 1.39 - Vilar and co-worker's palladium based anion receptor.

A single crystal X-ray structure of **42** was obtained which interestingly encapsulates one of the triflate counter-anions (*fig.* 1.37). As can been, the anion is bound by the urea NH groups on the ligand arms to the oxygens of the triflate (N-H···O 3.13 – 3.23 Å).[48]

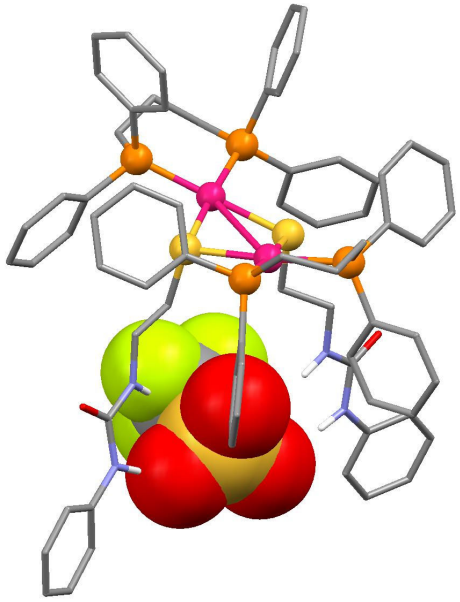

Figure 1.40 - X-ray crystal structure of 42 showing it binding its triflate counter-anion.

The same workers have also used a similar architecture to synthesise some palladium based macrocycles composed of bridging, functionalised pyridyl ligands. Despite the wealth of literature exploring palladium based cages and boxes there had been relatively few studies of metal receptors with bridging ligands that also function as hydrogen bonding units.[50]

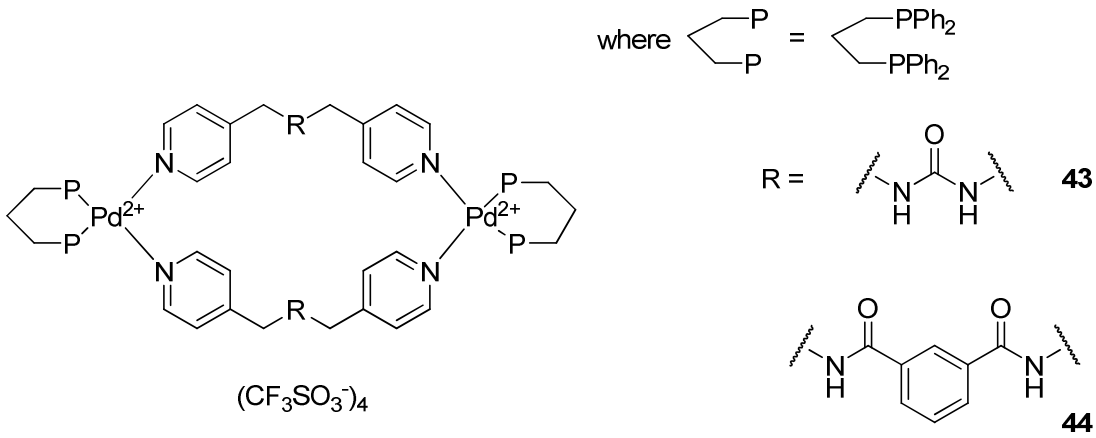

Figure 1.41 - Vilar and co-worker's palladium based macrocycles.

It was reasoned that the synthesis of **43** and **44** could lead to the formation of a range of different acyclic and cyclic products, especially taken into account how labile palladium/pyridine bonds are. This would mean that an equilibrium of different assemblies would likely be established. X-ray suitable crystals were grown from the reaction mixtures which revealed formation of the [2+2] macrocycles for both **43** and **44**. As seen in their earlier work with receptor **42**, **43** encapsulates a triflate counter-anion which is interacting with the central cavity whilst the palladium centres are in a distorted geometry.[49, 50]

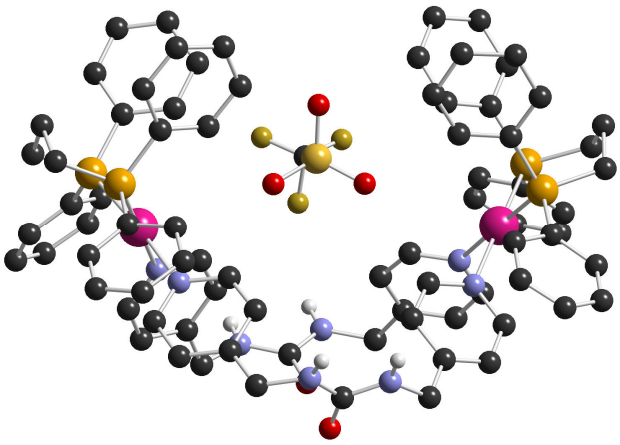

Figure 1.42 - X-ray crystal structure of 43 showing the encapsulation of a triflate counter-anion.[21]
Reproduced by permission of The Royal Society of Chemistry.

The same structure was observed for receptor **44**, showing the bowl structure with a triflate encapsulated inside. However, despite these crystal structures, ^{1}H-NMR studies revealed that more than one species co-existed in solution. In fact, the studies revealed that indeed, an equilibrium did exist between a [2+2] and [3+3] macrocycle. Of

significant interest was that this equilibrium was found to be affected by, the solvent system, concentration, temperature and the presence of particular anions: *viz.* when dihydrogen phosphate was added, the [2+2] macrocycle was favoured over the [3+3]. The same effect was noticed with the addition of di-carboxylates such as malonate or oxalate. Yet with hydrogen sulfate, no significant changes were observed in the relative integration of the peaks assigned to the two different assemblies [2+2] or [3+3]. The authors believe this work will lead on to the development of complex dynamic combinatorial libraries by mixing other hydrogen bonding ligands with the *cis*-palladium centres.[49]

1.5 Neutral Molecule Receptors and Hydrogen Bonded Arrays

The binding of neutral guests is a particularly challenging task simply because of their lack of charge. When guests are charged (anionic or cationic), electrostatic interactions with the host play a key role in enhancing binding affinity. So unless the host is charged, neutral guest binding must rely on other intermolecular interactions.

As in anion recognition, the majority of inspiration in this area has come from nature. Of course DNA consists of a hydrogen bonded array of neutral complementary base pairs on a poly-anionic backbone, which remarkably assembles in the most competitive of solvent environments, water. Indeed a lot of early work in this area involved developing receptors for binding specific nucleotides or nucleotide base pairs. A fine example can be provided by Andew Hamilton who designed a receptor for the recognition of thymine derivatives.[51] As was the theme of most of Hamilton's seminal work, the design of the receptor was remarkably simple, consisting of an easy to prepare, amide based macrocycle **45**.

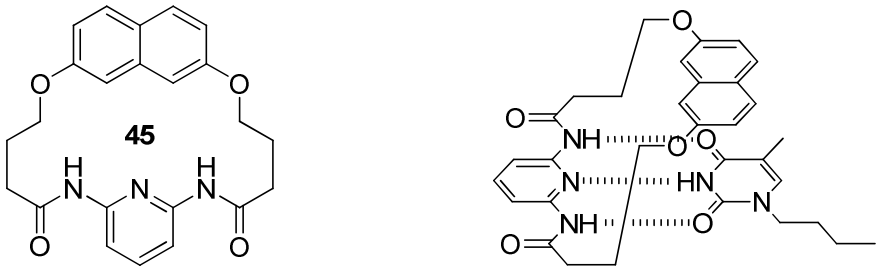

Figure 1.43 - Hamilton's macrocyclic receptor for thymine derivatives (left) and its mode of binding to butyl-thymine (right).

The role of the naphthalene unit is to complement the hydrogen bonding by π-π stacking with the thymine ring (as depicted in *fig.* 1.40 right). This was proved by X-ray crystal structure analysis (*fig.* 1.41) which neatly shows the three hydrogen bonds (N···N 3.06, N···O 2.87&2.99 Å) and naphthalene unit lying parallel to the thymine (inter-plane contact 3.37 Å).[51]

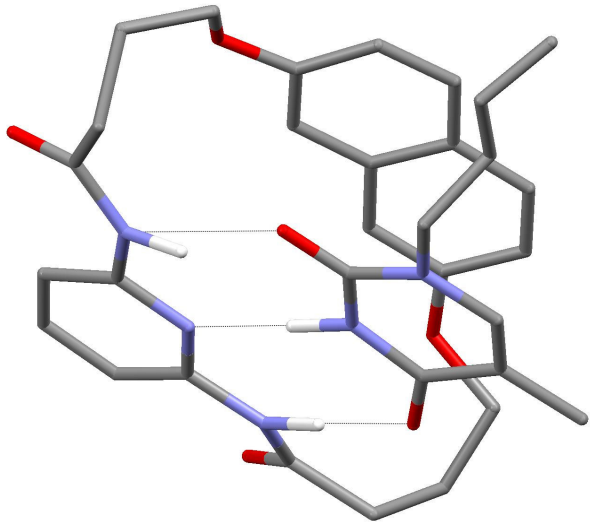

Figure 1.44 - X-ray crystal structure of 45 with butyl-thymine.

By adding butyl-thymine to a $CDCl_3$ solution of **45** the NH protons on each species were significantly shifted downfield on the ^{1}H-NMR spectrum (2.6 and 2.25 ppm respectively).

What this work chiefly highlights is the two most important intermolecular interactions implemented in neutral molecule receptor chemistry; hydrogen bonding and π-π interactions. Other work which has exploited both these interactions for neutral guest recognition includes the early research of Hunter and Purvis. This involved the design of macrocycles **46** and **47** for binding quinones. Their synthesis was effected from the corresponding diamine and bis-acid chloride in a two-step high dilution synthesis.[12, 52]

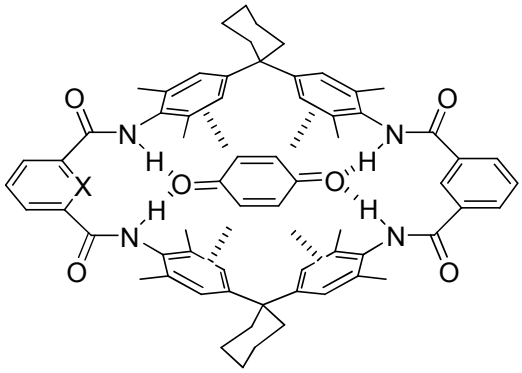

46 X = CH
47 X = N

Figure 1.45 - Hunter and Purvis's macrocyclic receptors for *p*-benzoquinone.

Interestingly the synthesis also yielded [2]-catenane and cyclic tetramer versions of **46** and **47**, which were later investigated[53, 54] but are not detailed herein. The *p*-

benzoquinone can potentially bind to the macrocycles by hydrogen bonding to the four amide groups and through π-π interactions from the bis-phenyl linkers (*fig.* 1.45).

Proton-NMR binding studies were conducted in $CDCl_3$ with **46** and **47** with *p*-benzoquinone which gave remarkably high (for a neutral molecule binding event) binding constants of 1200 and 1800 M^{-1} respectively.[12] A titration of **46** with *p*-benzoquinone in the competitive solvent mixture, $CDCl_3$-CD_3OD (9:1), gave an association constant of only 100 M^{-1} which suggests that the π-π interactions must be making a sizeable contribution to the binding energy.

1.5.1 Hydrogen Bonded Arrays

Hydrogen bonds are believed to be a complex conglomerate of different intermolecular interactions, one of which is electrostatics (see earlier). The highly directional hydrogen bond is the primary interaction between a hydrogen bond donor (D) and acceptor (A) but secondary, diagonal electrostatic interactions can also supplement this primary interaction to form a strengthened array.[55] This concept can be realised by considering the following triple hydrogen bond arrays:

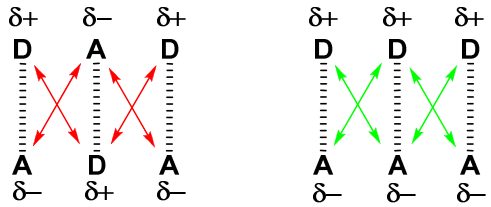

Figure 1.46 - Dimers between triple hydrogen bond arrays, showing attractive (green) and repulsive (red) electrostatic interactions between the donors (D) and acceptors (A).

In the array, like charges repel each other diagonally, weakening the binding whilst opposite charges attract, strengthening the binding. So the DDD.AAA array has only attractive electrostatic interactions, hence it forms the most strong complex.[55] This hypothesis was elegantly proven by the research group of Steve Zimmerman through his investigations of amino- and ureido-naphthyridines.[56-58]

Recently, Wilson and co-workers have investigated how to strengthen a pyridyl-urea DDA.AAD array using imidazoles.[59] Pyridyl-ureas are considered attractive DDA building blocks because of their ease of synthesis but they are susceptible to

intramolecular hydrogen bonding interactions, which means they have poor association constants due to the entropic energy barrier needed to be overcome (*fig.* 1.47).

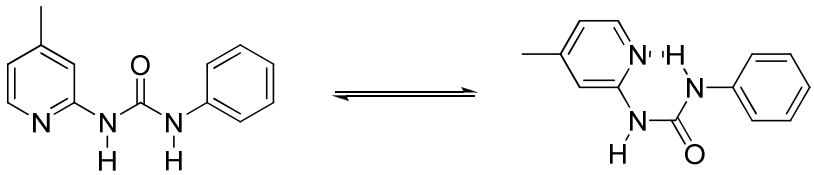

48

Figure 1.47 - The pyridyl-urea studied and how it can intramolecularly interact.

This problem was addressed by using an imidazole instead of the pyridyl- which can pre-organise itself through intramolecular hydrogen bonds. An equilibrium would still exist between two conformers but each would potentially be able to form two different DDA arrays (see *fig.* 1.48).[59]

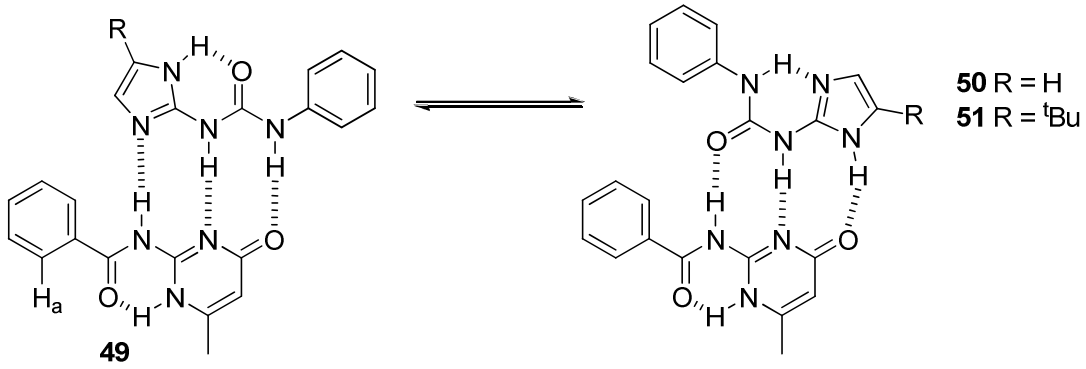

49

Figure 1.48 - Wilson and co-worker's proposed DDA.AAD arrays.

Compound **50** was initially synthesised but it was not soluble enough to study in $CDCl_3$ so the more soluble **51** was made and tested with a complimentary AAD array, amidoisocytosine (**49**). No crystals of the proposed dimers between **50/51** and **49** were obtained but crystals of the self-associating dimers of **50** and **49** were. The structure of compound **50** revealed only the NH···O conformer was formed but a ^{1}H-NMR in DMSO-d_6 showed interconversion between the two conformers (*fig.* 1.49).[59]

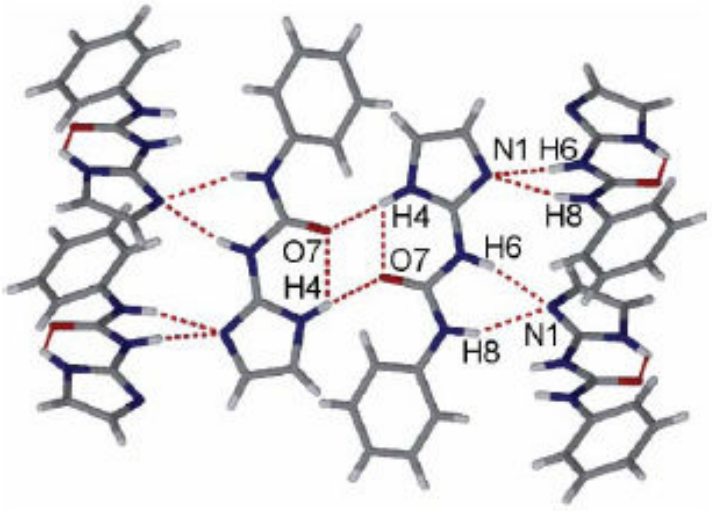

Figure 1.49 - X-ray crystal structure of the self-associating dimer of 50.[59] ***Reproduced by permission of The Royal Society of Chemistry.***

The crystal structure of **49** revealed the presence of the intramolecular binding that was predicted, with only weak intermolecular hydrogen bonds (*fig*. 1.50).

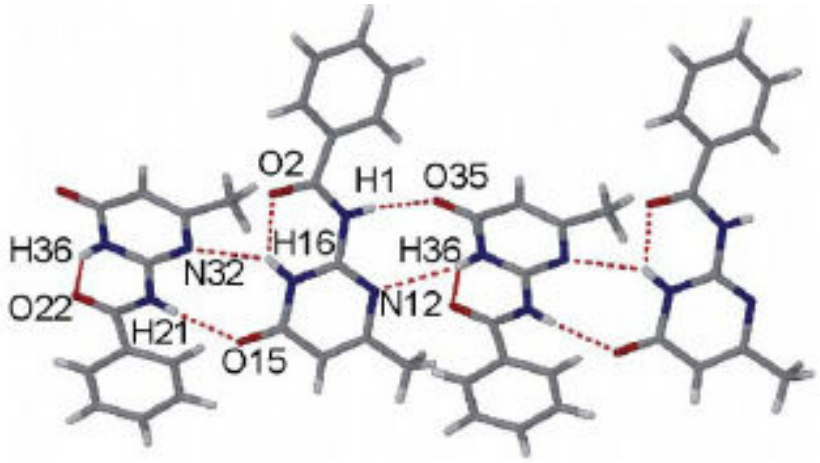

Figure 1.50 - X-ray crystal of the self-associating dimer of 49.[59] ***Reproduced by permission of The Royal Society of Chemistry.***

In solution, addition of aliquots of **49** to **51** in $CDCl_3$ produced large shifts of the H_a proton on **49** (see *fig*. 1.48 for proton labelling). Curve fitting with HypNMR[60] produced an exceptionally high binding constant of 8400 M^{-1} compared to just 84 M^{-1} with **48** and **49**; a nearly three order of magnitude difference.

Of course, increasing the number of hydrogen bond donors and acceptors can lead to even more possible arrays of increased stability. For example, quadruple

hydrogen bonded dimers have six possible arrays, two of which are self-complimentary (*fig.* 1.48).[61]

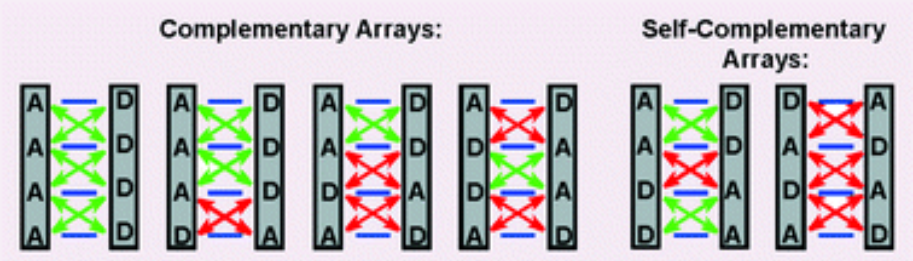

Figure 1.51 - The six possible arrays of a quadruple hydrogen bonded dimer.[61] ***Reproduced by permission of The Royal Society of Chemistry.***

Since 1988 there has been a vast amount of literature on quadruple hydrogen bonded arrays but perhaps the most prominent work was that of Meijer and co-workers.[61] This group used ureidotriazines for self-assembling 'supramolecular polymers' in alkanes, chloroform and water.[62]

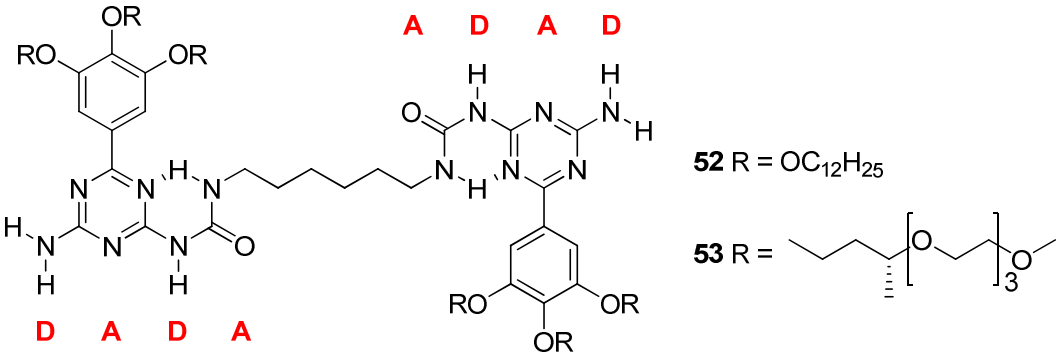

Figure 1. 52 - Meijer and coworker's supramolecular polymers.

As can be seen (*fig.* 1.52), the ureidotriazoles can form the self-complimentary DADA array (see *fig.* 1.51). The bifunctional unit **52** only forms a monomer in polar solvents such as DMSO but in $CDCl_3$ can self-assemble into random coil polymers. In dodecane, solvophobic interactions induce stacking of the dimerized ureidotriazine units to form highly ordered, helical, columnar polymers (see *fig.* 1.53).[61, 62]

Figure 1.53 - Pictorial representation of the helical polymer formed by 52 in dodecane.[61] ***Copyright Wiley-VCH Verlag GmbH & Co. KGaA. Reproduced with permission.***

The inclusion of chiral oligoethylene chains on **53** renders it water soluble and to the authors' amazement the quadruple hydrogen bond arrays still formed in this highly competitive solvent. It was thought that this was facilitated by the hydrophobic microenvironment created by the stacking of the planar trialkoxyphenyltriazine moieties in which disruption of the hydrogen bonds by water molecules is prevented.[61, 62]

1.6 Aims of This Thesis

This chapter has introduced just a few examples of previous work in each of the subject areas of this thesis. The work has predominantly shown that hydrogen bonding is the primary tool for efficient and selective anion recognition. Metal based anion receptors can potentially provide complementary electrostatic interactions for more enhanced anion affinities. This chapter has demonstrated that there are many different functional groups and subsequent hydrogen bonding motifs that can be used to bind anions. This thesis will build on previous studies with the report of novel hydrogen bonding motifs both for binding anions and neutral molecules. Because of the diversity of the topics studied this thesis has been divided into three sections:

1. The synthesis of platinum(II) based receptors and a study of their anion binding properties both in solution and the solid state.

2. The synthesis of a simple benzimidazole cleft receptor for barbiturates and ureas. This receptor will be tested against several control analogues to probe various aspects of the receptor. This section will also include a brief investigation into the design and synthesis of a neutral guest templated catenane.

3. Finally a new triazole strapped calix[4]pyrrole will be described and its solution behaviour investigated. A brief investigation into the novel use of triptycenes in anion receptor design will also be included in this section.

Chapter 2 – Metal-Organic Anion Receptors

2.1 Introduction

In 1997, Steve Loeb from the University of Windsor (Canada) reported the synthesis and study of a range of calix[4]arene based anion receptors; functionalised with amides at the 1,3-positions on the upper rim (*fig.* 2.1).[63]

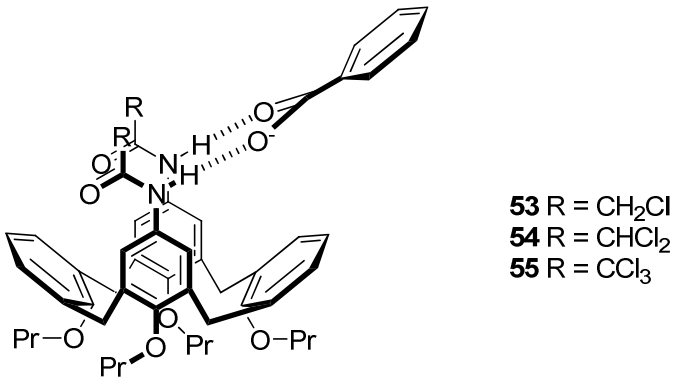

Figure 2.1 - Cameron and Loeb's calix[4]arene based anion receptor.

In $CDCl_3$, ^{1}H-NMR studies revealed receptor **54** had a selectivity for 'Y'-shaped anions such as the benzoate anion (*fig.* 2.1) which gave a binding constant (K_a) of 5160 M^{-1}. The binding is accommodated by the calix[4]arene adopting a pinched cone conformation, with the amides arranged in a complimentary fashion for 'Y'-shaped anions.

This work demonstrates how an organic scaffold can be utilised to organise hydrogen bond donors for selective anion recognition. As a progression of this concept, Gale and Loeb wanted to investigate an analogous 'inorganic' scaffold for organising hydrogen bond donors. In order to acheive the right pre-organised orientation of the hydrogen bond donor groups, a transition metal of appropriate geometry with appropriate

organic ligands was required. At the time, this concept was largely unexplored and in particular, no research had been done with platinum(II) metal-organic anion receptors. These 2+ charged metal complexes were considered ideal for the following reasons:

a) Because of platinum(II)'s d^8 electronic configuration, it adopts a 4-coordinate, square-planar geometry.

b) The complexes were considered inert to ligand substitution.

c) They are usually stable complexes in air and moisture.

d) They were considered easy to prepare in comparison to organic scaffolds such as synthetically challenging calix[4]arenes.

e) There is potential for the charge on the metal centre to supplement the hydrogen bonding to an anion with electrostatic interactions.

Initially, it was decided to focus on amide based ligands because of the results from the calix[4]arene work (see earlier), and so the easy to prepare, nicotinamide ligand was chosen, to result in a homoleptic $[PtL_4]^{2+}$ complex **56** (*fig*. 2.2).[64]

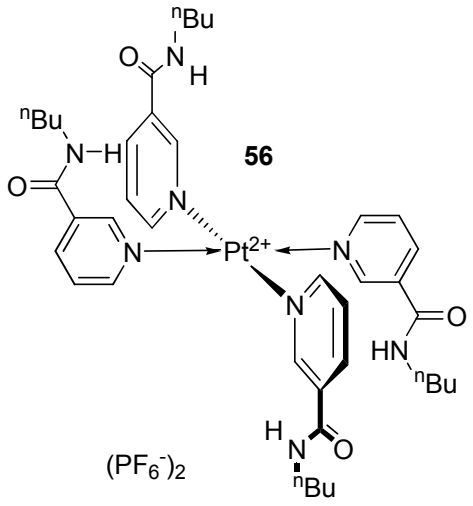

Figure 2.2 – Gale and Loeb's Pt-nicotinamide based anion receptor.

The large, charge diffuse PF_6^- ion was chosen as the counter-anion, as it was presumed it would have minimum interactions with the receptor. The ligand was synthesised from the nicotinamide ethylester and *n*-butylamine by standard methods.[64, 65] The platinum(II) complex was prepared by reacting one equivalent of $PtCl_2(EtCN)_2$ with four equivalents of ligand and two equivalents of $AgBF_4$ in MeCN solution at reflux. After

filtration to remove residual AgCl, the crude product was recrystallised from MeCN/Et_2O to give the product in 87% yield.[64]

By drawing analogy to calix[4]arene nomenclature, four different conformations were conceived for the platinum complex because of free rotation about the Pt-N bonds (see *fig.* 2.3 below).

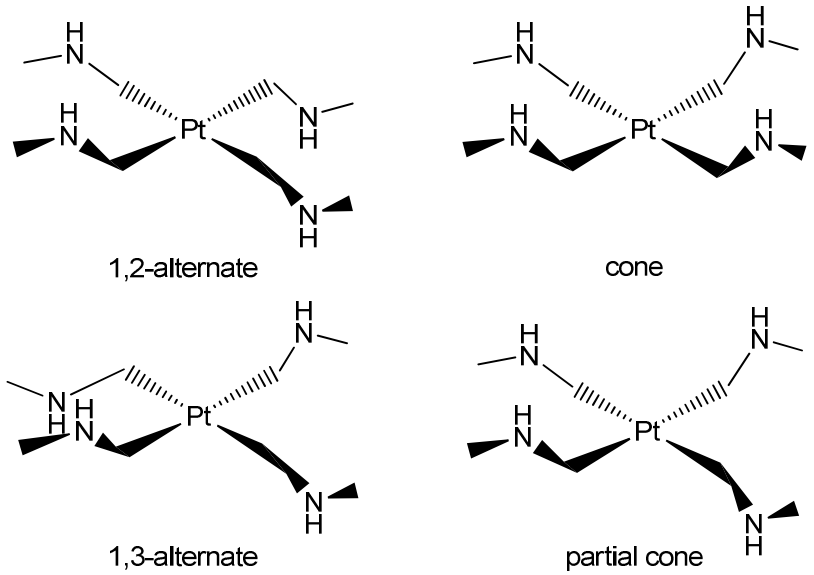

Figure 2.3 - The four different conformations that receptor 56 can adopt.

Single crystals of **56** were obtained by recrystallisation from a CH_2Cl_2/Pr^i_2O solvent mixture. These provided an X-ray structure of **56** with two molecules of CH_2Cl_2 in the structure (*fig.* 2.4). Interestingly the complex adopted the 1,2-alternate, centrosymmetric conformation, with the two CH_2Cl_2 molecules hydrogen bonding to the amide oxygens (CH···O distances 2.40-2.47 Å). The PF_6^- counter-anions sit above and below the metal centre and do not interact with the amide NH groups. This ratified the assumption that the counter-ions would not compete for binding with anions. Also, because of the 1,2-alternate conformation adopted, it was considered that the receptor would predominantly form 2:1 anion:host species in solution.[64]

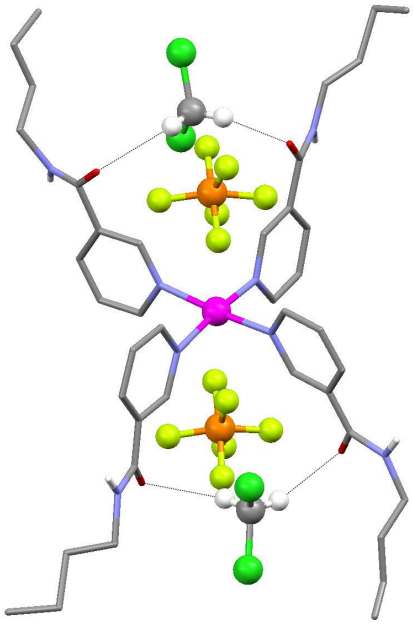

Figure 2.4 - X-ray crystal structure of 56 with CH_2Cl_2.

Solution studies in the form of ^{1}H-NMR titrations, were conducted in a variety of solvent mixtures due to solubility problems encountered and are shown in Table 2.1.

Anion	Solvent	K_a (M^{-1})
$CF_3SO_3^-$	CD_3CN	129
ReO_4^-	CD_3CN	150
NO_3^-	CD_3CN	K_1 = 562, K_2 = 132
HSO_4^-	CD_3CN/DMSO-d_6 3:1 v/v	149
$CH_3CO_2^-$	CD_3CN/DMSO-d_6 3:1 v/v	Precipitated
$H_2PO_4^-$	CD_3CN/DMSO-d_6 1:9 v/v	Precipitated
$CH_3CO_2^-$	CD_3CN/DMSO-d_6 1:9 v/v	K_1 = 230, K_2 = 491

Table 2.1 - Stability constants (K_a/M^{-1}) for receptor 56 with tetrabutylammonium salts under standard conditions.[64]

The results showed the receptor binds trigonal planar oxyanions such as carboxylate and nitrate, with the predicted 2:1 binding stoichiometry observed. Interestingly the K_2 value for acetate is greater than the K_1 value, which infers that the binding of the first anion has a positive allosteric effect which favours the binding of the second. Unfortunately, the solubility problems prevented a direct comparison of all the anions in the same solvent, so no selectivity could be deduced. The tetrahedral or pseudo-tetrahedral anions were found to be more weakly bound in a 1:1 binding stoichiometry, or

with a K_2 too small to calculate. This observation was supported by the resolution of the crystal structure of single crystals of **56** with ReO_4^- (*fig*. 2.5).[64]

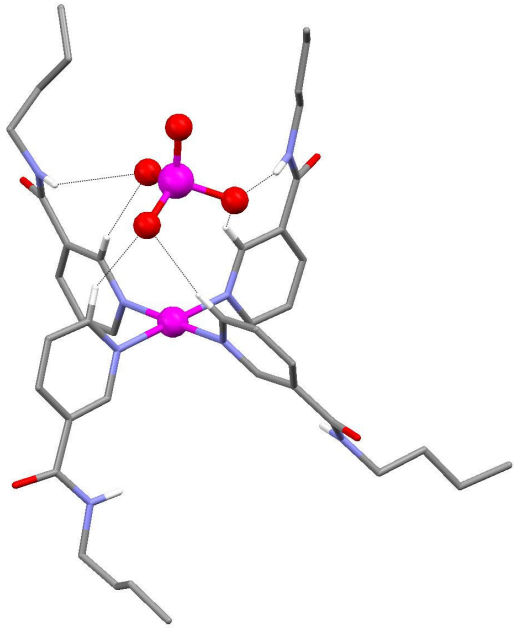

Figure 2.5 - X-ray crystal structure of 56 with ReO_4^-.

The ReO_4^- is bound by not only hydrogen bonds from the amide NH groups, but also from the CH groups on the aryl rings of the ligands. To do this, the complex distorts from centrosymmetry which it was presumed, disfavours the binding of a second anion.[64]

The platinum(II) complex, **56**, had shown promise as a receptor for trigonal planar anions in a 2:1 binding stoichiometry, with an allosteric effect observed with acetate. So the workers reasoned that designing a receptor that was preorganised in a 1,2-alternate conformation for 2:1 binding was a natural progression. This resulted in the synthesis and study of a second generation receptor; the bipy-tetraamide platinum(II) based receptor **57** (*fig*. 2.6).[66] The ligand was prepared from a literature procedure[67], whilst the complex was prepared by reaction of one equivalent of [$PtCl_2$(4,4'-*t*Bu-2,2'-bipy)] with two equivalents each, of ligand and $AgPF_6$ at reflux.

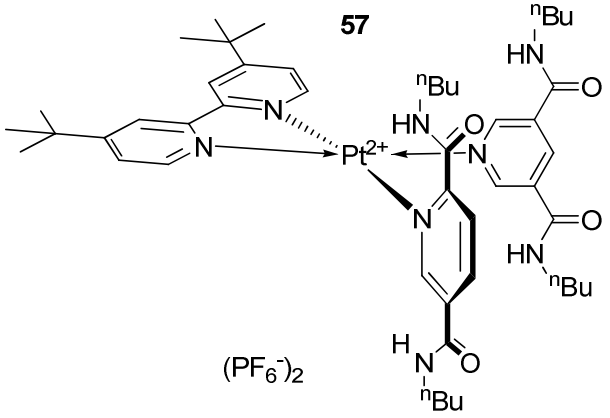

Figure 2.6 - 2nd generation platinum(II) based anion receptor 57.

Proton-NMR studies in MeCN and MeCN/DMSO mixtures showed little change in binding constants for the tetrahedral anions when compared to receptor **56** (*tbl.* 2.2).

Anion	Solvent	K_a (M^{-1})
$CF_3SO_3^-$	CD_3CN	101
ReO_4^-	CD_3CN	148
NO_3^-	CD_3CN	$K_1 = 283$, $K_2 = 2$
HSO_4^-	CD_3CN/5% DMSO-d_6	Decomposed
$CH_3CO_2^-$	CD_3CN/5% DMSO-d_6	Decomposed
$H_2PO_4^-$	CD_3CN/5% DMSO-d_6	Decomposed
$C_6H_5CO_2^-$	CD_3CN/5% DMSO-d_6	Decomposed

Table 2.2 – Association constants for receptor 57 with various anions as tetrabutylammonium salts. Values calculated using Win-EQNMR with errors estimated <10%.

This was expected though, since the conformation of receptor **56** didn't match the shape of these anions. However surprisingly, receptor **57** was less effective for nitrate in the same solvent and with the other trigonal planar anions it completely decomposed. They attributed this to the fact the complex is inherently less stable because the pyridine ligands have two electron withdrawing amide groups on them, which makes their Pt-N bonds weaker than those on receptor **56**. In fact, this theory was proved by the isolation of single crystals of the decomposition product in the titration of **57** with benzoate (see *fig.* 2.7).[66]

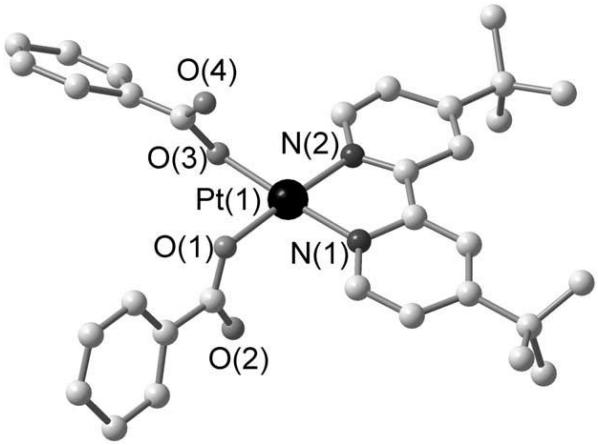

Figure 2.7 - X-ray structure of a decomposition product of the titration of 57 with benzoate.

The structure shows the amido ligands have been substituted with benzoate anions to form a neutral complex. This clearly demonstrates that some platinum(II) complexes are not completely inert to ligand substitution by certain anions.

The lower values for the binding of the nitrate anion to receptor **57** were also rationalised by a crystal structure (*fig.* 2.8). The structure of **57** with nitrate shows how the binding of the anion to the bottom cavity pinches the amide groups inwards to form two hydrogen bonds to it. This effectively pulls the top amides apart, which destroys the second binding site and so the top nitrate only has one hydrogen bond to it. This means that the two binding sites are not independent of each other and so it can be concluded that the more flexible ligands on **56** are far more effective for accommodating anions.[66]

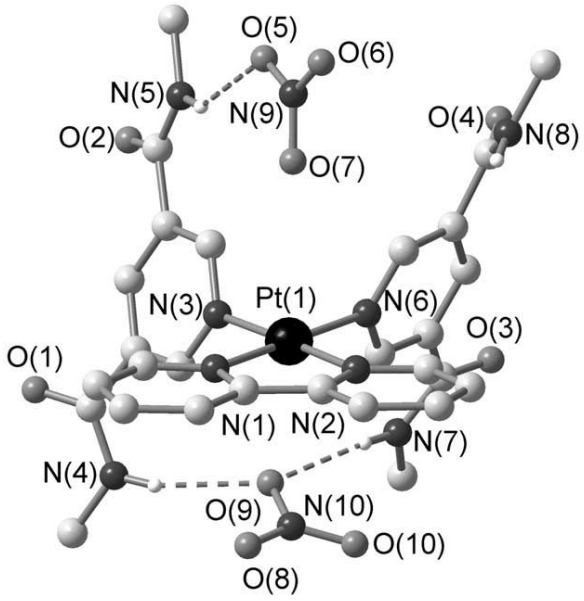

Figure 2.8 – X-ray crystal structure of 57 with nitrate, omitting the *t*-butyl groups for clarity.[66]

Clearly the design of a third generation receptor had to take heed of the problems encountered with receptor **57**; *viz.*, a less labile ligand, with free rotation about the coordinating bond and a stronger hydrogen bond donor group was required. To these ends, receptor **58** was designed and synthesised,[68] which included the following improvements:

1. Urea groups for more enhanced anion binding.
2. More rigidity and pre-organisation of the hydrogen-bond donor groups by the isoquinoline framework.

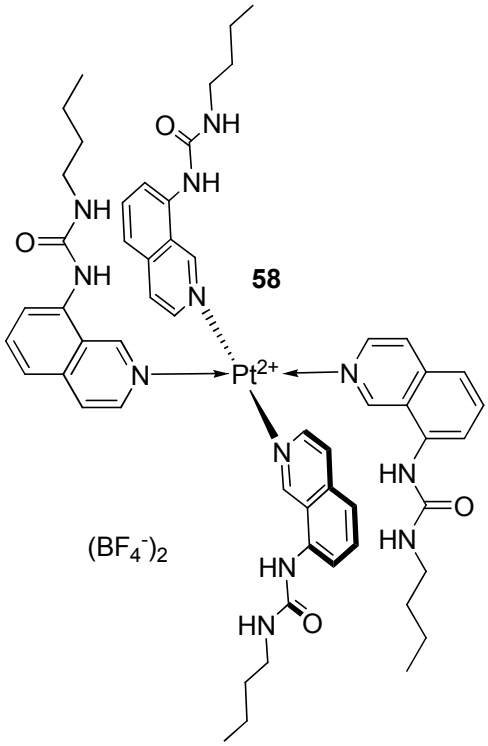

Figure 2.9 – Third generation platinum(II) based anion receptor 58.

The ligand was prepared from the corresponding aminoisoquinoline and *n*-butylisocyanate in 91% yield. The receptor was prepared as a tetrafluoroborate salt by refluxing $PtCl_2(EtCN)_2$ with two equivalents of $AgBF_4$ and four equivalents of the ligand in acetonitrile for 24hrs. After filtration of residual AgCl and further workup, the product was isolated as a yellow powder in 60% yield.[68]

Once again, in solution or solid state, the receptor could potentially adopt any of the four conformations discussed for receptor **56**. The limited solubility of **58** meant the solution studies could only be done in the polar, competitive donor solvent, DMSO-d_6. In

this solvent there were negligible interactions with the weakly coordinating anions, ReO_4^-, $CF_3SO_3^-$ and NO_3^-. Nevertheless, ^{1}H-NMR titrations with other anions in this solvent showed promising results and these are shown in Table 2.3. The halides all bound in a 2:1 anion-receptor stoichiometry, potentially in the 1,2- or 1,3-alternate conformation. The K_2 values are lower than the K_1 values, indicating that there could be a reduction in electrostatic interactions upon the first anion binding; this is known as a negative cooperative effect. However, more likely, is that the lower K_2 value is due to a non-cooperative or statistical effect. That is, the binding of the first equivalent of anion limits the number of binding sites available for the binding of a second equivalent of anion. This would statistically lower the probability of binding a second equivalent of anion which would make K_2 lower than K_1.

Anion	**K_a (M^{-1})**
Cl^-	K_1 = 11700
	K_2 = 2220
Br^-	K_1 = 1360
	K_2 = 450
I^-	K_1 = 1430
	K_2 = 52
SO_4^{2-}	$> 10^{4*}$
$H_2PO_4^-$	$> 10^{4‡}$

Table 2.3 – Stability constants (K_a/M^{-1}) for receptor 58 with tetrabutylammonium anion salts (unless stated otherwise) in DMSO-*d_6* at 300 K. * SO_4^- added as K_2SO_4 with the effects of ion pairing ignored. ‡ Estimated value – saturation is seen on addition of 1 equiv. of anion.[68]

The binding constants for SO_4^{2-} and $H_2PO_4^-$ were very high, which is remarkable considering how competitive the solvent is. The value for $H_2PO_4^-$ is estimated since NMR methods[69] cannot accurately calculate binding constants above 10^4 M^{-1}. The interaction with sulfate was slow on the NMR timescale. This results in a broad spectrum at sub-stoichiometric amounts of anion addition and peaks representing both the complexed and uncomplexed receptor. At equimolar amounts of receptor and anion the complexed peaks become sharp, the uncomplexed peaks disappear and no further change in chemical shift is observed.

Determination of the X-ray crystal structure of the chloride complex of receptor **58**, revealed adoption of a 2:1 anion-receptor stoichiometry in a 1,2-alternate conformation. The anions are each bound slightly off-set from the central axis, through four urea NH···Cl^- (in the range N···Cl 3.33-3.40 Å) and two aromatic CH···Cl^- (in the range C···Cl

3.50-3.53 Å) hydrogen bonds. Interestingly, the aromatic CH interactions were also observed in the solution studies with particularly large shifts with chloride (1.44 ppm). The X-ray structure of the sulfate complex of **58**, showed the binding of the anion in a 1:1 cone conformation with a full complement of eight urea NH···SO_4^- (in the range N···O 2.89-3.23 Å) and four CH···SO_4^- (in the range C···O 3.03-3.36 Å) hydrogen bonds. The anion sits tightly in the cavity, shielded from interactions with surrounding solvent and with possible strong electrostatic contributions from the complimentarily charged 2+ metal centre.[68]

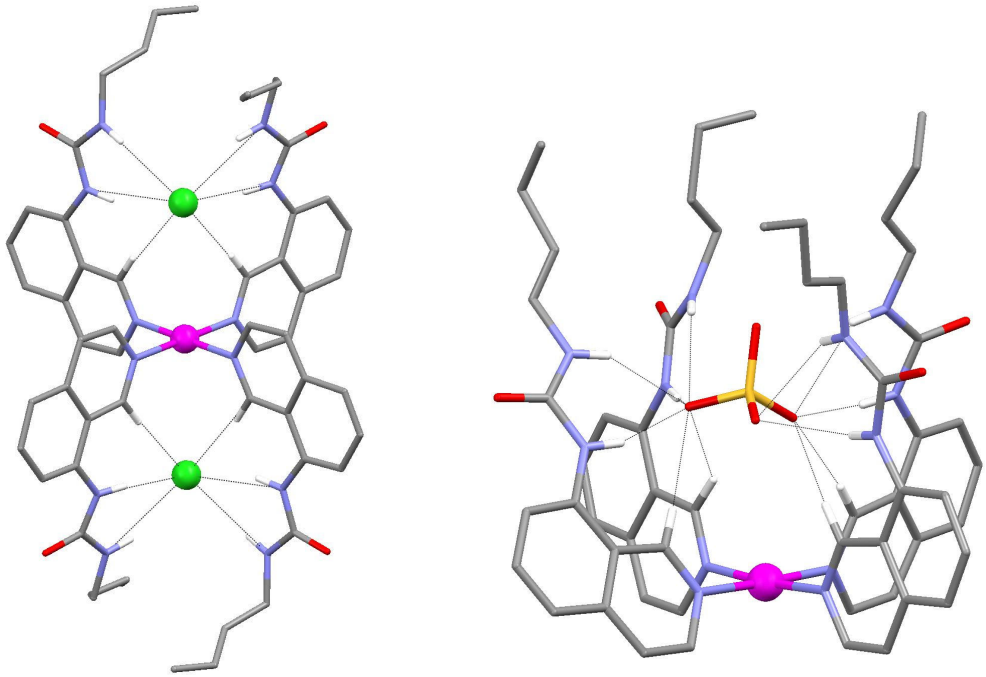

Figure 2.10 – X-Ray crystal structure of receptor 58 with chloride (left) and sulfate (right), omitting non-coordinating hydrogens for clarity.

These structures go a significant way towards explaining what is happening in solution, especially the high stability of the sulfate complex and slow complexation-decomplexation kinetics relative to the NMR timescale.[68]

2.2 A Platinum(II) Tetra(urea-pyridine) Complex: Investigating Pre-organisation and Ligand Rigidity

As part of our collaboration with the Loeb group, we wished to further explore the designs and behaviour of the platinum(II) based anion receptors just discussed. Initially it was decided to investigate how fundamental it was to have an isoquinoline based ligand, for both pre-organising the hydrogen bond donor groups and rigidifying the ligand structure. To this end, receptor **59** was designed, with methyl-pyridine ligands replacing the isoquinolines of receptor **58** (*fig.* 2.11).

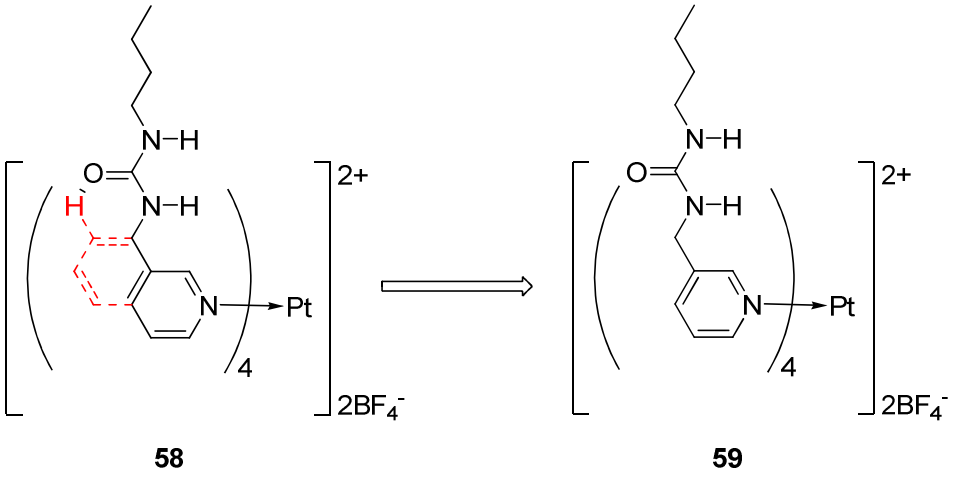

Figure 2.11 - The design principle of receptor 59.

Receptor **59** lacks the rigid backbone provided by the second aromatic ring (red lines in *fig.* 2.11) of the isoquinoline on **58**. In addition to this, **59** lacks the pre-organisation of the urea group by the intramolecular hydrogen bonding of the isoquinoline ring. It was hoped further insights into the behaviour of homoleptic Pt-L_4 complexes could be gained by the study of this system.

2.2.1 Synthesis

The synthesis of the methyl-pyridine ligand for receptor **59,** was achieved by reaction of 3-aminomethylpyridine with *n*-butylisocyanate in dry DCM for 5 days at room temperature, to afford the product as a fine white powder in 89% yield (*sch.* 2.1).

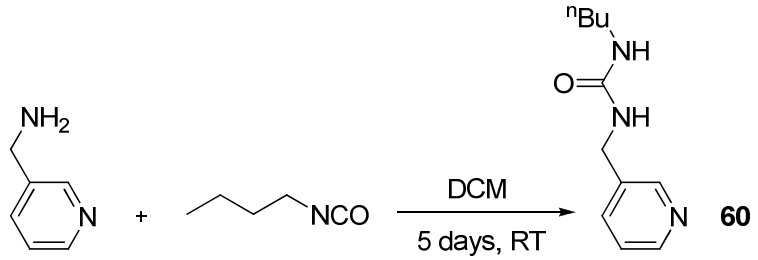

Scheme 2.1 – Synthesis of methyl-pyridine ligand 60, for the preparation of receptor 59.

The platinum starting material, *cis*-$[PtCl_2(EtCN)_2]$, needed for the preparation of the receptor, was made according to a literature procedure.[70] This involved allowing propionitrile to diffuse into a concentrated aqueous solution of K_2PtCl_4 over period of 3 days to crystallise the product as large yellow crystals.

The receptor was prepared by refluxing four equivalents of the ligand with one equivalent of *cis*-$[PtCl_2(EtCN)_2]$ and 2.2 equivalents of $AgBF_4$ in darkness for 24 hours (*sch.* 2.2). After cooling and filtration of residual AgCl, the crude product was recovered by precipitation of the MeCN solution by addition of Et_2O. This was further purified by recrystallisation via a slow evaporation of a $MeNO_2$ solution of the crude receptor, to leave the product as grey crystals in 35% yield.

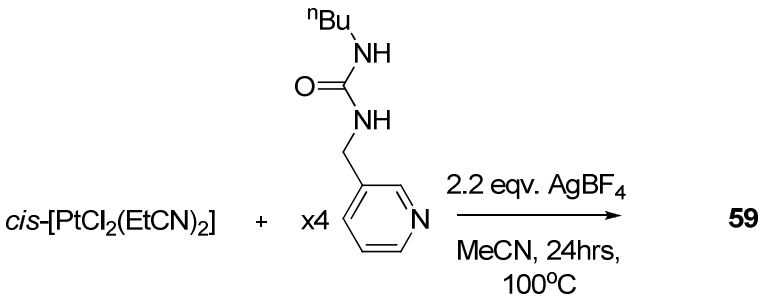

Scheme 2.2 – Synthesis of receptor 59.

2.2.2 Solution Studies

Stability constants for receptor **59** were obtained by ^{1}H-NMR titration experiments in DMSO-d_6 at 300 K, using the anions tested with **58**[68] as their tetrabutylammonium salts. Changes in the chemical shift of one of the binding proton resonances, upon addition of increasing aliquots of anion solution, were recorded and the data fitted to a 1:1 or 2:1 binding model with Win-EQNMR.[69] The results were compared with those from the studies with **58** and are shown in Table 2.4.

	Receptor	
Anion	**58**[a]	**59**
Cl^-	$K_1 = 11700$	Decomposed
	$K_2 = 2220$	
Br^-	$K_1 = 1360$	$K_1 = 137$
	$K_2 = 450$	$K_2 = 14$
I^-	$K_1 = 1430$	$K_a < 10$
	$K_2 = 52$	
SO_4^{2-}	$K_a > 10^4$	No data
$H_2PO_4^-$	$K_a > 10^4$	$K_1 = 10059$
		$K_2 = 62$
$CH_3CO_2^-$	No data	$K_1 > 10^4$
		$K_2 = 54$
$CF_3CO_2^-$	$K_a < 10$	$K_a < 10$
NO_3^-	$K_a < 10$	$K_a < 10$
ReO_4^-	$K_a < 10$	$K_a < 10$
HSO_4^-	No data	$K_a < 10$

Table 2.4 – Stability constants (K_a/M^{-1}) for receptors 58 and 59 with tetrabutylammonium anion salts in DMSO-d_6 at 300 K. All data fitted with Win-EQNMR and errors estimated ≤10%. [a]Data from reference 68.

The results show that **59** forms much less stable complexes with anions than **58**. The receptor completely decomposed after addition of one equivalent of TBA chloride, which is thought to be the result of chloride displacement of the ligands. Bromide showed only weak 2:1 coordination to the receptor, in stark contrast to the strong binding observed with **58**. The results for **58** with sulfate were obtained by step-wise addition of solid K_2SO_4 to the receptor solution, followed by sonication and observation of the proton resonances, which showed a slow interaction relative to the NMR timescale. A binding constant could not be obtained with **59** using this method since the peaks became too broad and untraceable.

The binding constant was still high with $H_2PO_4^-$ and interestingly it bound in a 2:1 conformation. Although not tested with **58**, the acetate anion was titrated with **59** and showed a particularly high 2:1 binding.

These results clearly show how vital it is to have the rigidifying and pre-organising components of the isoquinoline version. Without these factors, the entropy of the system is increased, which leads to weaker anion complexes with lower stability constants. The isoquinoline ligand has also been shown to be less susceptible to ligand substitution

compared to this methyl-pyridine analogue, which is also an important observation to consider in the designs of these systems.

2.2.3 Solid State Analysis

X-ray quality crystals of the hydrogen sulfate complex of **59** were obtained by slow evaporation of a $MeNO_2$ solution of **59** in the presence of excess $TBA^+HSO_4^-$ (*fig.* 2.12).

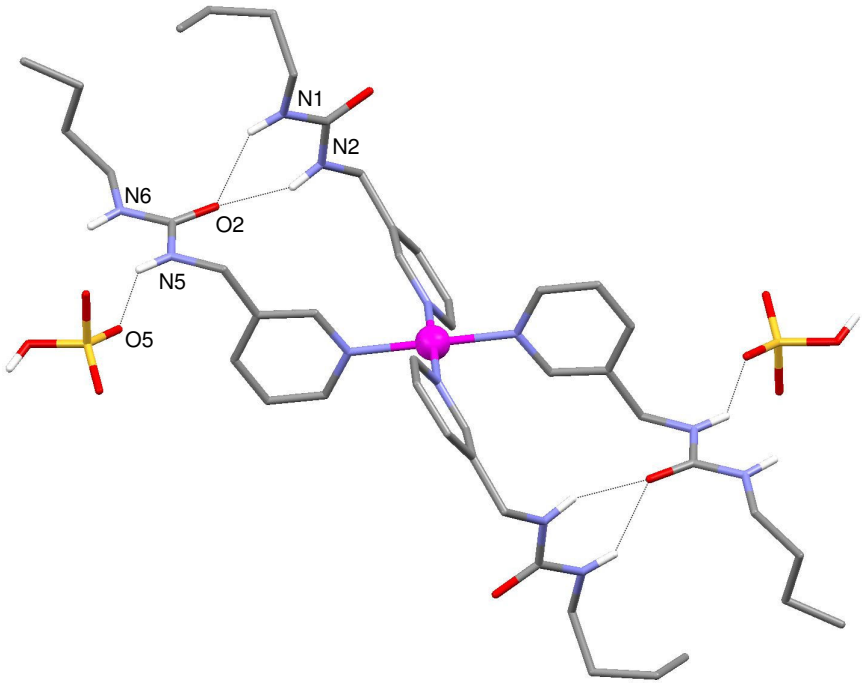

Figure 2.12 – X-ray crystal structure of the HSO_4^- complex of receptor 59. Non-acidic protons have been omitted for clarity.

The structure shows the flexible nature of the pendant arms of the pyridine ligands, have allowed them twist and intramolecularly hydrogen bond to their neighbouring ligands (N2···O2 2.893(12) Å, N1···O2 2.873(14) Å). The HSO_4^- anions are only coordinated via one hydrogen bond to one of the urea NH groups (N5···O5 2.849(11) Å). A clearer idea of what is happening can be gained by looking at the hydrogen bonded ladder of **59** (*fig.* 2.13). This shows that the urea groups are also intermolecularly hydrogen bonding to urea groups on neighbouring complexes, to form a hydrogen bonded network interlaced with HSO_4^- anions (intermolecular N···O 2.798(14) & 3.272(12) Å).

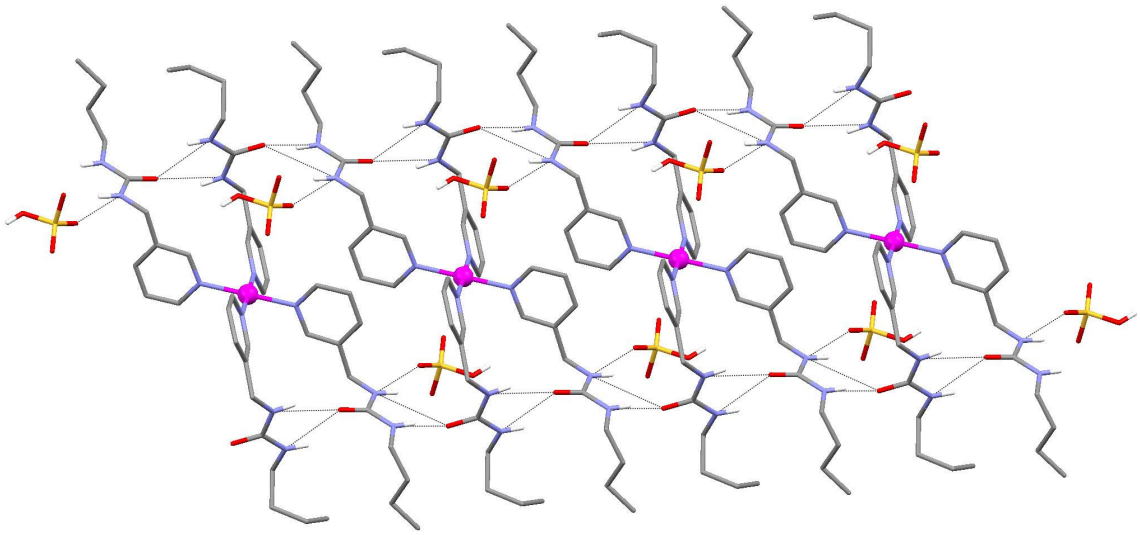

Figure 2.13 - Hydrogen bonded ladder of 59 running down the b axis.

Looking at the top view of the ladder (*fig.* 2.14), the hydrogen sulfate anions can be seen off-set from the ideal axial position that is running through the platinum metal centre.

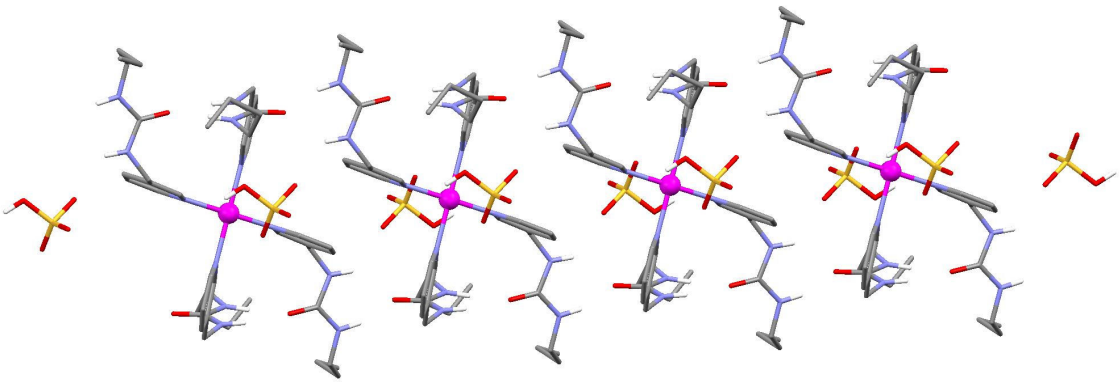

Figure 2.14 – Top view of the hydrogen bonded ladder.

The high degree of twisting of the ligands in the solid state can certainly support the theory that the ligands are too flexible with little pre-organisation in solution, which leads to greater disorder in the system and hence poor anion complexation.

2.3 Changing The Hydrogen Bond Donor Group: Platinum(II) Based Receptors with Pyrrole Functionalised Ligands

The next progression was to investigate changing the hydrogen bond donor group from the urea or amide systems previously investigated. From extensive research over the last decade, both within our group and others, the pyrrole motif has emerged as a highly important tool for binding anions.[23] We therefore wished to investigate the inclusion of this functionality in the platinum(II) based receptors. This resulted in the design of receptor **60** and the control analogue **61** (*fig.* 2.15).

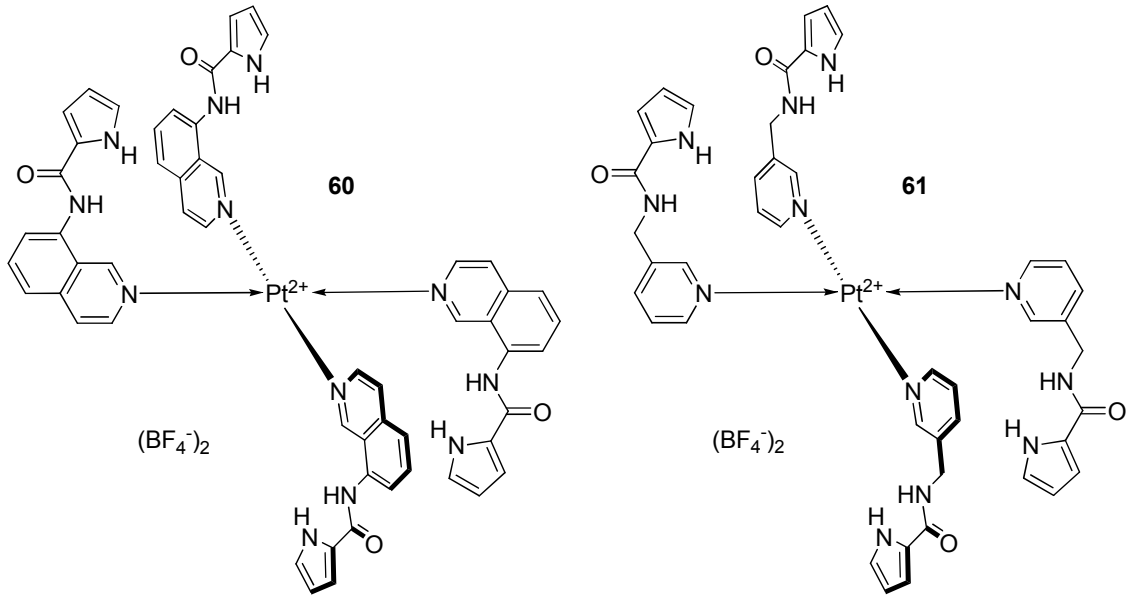

Figure 2.15 – Design of receptors 60 and 61.

Because of the nature of the pyrrole carboxamide group, the pyrrole NH converges with the amide NH, which could hopefully form a more encapsulated cavity for binding spherical anions such as chloride.

2.3.1 Synthesis

The ligand for **60** was synthesised from the corresponding 8-aminoisoquinoline (used in the synthesis of **58**) and the pyrrole acid chloride. The 8-aminoisoquinoline (**64**) was prepared from 5-aminoisoquinoline by literature procedures as shown in Scheme 2.3.[71, 72]

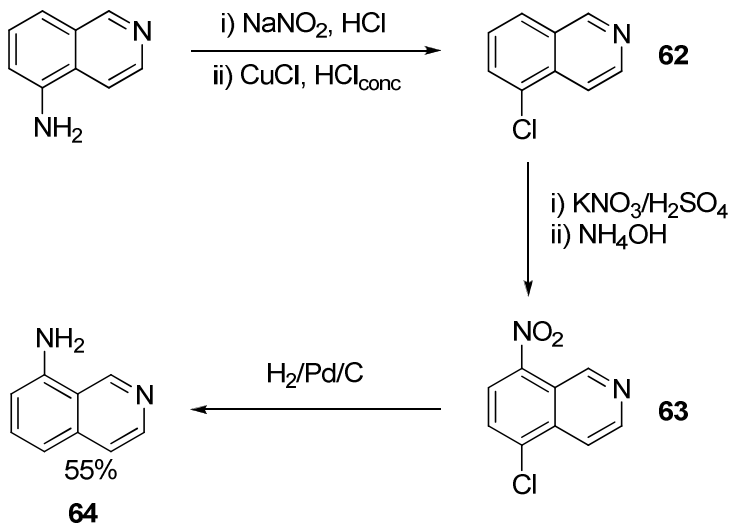

Scheme 2.3 – Synthesis of 8-aminoisoquinoline 64.

The next step involved the generation of the unstable pyrrole acid chloride, by activation of pyrrole-2-carboxylic acid with thionyl chloride. This was then coupled to **64** in the presence of triethylamine (TEA) and a catalytic amount of dimethylaminopyridine (DMAP) to give **65** in 41% yield (*sch.* 2.4).

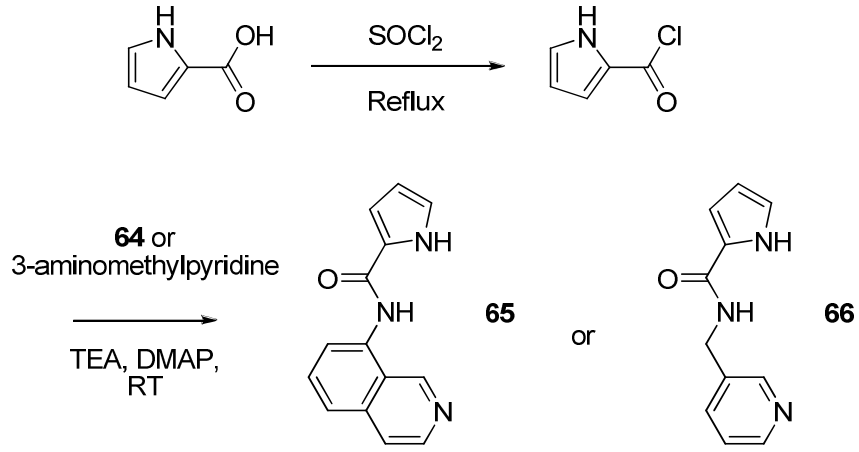

Scheme 2.4 – Synthesis of ligands 65 and 66.

The ligand for **61** was generated using the same method as for **65**, except using the commercially available 3-aminomethylpyridine and was made in 25% yield.

The synthesis of **60** and **61** was unsuccessful using the one-pot method (*sch.* 2.2) used for the preparation of receptor **59**. So an improved two-step method was developed which involved generation of a reactive intermediate (*sch.* 2.5).

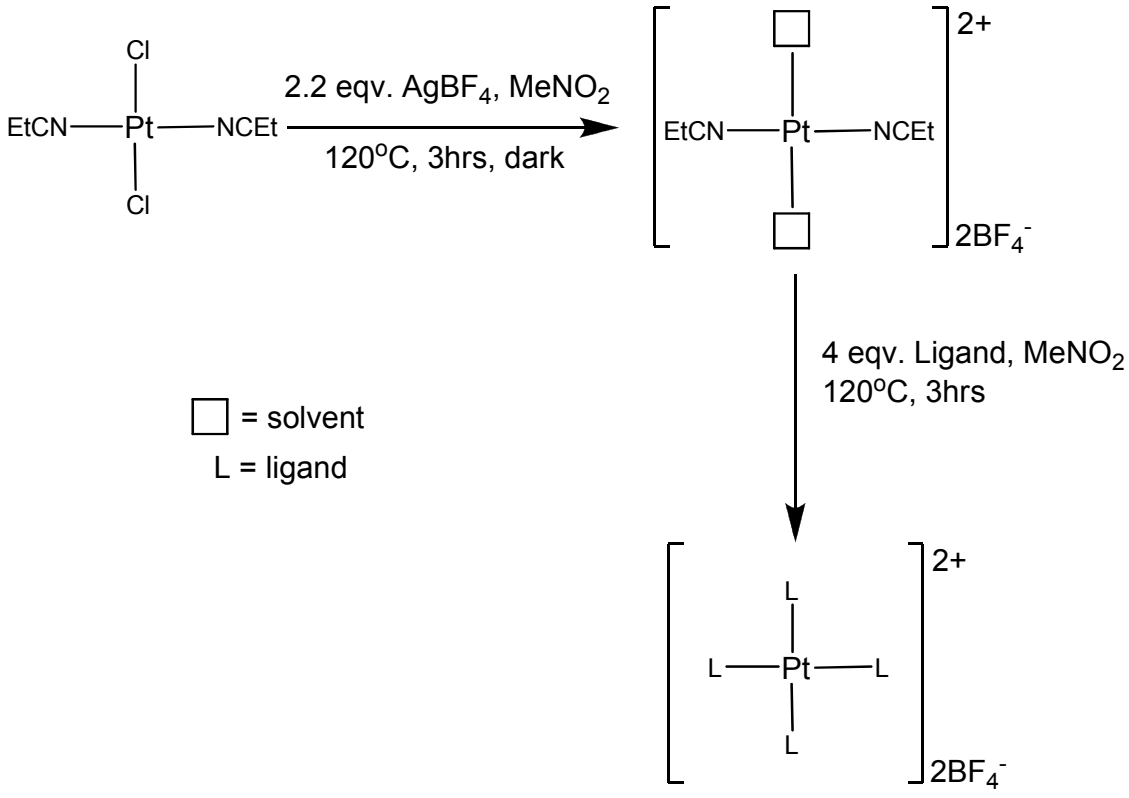

Scheme 2.5 – Two-step synthesis of homoleptic $[PtL_4]2BF_4$ complexes.

This method involves refluxing the starting material with $AgBF_4$ in the absence of ligand, followed by removal of the AgCl generated, before addition of the ligand and further refluxing. This synthetic route proved far more successful, generating receptor **59** and **60** in 61% and 48% yields respectively.

2.3.2 Solution Studies

Proton-NMR titration experiments were conducted on receptors **60** and **61** with a variety of different anions as their TBA salts in DMSO-d_6 solution at 300 K. The resulting data was fitted to either a 1:1 or 2:1 binding model using Win-EQNMR[69] and the results are presented in Table 2.5 below.

	Receptor	
Anion	**60**	**61**
Cl^-	$K_1 = 6840^a$	Decomposed
	$K_2 = 60^a$	
Br^-	$K_a < 10$	$K_a < 10$
I^-	$K_a < 10$	$K_a < 10$
HSO_4^-	$K_a < 10$	$K_a < 10$
NO_3^-	$K_a < 10$	$K_a < 10$
$H_2PO_4^-$	$K_1 = 1920$	Poor fitting
	$K_2 = 30$	
$C_6H_5CO_2^-$	$K_1 = 15200$	$K_1 = 7800$
	$K_2 = 39$	$K_2 = 41$
$CH_3CO_2^-$	$K_1 = 1662^b$	$K_1 = 181^b$
	$K_2 = 197^b$	$K_2 = 46^b$

Table 2.5 – Stability constants for receptors 60 and 61 in DMSO-d_6 with anions as their TBA salts at 300 K. Data was fitted using the pyrrole NH unless otherwise stated. All errors estimated ≤ 10%. [a]Decomposition occurred after addition of 1.5 eqv. of anion in this case. [b]Data fitted to chemical shift of pyridine or isoquinoline CH at 2-position due to broadening of pyrrole NH resonance.

Surprisingly, **60** and **61** were ineffective for binding halides, even decomposing in the presence of chloride in both cases. Receptor **60** showed interaction with the tetrahedral $H_2PO_4^-$ anion but, despite repeated attempts, a good set of data could not be collected for **61** with this anion.

Nevertheless, the receptors showed a good selectivity and stability with the carboxylate anions, binding in a 2:1 anion-receptor binding stoichiometry. In the case of acetate, the pyrrole NH resonances on both receptors moved considerably downfield upon first addition of anion, with the peaks quickly becoming too broad to fit data with. This indicates a particularly strong binding interaction.

2.4 Investigating The Sulfate Binding and CH Interactions: *Trans*-functionalised Platinum(II) Complexes

2.4.1 Introduction

Receptor **58** had proved to be particularly effective for binding sulfate, both in solution and the solid state, with the receptor adopting the desired cone shape. Recently, there has been an intense interest in the recognition of sulfate,[25, 26, 73-77] not least because of the importance of this anion in biological systems. For example, the sulfate binding protein (*fig.* 2.16) found in *Salmonella typhimurium*, binds sulfate through just seven hydrogen bonds with very high selectivity (binding constant $K_a \approx 10^6$ M^{-1} in water).[78, 79]

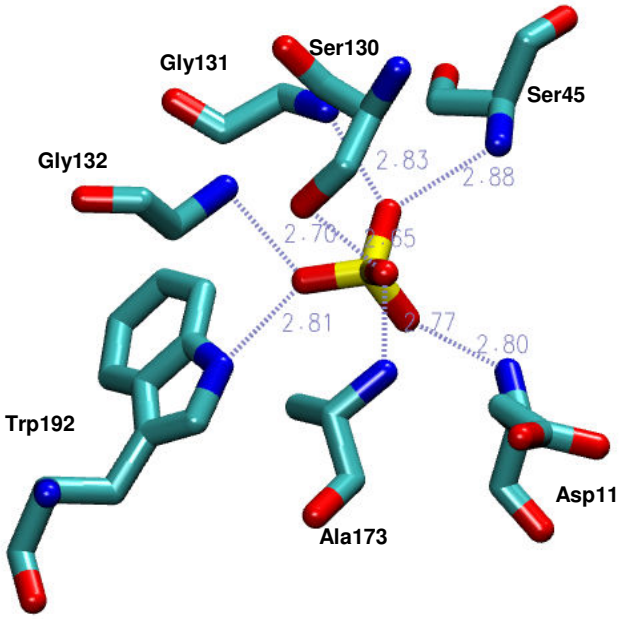

Figure 2.16 – Active site of the sulfate binding protein of *Salmonella typhimurium* showing the encapsulation of the anion by seven residues.[78]

What is remarkable about the binding, is that the 2^- charged sulfate is deeply buried and completely inaccessible to solvent and appears to have no surrounding (*i.e.* within Van der Waals distance) neutralising or stabilising positive charge.[78] Following this crystallographic report, researchers have sought to design selective receptors for oxo-anions such as sulfate that mimic natural hosts.[80] Compounds which can bind sulfate are also of interest because of their applications in sulfate extraction processes, such as its removal from nuclear waste.[81]

Progress to towards synthetic sulfate recognition hosts, includes the tren-based tris-urea receptor, highlighted earlier (see *Chapter* 1), which can coordinate sulfate through twelve hydrogen bonds. Receptor **58** can also coordinate sulfate through twelve hydrogen bonds (8 NH and 4 CH), which is postulated to be[82] the maximum coordination preference for sulfate by urea based receptors.

A key point about the sulfate complex of **58** is that four of the twelve hydrogen bonds to the anion are CH···O interactions. There were also CH···anion interactions observed between the halides and **58**, both in solution and the solid state. These observations motivated previous members of our group to investigate the role these CH···anion hydrogen bonds play in stabilising anion complexes in solution, by studying a test series of platinum (II) based receptors (*fig.* 2.17).[83]

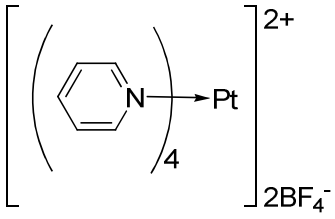

67

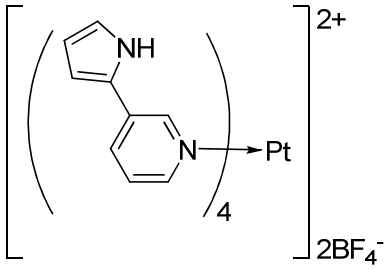

68

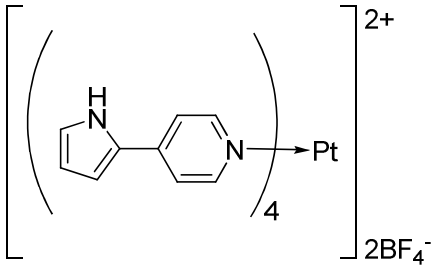

69

Figure 2.17 – The platinum(II) receptors used in the CH *vs.* NH hydrogen bond study.[83]

As can be seen, one of the receptors offers only CH hydrogen bond donors (**67**), whilst the others (**68** and **69**), offer a choice of hydrogen bond donor (NH or CH) as the pyrrole is free to rotate about the pyridine-pyrrole bond.[83]

The anion binding properties of these complexes were explored using ^{1}H-NMR techniques in DMSO-d_6 and the results are shown in Table 2.6.

	Receptor		
Anion	**67**	**68**	**69**
Cl^-	195	960	216
Br^-	121	796	211
I^-	50	462	113
HSO_4^-	< 10	837	< 10
NO_3^-	-	29	< 10
$CH_3CO_2^-$	84	K_1= 216‡	117‡
	-	K_2 = 2400‡	-
$C_6H_5CO_2^-$	132	Precipitated	111‡
$MeSO_3^-$	45	1115	< 10

Table 2.6 – Stability constants for receptors 67 – 69 with anionic guests as TBA salts in DMSO-d_6 at 298 K. Data fitted to a 1:1 binding model using the shift of the CH at the α-position on the pyridine ring unless otherwise stated. ‡Fitted using the pyrrole NH proton shift.[83]

Despite **67** not having any NH hydrogen bond donor groups there were significant shifts downfield of the α-proton on the pyridine ring and a set of stability constants could be calculated. The interaction was strongest with chloride and the receptor bound 1:1 in all cases.[83]

Receptor **69** does not contain any convergent binding site that would utilise all four pyrrole NH groups. The lower stability constants reflect this, with only the α-proton on the pyridine moving downfield during the titrations. The only exception was with the carboxylate anions which shifted the pyrrole NH resonance 0.61 and 0.85 ppm for benzoate and acetate respectively.[83]

However, the most interesting behaviour was observed with **68**, whereby the pyrrole NH proton did not significantly shift as expected, upon addition of Cl^-, Br^-, I^-, HSO_4^-, $MeSO_3^-$ or NO_3^-. Only with the most basic anions (benzoate and acetate), did the NH resonance shift downfield by 1.03 and 1.36 ppm respectively. Conversely, the resonance of the CH at the 3-position on the pyrrole ring moved downfield with the former anions but not with the latter anions. By changing the solvent to $MeNO_3$-d_3, more typical behaviour was observed with **68** upon the addition of anions. For example upon addition of TBA methanesulfonate, the pyrrole NH resonance moved downfield by up to 1.77 ppm. This led to the conclusion that a solvent competition mechanism (see *fig.* 2.18) may have been operating in the DMSO solution. In the good hydrogen bond acceptor solvent, DMSO, less basic anions such as $MeSO_3^-$ will bind to the less acidic CH, with the more acidic NH binding the DMSO. Whereas in the poor hydrogen bond acceptor solvent,

$MeNO_2$, the $MeSO_3^-$ will bind to the more acidic NH with the less acidic CH interacting with the solvent. However, if the anion is more basic, such as a carboxylate, then it will bind the more acidic NH even in DMSO solution.[83]

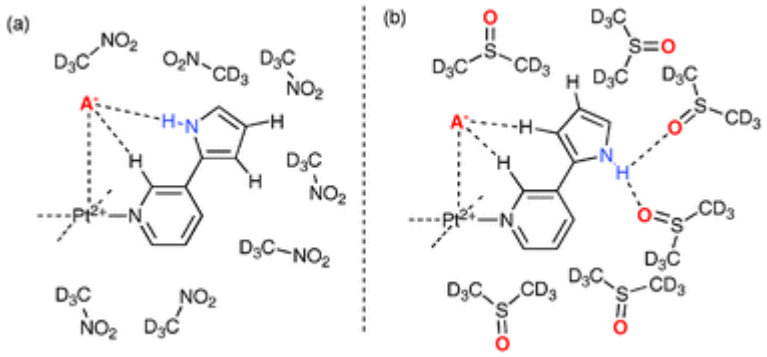

Figure 2.18 – Binding modes of one equivalent of $MeSO_3^-$ (A^-) to 68 in (a) nitromethane-d_3 and (b) DMSO-d_6 solution.[83] ***Reproduced by permission of The Royal Society of Chemistry.***

Crystals of the $MeSO_3^-$ salt of **68** were grown by slow evaporation of a nitromethane solution of the complex (*fig.* 2.19). The comlex adopted a 1,2-alternate conformation with the anion binding through the pyrrole NH groups and the protons at the α-positions on the pyridine rings (N···O 2.926(8) & 2.850(8) Å and C···O 3.542(7) & 3.100(6) Å).

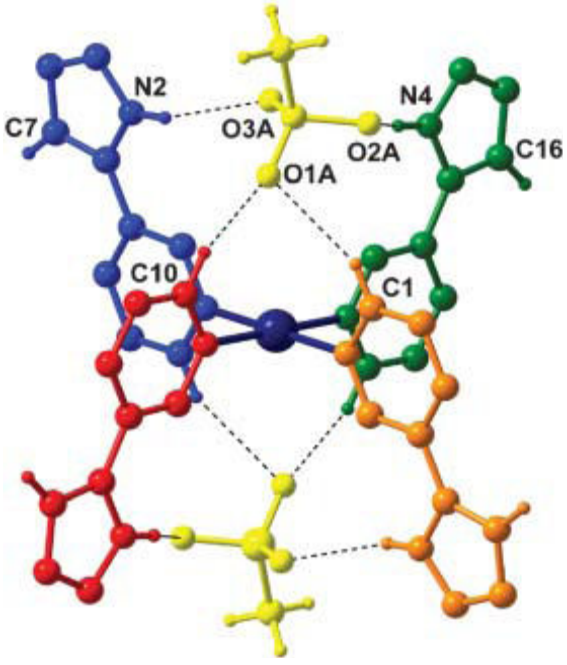

Figure 2.19 – X-ray crystal structure of the $MeSO_3^-$ salt of 68. ***Reproduced by permission of The Royal Society of Chemistry.***

This crystal structure serves to prove that the binding observed in the solid state does not always reflect what may happen in solution as there is no evidence of the pyrrole NH groups interacting with this anion in DMSO solution.[83]

Since the publication of this work there have been extensive computational molecular modelling investigations into CH···anion interactions by Hay and Bryantsev.[84, 85] This theoretical work involved studying various arene systems (even as simple as benzene) and their interaction with various anions.

As a continuum of this body of work, we thought it interesting to investigate the role of CH···anion binding in stabilising the anion complexes of receptor **58**. In particular, we also wished to further explore the binding conformation of sulfate to this class of receptor. To these ends, a *trans*-functionalised, heteroleptic version of the homoleptic receptor **58** was prepared (receptor **70**, *fig.* 2.20).

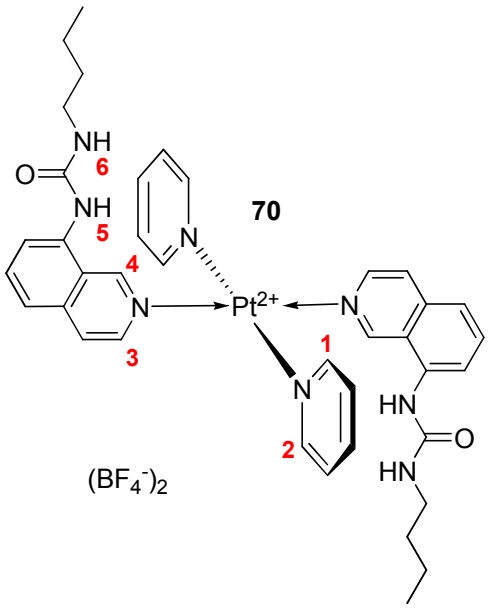

Figure 2.20 – The *trans*-functionalised receptor used for this study.

2.4.2 Synthesis

The ureido-isoquinoline ligand required for the synthesis was prepared from 8-aminoisoquinoline[71, 72] and *n*-butylisocyanate in 58% yield (*sch*. 2.6).[68]

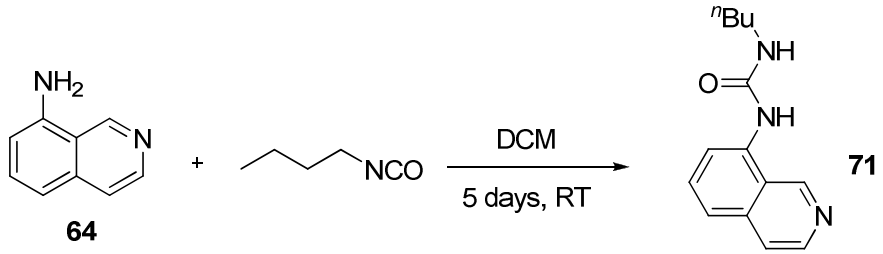

Scheme 2.6 – Synthesis of ligand 71.[68]

The receptor was prepared using a similar two-step method to that of **60** and **61**, except using *trans*-dichlorobis(pyridine)platinum(II)[86] as the starting material (see *sch*. 2.7).

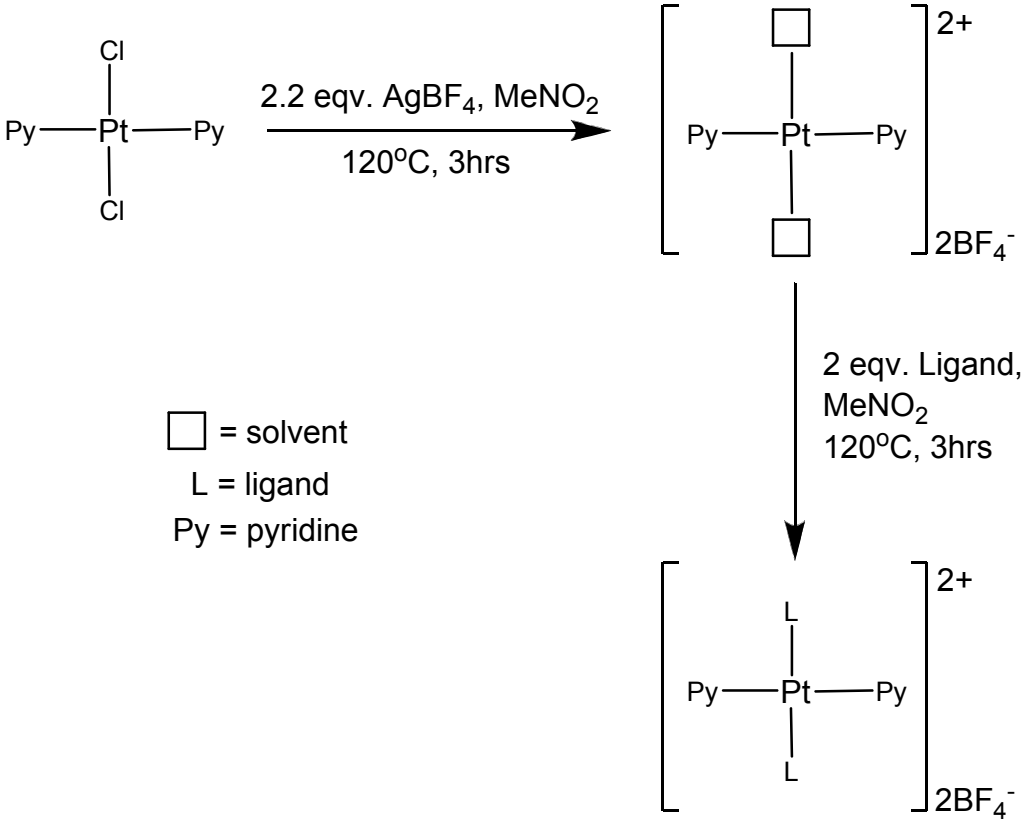

Scheme 2.7 – Synthesis of heteroleptic *trans*-$[Pt(Py)_2L_2]2BF_4$ complexes.

The crude material was purified by washing with acetonitrile, followed by repeated hot-filtration of a DCM/Et_2O slurry of the material to give the product in 48% yield.

2.4.3 Solution Studies

As with receptor **58**, anion binding studies were conducted by ^{1}H-NMR titration techniques in highly competitive DMSO-d_6. Where possible, Win-EQNMR[69] was used to curve-fit the titration data and the results are compared with those for **58** in Table 2.7.

	Receptor	
Anion	**58**[a]	**70**
Cl^-	$K_1 = 11700$	$K_1 = 2350$
	$K_2 = 2220$	$K_2 = 450$
Br^-	$K_1 = 1360$	$K_1 = 942$
	$K_2 = 450$	$K_2 = 131$
I^-	$K_1 = 1430$	$K_1 = 161$
	$K_2 = 52$	$K_2 = 16$
SO_4^{2-}	$K_a > 10^4$	$K_1 > 10^4$[b]
		$K_2 = 7800$[c]
$H_2PO_4^-$	$K_a > 10^4$	$K_a > 10^4$[d]

Table 2.7 – Stability constants (K_a/M^{-1}) for receptors 57 and 70 with anions as their TBA salts in DMSO-d_6 at 300 K. All errors estimated < 10%. [a]Data from reference 6. [b]Estimated value. [c]Estimated using a single point method. [d]Saturation is seen upon addition of 1 eqv. of anion, further addition of anion causes precipitation which infers strong binding.

As expected, the binding constants are lower than for receptor **70** than **58** due to the lower number of hydrogen-bond donor groups in this system. However, the same 1:2 receptor-halide stoichiometry with a high K_1 and lower K_2 was observed. This can be interpreted as the receptor adopting an *up-up* conformation at low anion concentrations wherein the anion is bound by two urea groups orientated in the same direction on one face of the complex. Whereas as at higher anion concentrations, the receptor switches to an *up-down* conformation, with the urea groups oriented on different faces of the complex and each urea binding a different anion.

With dihydrogen phosphate, a slow exchange relative to the NMR timescale was observed. This can best be explained by referring to the NMR titration stack-plot shown in Figure 2.21 below.

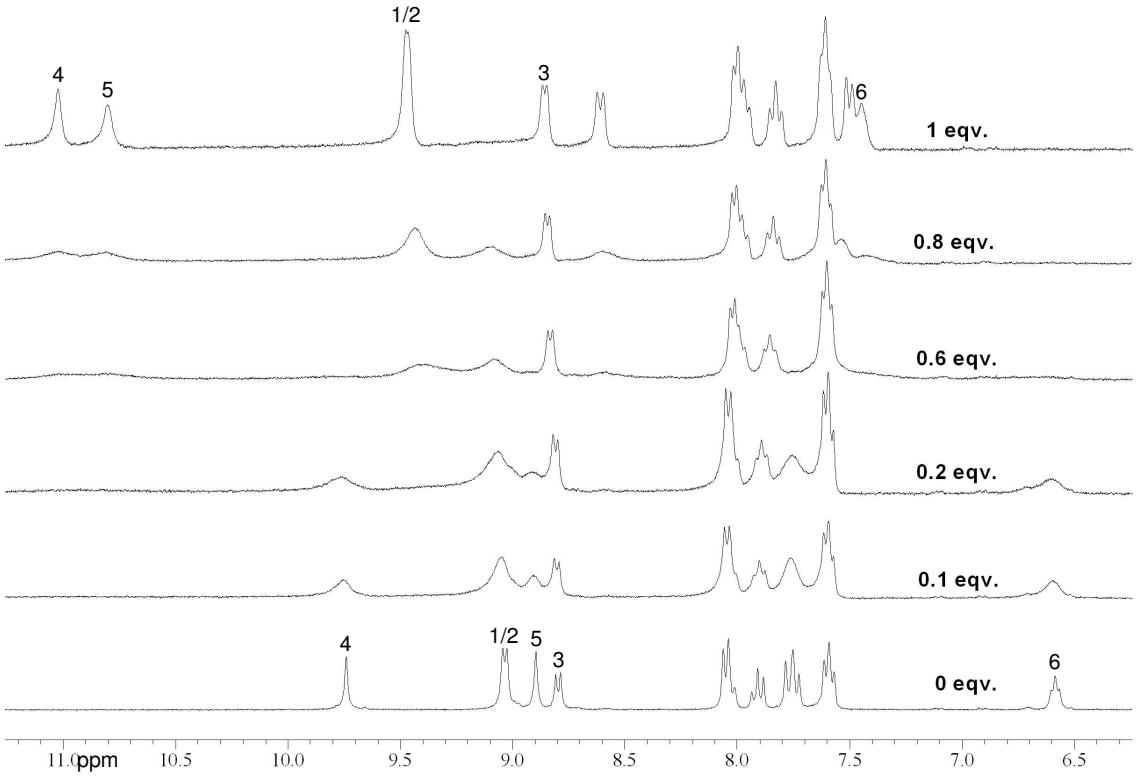

Figure 2.21 – Proton NMR titration stack-plot of 70 with TBA dihydrogen phosphate, see page 64 for the proton numbering scheme used.

At sub-stoichiometric amounts of anion addition there are peaks (although they are very broad in this case) representing both the complexed and uncomplexed receptor. At equimolar amounts of receptor and anion the complexed peaks become sharp, the uncomplexed peaks disappear and no further change in chemical shift is observed. Upon excess addition of the anion, the complex precipitates. This suggests a very strong binding interaction with a stability constant $>10^4\,M^{-1}$.

It was discovered[87] that it is possible to prepare anhydrous tetrabutylammonium sulfate for titrations. This was done by taking a 50 wt. % aqueous solution of tetrabutylammonium sulfate and reducing it to a gel *in-vacuo*. Further drying over phosphorous pentoxide on a high-vacuum line produced the salt as a crystalline material suitable for ^{1}H-NMR titrations.

Sulfate had a very strong interaction with **70** in DMSO-d_6, with a fast exchange process observed up to one equivalent of added tetrabutylammonium sulfate. Fitting this portion of the NMR titration using a 1:1 binding model in Win-EQNMR[69] gave a binding constant $K_1 > 10^4\,M^{-1}$.

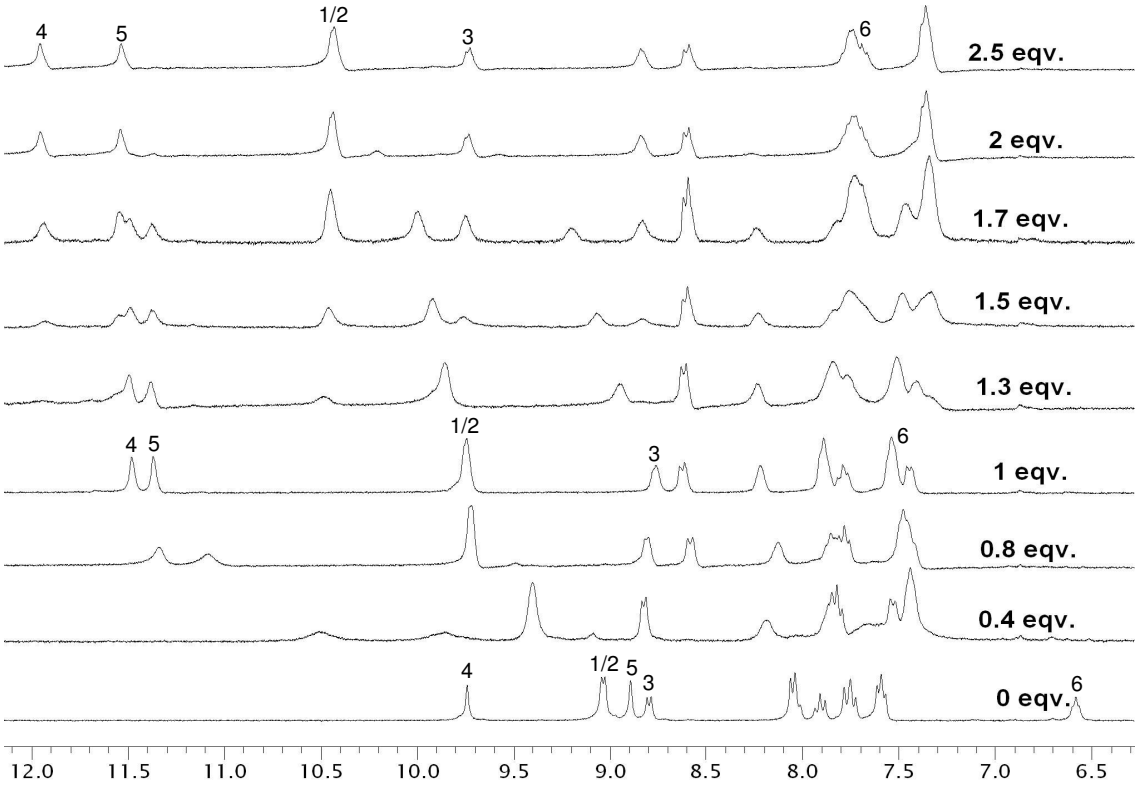

Figure 2.22 - Proton NMR titration stack-plot of 70 with $(TBA)_2$ sulfate, see page 64 for proton numbering system used.

Interestingly, at this point, further additions of anion result in a slow exchange process whereby peaks representing a new 2:1 complex appear with the 1:1 complex peaks at sub-stoichiometric amounts of anion (see *fig.* 2.22). So in Figure 2.22, two sets of peaks for the two different complexes can be clearly seen at 1.5 equivalents of anion addition. At 2 equivalents the 1:1 complex peaks disappear leaving just the peaks for the 2:1 complex. This process is summarised in Scheme 2.8 below.

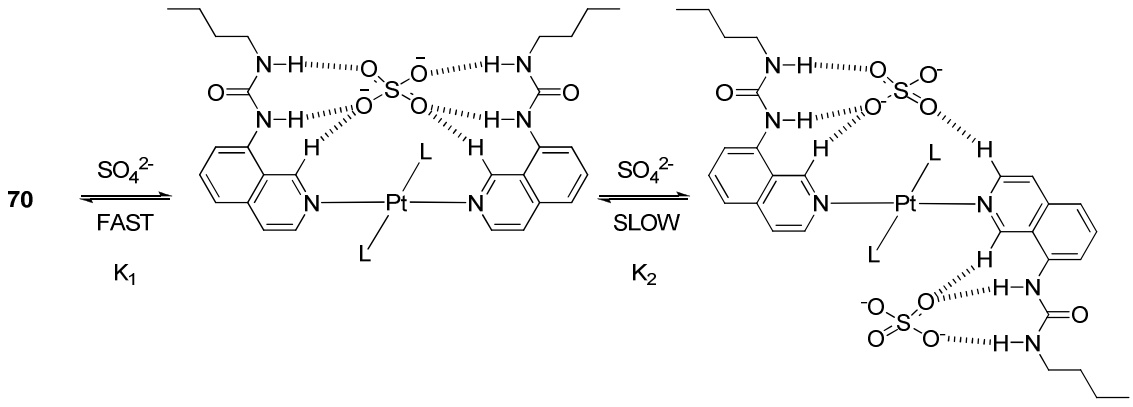

Scheme 2.8 – Proposed model for the behaviour of 70 in the presence of sulfate in DMSO solution.

A stability constant (K_2) for this slow exchange process was calculated by taking a single point in the titration at 1.7 equivalents of anion addition and applying some simple mathematic methodology:-

By assuming a simple equilibrium (where R = 1:1 receptor/anion complex and A = anion):

$$R + A \underset{}{\overset{K_2}{\rightleftharpoons}} RA$$

K_2 can be expressed as:

$$K_2 = \frac{[RA]}{[R][A]} \qquad (1)$$

Where:

[R] = Concentration of 1:1 receptor/anion complex.

[A] = Concentration of anion.

[RA] = Concentration of 1:2 receptor/anion complex.

At a single point in the NMR titration:

$$\frac{[RA]}{[R]} = \frac{Integration\ of\ RA\ proton\ peak}{Integration\ of\ R\ proton\ peak} \qquad (2)$$

So using the bottom urea proton peaks on the isoquinoline ligands at 1.7 eqv. of anion addition for 1:1 and 1:2 receptor:

$$\frac{[RA]}{[R]} = 1.67 \qquad (3)$$

The following relationships are also known at 1.7 eqv:

$$[R_{total}] = [R] + [RA] \qquad (4)$$

$$[A_{total}] = [A] + [RA] \qquad (5)$$

Where:

$[R_{total}]$ = Total concentration of receptor at 1.7 eqv. of anion.

$[A_{total}]$ = Total concentration of anion at 1.7 eqv. of anion.

By rearranging equation (3) and substituting [RA] into equation (4):

$$[R] = \frac{[R_{total}]}{2.67} \qquad (6)$$

and doing likewise for equation (5):

$$[A] = [A_{total}] - 1.67[R] \qquad (7)$$

So from equations (6) and (7):

$$[R] = 3.1192E^{-3} \text{ and } [A] = 2.1473E^{-4}$$

and by rearranging (3):

$$[RA] = 1.67[R] = 5.2091E^{-3} \qquad (8)$$

So finally:

$$K_2 = \frac{[RA]}{[R][A]} = 7777.1$$

So $K_2 \approx 7800M^{-1}$

2.4.4 Solid State Analysis

Crystals of the bromide complex of **70** were grown by slow evaporation of a nitromethane solution of the receptor in the presence of excess tetrabutylammonium bromide (*fig.* 2.23).

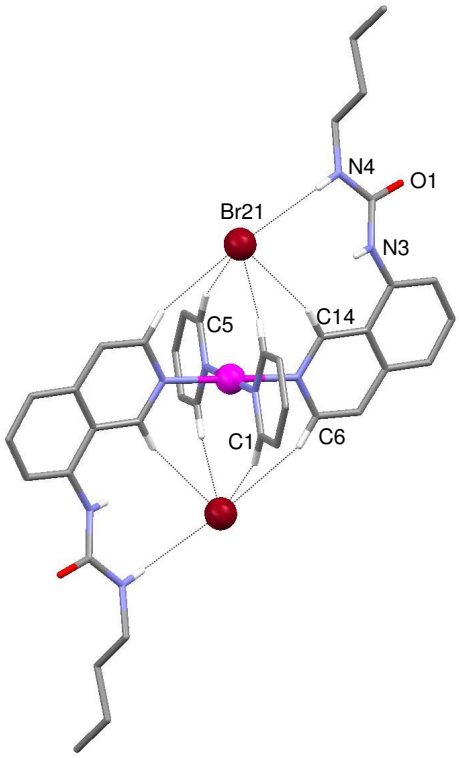

Figure 2.23 – X-ray crystal structure of the bromide complex of 70, omitting non-coordinating protons for clarity.

The structure reveals that the receptor adopts an *up-down* conformation in the solid state, binding each bromide anion via four CH···Br^- hydrogen bonds (C14···Br21 3.654(4) Å, C5···Br21 3.775(5) Å) and a single urea NH···Br^- hydrogen bond (N4···Br21 3.474(4) Å). The other urea NH appended to the isoquinoline does not interact with the bromide but instead forms an intermolecular hydrogen bond to an adjacent complex in the crystal (see *fig.* 2.24).

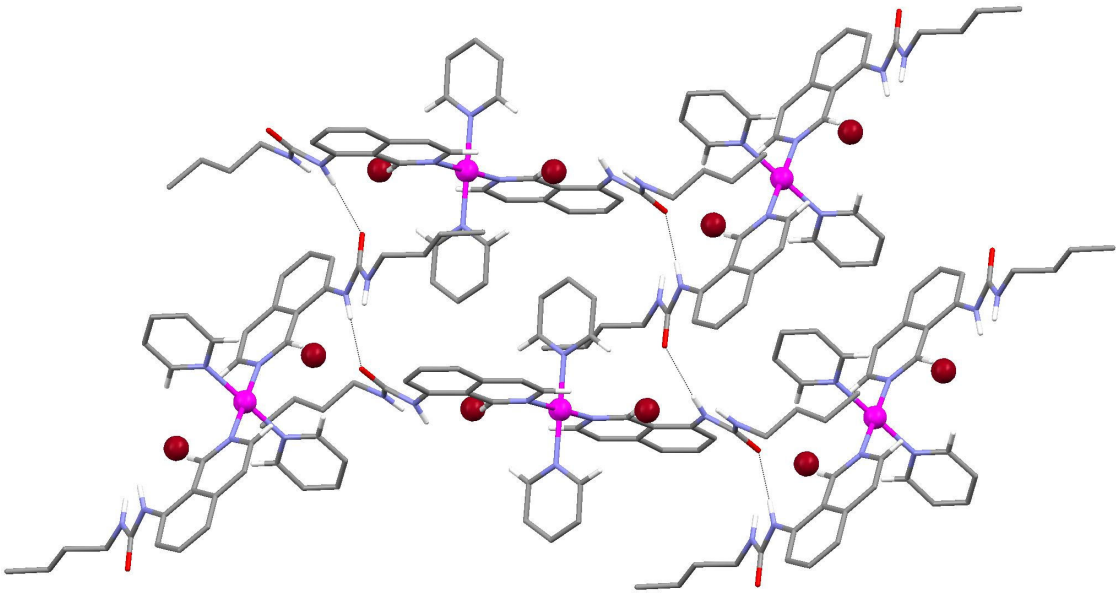

Figure 2.24 – Hydrogen bonded network of the bromide complex of 64, showing the intermolecular hydrogen bonds between N3 and O1.

Remarkably, it was possible to obtain two different crystal structures of the complex of **70** with sulfate. The first crystals were grown by a slow evaporation of a nitromethane solution of **70** in the presence of one equivalent of tetrabutylammonium sulfate (*fig.* 2.25).

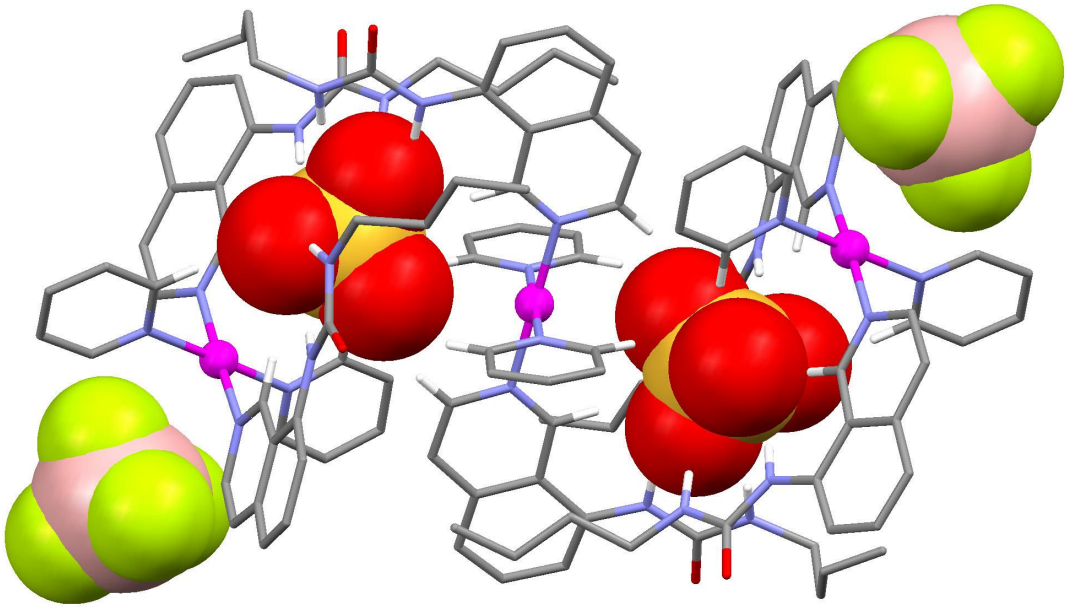

Figure 2.25 – X-ray crystal structure of the sulfate complex of receptor 70 from a 1:1 nitromethane solution. Sulfate and tetrafluoroborate have been shown in a space filling representation and non-coordinating hydrogens have been omitted for clarity.

The structure reveals the formation of a 3:2 receptor-sulfate complex with tetrafluoroborate anions also coordinating to the platinum complexes *via* CH···F interactions at the periphery of the structure. The existence of the two different conformations of the receptor can be observed, whereby the central complex adopts an *up-down* conformation with each urea group bound to a sulfate anion. Each of these sulfate anions is also bound to another platinum complex adopting the *up-up* conformation. Hence, each sulfate is bound to three urea groups. In addition, the aromatic CH groups in the α-position of the isoquinoline and pyridine rings of two platinum complexes form CH···O hydrogen bonding interactions with the sulfate ions. So in total, there an unprecedented fourteen NH and CH hydrogen-bond donor groups binding each sulfate anion. This is more coordination than was theoretically calculated to be the optimum coordination number for sulfate by Hay and co-workers.[82] By referring to the fragmented depiction of the complex in Figure 2.26, it is possible to see more clearly the two different binding modes and their associated hydrogen bonds in the crystal.

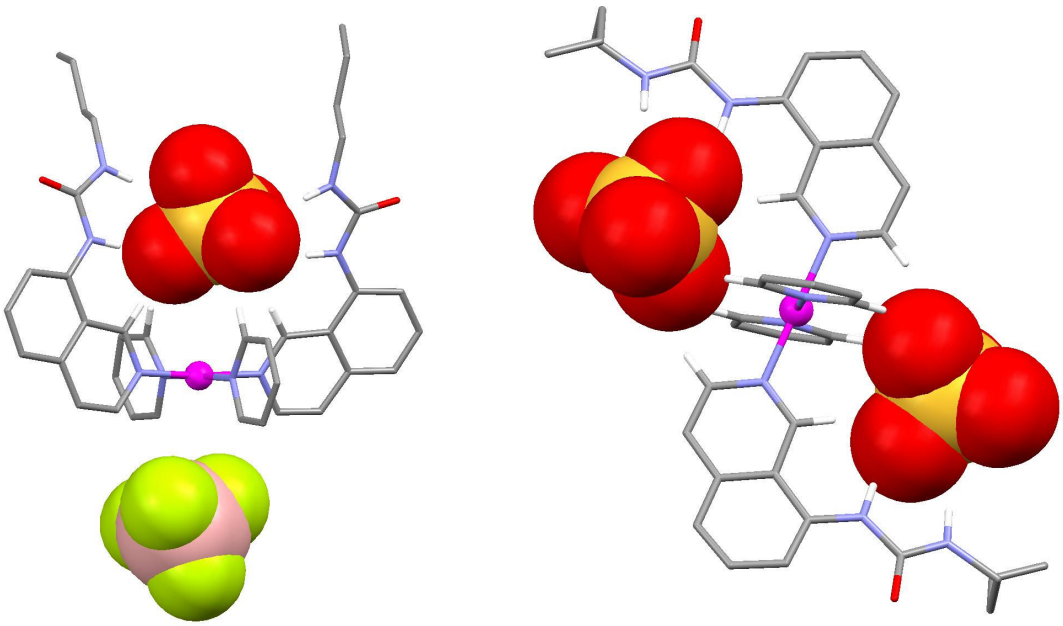

Figure 2.26 – Breakdown of the 3:2 crystal structure of 70 with sulfate, showing the periphery *up-up* platinum complex binding the sulfate (left) and the central *up-down* complex binding sulfate (right).

The second crystals were grown by a slow evaporation of a DMSO solution of **70** in the presence of *excess* tetrabutylammonium sulfate and these gave a completely different X-ray crystal structure (*fig.* 2.27).

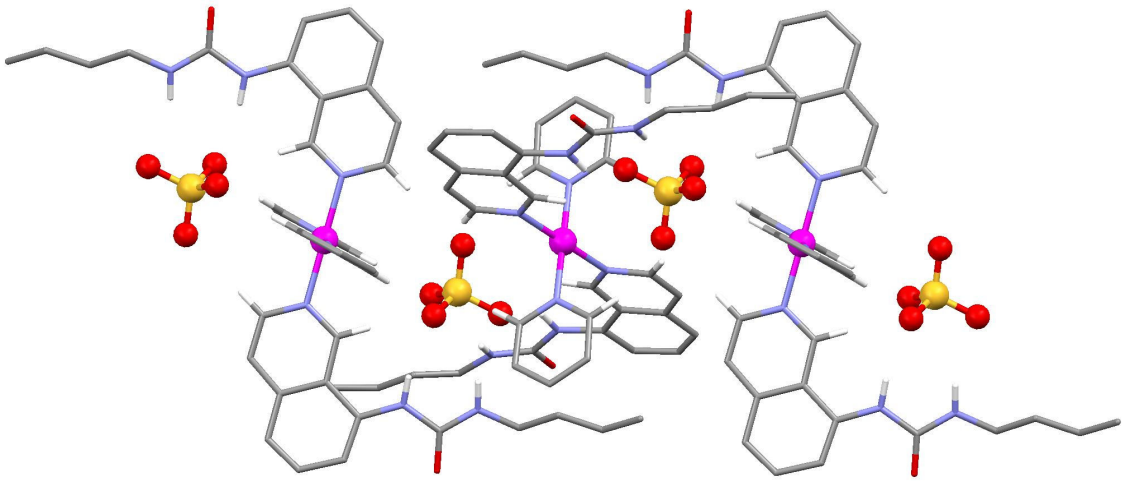

Figure 2.27 – X-ray crystal structure of the sulfate complex of 70 from a DMSO solution of the receptor in the presence of excess sulfate. Non-coordinating hydrogens have been omitted for clarity.

This structure reveals each sulfate is coordinated to two platinum complexes which are each in the *up-down* conformation. There is no presence of the *up-up* conformation seen in the other structure and each sulfate is coordinated by two urea groups. In addition there are eight CH···O interactions with the sulfate ions from the α-position CH groups on the isoquinoline and pyridine rings. In total there are twelve NH and CH hydrogen-bond interactions with each sulfate anion. Also there are no tetrafluoroborate anions in this crystal structure.

The achievement of obtaining two different crystal structures for the sulfate complex of **70** is quite remarkable and suggests there can be potential for designing specific platinum(II) based architectures for binding sulfate. For example, receptor **58** could be co-crystallised with receptor **70** and sulfate in various stoichiometric ratios. Or a new heteroleptic receptor with one isoquinoline ligand and three pyridine ligands can be co-crystallised with **70** or **58** and sulfate. This can then lead to the creation of combinatorial crystallographic libraries to study the binding behaviour of sulfate to this class of receptor.

2.5 Conclusions

This chapter has documented the extensive further investigations into the original platinum(II) based anion receptors developed by our collaborators in Canada. Different variables have been studied, such as changing the rigidity and pre-organisation of the hydrogen-bond donor groups of the ligands relative to those of receptor **58**. In solution, this resulted in a much less stable complex in the presence of certain anions. In addition, the binding constants were drastically much lower than those for receptor **58** in the same solvent and conditions. The crystallographic studies revealed a twisting of the pendant urea arms which were intermolecularly hydrogen bonded instead of discretely complexing the hydrogen sulfate anion. The greater disorder in this system meant entropic barriers were greater to overcome which lead to weaker anion complexation.

Changing the hydrogen-bond donor group to a pyrrole-amide produced a sub-class of receptors with surprisingly different properties to receptor **58**. With the different functionality, even the isoquinoline version (**60**) was not stable in the presence of chloride in solution. Both receptors **60** and **61** were not effective for halides in DMSO solution as expected. They were however effective for the carboxylate anions benzoate and acetate, with high binding constants and strong broadening of the pyrrole peak on the ^{1}H-NMR titration spectra.

Synthesis of the *trans*-functionalised bis-pyridyl version of receptor **58** allowed further investigation into the sulfate binding conformation and explored the role of CH···anion interactions in these complexes. The solution studies revealed an interesting interaction of **70** with sulfate, whereby at low anion concentration a fast exchange strong 1:1 binding in an *up-up* conformation was observed. After addition of one equivalent of this anion, a slow exchange process was observed with the complex switching to a 2:1 anion-receptor system in an *up-down* conformation.

In the solid state, receptor **70** could form two different crystal structures depending on the crystallisation conditions. By slow evaporation of a nitromethane solution of **70** in the presence of one equivalent of tetrabutylammonium sulfate, a unique 3:2 receptor-sulfate complex formed with the anion bound in a pocket lined with fourteen NH and CH hydrogen bond donor groups. By slow evaporation of a DMSO solution of **70** in the presence of an excess of sulfate, a 2:1 sulfate-receptor complex formed with the sulfate anions also binding to adjacent receptors through a total of twelve hydrogen bonds. These

findings leave scope for further crystallographic investigations into this class of receptor's complexation with sulfate.

Chapter 3 – Benzimidazole Based Receptors for Neutral Guest Complexation

3.1 Introduction

Since the late 1980s there have been many reports of artificial receptors for neutral molecules such as ureas and barbiturates. It was the early investigations of Hamilton's group that particularly focused on the molecular recognition of barbiturates which were considered attractive targets due to their biological activity.[88]

Hamilton's approach was to use an isophthalamide core with two appended diamidopyridine units to provide the basis of some elegant macrocycles **72** and **73** (*fig.* 3.1).[88, 89]

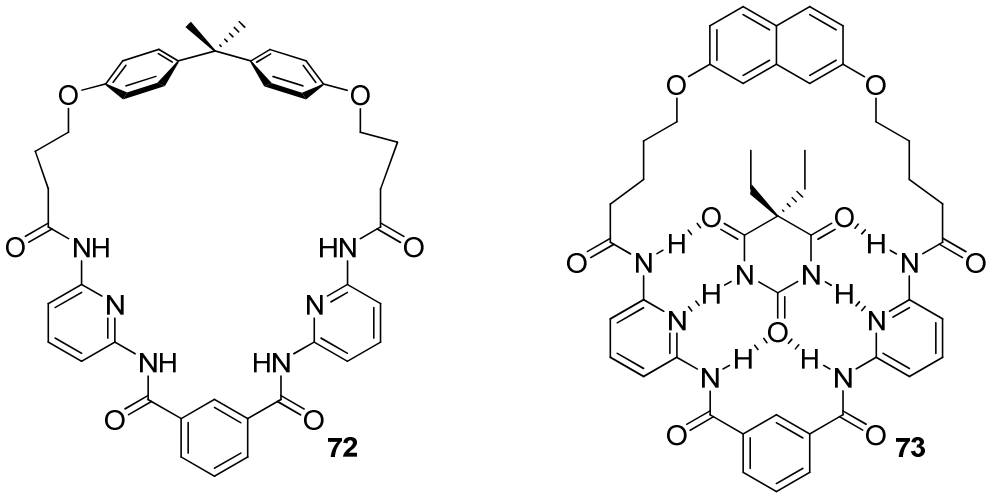

Figure 3.1 – Hamilton's macrocycles for barbiturates showing the expected binding mode of barbital to receptor 73.

The synthesis of the macrocycles was remarkably facile, involving two steps from isophthaloyl dichloride and producing macrocycles **72** and **73** in 12 and 14% yields

respectively.[89] The complexation properties of the receptors were tested by ^{1}H-NMR titrations (in CD_2Cl_2 or $CDCl_3$), or by UV-vis titrations (in CH_2Cl_2) where the association constants were too high to measure by ^{1}H-NMR. The results showed that the macrocycles bound barbital (5,5-diethylbarbituric acid) in a 1:1 stoichiometry with very high affinities (K_a = 6x10^5 and 2.5x10^5 M^{-1} for **72** and **73** respectively). Such high binding constants are remarkable considering that both species in the complex are neutral. Characteristic changes in the ^{1}H-NMR spectra during titrations of the macrocycles with barbital, revealed the guest binds through six hydrogen bonds as shown in Figure 3.1.[89]

The binding behaviour observed in solution was supported by X-ray crystallographic analysis of the barbital complex of **73** (*fig.* 3.2). The structure shows the barbital in the centre of the macrocycle forming three hydrogen bonds to each diamidopyridine unit (N···O distances 2.87-3.23 Å and N···N 2.95 and 3.00 Å). The barbital is not coplanar to the macrocycle but lies at 27^o angle relative to the plane of the pyridine rings.[89]

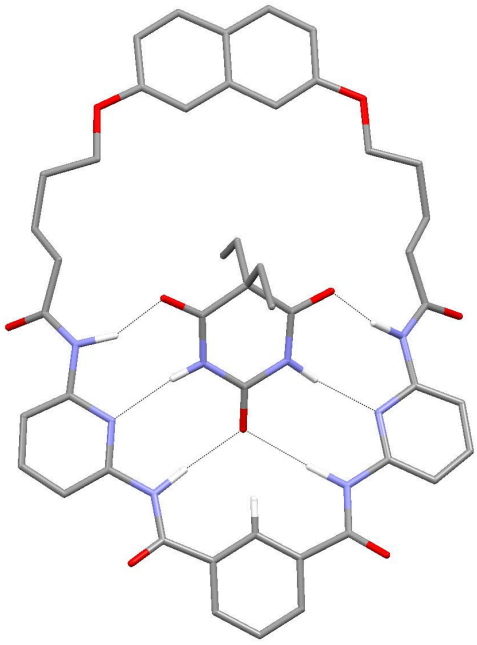

Figure 3.2 – X-Ray crystal structure of the barbital complex of macrocycle 73.

Hamilton further developed this motif to make receptors with specific functions such as catalysts[90] or multi-component chromophores.[91]

At the same time Whitesides and later Reinhoudt initiated their extensive studies into melamine based receptors for barbiturates which they used to assemble a vast array of hydrogen bonded crystalline architectures.[92-94] One of the more simple architectures was

the tris-melamine based [2x2] hydrogen bonded grid of Reinhoudt and co-workers.[95] The components, **74** and **75**, could potentially form three different structures including a [1x1] grid and a polymer. However, the ^{1}H-NMR spectrum of a 1:1 mixture of **74** and **75** in $CDCl_3$ confirmed the exclusive formation of the [2x2] grid $(\mathbf{74})_2\bullet(\mathbf{75})_2$. Proton-NMR studies also confirmed the increased kinetic and thermodynamic stability of the grid when compared with the 1:2 barbital complex of **74**.[95]

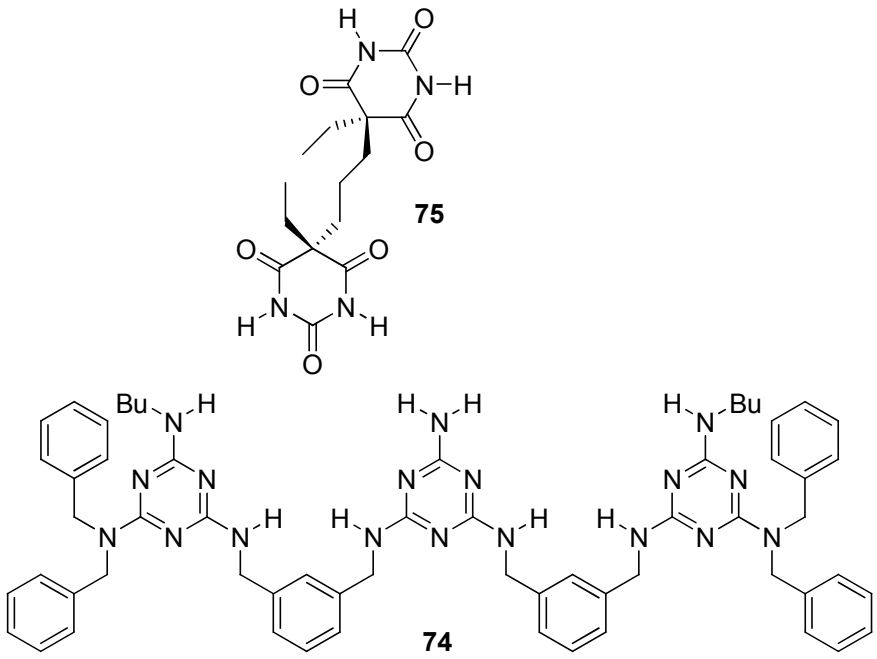

Figure 3.3 – The components for Reinhoudt's [2x2] hydrogen bonded grid.

Other groups have further explored melamine based frameworks for the recognition of barbiturates. For example Champness and co-workers have looked at the effects on barbital binding when hydrogen bond donors are removed from bis-melamine cleft receptors.[96] Also, Kondo and co-workers have borrowed from Hamilton, Whitesides and Reinhoudt's ideas and used melamines to synthesise a series of macrocycles (**77**-**79**) for barbiturates (*fig.* 3.4).[97] The acyclic receptor **76** was prepared as a control analogue, macrocycle **77** has an alkyl spacer, **78** has the spacer used in Hamilton's macrocycles[88] and **79** is a symmetrical tris-melamine analogue.

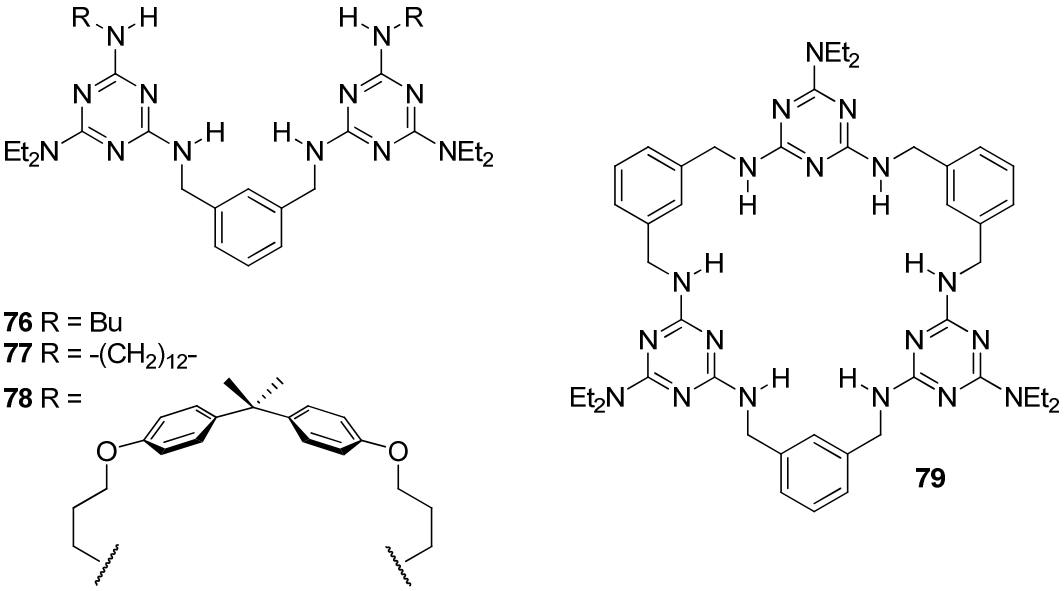

Figure 3.4 – Kondo and co-worker's melamine based macrocycles 77-79 and an acyclic analogue 76.

An anthryl chromophore substituted barbiturate (**80**) was synthesised to test the compounds by UV-vis titrations since none of the compounds were UV-vis active.

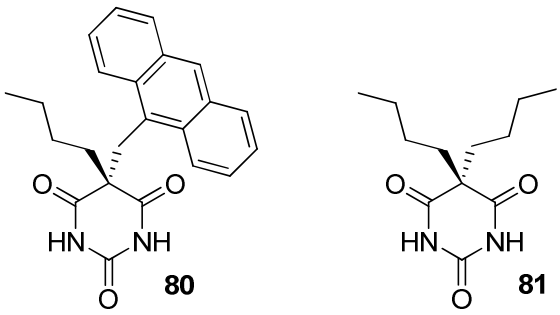

Figure 3.5 – The barbiturate guests used for the study of compounds 76-79.

The UV-vis titrations (conducted in $CHCl_3$) revealed very high association constants for all the compounds with barbiturate **80**, including the acyclic receptor **76**, with the largest value found for receptor **78** ($K_a = 1.29 \times 10^5\ M^{-1}$). The binding constant for **79** ($K_a = 43500\ M^{-1}$) was similar to that of **76** ($K_a = 50000\ M^{-1}$) suggesting that the steric hinderance presented by the 5,5-substituents on the barbiturate prevents efficient binding with this macrocycle. Proton-NMR titrations in $CDCl_3$ were also carried out with the receptors and barbiturate **81** to compliment the UV-vis studies.

An X-ray crystal structure of compound **79** with barbiturate **81** was obtained which showed two of the melamines binding a barbiturate through six hydrogen bonds. Whilst the other melamine unit was orientated out of the cavity and binding another barbiturate

through three hydrogen bonds which was bound to another macrocycle to form a dimer. This resulted in the formation of a 2:4 receptor:barbiturate complex.

Since 1997, Tucker and co-workers have synthesised many ferrocene and cobaltocene based receptors for neutral molecules such as bis-carboxylic acids[98, 99] and later ureas and barbiturates.[100, 101] The latter work included a study of 1,1'- and 1,3-substituted ferrocene receptors (**82**-**87**) based on Hamilton's diamidopyridine frameworks[88] discussed earlier.[101]

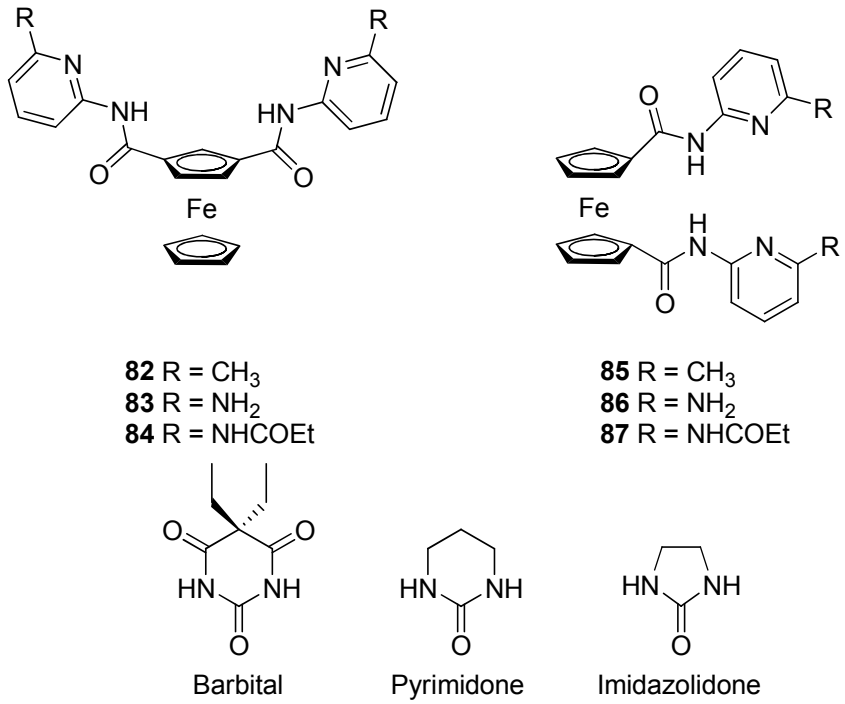

Figure 3.6 – Tucker and co-worker's organometallic neutral guest receptors.

It was thought that introduction of the ferrocene spacer groups would serve to both allow control of the binding strength of the receptor through oxidation of the metal centre, and allow the binding event to be monitored by cyclic voltammetry.[101]

Proton-NMR titrations were conducted on receptors **82**-**87** in $CDCl_3$ with the selection of guests shown in Figure 3.6 and the association constants obtained using WIN-EQNMR.[69] With the exception of receptors **82** and **85**, the results showed all the receptors to have the strongest interaction with barbital. Receptors **82** and **85** had higher binding constants with pyrimidone (K_a = 600 & 240 M^{-1} respectively) compared to barbital (K_a = 195 & 200 M^{-1} respectively) which they thought was due to unfavourable secondary hydrogen bond interactions. Another unsual result was that the association constants for the amide receptors (**84** & **87**) were lower than those for the amine receptors (**83** & **86**).

This was thought due to either; unfavourable steric effects or that the pyridine nitrogen is a better hydrogen bond acceptor when the more electron rich amine is attached to the pyridine ring.[101]

X-Ray crystals of the barbital complex of receptor **84** were obtained by slow diffusion of diethyl ether into a chloroform solution of the complex. The structure (*fig.* 3.7) shows the formation of a 1:1 complex with the barbital bound through six hydrogen bonds as expected. The barbital lies at a 38° angle relative to the plane of the pyridine rings which is similar to the effect observed in Hamilton's isophthaloyl macrocycles described earlier.[100]

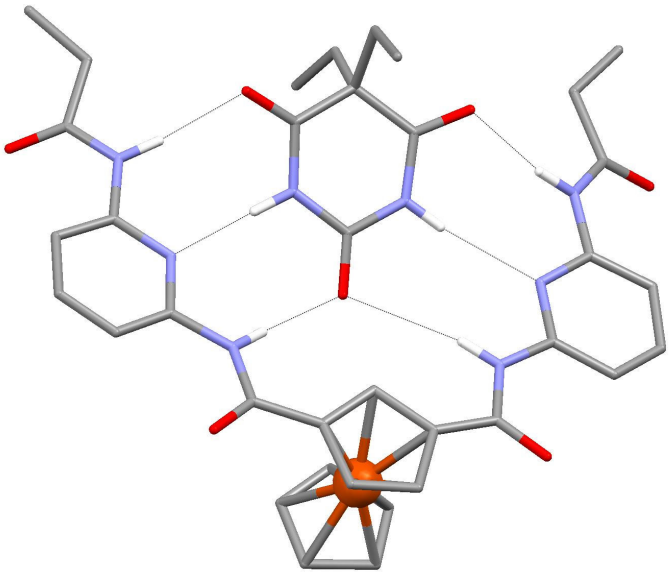

Figure 3.7 – X-Ray crystal structure of receptor 84 with barbital.

Cyclic voltammetry experiments in dry DCM were conducted on all the receptors except the amine based receptors **83** and **86**, since these posed problems which was thought to be possibly due to them being absorbed onto the electrode surface. The tested receptors all showed reversible, one electron reduction processes with similar formal potentials ($E^{o'}$). To test their behaviour in the presence of the guests, at least twenty equivalents of guest was added to the host solution. In all cases (except where poorly defined voltagrams were encountered), $E^{o'}$ shifted negatively relative to that of the receptor alone. Shifts of up to -60 mV were observed. These negative shifts are consistent with the hydrogen bond between the receptor's amide NH groups and the oxygen of the guest increasing the electron density on the receptor, which makes the ferrocene unit easier to oxidize.[101]

There have been many other studies into barbiturate and urea receptors including chiral,[102] indole based[103] and metal based[104] receptors which further demonstrate the scope and depth of this field of chemistry.

3.2 Simple Benzimidazole Based Clefts

Previous work in the Gale group has involved the extensive synthesis and study of novel hydrogen bonding motifs for anion recognition. In particular, intramolecular hydrogen bonding has been used to preorganise receptors for enhanced anion binding as seen in our macrocyclic receptors for carboxylate recognition[13, 105] and in acyclic membrane transporters for chloride[15] and HCl.[106] In the case of the latter, methylimidazole groups were employed and the success with this approach prompted a further search for analogous functionalities such as benzimidazoles. The ready commercial availability of 2-aminobenzimidazoles led to the design of a simple symmetric bisamidobenzimidazole cleft receptor **88** (*fig.* 3.8).

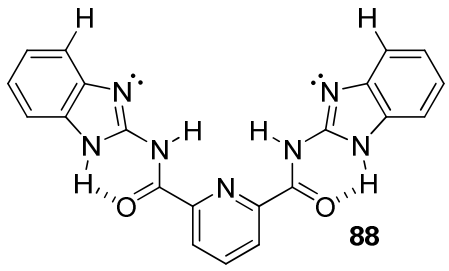

88

Figure 3.8 – Original benzimidazole cleft receptor

The ^{1}H-NMR of receptor **88** in DMSO-d_6 revealed the benzimidazole NH proton to be shifted unusually far downfield to a remarkable 12.87 ppm. This suggests that in solution the receptor adopts the *syn-syn* conformation depicted in Figure 3.8, with the benzimidazole NH protons intramolecularly hydrogen bonding to the amide carbonyl which preorganises the structure. A ^{1}H-NMR titration of **82** with TBA^+Cl^- revealed no binding of chloride, which is likely due to the lone pair electrons on the benzimidazole nitrogens projecting into the cleft and repelling the anion.

However, it was immediately apparent that compound **88** had the DADDAD hydrogen bond donor (D)/acceptor(A) array which is complimentary for neutral guests such as barbiturates and ureas. In order to study the interaction of such guests with receptor **88**, some control analogues (**89**-**92**) were synthesised to probe various aspects of the receptor (*fig.* 3.9).

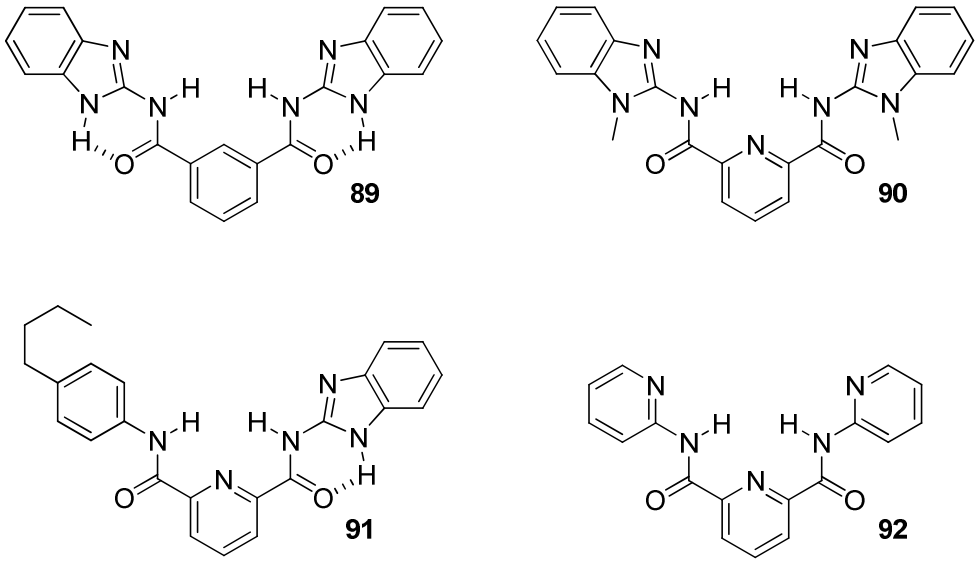

Figure 3.9 – Model compounds for the study of receptor 88.

Compound **89** has an isophthaloyl core in place of the pyridine one on **88** which removes a degree of preorganisation and may twist the structure because of the CH on the iosphthaloyl ring pointing into the cleft. Compound **90** lacks the benzimidazole NH group and hence possesses a lower degree of preorganisation than **88**. Asymmetric compound **91** lacks one of the amidobenzimidazole groups thus removing both a hydrogen bond donor and acceptor. Compound **92** is a pyridine analogue of compound **88** and again lacks the same degree of preorganisation as **88**.

3.2.1 Synthesis

Compounds **88**-**90** were synthesised by the condensation of 2-aminobenzimidazole or 2-amino-1-methylbenzimidazole with either 2,6-pyridinedicarbonyl dichloride or isophthaloyl dichloride in yields of 81, 54 and 86% respectively (*sch.* 3.1).

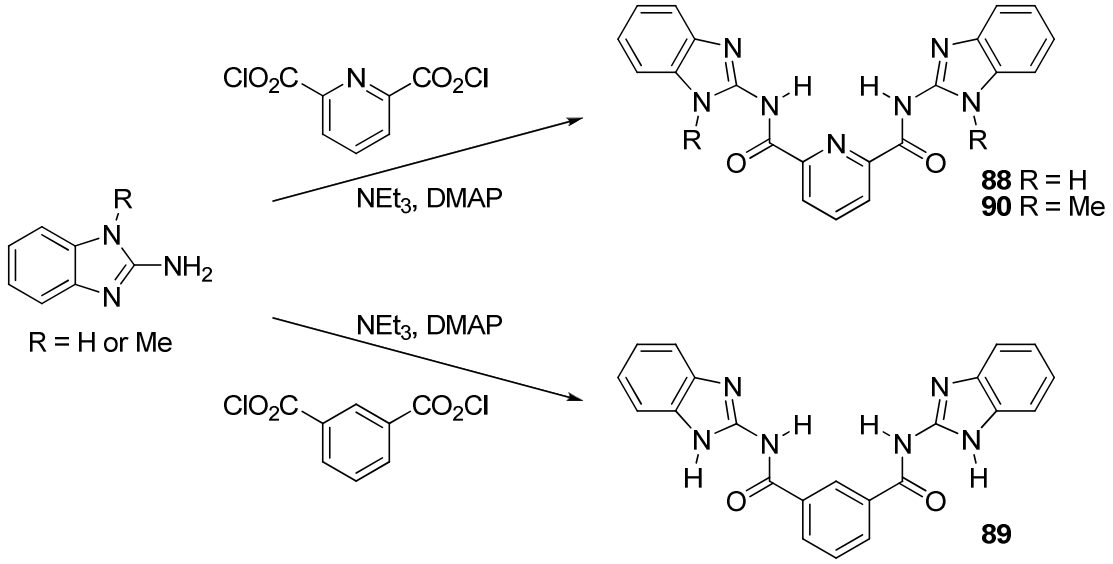

Scheme 3.1 – Synthesis of compounds 88-90.

Compound **91** was synthesised according to Scheme 3.2 with the last step proceeding in 54% yield. The synthesis of intermediate **94** was carried out according to a literature procedure.[107] This involved esterification of 2,6-pyridinedicarboxylic acid in methanol in the presence of a catalytic amount of sulphuric acid. Treatment of the bisester with one equivalent of potassium hydroxide at 0 ^{o}C afforded predominantly the monoester-monoacid which was purified by recrystallisation from isopropanol. Intermediate **95** proved unstable to treatment with thionyl chloride so a suitable coupling agent route was employed instead.

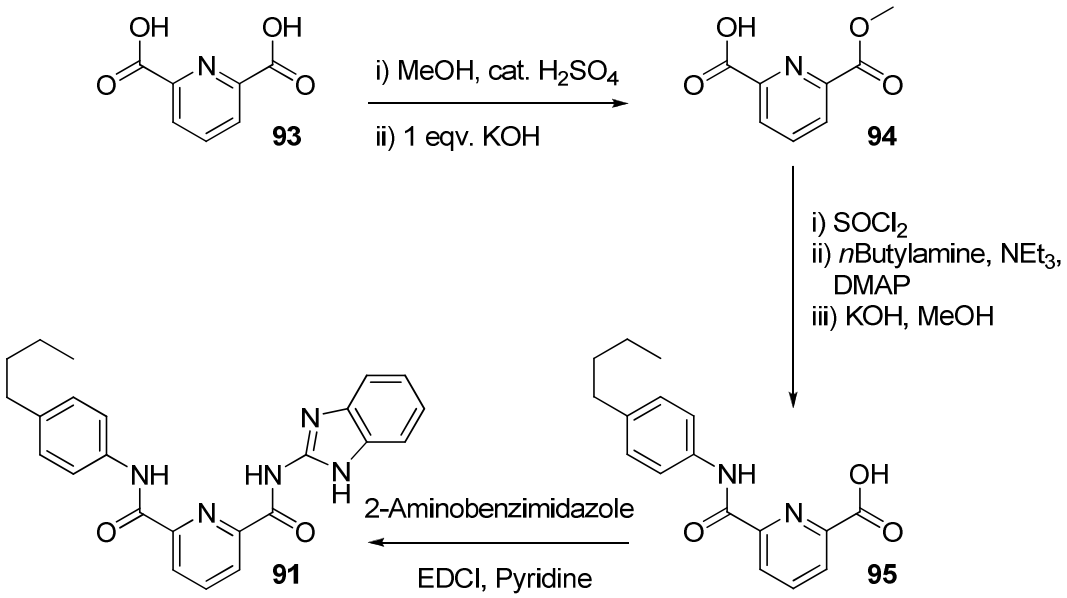

Scheme 3.2 – Synthesis of compound 91.

Finally, compound **92** was synthesised according to a literature procedure[108] from 2-aminopyridine and 2,6-pyridinedicarbonyl dichloride.

3.2.2 Solid State Analysis

X-ray quality crystals of compound **88** were obtained by the slow evaporation of a DMSO solution of the receptor. The structure (*fig.* 3.10) shows the receptor adopting a *syn-syn* conformation with a DMSO molecule bound to the amide NH groups.

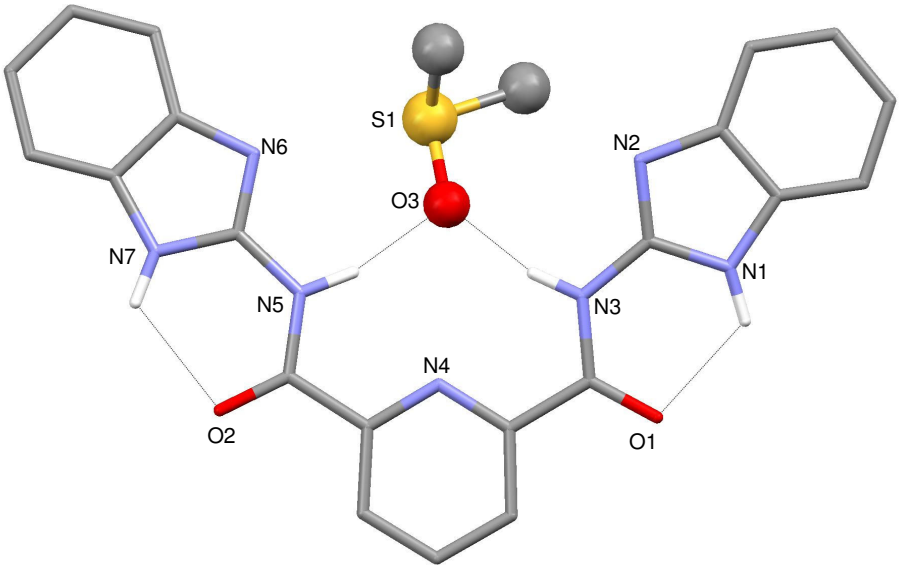

Figure 3.10 – X-Ray crystal structure of the DMSO solvate of compound 88. Non-acidic hydrogen atoms have been omitted for clarity.

In addition, there are intramolecular hydrogen bonding interactions N1···O1 (2.666(2) Å) and N7···O2 (2.741(2) Å) which presumably stabilise the structure in the solid state. This observation supports the similar findings in DMSO solution, confirming the reasoning behind the high downfield shift of the benzimidazole NH proton.

It was not possible to obtain X-ray quality crystals of compound **90** from a DMSO solution. However, crystals of the compound were instead obtained by slow evaporation of a DMF solution of the compound.

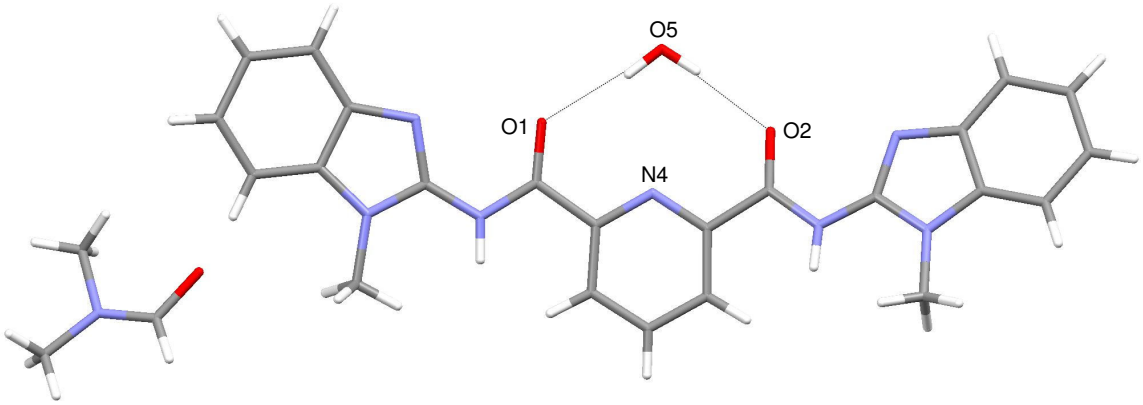

Figure 3.11 – X-ray crystal structure of the DMF/H_2O solvate of compound 90.

The structure (*fig.* 3.11) shows the compound adopting an *anti-anti* conformation with a water molecule bound (O1···O5 2.856(2) Å & O2···O5 2.872(2) Å) to the amide carbonyls. This result is quite remarkable considering that it has been well documented that this is the most high energy conformation.[12, 14] As briefly mentioned (*Chapter* 1), 2,6-pyridine diamides usually prefer to adopt a *syn-syn* conformation because of stabilising, favourable electrostatic interactions between the amide protons and the pyridine nitrogen atom. The *anti-anti* conformation has unfavourable electron repulsions between the pyridine nitrogen lone pair (l.p) electrons and carbonyl oxygen l.p electrons, making it higher energy (*fig.* 3.12).

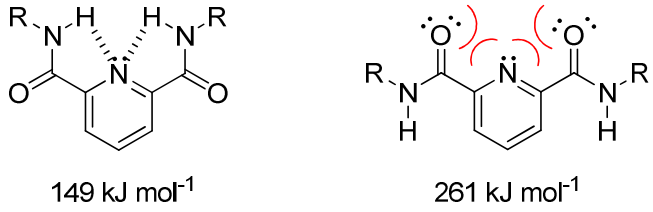

Figure 3.12 – Favourable and unfavourable conformations of 2,6-pyridine diamides. The energies are quoted from Reference 12 and were calculated using a CHARMm force field with no solvent included in the calculations.[12]

However in this case, the hydrogen bonded water molecule is presumably stabilising the *anti-anti* conformation in the solid state.

Single crystals of compound **91** were grown by slow evaporation of a methanolic solution of the compound (*fig.* 3.13).

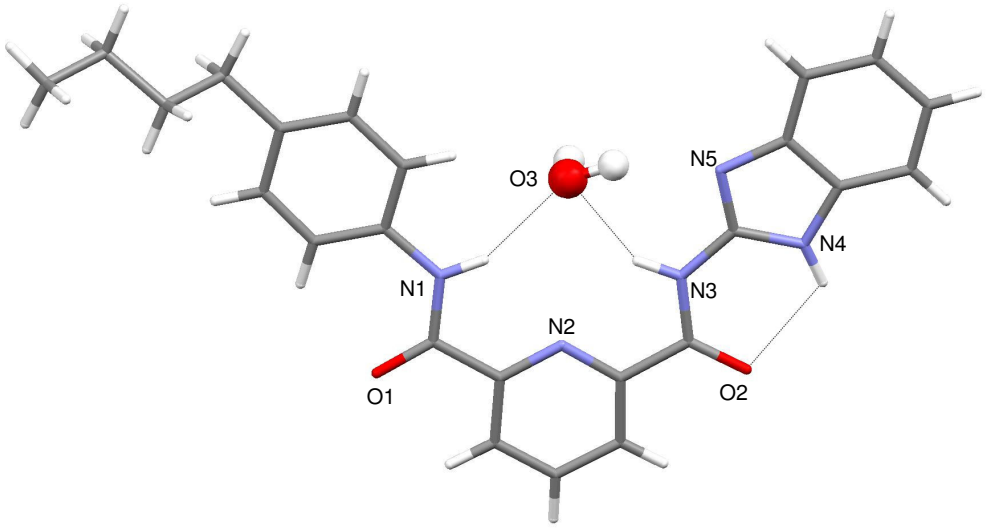

Figure 3.13 – X-Ray crystal structure of compound 91.

The structure shows the compound adopting a *syn-syn* conformation with a water molecule bound to the amide protons in the cleft (N1···O3 3.055(4) Å & N3···O3 2.908(3) Å). The benzimidazole NH/carbonyl intramolecular hydrogen bond is also present (N4···O2 2.781(3) Å).

Crystals of the barbital complex of receptor **88** were grown by the slow evaporation of a DMSO solution of the complex (*fig.* 3.14). The barbital is held by a total of six hydrogen bonds; N2···N9 (2.7700(4) Å), N3···O3 (2.9769(4) Å), N5···O3 (2.172(3) Å), N6···N8 (2.7406(4) Å), C5···O3 (3.4011(5) Å) and C17···O4 (3.3921(6) Å). Intramolecular hydrogen bonds N1···O1 (2.6906(3) Å) and N7···O2 (2.7198(4) Å) are

also present in the complex and, interestingly, each benzimidazole NH group also forms a hydrogen bond to a DMSO molecule.

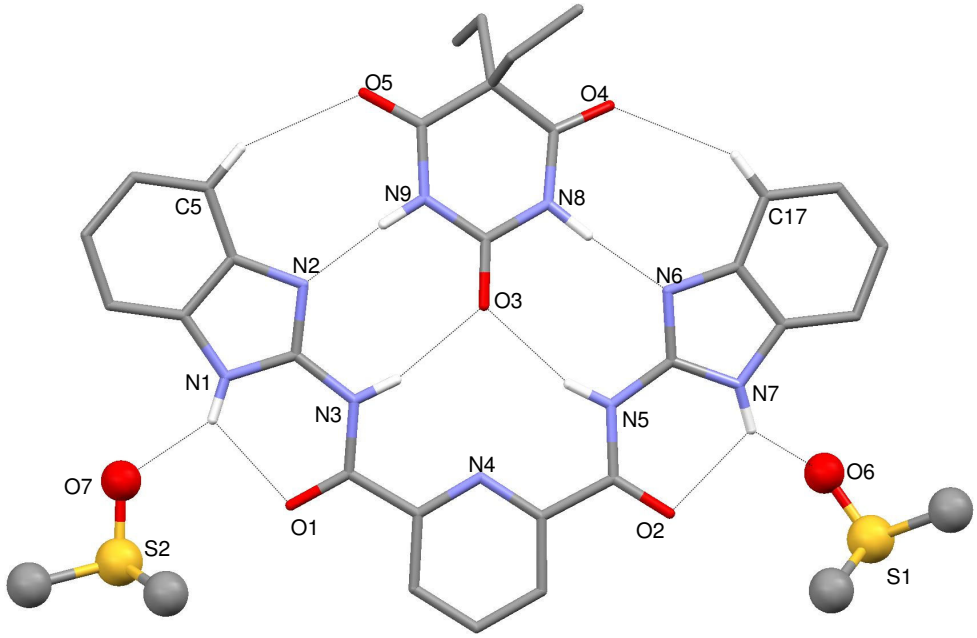

Figure 3.14 – X-Ray crystal structure of the barbital complex of receptor 88. Non-coordinating/acidic hydrogens have been omitted for clarity.

3.2.3 Solution Studies

The compounds were tested against the neutral guests shown in Figure 3.15. Compounds **88**-**90** were only completely soluble in more polar solvents such as DMF or DMSO. In particular compound **89** was only soluble in warm DMSO. Preliminary ^{1}H-NMR titrations in DMSO revealed none of the compounds interacted with the guests chosen for the study.

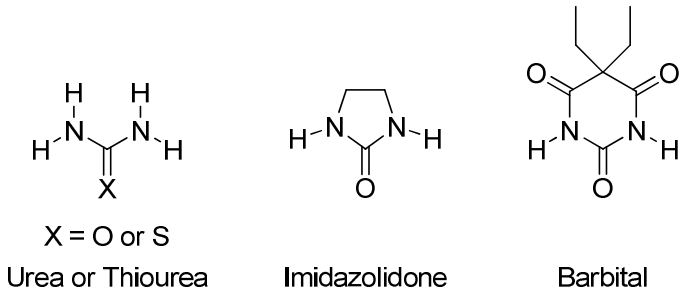

Figure 3.15 – The neutral guests used in the solution studies.

However, compounds **88** and **90** were found to be soluble in the less polar nitromethane, but the only guest soluble in this solvent was barbital. Addition of a nitromethane solution of barbital to receptor **88** resulted in precipitation which is indicative of strong binding. So the binding studies were conducted by ^{1}H-NMR titrations in solutions of nitromethane-d_3 diluted with DMSO-d_6 (either $MeNO_2$-d_3/20% DMSO-d_6 or $MeNO_2$-d_3/30% DMSO-d_6). Only compound **89** was not soluble in these solvent systems so no data was collected for it. The stability constants were determined using the WIN-EQNMR program.[69]

The crystal structure of receptor **88** shows that DMSO binds to the amide groups. Hence, it is reasonable to expect that, in solution, the neutral guests must compete with this solvent for the guest binding site. The results for the titrations are shown in Table 3.1.

	88	**88**[a]	**90**	**91**	**92**
Thiourea	0	0	0	0	0
Urea	28	<10	0	0	0
Imidazolidone	45	13	0	0	0
Barbital	Precipitate	59	0	0	0

Table 3.1 – Binding constants K_a (M^{-1}) for compounds 88, and 90-92 with a selection of neutral guests in 20% DMSO-d_6/$MeNO_2$-d_3 unless noted otherwise at 298 K. All errors are estimated to be <10%. [a] In 30% DMSO-d_6/$MeNO_2$-d_3.

In 20% DMSO-d_6/$MeNO_2$-d_3, receptor **88** was found to bind urea and imidazolidone but precipitate upon the addition of barbital. Switching to 30% DMSO-d_6/$MeNO_2$-d_3 allowed a stability constant of 59 M^{-1} to be determined for the formation of the **88**-barbital complex under these more polar solvent conditions. Compounds **90**-**92** showed no interaction with the guests under these conditions. Compound **91** was able to be tested in acetonitrile with barbital and even in these less polar solvent conditions it still showed no interaction with the guest. Interestingly, thiourea does not interact with receptor **88** under either set of solvent conditions, whereas urea is bound (albeit very weakly). This is presumably due to the poor hydrogen bond acceptor ability of the thiourea sulphur atom compared to the urea oxygen.

The achievement of binding these neutral guests in such a polar solvent system is quite significant since, to the best of our knowledge, previous studies have only bound such guests in non-polar mediums such as DCM.

3.3 Towards a More Soluble Simple Cleft Receptor

Given the solubility problems encountered with receptors **88**-**92**, we thought it necessary to try and make a more soluble version of receptor **88**. This can feasibly be done by appending a 'greasy' alkyl chain to either the benzimidazole groups or the 4-position on the pyridine ring. Receptor **96** employed the latter with a butyloxy chain appended onto the pyridine ring (*fig*. 3.16).

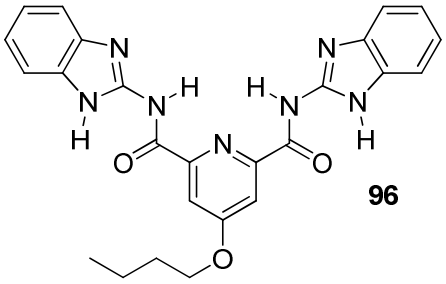

96

Figure 3.16 – Butyloxy substituted version of receptor 88.

3.3.1 Synthesis

Receptor **96** was synthesised from chelidamic acid monohydrate in 5 steps (*sch.* 3.3). The first step involved a simple esterification of the carboxylic acid in methanol with a catalytic amount of sulfuric acid as described in the literature.[109] The butyloxy chain was appended by reacting the bisester with butyl iodide in the presence of potassium carbonate as described in Dr. Joachim Garric's thesis.[110] Conversion of the pyridine bisester into the bisacid was followed by treatment with thionyl chloride and finally reaction with 2-aminobenzimidazole in the presence of triethylamine to afford the product in 82% yield.

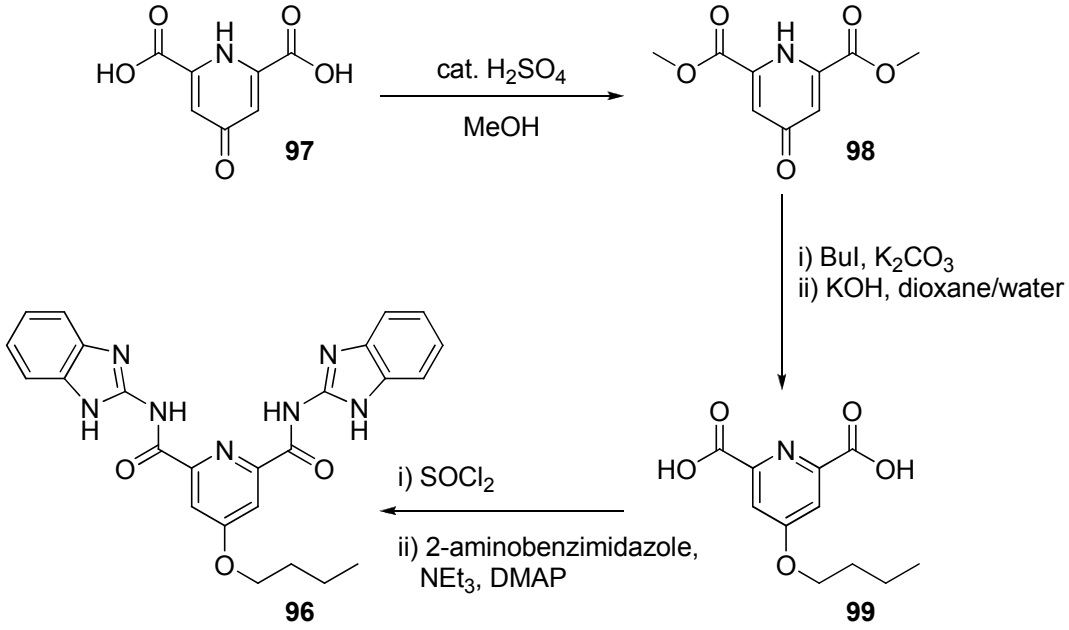

Scheme 3.3 – Synthesis of receptor 96.

3.3.2 Solid State Analysis

Crystals of the barbital complex of receptor **96** were grown by the slow evaporation of a DMSO solution of the complex (*fig.* 3.17). As expected, the barbital is held by six hydrogen bonds as with the receptor **88** complex; N2···N8 (2.779(4) Å), N3···O4 (2.985(3) Å), N5···O4 (3.019(4) Å), N6···N9 (2.783(4) Å), C2···O5 (2.668 Å) and C17···O6 (2.757 Å). Again, the intramolecular hydrogen bonds are also present; N1···O1 (2.660(4) Å) and N7···O2 (2.686(4) Å) as is a hydrogen bond from a benzimidazole NH to a DMSO molecule.

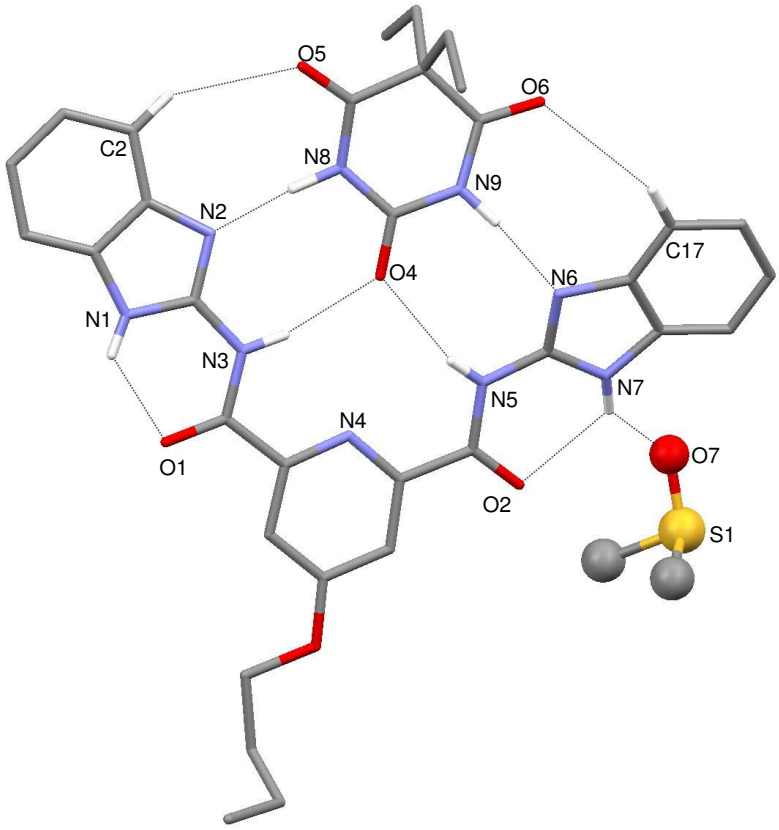

Figure 3.17 – X-Ray crystal structure of the barbital complex of receptor 96. Non-coordinating/acidic protons have been omitted for clarity.

3.3.3 Solution Studies

In solution it was discovered that receptor **96** had the same solubility properties as receptor **88**. The addition of the butyloxy chain appeared to have little or no effect on making the receptor more soluble in less polar solvents. Nevertheless, binding studies, in the form of ^{1}H-NMR titrations, were carried out in the same solvent conditions as those for the previous study (*tbl.* 3.2).

	88 (20%)	**88** (30%)	**96** (20%)	**96** (30%)	**96** (40%)
Thiourea	0	0	0	0	0
Urea	28	<10	33	<10	0
Imidazolidone	45	13	51	<10	0
Barbital	Precip.	59	Precip.	Precip.	Precip.

Table 3.2 - Binding constants K_a (M^{-1}) for receptor 96 and their comparison to receptor 88 with a selection of neutral guests in DMSO-d_6/$MeNO_2$-d_3 solutions with the percentage of DMSO used in brackets. All at 298 K and all errors estimated to be <10%.

In 20% DMSO-d_6/$MeNO_2$-d_3, receptor **96** gave the same results (within error limits) as those for receptor **88** in these solvent conditions, with addition of barbital again

causing precipitation. Changing to 30% DMSO-d_6/$MeNO_2$-d_3 also gave the same results with thiourea, urea and imidazolidone. However, addition of the barbital solution resulted in precipitation and so it was decided to switch to even more concentrated DMSO. In 40% DMSO-d_6/$MeNO_2$-d_3, precipitation was still observed which was surprising considering the butyloxy chain on this receptor was supposed to make the free receptor and resultant barbital complex more soluble.

3.4 A Bis(aminobenzimidazole) Analogue That Functions as an Anion Receptor

An analogue of receptor **88** which lacks the amide groups was prepared (compound **100**, *fig.* 3.18). Studies with this receptor would investigate the importance of the amide groups in preorganising the receptor through intramolecular hydrogen bonding.

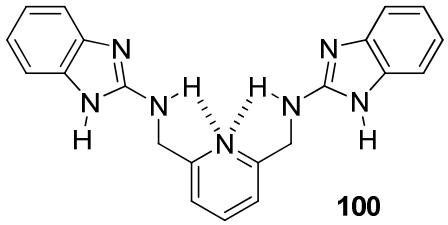

100

Figure 3.18 – Bisaminobenzimidazole analogue of receptor 88.

The favourable electrostatic interactions between the amine NH groups and the pyridine nitrogen atom should still be present which may preorganise the receptor into a cleft. However, without the amide groups, the benzimidazole groups are free to rotate in solution which should affect the neutral guest binding.

3.4.1 Synthesis

The synthesis of compound **100** was effected in three steps from 2,6-pyridinedimethanol. The first step involves oxidation of the alcohol to the aldehyde using selenium dioxide according to a literature procedure (*sch.* 3.4).[111]

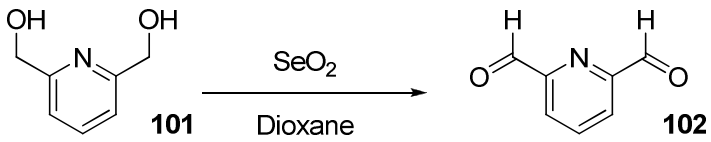

Scheme 3.4 - Synthesis of the aldehyde required for the preparation of 100.

The aldehyde was then reacted with two equivalents of 2-aminobenzimidazole to generate the Schiff base version of compound **100** which is immediately reduced using borohydride reducing agents to yield the product (*sch.* 3.5).

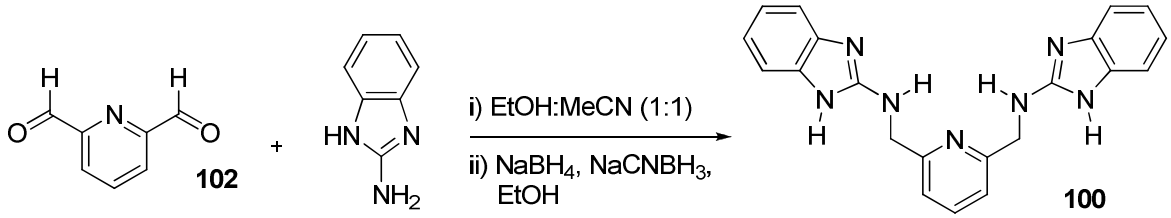

Scheme 3.5 - Synthesis of compound 100.

3.4.2 Solution Studies

Receptor **100** had similar solubility properties as receptor **88** being only soluble in more polar solvents such as nitromethane or DMSO. Proton-NMR titrations with receptor **100** and barbital in $MeNO_2$-d_3/DMSO-d_6 solutions showed no interaction between the two species. This finding confirms that without the amide groups the receptor is more disordered and cannot complex with neutral guests.

Although receptor **100** showed no interaction with barbital we reasoned that without the preorganisation of the benzimidazole groups the receptor might now be able to function as an anion receptor. Receptor **100** was titrated with a selection of anions in DMSO-d_6/0.5% H_2O solution (*tbl.* 3.3).

The results show the receptor is not very effective for binding anions in DMSO solution with even the more basic anions such as acetate giving a low association constant. And with the very basic fluoride anion, the receptor is deprotonated. However, the receptor did show a very high affinity for the tetrahedral 2^- charged sulfate anion. The affinity was so strong that it could not be measured by ^{1}H-NMR methods.[112]

Anion	K_a
F^-	Deprotonation
Cl^-	< 10
Br^-	< 10
I^-	< 10
NO_3^-	< 10
SO_4^{2-}	$>10^4$
$C_6H_5CO_2^-$	66
$CH_3CO_2^-$	94

Table 3.3 - Binding constants K_a (M^{-1}) for receptor 100 with a selection of anions as their TBA salts in DMSO-d_6/0.5% H_2O solution. All at 298 K and all errors estimated to be <10%.

Figure 3.19 shows the titration profile of sulfate with receptor **100** which plots concentration of anion (mol dm^{-3}) against chemical shift (ppm). The graph shows how the curve rises very steeply up to one equivalent of anion added and then levels out to a plateau. This is typical behaviour for a very strong 1:1 binding event.

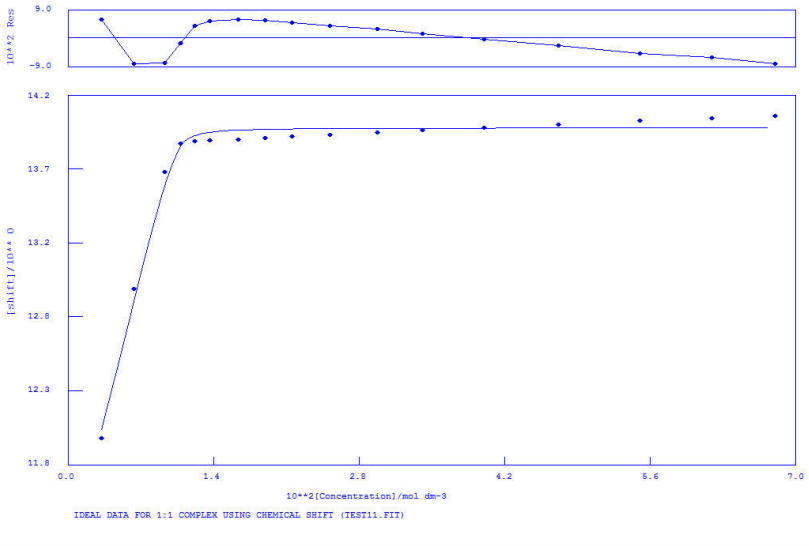

Figure 3.19 – Titration binding profile for receptor 100 with $(TBA)_2SO_4$ in DMSO-d_6.

Such a high selectivity for this anion compared to the other anions is remarkable and may not have arisen simply because it 2^- charged. This prompts a need for further binding studies to be carried out with this receptor and other tetrahedral anions, such as phosphates and 2^- charged anions, such as carbonate.

3.5 Towards a Neutral Guest Templated [2]-Catenane

The complexation of a barbiturate to receptor **88** in such a polar solvent system was an encouraging result. This motivated us to consider using this system in an attempt to construct a neutral guest templated [2]-catenane. This concept was intriguing because there are no catenanes reported (to the best of the author's knowledge) that have been templated using a neutral guest.

3.5.1 Catenane Design and the Synthetic Routes Attempted

It was decided to synthesise an extended version of receptor **88** to use as a precursor that could be macrocyclised to form the catenane rings. A ring closing metathesis using Grubb's catalyst was chosen to perform this macrocyclisation and interlock the rings upon guest templation, since it is well documented[113] and usually high yielding. This route would require pendant arms with terminal alkenes.

An ideal neutral template for this system was thought to be a spirobarbiturate species such as compound **103** (*fig.* 3.20). This spiro-compound is the smallest way to design the template and the twist in the structure at the 5-position on the barbiturate rings would provide the ideal shape to template the catenane formation.

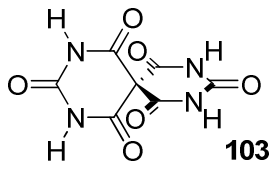

103

Figure 3.20 - Design of the neutral guest required for the templation of a [2]-catenane.

3.5.1.1 Preliminary Investigations

It was decided that adding better hydrogen-bond donor groups such as amide groups to receptor **88** would likely coordinate to the carbonyls at the 4- and 6-positions on the barbiturate rings. This would enhance binding and provide a way of appending the arms required for macrocyclisation. Compound **104** (*fig.* 3.21) was therefore hypothesised which would require the synthesis of a novel 2-aminobenzimidazole.

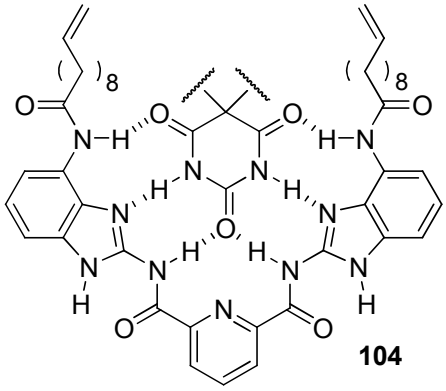

104

Figure 3.21 – Initial idea for the design of the catenane macrocycle.

In general, substituted 2-aminobenzimidazoles can be synthesised according to Scheme 3.6 which involves reaction of the corresponding benzene diamine with cyanogen bromide.[114]

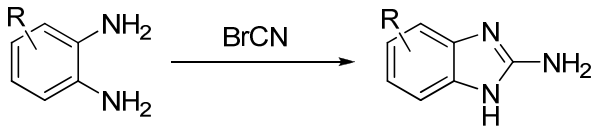

Scheme 3.6 – General synthesis of 2-aminobenzimidazoles.

Clearly the synthesis of compound **104** could proceed through 2-amino-4-nitrobenzimidazole **105** which could then be reacted with 2,6-pyridinedicarbonyl dichloride and reduced to the bisamine **106** (*sch.* 3.7).

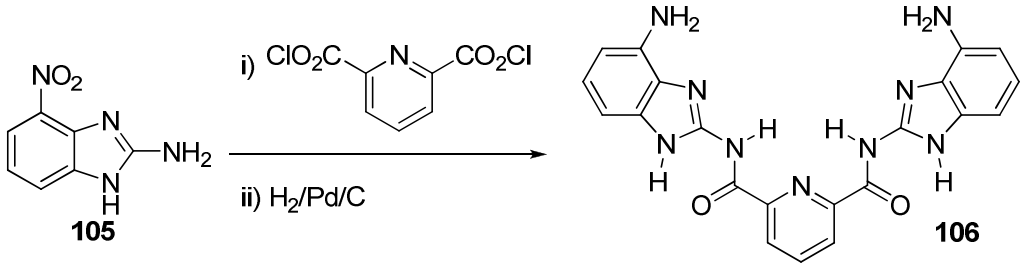

Scheme 3.7 – Proposed first step in the synthesis of compound 98.

However, reaction of **105** with the acid chloride did not work as it was found that with the nitro group on the benzene ring, the benzimidazole NH position was now more reactive than the amine. Subsequently, the benzimidazole NH was protected with a BOC group. Reaction of the protected benzimidazole with the acid chloride followed by deprotection did work but in very low yield and the product was very difficult to purify.

Nevertheless, it was possible to recrystallise the crude material from the reaction by slow evaporation of a DMSO solution of the crude solid.

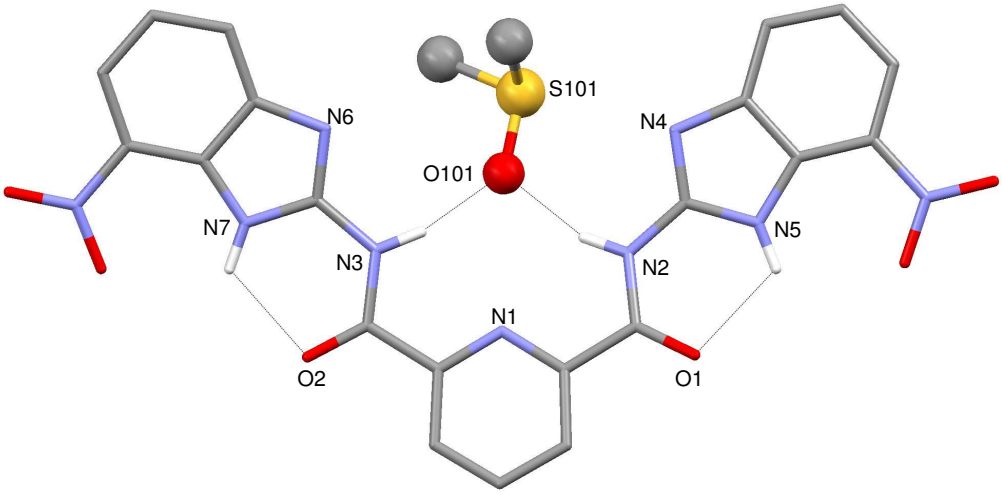

Figure 3.22 – X-Ray crystal structure of the nitro-product of the reaction to make compound 106. Non-acidic hydrogens have been omitted for clarity.

The structure (*fig.* 3.22) shows the compound binding a DMSO molecule with the expected intramolecular hydrogen bonding observed (N7···O2 2.723(5) Å, N5···O1 2.653(5) Å, N2···O101 2.834(5) Å, N3···O101 2.797(5) Å). Interestingly, the nitro-groups are both orientated out of the cleft rather than one in/one out or both in. It would be reasonable to assume that this conformation is also the most stable in solution. The nitro-groups would therefore be poorly aligned for the subsequent reduction and macrocyclisation.

Another approach was to reduce the nitro-group on the benzimidazole and form the amide before attaching it to the pyridine core. This required the BOC protection of the amine and benzimidazole groups. Stirring compound **99** with di-^{t}butyl dicarbonate at room temperature only resulted in BOC protection at the benzimidazole NH position, so heat and a base catalyst was needed to protect the amine as well. Subsequent reduction of the nitro-group did not work as the amine seemed to be unstable and would not react cleanly in the next step so this approach was abandoned.

3.5.1.2 Final Ideas

The second approach tried, required the attachment of ethylene glycol chains with terminal alkenes to the 5-position on the benzimidazole ring to result in macrocycle precursor **107** (*fig.* 3.23).

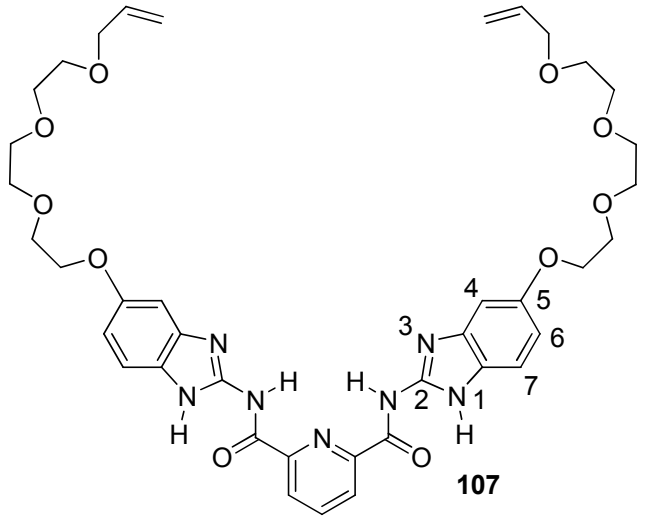

Figure 3.23 – Macrocycle precursor 107 and the benzimidazole numbering system.

In-house molecular modelling using SPARTAN revealed that the optimum number of atoms required to fit around the guest template and opposing catenane ring was 24 atoms. It was reasoned that even if there were tautomers where the glycol chains were attached to the 6-position, the precursor would still be able to macrocyclise.

Figure 3.24 shows how the catenane structure was envisaged showing how the spirobarbiturate guest would bind.

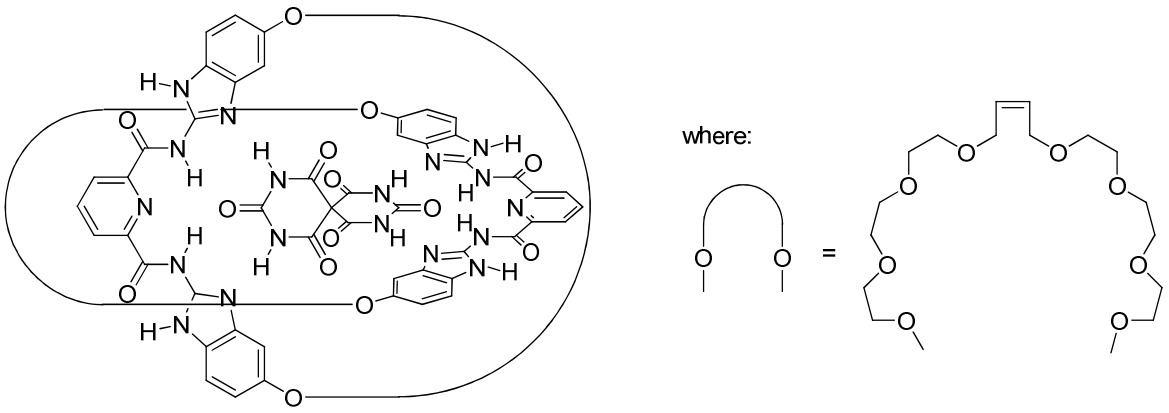

Figure 3.24 – Proposed catenane design.

It was thought that the macrocycle precursor could be accessed through 2-amino-5-hydroxybenzimidazole **109** (*sch.* 3.8). Its methoxy-precursor **108**, could be synthesised according to the general method (see *sch.* 3.6).

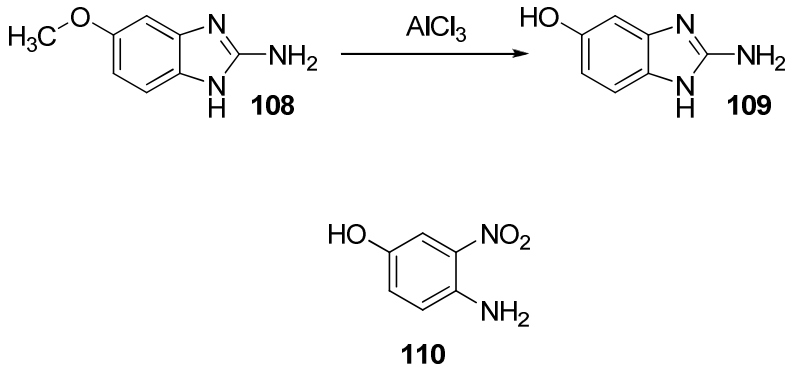

Scheme 3.8 – Synthesis of compound 109 and the alternative starting material 110.

However, it proved very difficult to purify the amino-alcohol and the next steps would require more BOC protections. So it was decided to start with the commercially available compound **110** which could be functionalised before conversion into the aminobenzimidazole (*sch.* 3.9).

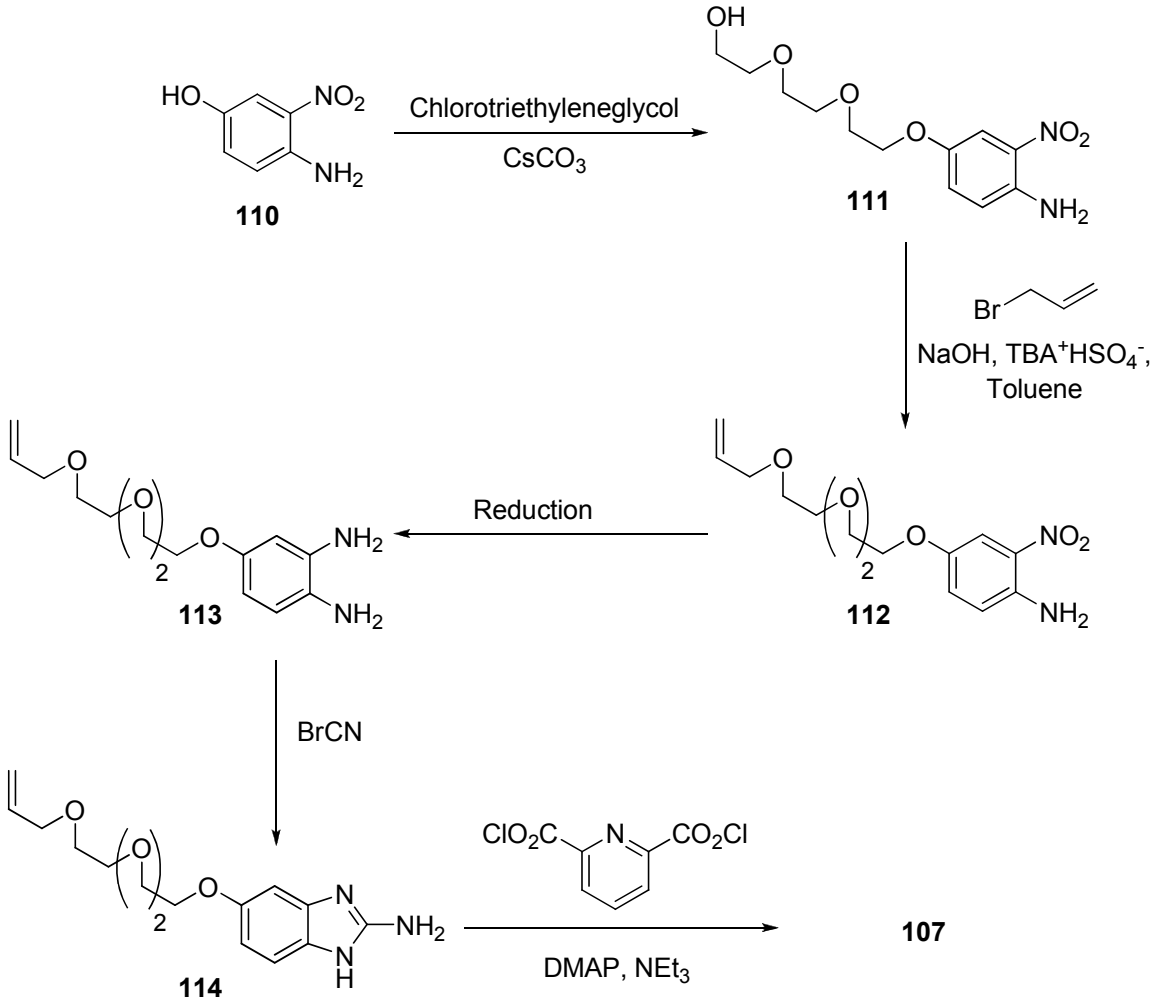

Scheme 3.9 – Alternative proposal for the synthesis of precursor 107.

The first step in the proposed synthesis worked well in high yield but there were immediately apparent problems with the synthesis. The second step worked in low yield because of substitution of allyl bromide onto the amine as well as the alcohol. BOC protecting the amine group could have solved this problem but the synthesis was not continued for the following reasons:

i) It was envisaged there would be problems reducing the nitro-group without saturating the alkene.

ii) It was also realised that the cyanogen bromide used to treat the diamine would also react with the alkene groups.

The first problem could be solved by using the nitro-selective tin(II) chloride as a reducing agent but the synthesis was becoming too complicated. Eventually it was decided

to reduce compound **111** and form the benzimidazole to make a hydroxyl-version of compound **107**. This did not work in sufficient yield or purity to perform any studies with.

The synthesis of the spirobarbiturate **103** was also attempted. From a literature review it was discovered that there were two approaches that could be taken to synthesise this compound.

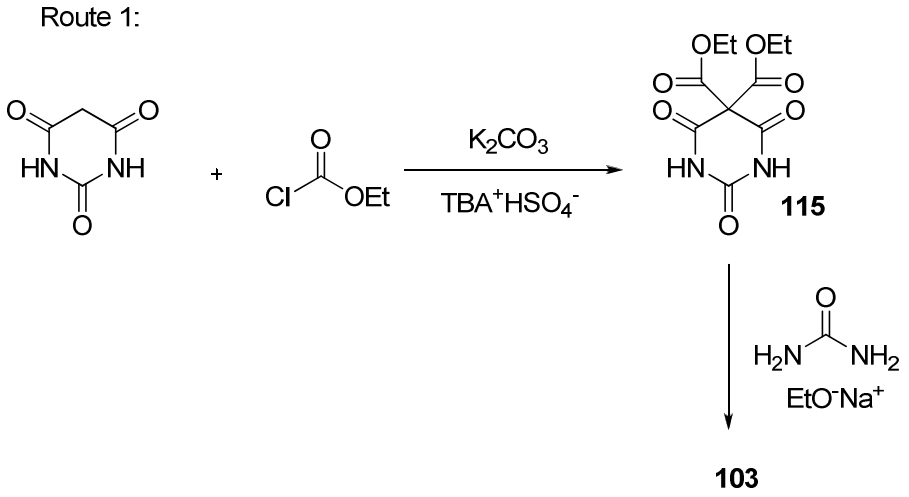

Scheme 3.10 – First route attempted for the synthesis of 103.

The first route was based on the realisation that the CH_2 position on barbituric acid could easily be deprotonated by a standard base such as potassium carbonate. So a 5,5-substitution of ethoxy-esters could be carried out (*sch.* 3.10). The reaction worked but the bis-substituted version (**115**) was not stable and decayed to the more stable mono-substituted version. Repeating the reaction and taking it straight through to the next step did not result in the product, presumably due to the unstable nature of compound **115**.

Route 2:

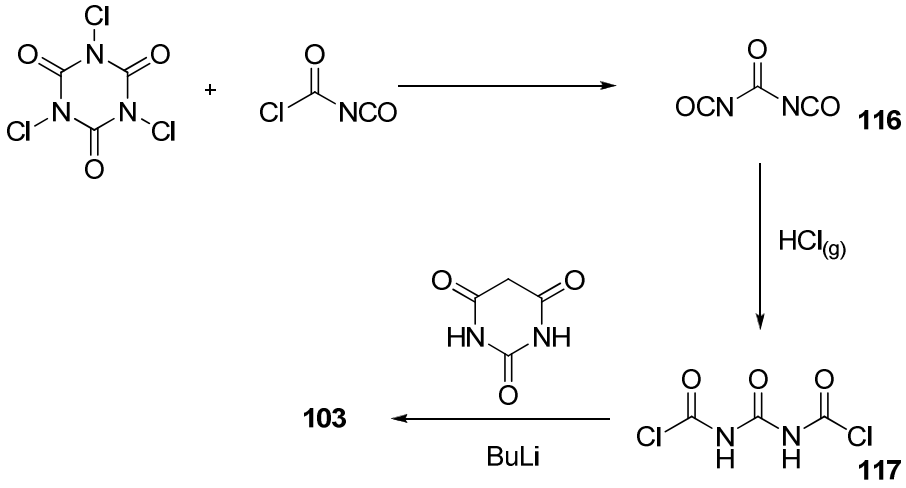

Scheme 3.11 – Second route attempted for the synthesis of 103.

The second route involves the generation of a urea bis-acid chloride (**117**) which is reported in the literature.[115, 116] The final product was insoluble in all organic solvents and this was thought to be because it may have been isolated as a lithium salt. Subsequent washing with HCl solution to remove the lithium did not make the compound more soluble, which made it difficult to characterise and confirm the product. A ^{1}H-NMR of the material in warm DMSO-d_6 revealed one peak for the four urea NH groups and a ^{13}C-NMR revealed the correct number of carbon atoms. A mass spectrum from DMSO also revealed a peak for the product but an accurate elemental analysis could not be obtained.

3.6 Conclusions

This chapter has explored the properties of some simple benzimidazole based receptors for neutral guest recognition. Building upon these results, we have then tried to exploit these simple clefts for the design of a more complex structure in the form a neutral guest templated [2]-catenane.

The structurally simple bis-benzimidazole functionalised 2,6-diamidopyridine **88** is capable of binding neutral guests in a highly polar solvent mixture such as 30% DMSO-d_6/$MeNO_2$-d_3. Whereas compounds possessing similar hydrogen bonding arrays but lacking some of the intramolecular hydrogen bonding interactions present in compound **88** do not, under these conditions, interact with the neutral guests studied. For example, removing the amide groups (compound **100**), methylating the benzimidazoles (compound **90**) or removing one of the benzimidazole (compound **91**) groups resulted in no interaction with the guests studied.

Unfortunately, more substituted benzimidazoles proved more difficult to work with due to their reactivity, difficulty to purify and sometimes their associated solubility problems. This made construction of the more complex catenane architecture a significant challenge.

Ideas for further work with these systems should include further investigations into their potential for use as HCl, chloride or bicarbonate membrane transporters. An encouraging preliminary investigation of compound **91** involved crystalising it in the presence of HCl which resulted in the crystal structure shown in Figure 3.25.

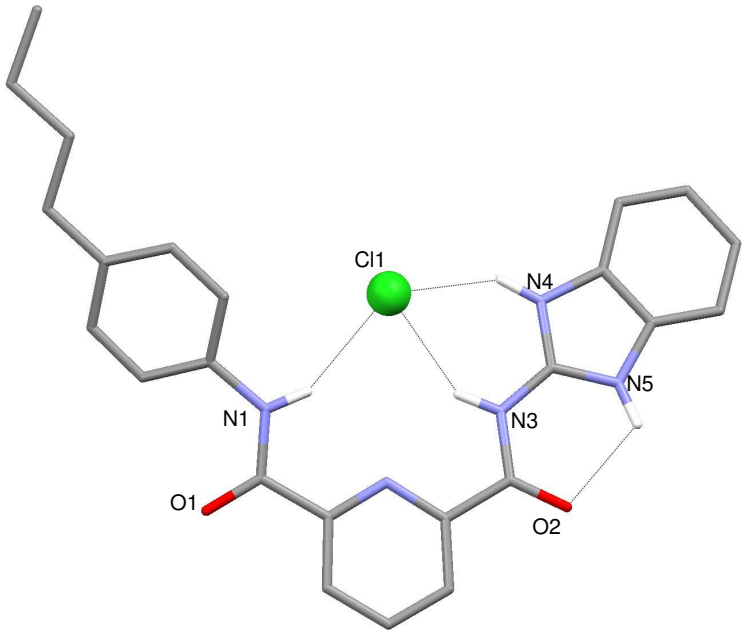

Figure 3.25 – HCl complex of compound 91. Non-acidic hydrogens omitted for clarity.

The crystals were grown by a slow evaporation of a methanolic HCl solution of compound **91**. The structure shows a chloride anion bound in the cleft through three hydrogen bonds (N1···Cl1 3.365(2) Å, N3···Cl1 3.150(2) Å, N4···Cl1 3.041(2) Å) with an intramolecular hydrogen bond between the benzimidazole NH and the amide carbonyl (N5···O2 2.743(3) Å). One of the hydrogens involved in the complexation is from the protonated benzimidazole nitrogen group. The complex actually forms a hydrogen bonded dimer through hydrogen bonded methanol molecules in the structure (*fig*. 3.26).

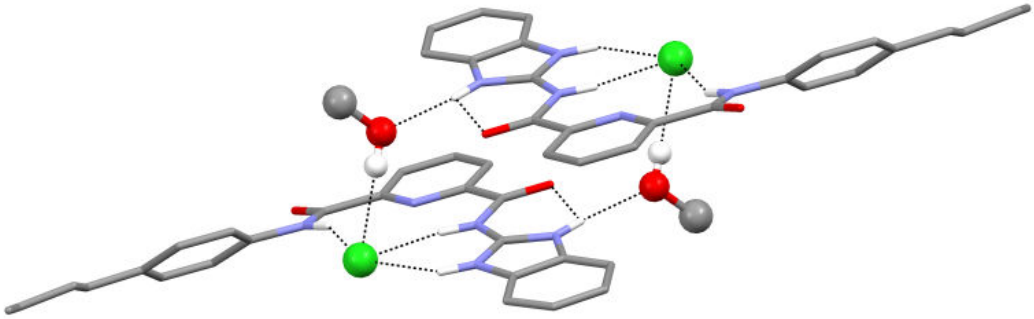

Figure 3.26 – Hydrogen bonded dimer of the HCl complex of compound 85.

Although the crystal structure result was encouraging, unfortunately, vesicle transport screening studies in our group (conducted by Dr. Joachim Garric) revealed that the HCl complex of **91** did not remain soluble in the medium (water/DMSO) used in the study.

It seemed that much of the problems with this chemistry arose from lack of solubility of the compounds. An attempt to rectify this problem with the synthesis of receptor **96** failed. However, more can be done to make these compounds more soluble, such as attaching longer, branched alkyl chains to the receptors or appending glycol chains.

Chapter 4 – Triazoles in Anion Receptor Chemistry

4.1 Introduction

In 1963 Rolf Huisgen published an extensive review of 1,3-dipolar cyclocadditions., which included a synthesis for a 1,2,3-triazole from alkyne and azide precursors.[117, 118] It followed that these syntheses became known as Huisgen 1,3-dipolar cycloadditions and the 1,2,3-triazole synthesis is shown in Figure 4.1.

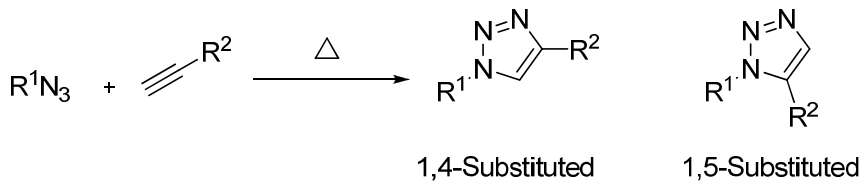

Figure 4.1 – Synthesis of triazoles by Huisgen 1,3-dipolar cycloaddition.

However, the problem with the reaction was that it requires prolonged heating to work and results in both the 1,4- and 1,5-substituted products in roughly equal proportions which somewhat limited its application.

In 2001 K. Barry Sharpless and co-workers introduced the concept of 'click' chemistry which was supposed to be a 'guiding principle'.[119] The principle revolved around the endeavour to generate substances by simple reactions from readily available starting materials under kinetic control, with high yields, inoffensive by-products and very simple non-chromatographic workup.[119] It was inspired by nature's processes and was devised to meet the demands of modern day chemistry and in particular, the demands of drug discovery.[119, 120] The Huisgen synthesis of triazoles provided an excellent example of a reaction that could potentially meet these stringent requirements: the starting materials are usually easily synthesised or commercially available, kinetically stable and tolerant to a wide range of functional groups and reaction conditions.[120] It was then discovered[121, 122] that this reaction could be greatly accelerated by a copper(I) catalyst in the presence of water to form exclusively the 1,4-substituted product, usually in high yields. In addition,

the products of these reactions usually require a very simple work-up with no chromatography. It is obvious that this near perfect reaction fits all the principles of 'click' chemistry, so the term has evolved to become synonymous with the copper(I) catalysed Huisgen synthesis of 1,4-substituted 1,2,3-triazoles.

The 1,2,3-triazole heterocycle has interesting properties that give rise to a fascinating array of applications.[120, 123] These properties were neatly summarised in a recent paper by Li and Flood[124] as follows:

i) it can be deduced that the electronegativities of the three nitrogens combine to polarise the CH bond and,

ii) the lone pairs of electrons on the nitrogen atoms act to establish and orient along the CH bond to create a large dipole (~5D) whose positive end points towards to the hydrogen atom.

These features make the CH group a remarkably good hydrogen bond donor whilst the nitrogens at the 2- or 3-positions are good hydrogen bond acceptors. As a result of these characteristics, triazoles have been thought of as candidates for amide bond surrogates.[124]

Given these properties, one of the useful applications of the triazole group would be to employ it in a receptor for anions. One of the first examples of such an application, reported in 2008 by Li and Flood, was a 1,2,3-triazole-phenyl based macrocycle (**118**) which has a high affinity for chloride in DCM.[125]

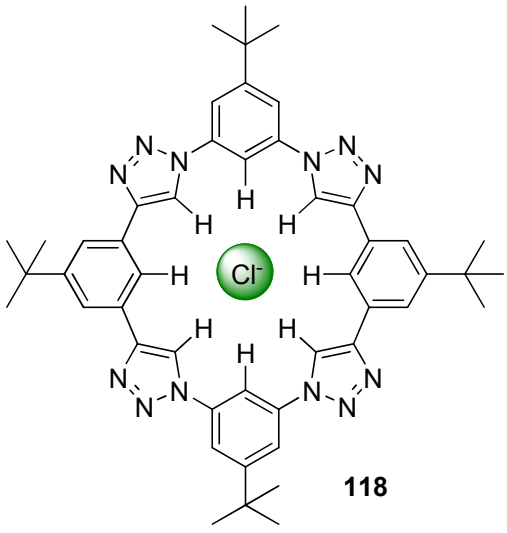

118

Figure 4.2 – Triazole macrocycle for chloride.

The macrocycle consists of eight conjoined ring systems wherein four triazoles alternate with four phenyl rings. The design allows for minimal deviations from ideal bond angles and minor steric interactions between hydrogens on adjacent ring systems.[125]

The synthesis of **118** was efficient; proceeding in 27% yield over seven steps using Sharpless-Meldal click chemistry and standard Sonogashira coupling reactions. A UV-vis titration of the macrocycle in DCM revealed a 1:1 binding stoichiometry and an association constant (K_a) of 130000 M^{-1}. A ^{1}H-NMR titration of **118** with tetrabutylammonium chloride in CD_2Cl_2 resulted in a shift of the triazole CH peaks and the phenyl CH peaks pointing into the cleft which confirms there are eight CH···Cl^- hydrogen bonds. It is important to note that the binding affinity relies heavily on the fact that the triazoles are rigidly preorganised in this example, as suggested by a much lower binding constant ($7M^{-1}$) of an acyclic analogue of **118**.

Further studies[124, 126] with this macrocycle revealed that it had a selectivity for chloride over other halides in DCM as follows; Cl^- ($1.1x10^7$ M^{-1}) > Br^- ($7.5x10^6$ M^{-1}) >> F^- ($2.8x10^5$ M^{-1}) >> I^- ($1.7x10^4$ M^{-1}),[124] which infers that the fluoride anion was too small for the cavity, whilst the iodide anion was too large for the cavity. And in fact it was found[126] that the iodide anion forms a sandwich complex with two equivalents of the macrocycle in solution.

Other examples which illustrate the versatility of the 1,2,3-triazole-phenyl motif in foldamers[127] and linear nonamers[128] have been reported by other authors.

The first anion receptor to employ 'click' chemistry in its construction was that of Pandey and co-workers who united click chemistry with the established[129, 130] tool of using steroid based frameworks to append hydrogen bond donor groups for anion recognition.[131] They first synthesised two bis-triazole macrocycles and then treated them with methyl iodide, followed by ammonium PF_6^- to form the charged methyl-triazolium macrocycles **119** and **120** (*fig.* 4.3). An acyclic analogue (**121**) of the macrocycles was also prepared as a control compound.

Proton-NMR titrations of the compounds were conducted in $CDCl_3$ with a selection of anions as their tetrabutylammonium salts. The results showed that all the receptors bound in a 1:1 stoichiometry with similar binding constants in the range 100-690 M^{-1} for the halides.[131]

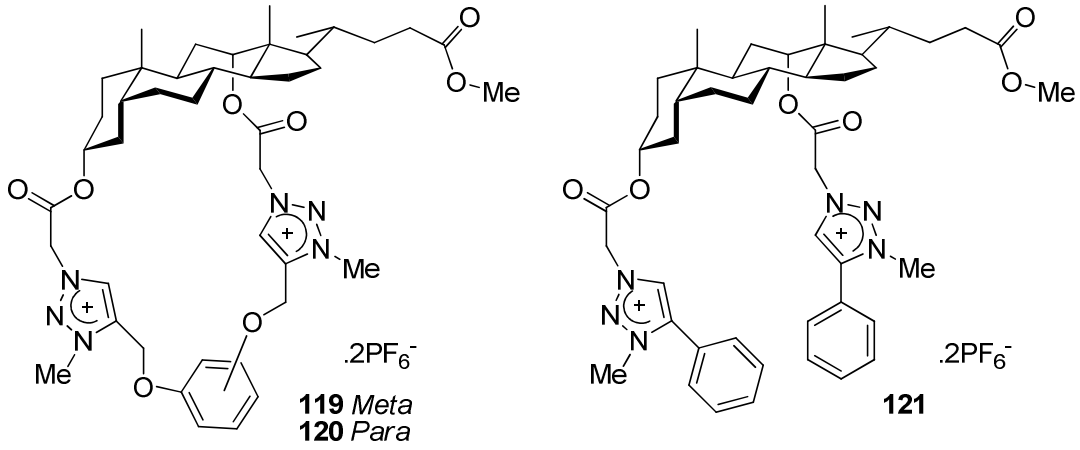

Figure 4.3 – Pandey and co-worker's triazolium-steroid macrocycles and an acyclic control analogue.

Interestingly, macrocycle **120** and the acyclic **121** showed a slight selectivity for $H_2PO_4^-$ (K_a = 1100 and 1920 M^{-1} respectively), whereas the *meta*-substituted **119** did not show any interaction with this anion. The authors hypothesised that the *para*-substituted **120** presents a larger cavity so it is able to accommodate the larger anion, whilst the acyclic **121** has more flexibility to arrange around the anion.[131] Overall, the results showed that there was no significant advantage to having a macrocyclic framework in the case of these receptors.

4.1.1 Strapped Calix[4]pyrroles

Given the useful properties of triazoles and interesting applications of them by other groups, particularly in anion recognition, it was thought interesting to apply this chemistry to our lines of work. Gale and Sessler have reported that *meso*-octamethylcalix[4]pyrrole (**23**, *fig.* 4.4) is a highly efficient receptor for fluoride and chloride (see Chapter 1). Ways of functionalising the basic calix[4]pyrrole framework followed and some of the possible modifications are shown in Figure 4.4.[132]

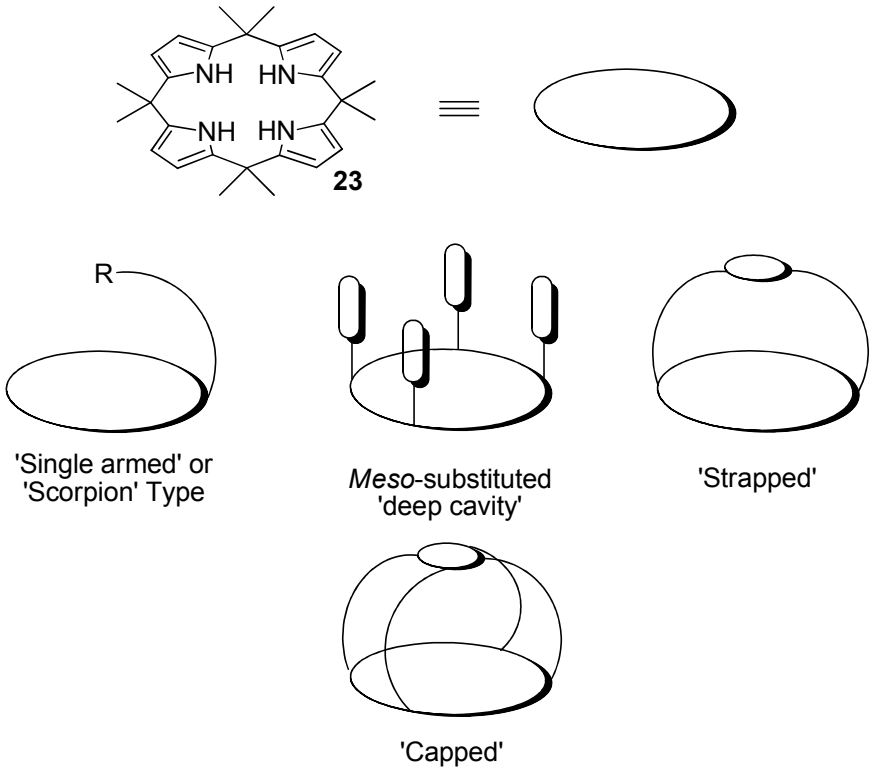

Figure 4.4 – Schematic representation of possible ways to modify the basic calix[4]pyrrole core.[132]

Early modifications of calix[4]pyrrole involved functionalising the β-pyrrolic or *meso*-positions since these are the easiest changes to effect. Whilst highly versatile, these systems have some limitations, particularly with regard to potential enhancements in selectivity and affinity.[132] Further developments led to the single armed versions which were inspired by similar modifications applied to sapphyrin based receptors.[23] However, the idea of strapped or capped calix[4]pyrroles was most attractive, because they would have added preorganisation which would improve anion binding and allow selectivity for specific sized anions. Research has particularly focused on the former because it was considered[132] that capped calixpyrroles could be *too* rigid, which may reduce anion affinity. In addition, they are inherently more complex to synthesise.

It was not until 2002 that Lee and co-workers first reported the successful synthesis of a strapped calixpyrrole **122** (*fig*. 4.5).[133] The role of the CH in the anion binding with these strapped calix[4]pyrroles was studied by comparing **122** to pyrrole (**123**) and furan (**124**) strapped analogues.[134] Binding constants were determined by isothermal calorimetry (ITC) in dry acetonitrile with tetrabutylammonium chloride for **122**, **123** and **124** and compared against the original octamethylcalix[4]pyrrole **23** (shown in *fig*. 4.4 and discussed in Chapter 1).

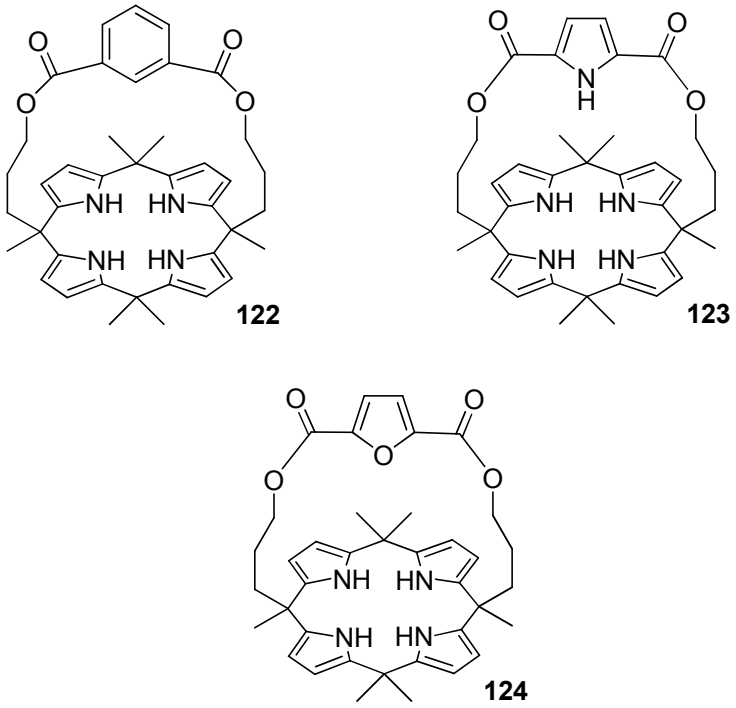

Figure 4.5 – The first strapped calixpyrrole (122) and the recent pyrrole (123) or furan (124) strapped versions for comparative analysis.

The results showed that **122** had a ten-fold increase in affinity for chloride (K_a = $2.2x10^6$ M^{-1}), whilst **123** had an 80 fold increase (K_a = $1.8x10^7$ M^{-1}) when compared to the parent calix[4]pyrrole **23** (K_a = $2.2x10^5 M^{-1}$). Conversely, compound **124** had a slightly lower binding constant (K_a = $1.9x10^5$ M^{-1}), which suggests the significant role the CH plays in binding the anion.

The crystal structure (*fig.* 4.6) of calixpyrrole **122** with tetraethylammonium chloride revealed the binding of the anion via a total of five hydrogen bonds; four pyrrole NH···Cl^- (average N···Cl^- distance 3.285 Å) and a CH···Cl^- (C···Cl^- 3.793 Å). The phenyl group of the strap is canted ~70° relative to the centre of the calix[4]pyrrole ring. This is because of the need to accommodate a tetraethylammonium cation which is not shown in this representation.[135]

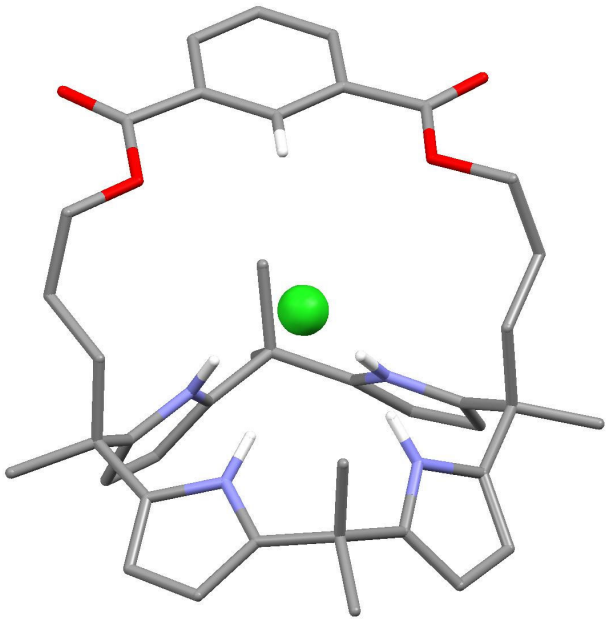

Figure 4.6 – X-ray crystal structure of 122 with chloride.

Studies that vary the length of the strap on compound **122**, to investigate the effects on binding affinity, have shown that selectivities for certain size anions can be achieved by simply making the strap larger or smaller in the case of these isophthaloyl strapped calixpyrroles.[135]

The synthesis of strapped calixpyrroles is particularly versatile which has lead to many other variations of strapped calixpyrroles not detailed here.[132, 136, 137] As a progression of this body of work, we introduced a triazole strap into the calix[4]pyrrole using 'click' chemistry.

4.2 'Clicked'-calix[4]pyrrole

Initially it was decided to introduce one triazole into the strap to keep the complexity of the receptor to a minimum. The length of the strap was also an important consideration: most strapped calix[4]pyrroles reported to date have a strap length of 17±1 atoms (see *fig.* 4.7 for strap length numbering system used). Indeed, Sessler and co-worker's study into varying the strap length on their strapped calix[4]pyrroles had shown this to be the optimum length for binding chloride.[135] Finally, using simple alkyl chains in the strap construction, 'clicked'-calix[4]pyrrole **125** was envisaged (*fig.* 4.7).

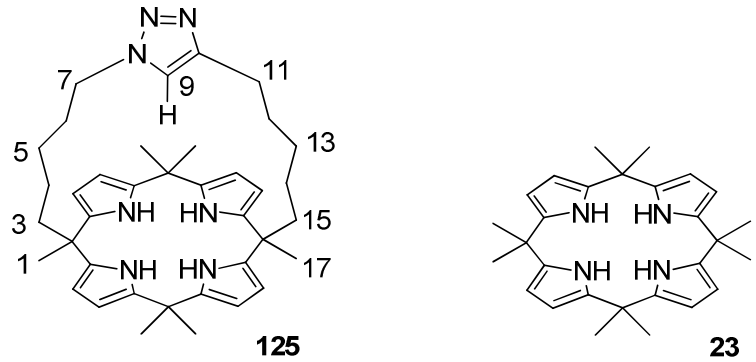

Figure 4.7 – 'Clicked'-calix[4]pyrrole design and the parent calix[4]pyrrole 23.

The additional CH hydrogen-bond donor provided by the triazole, was expected to increase the affinity for anions of interest (compared to **23**), and produce interesting complexation behaviour in solution and the solid state.

4.2.1 Synthesis

In general, the synthesis of strapped calix[4]pyrroles can potentially be achieved by two ways: either initial construction of the calixpyrrole core, followed by spanning with a strap or, creation of a linked precursor (incipient strap) followed by calixpyrrole ring formation.[132] The latter method was adopted for the synthesis of **125** because it was the first[133] and most successful approach used to date. The main drawback to this synthetic route is that the final step (calixpyrrole ring formation) is often extremely low yielding (typical yields reported; 4-16%).

The 'clicked'-calix[4]pyrrole **125** was successfully synthesised according to the route outlined in Scheme 4.2. The first step involves generating the appropriate terminal alkyne and azide linkers which can be 'clicked' together to form the strap. This was achieved by first synthesising a bromoketone precursor according to a literature procedure (*sch*. 4.1).[138]

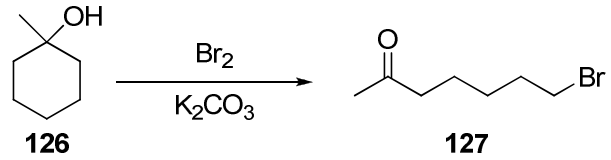

Scheme 4.1 – Synthesis of the bromoketone.

The ketone was protected as a cycloketal[139] then converted to the alkyne (**129a**) and azide (**129b**) by nucleophilic substitution of the bromine using $NaCCH_3$ and NaN_3 respectively (*sch*. 4.2). The triazole was formed by reacting **129a** and **129b** in the presence of a copper(I) catalyst. There are a range of different methods[140] of sourcing copper(I) for the cycloaddition; although it can be sourced directly (*e.g.* copper(I) iodide), it is better generated *in-situ* by reduction of copper(II) salts, which are less costly and often purer than copper(I) salts.[121] We employed the most widely used method; copper(II) sulfate mixed with sodium ascorbate as the reductant.

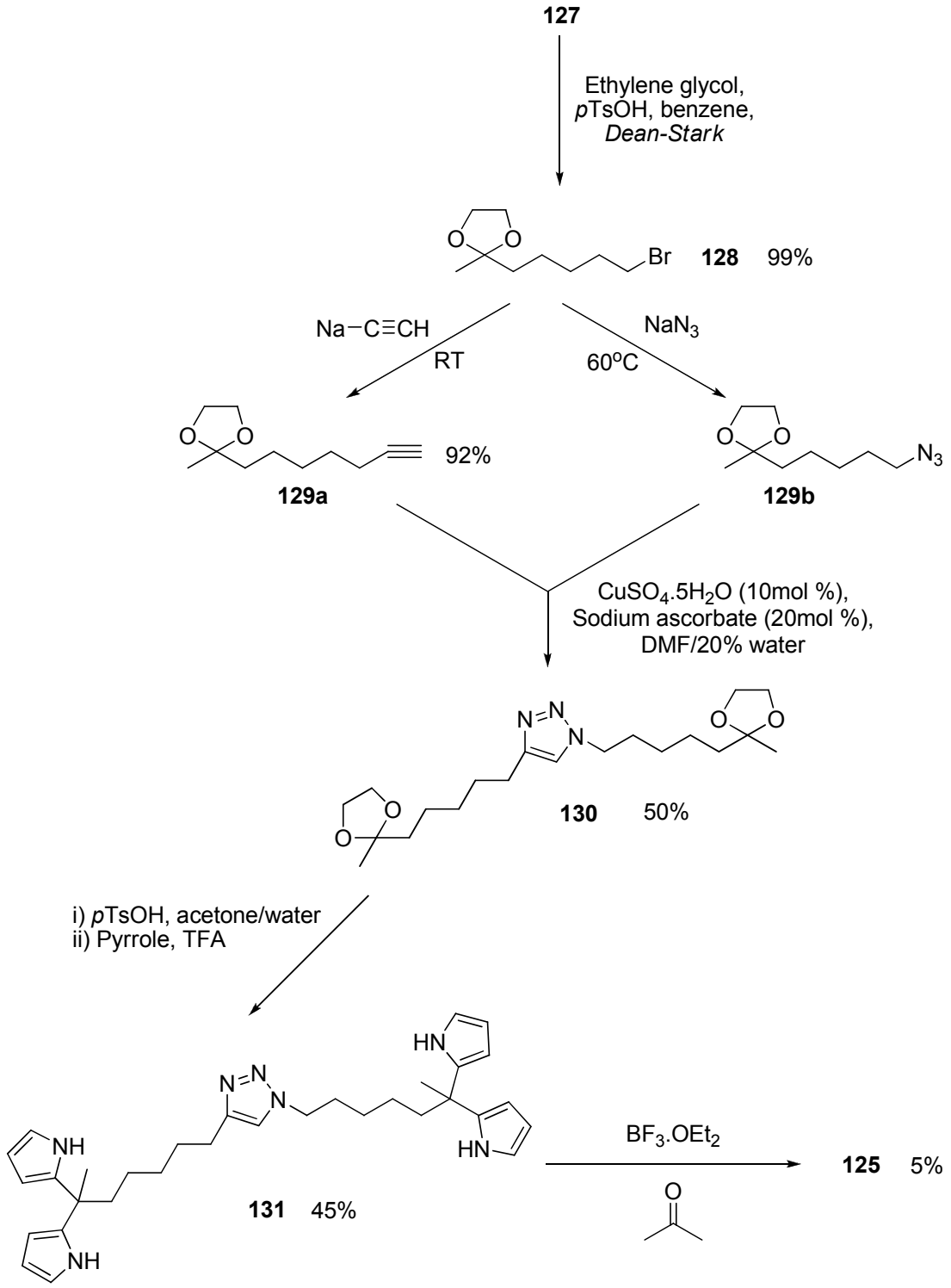

Scheme 4.2 – Synthesis of 'clicked'-calix[4]pyrrole 119.

The appended triazole **130** was deprotected to yield the diketone and was reacted in pyrrole with a TFA catalyst to form the 'dipyrromethane' precursor **131**. Finally, the 'clicked'-calix[4]pyrrole **125** was generated by reaction by reaction in acetone with a catalytic amount of BF_3OEt_2.

This synthesis is efficient because it is convergent and, with the exception of the last step, is moderately high yielding. The 'clicked'-calixpyrrole **125** could not be purified by column chromatography and so required recrystallisation from methanol which isolated a methanol solvate of the pure material.

4.2.2 Solid State Analysis

Single crystals of compound **125** were prepared by recrystallisation from methanol/diethyl ether. The structure (*fig.* 4.8) reveals the calixpyrrole adopting a 1,2-alternate conformation in which two methanol molecules are each bound to two pyrrole NH groups.

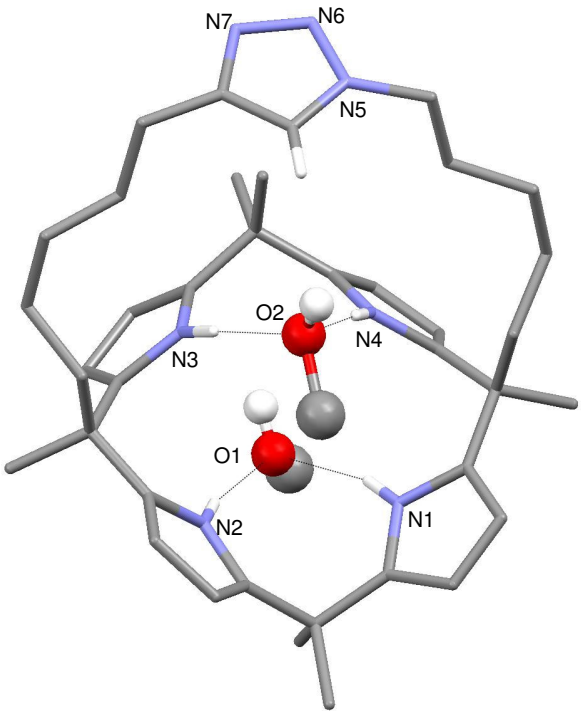

Figure 4.8 – X-ray crystal structure of the methanol solvate of compound 125 showing the calixpyrrole macrocycle adopting the 1,2-alternate confirmation.

Compound **125** also spontaneously crystallised by wetting the material with a few drops of DMSO. Again, the structure (*fig.* 4.9) shows the calixpyrrole adopting a 1,2-alternate confirmation with two molecules of DMSO each bound to two pyrrole NH groups and one bound to the triazole CH. The triazole ring in the structure is disordered.

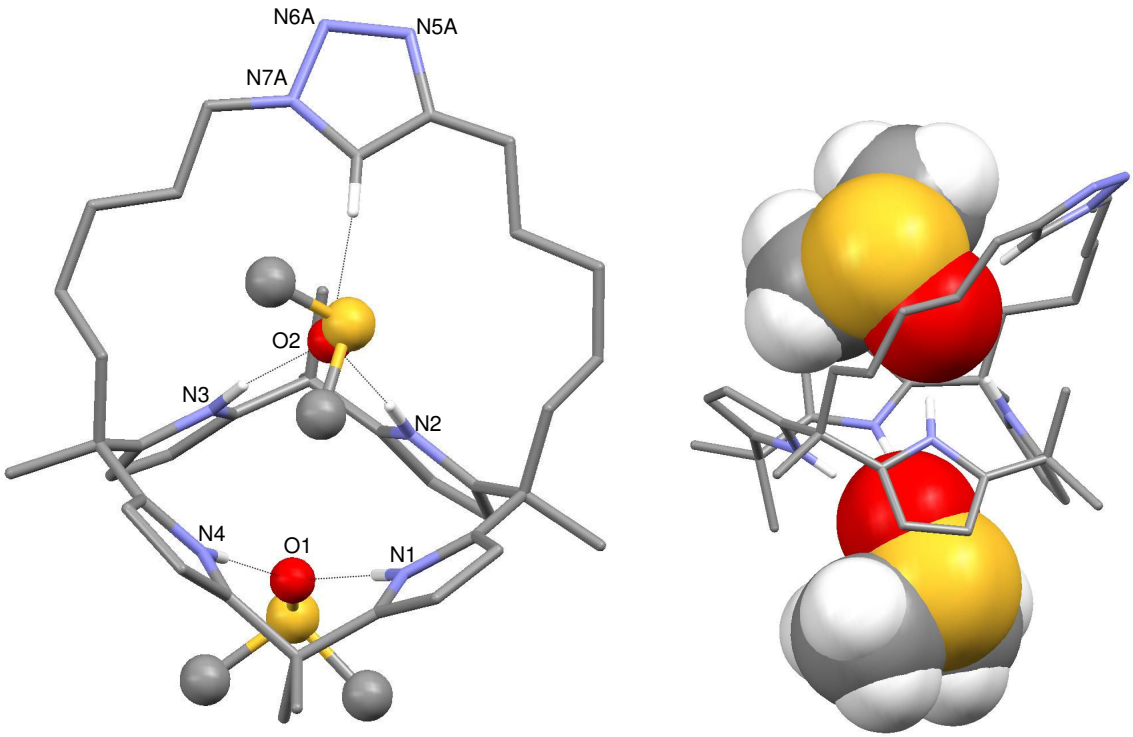

Figure 4.9 – X-ray crystal structure (left) of the DMSO solvate of compound 125 from the minimum amount of DMSO. Also shown, is the structure with the DMSO molecules depicted in a space filling representation (right).

From the space filling representation it can be seen that the strap is tilted off at an angle in order to accommodate the DMSO molecule. This is similar to the effect observed with Sessler and Lee's strapped calix[4]pyrroles.[133, 135]

X-ray quality crystals of a pseudopolymorph of the DMSO structure described above were obtained from dilute solutions of **125**. In this structure (*fig*. 4.10) the calixpyrrole still adopts the 1,2-alternate conformation but binds three DMSO molecules instead of two: one molecule of DMSO binds the triazole CH and the other two each bind to two of the pyrrole NH groups. The triazole ring is also not disordered in contrast to the other structure.

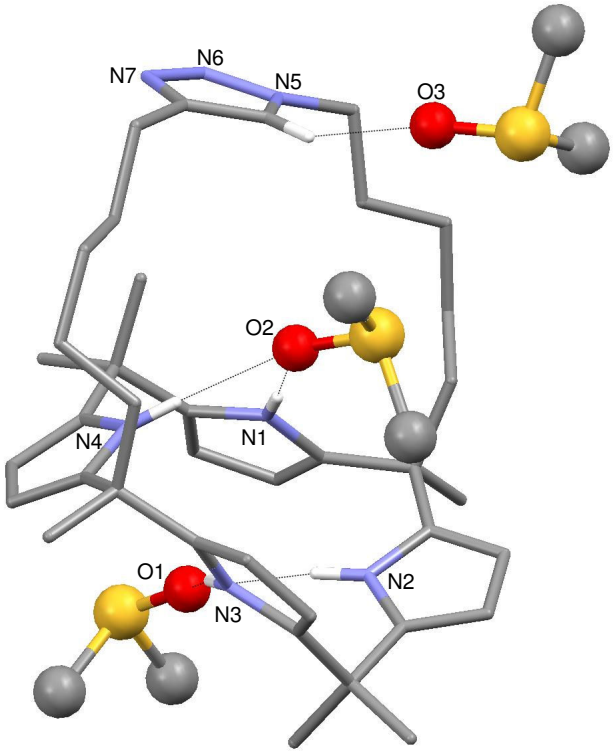

Figure 4.10 – X-ray crystal structure of the pseudopolymorph of the DMSO solvate of compound 125 from a dilute DMSO solution.

4.2.3 Binding Studies in Solution

It was predicted that the binding constants would be too high ($K_a > 10^4\ M^{-1}$) to accurately measure by NMR techniques.[112, 135] However, it was fundamental to use this technique to demonstrate that the triazole CH is involved in hydrogen bonding to anions in solution. So the anion binding properties of **125** were studied by ^{1}H-NMR titrations in acetonitrile-d_3 solution at 298 K. Under these conditions addition of tetrabutylammonium chloride resulted in slow exchange on the NMR timescale, with peaks representing both complexed and uncomplexed receptor at 0.5 equivalents of chloride addition (see *fig.* 4.11). At 1 equivalent of anion addition, the uncomplexed peaks disappear and further addition of anion results in no further change in the spectrum. The triazole CH peak shifted significantly downfield (by 1.33 ppm) in this process which suggests strong hydrogen-bond formation. In addition, the β-pyrrole CH groups shift upfield slightly which may be due to the presence of tetrabutylammonium in the vacant 'cup' under the calixpyrrole.

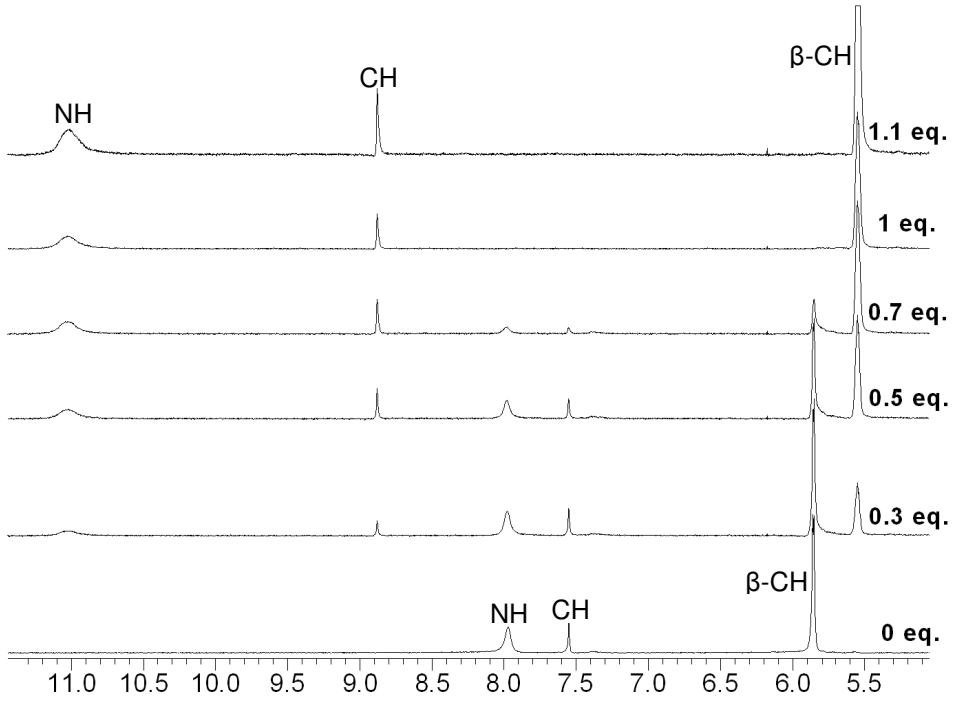

Figure 4.11 – Partial ^{1}H-NMR spectrum of compound 125 upon addition of tetrabutylammonium chloride in acetonitrile-d_3 solution at 298 K.

Proton-NMR titrations with bromide, dihydrogen phosphate, acetate and bicarbonate all revealed strong binding events, with triazole CH hydrogen bonding in all cases (see *Appendix* for NMR stack plots with these anions). Addition of tetrabutylammonium nitrate to compound **125** resulted in weak enough binding to allow an association constant (K_a) of 3790 M^{-1} to be calculated.

Work by the groups of Sessler[135] and Schmidtchen[32] has determined that isothermal calorimetry (ITC) is the most reliable method for determining binding constants for calix[4]pyrrole species, especially when $K_a > 10^4$ M^{-1}. Hence ITC titrations with compound **125** were conducted by Professor Franz P. Schmidtchen at the Technical University of Munich (Germany).

The preliminary ITC titrations were conducted with various tetraalkylammonium anion salts in absolute (<10 ppm water) acetonitrile at 303 K. The molecular weights were calculated on the basis of two additional molecules of methanol (as observed in the crystal structure and ^{1}H-NMR spectrum) per host compound. Absolute concentrations in the cell ranged from 0.3 mM to 1 mM with the concentrations in the syringe being about tenfold higher. Two types of measurements were conducted; the first (*tbl.* 4.1) involved the

titration of guest into host solution, whilst the second (*tbl.* 4.2) involved the titration of host into guest solution.

Salt	K_{ass} (M^{-1})	ΔG^o (cal K^{-1} mol^{-1})	ΔH^o (cal K^{-1} mol^{-1})	ΔS^o (cal K^{-1} mol^{-1})
TEA^+Cl^-	1.3 e6	-8.47 e3	-12.0 e3	-11.6
TEA^+BnO^-	6.0 e3	-5.23 e3	-9.90 e3	-15.4
$TBA^+H_2PO_4^-$	8.2 e3	-5.42 e3	-4.61 e3	+2.7
TEA^+NCO^-	1.1 e6	-8.38 e3	-13.35 e3	-16.3
$TEA^+HCO_3^-$	2.0 e5	-7.36 e3	-11.40 e3	-13.3

Table 4.1 – ITC titration results for compound 125 and various tetraalkylammonium salts in absolute acetonitrile at 303 K. In these experiments anionic guests were titrated into a solution of the host.

The results show that, with the exception of dihydrogenphosphate, all the host-guest interactions appear as clean 1:1 stoichiometric binding processes. An unusual binding stoichiometry is exhibited with dihydrogenphosphate. This could potentially be because the protons on this anion are acidic which means it can be deprotonated by the receptor. This can often lead to strange binding stoichiometries and complicates the fitting of data to an ideal model.

Salt	K_{ass} (M^{-1})	ΔG^o (cal K^{-1} mol^{-1})	ΔH^o (cal K^{-1} mol^{-1})	ΔS^o (cal K^{-1} mol^{-1})
TEA^+Cl^-	2.6 e6	-8.89 e3	-11.88 e3	-9.8
TBA^+F^-	1.6 e5	-7.19 e3	-11.34 e3	-13.6
TBA^+AcO^-	1.6 e5	-7.23 e3	-13.12 e3	-19.4
TBA^+*p*NO_2BnO^-	1.3 e3	-4.32 e3	-8.45 e3	-13.9

Table 4.2 – ITC titration results for compound 125 and various tetraalkylammonium salts in absolute acetonitrile at 303 K. In these experiments the host was titrated into solutions of the anionic guests.

In general, the smaller anions bind a lot more intensely to compound **125** than to the parent calix[4]pyrrole **23**.[32] Only if the steric bulk on the anion becomes too large, then the stabilities suffer substantially due to unfavourable association entropies.

Further preliminary ITC titrations were conducted in dry DCM with compound **125** by titrating a host solution into a selection of tetraalkylammonium anion solutions at 303K. Again, the molecular weights were calculated on the basis of two additional molecules of methanol per host compound. Absolute concentrations in the cell were ~0.6 mM with the concentrations in the syringe being about tenfold higher.

In the case of chloride, the results (*tbl.* 4.3) revealed that the association constants are reliant on the type of countercation, with tetraethylammonium chloride possessing an

affinity five times higher than tetrabutylammonium chloride. This phenomenon has recently been observed with the parent calixpyrrole **23** and various chloride salts.[30]

Salt	K_{ass} (M^{-1})	ΔG^o (cal K^{-1} mol^{-1})	ΔH^o (cal K^{-1} mol^{-1})	ΔS^o (cal K^{-1} mol^{-1})
TEA^+Cl^-	2.7 e6	-8.91 e3	-13.2 e3	-14.2
TBA^+Cl^-	4.7 e5	-7.86 e3	-11.8 e3	-13.0
$TEA^+NO_3^-$	6.1 e5	-8.38 e3	-7.68 e3	-8.0
$TEA^+HCO_3^-$	1.8 e3	-7.27 e3	-9.93 e3	-8.7

Table 4.3 - ITC titration results for compound 125 and various tetraalkylammonium salts in dry DCM at 303 K.

The results also show that, in contrast to compound **23**, the complex stabilities of **125** are not greatly enhanced in the less polar DCM when compared to the more polar acetonitrile. For example, in the case of TEA chloride (*tbl.* 4.4), the parent compound **23** in DCM binds chloride weaker than in the more polar acetonitrile because of an unfavourable complexation entropy overcompensating the more exothermic enthalpy output. However with the 'clicked'-calixpyrrole **125**, there is an almost ideal balance of the enthalpic/entropic gains and losses which attests to the less significant role of solvation in this case. However it must be noted that the high error values encountered during the ITC measurements of **125** in DCM (see *appendix*) may have distorted these results somewhat. These errors may have arisen from evaporation of the highly volatile solvent or electrical interference with the equipment during those measurements. Future experiments could involve using a less volatile chlorinated solvent such as DCE in place of the DCM to overcome these problems.

	Acetonitrile				Dichloromethane			
Host	K_{ass} [M^{-1}]	ΔG^o/ kcal mol^{-1}	ΔH^o/ kcal mol^{-1}	T ΔS^o/ kcal mol^{-1}	K_{ass} [M^{-1}]	ΔG^o/ kcal mol^{-1}	ΔH^o/ kcal mol^{-1}	T ΔS^o/ kcal mol^{-1}
23	1.9 e5	-7.19	-10.1	-3.07	4.9 e4	-6.33	-10.96	-4.63
125	2.6 e6	-8.89	-11.9	-2.96	2.7 e6	-8.91	-13.2	-4.3

Table 4.4 – Comparison of ITC titration results for compounds 23[30] and 125 with TEA chloride in dry solvents at 303 K. In all cases the host is titrated into a solution of the guest.

The comparison (*tbl.* 4.4) also shows that the enthalpy of the complexation with **125** is substantially more negative than that with **23** as is expected from the participation of an extra triazole CH···Cl^- hydrogen bond. This improved stickiness of **125** over **23** is also complemented by a depletion of the entropy component resulting in an outcome that improves affinity due to the triazole strap by an order of magnitude.

4.2.4 Membrane Transport Studies

Gale and co-workers have previously shown that *meso*-octamethylcalix[4]pyrrole **23** functions as a CsCl co-transporter across lipid bilayer membranes.[34] In fact much of the research in our group is geared towards the search for synthetic anion carriers.[34, 106, 141] So we decided to test the anion transport properties of 'clicked'-calix[4]pyrrole **125**.

4.2.4.1 Introduction to Membrane Transport

It has already been mentioned (Chapter 1) that cystic fibrosis is caused by the malfunction of the CFTR chloride channel in lung epithelia. However, there are many other diseases that have been associated with anion channel malfunction including, Best disease, Startle disease and Angelman syndrome.[142] So there is a great need for therapeutic agents that can provide an alternative transport system to the malfunctioning anion channels.

There are two strategies of research at present; i) is to develop artificial anion carriers to transport anions across membranes and ii) is to create synthetic anion channels to mediate anion transport. The latter will not be detailed here but progress towards both strategies has recently been reviewed by Smith and co-workers.[142]

There are a range of different methods to detect and quantify anion transport and they generally fall into two categories:

a) Methods employing vesicle suspensions in which transport in and out of the vesicles is examined. This is a 'bulk method' whereby macroscopic quantities of ions are transported across large areas of membrane (typically ~1 m^2).[142]

b) Conductance measurements on patches of synthetic or natural membranes, whole cells or sheets of tissue. This is a highly sensitive method which uses very small patches of membrane (~10^{-8} m^2).[142]

Vesicle methods are the most easily accessible methods to utilise in a chemical laboratory and so have been employed by our group. They are also the most suitable for studying charge neutral transport processes such as M^+X^- or H^+X^- cotransport (known as *symport*) or X^-/Y^- anion exchange (known as *antiport*).[142] Both mechanisms are depicted in Figure 4.12.

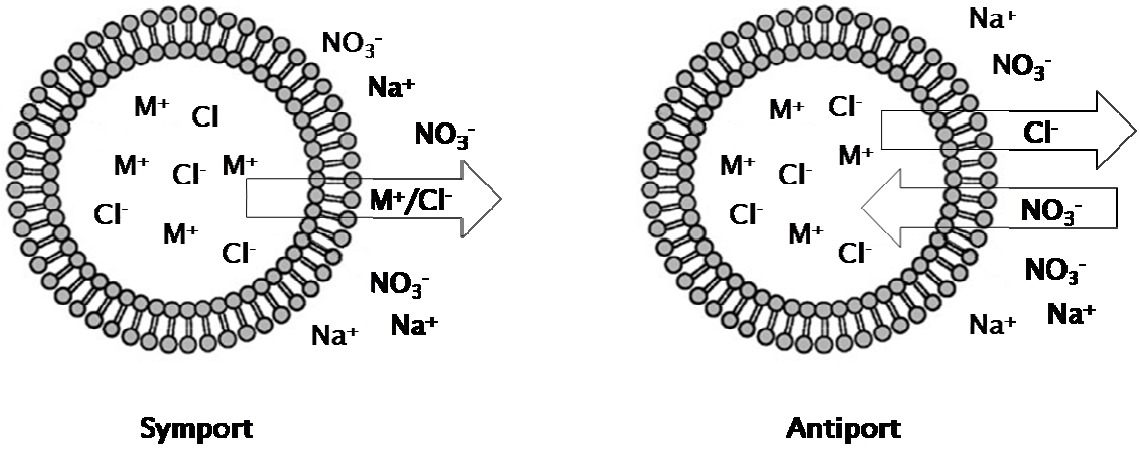

Figure 4.12 – Pictorial representation of symport and antiport mechanisms operating across the lipid bilayer of vesicles in a typical chloride/nitrate system where M is a group 1 metal.

Most vesicle methods employ unilamellar vesicles and, for our studies they are extruded through a nanoporous filter to a size of 200 nm. In a typical experiment the initial solution contains the components to be trapped inside the vesicles, such as NaCl or CsCl *etc*. The remaining material outside the vesicle is removed and replaced by a different salt, such as $NaNO_3$ or Na_2SO_4 by dialysis. This sets up a concentration gradient across the membrane that can be released by anion transporters. So far, two techniques have been developed to measure the transport of anions across the lipid bilayer:

i) By the use of dyes that respond to the appearance or disappearance of anions. The most common dye methods are; the pH sensitive pyranine dye, the fluorescing lucigenin dye and the electro-sensitive safranin O dye.

ii) By commercially available, specialist ion-selective electrodes.

We have so far employed the second method by means of a chloride selective electrode, capable of detecting chloride anions released by a transporter but not those encapsulated in the vesicles.[143] This method is the most direct and its only drawback is that kinetic experiments are limited due to the relatively slow response time of the electrode.

4.2.4.2 Results

Gale and co-workers used the chloride electrode method to measure the membrane transport properties of compound **23**.[34] Similar membrane transport studies with 'clicked'-calix[4]pyrrole **125** were conducted by Dr. Christine Tong from our research group and compared to the results with **23**.

In the first instance, separate samples of unilamellar POPC vesicles loaded with CsCl, RbCl, KCl and NaCl were prepared and suspended in an external $NaNO_3$ solution. A sample of either calixpyrrole **125** or **23** (4% carrier to lipid) was added as a DMSO solution and the resultant Cl^- efflux monitored using a chloride selective electrode. After five minutes the vesicles were lysed by addition of detergent and the final reading of the electrode used to calibrate the 100% release of chloride.

The results (*fig.* 4.13) show that calixpyrrole **125**, in contrast to the parent calixpyrrole **23**, is capable of transporting chloride from sodium, potassium and rubidium chloride containing vesicles with fastest release of the larger group 1 metal cation salts. It is also evident that the release of chloride from the caesium salt with **125** is slightly faster than the release with **23**.

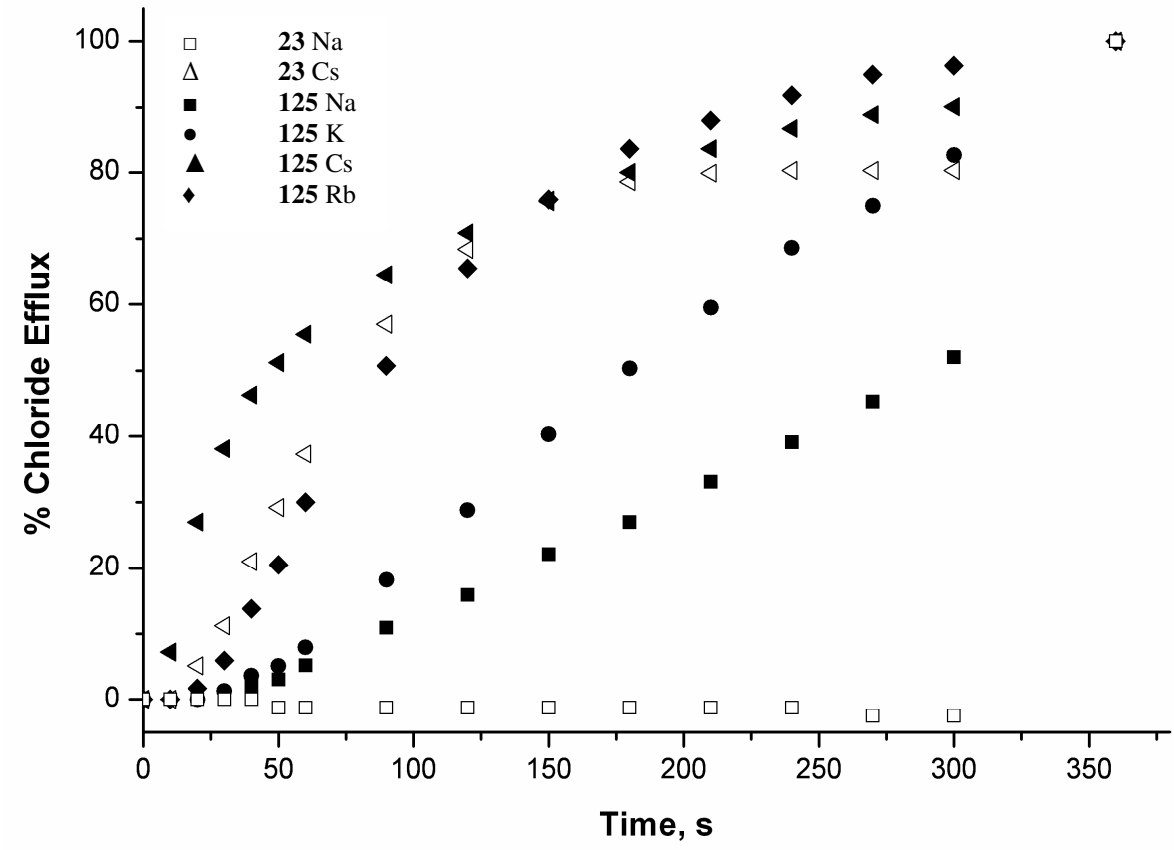

Figure 4.13 - Chloride efflux promoted by 23 (open symbols) and 125 (closed symbols), at 0.04 molar equivalents of carrier to lipid, across unilamellar POPC vesicles loaded with 489 mM MCl (M = Na, K, Cs, Rb) buffered to pH 7.2 with 5 mM phosphate. The vesicles were dispersed in 489 mM $NaNO_3$ buffered to pH 7.2 with 5 mM phosphate.

The influence of the composition of the external media on the transport activity shown by **125** was also investigated. For this purpose group 1 metal chloride loaded vesicles were suspended in a Na_2SO_4 buffer. The results (*fig.* 4.14) show that transport activity is essentially maintained although there is an increasing difference in the efficiency of transport as the metal ion size decreases. Sulfate is an extremely hydrophilic anion and it is not normally possible to extract this anion from an aqueous phase into a lipid bilayer membrane. In the case of the release of chloride mediated by compound **125** from caesium chloride containing vesicles, there is little difference between the rate of chloride release as the exterior anion is changed from nitrate to sulfate. However, as the cation size decreases there is an increasing difference in rate of release with, in the case of potassium and sodium, a considerably faster release of chloride from vesicles suspended in nitrate solution compared to those suspended in sulfate solution. This would suggest that both ion-pair co-transport and chloride/nitrate antiport mechanisms are responsible for the release of chloride. As the cation size decreases, the transport mechanism changes from a

predominantly ion-pair transport mechanism in the case of caesium chloride to a predominanty chloride/nitrate antiport process in the cases of sodium and potassium. Therefore the mechanism of transport responsible for chloride efflux with RbCl loaded vesicles is unclear.

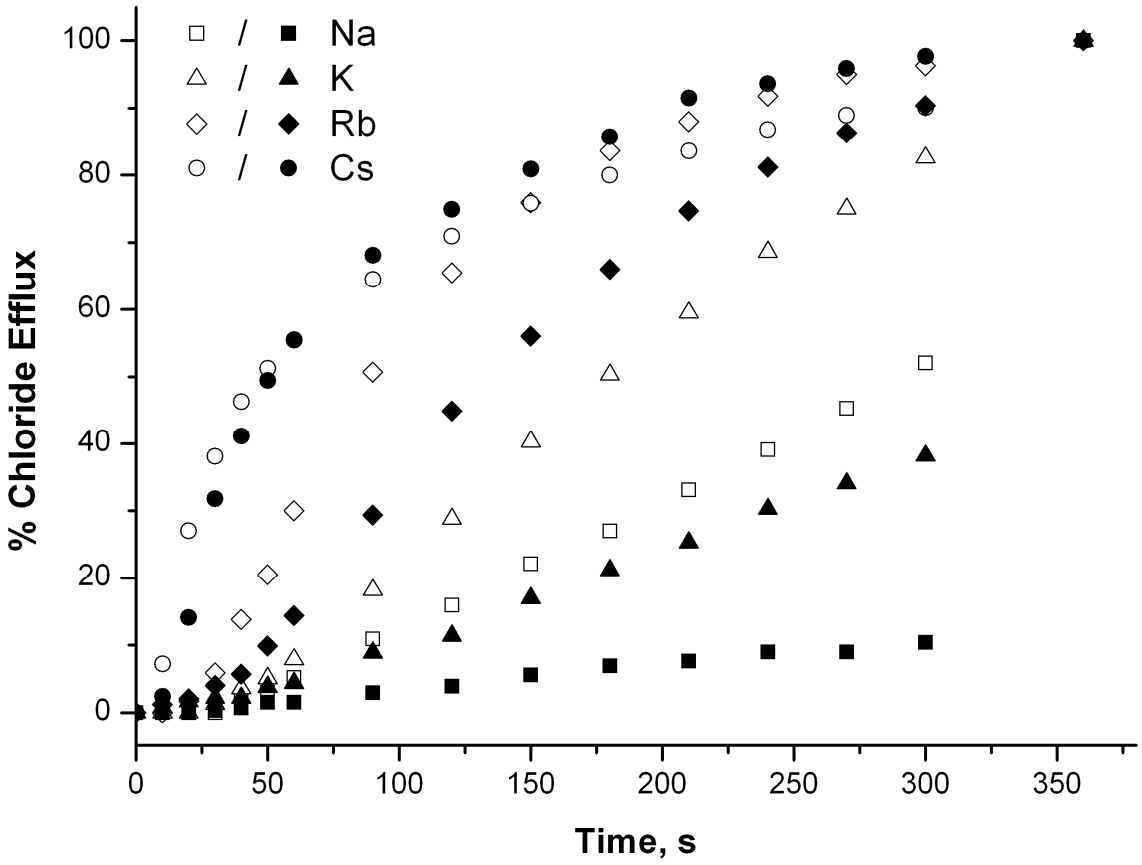

Figure 4.14 – Chloride efflux promoted by 125 at 0.04 molar equivalents of carrier to lipid, across unilamellar POPC vesicles loaded with 489mM NaCl (□/■), KCl (Δ/▲), RbCl (◊/♦) and CsCl (○/●) buffered to pH 7.2 with 5 mM phosphate dispersed in 489 mM $NaNO_3$ (open symbols) or 167 mM Na_2SO_4 (filled symbols) buffered to pH 7.2 with 5 mM phosphate.

In contrast, compound **23** only transports CsCl and when the external solution was changed to Na_2SO_4 the carrier activity was still maintained, which means this compound functions solely as a CsCl co-transporter. The CsCl selectivity and symport mechanism exhibited by both compounds was thought to be the result of the receptors being able to accommodate the caesium cation in the cup formed by the pyrrole rings upon chloride complexation. This ion pairing between compound **23** and CsCl has also been observed in solution[144] and the solid state[31] by Sessler and co-workers.

Finally, it was necessary to provide evidence to demonstrate that a mobile carrier mechanism was operating rather than an ion channel mimic mechanism. To do this,

transport assays were performed using vesicles composed of a 70:30 mixture of POPC and cholesterol. The presence of the steroid in the bilayer membrane significantly reduces its fluidity and so transport by a carrier should be reduced with the POPC-cholesterol vesicles; for transport by an anion channel, chloride efflux should be the same or similar to the results with the POPC vesicles.

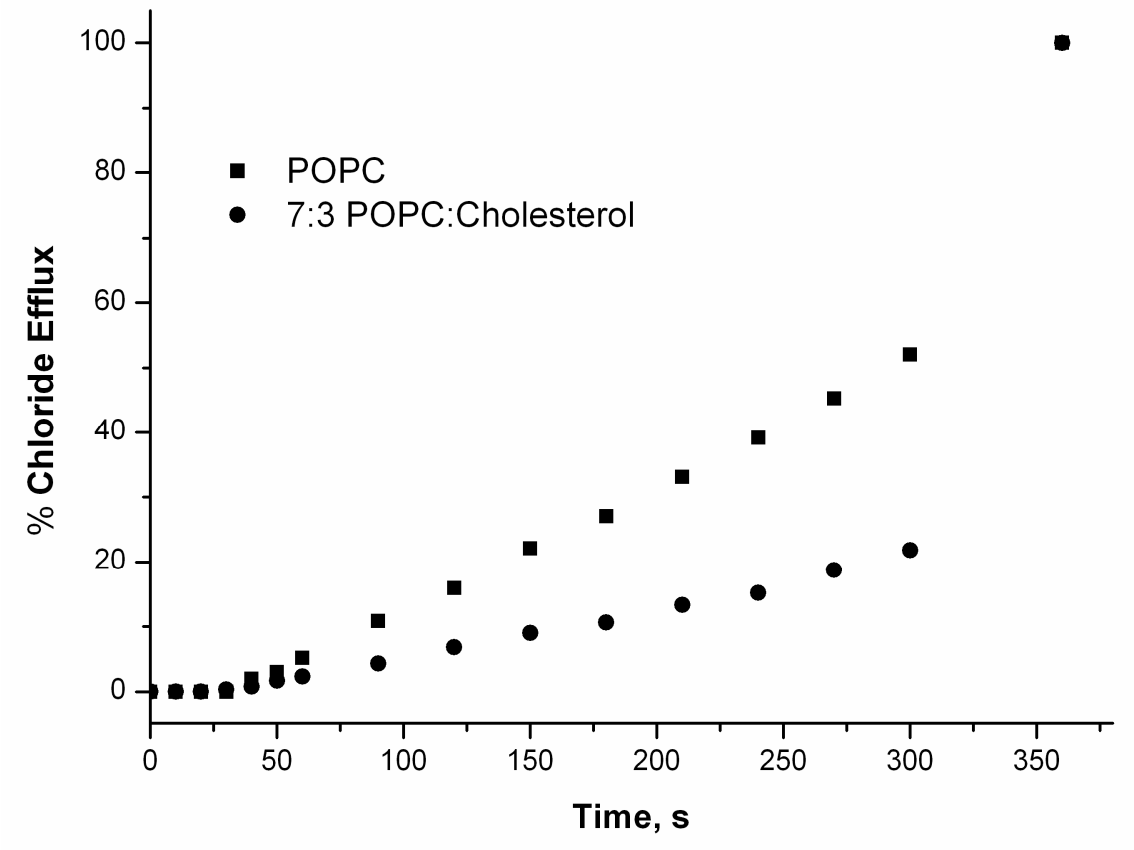

Figure 4.15 - Chloride efflux promoted by 125, at 0.04 molar equivalents of carrier to lipid, across unilamellar vesicles made of POPC (■) or POPC with 30 mol% of cholestrol (●) loaded with 489 mM NaCl buffered to pH 7.2 with 5 mM phosphate. The vesicles were dispersed in 489 mM $NaNO_3$.

The results shown in Figure 4.15 clearly indicate a significant reduction of the transport activity of **125** when the vesicle bilayer composition includes cholesterol. This result confirms the mobile carrier mechanism is operating. The same result was found with compound **23**.[34]

4.4 'Click' Chemistry and Triptycenes

4.4.1 Introduction

Jeff Davis and his group recently reported the synthesis and membrane transport properties of a C_3-symmetric triphenoxymethane (TPM) based receptor **132** (*fig.* 4.16).[145]

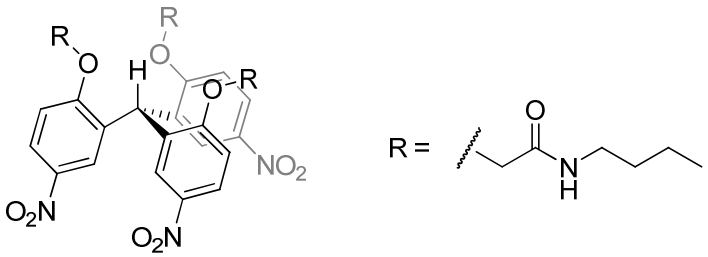

132

Figure 4.16 – Davis and co-worker's TPM based receptor for nitrate.

Proton-NMR titrations with compound **132** in CD_2Cl_2 revealed formation of a stronger complex with chloride (as a TBA salt, K_a = 816 M^{-1}) than with nitrate (as a TBA salt, K_a = 326 M^{-1}). However, membrane transport studies revealed that the compound selectively transports nitrate across liposomal membranes in preference to chloride. The nitrate transport was effectively achieved by a H^+/NO_3^- co-transport process.[145]

It was primarily this C_3-symmetric framework (but also others discussed in Chapter 1) that inspired us to consider the use of the more rigid C_3-symmetric triptycene framework (*fig.* 4.17) as a scaffold for appending hydrogen-bond donors for anion recognition.

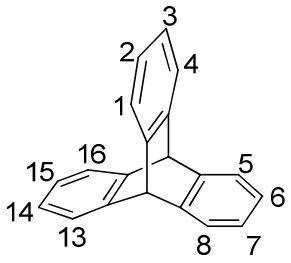

Figure 4.17 – Triptycene and the standard numbering of the ring systems.

The triptycene framework is similar to TPM, except it has an extra linkage for the benzene rings which makes it more rigid and thus allows the development of anion receptors with different binding properties. To the best of the author's knowledge,

triptycenes have not been used for anion receptors although they have been exploited for other supramolecular endeavours such as in molecular tweezers[146], rotaxanes[147] and motors.[148]

Our specific goal was to synthesis triptycenes that were substituted at the 1-, 8- and 13-positions (*syn*-triptycenes) as supposed to the undesired 1,8,16-substituted *anti*-triptycenes. Rogers and Averill published an extensive paper on the synthesis of these triptycenes[149] of which the most interesting version was the 1,8,13-tris(methoxycarbonyl)triptycene **133** (*sch.* 4.3). From this, the synthesis of 'clicked'-triptycene **136** was envisaged.

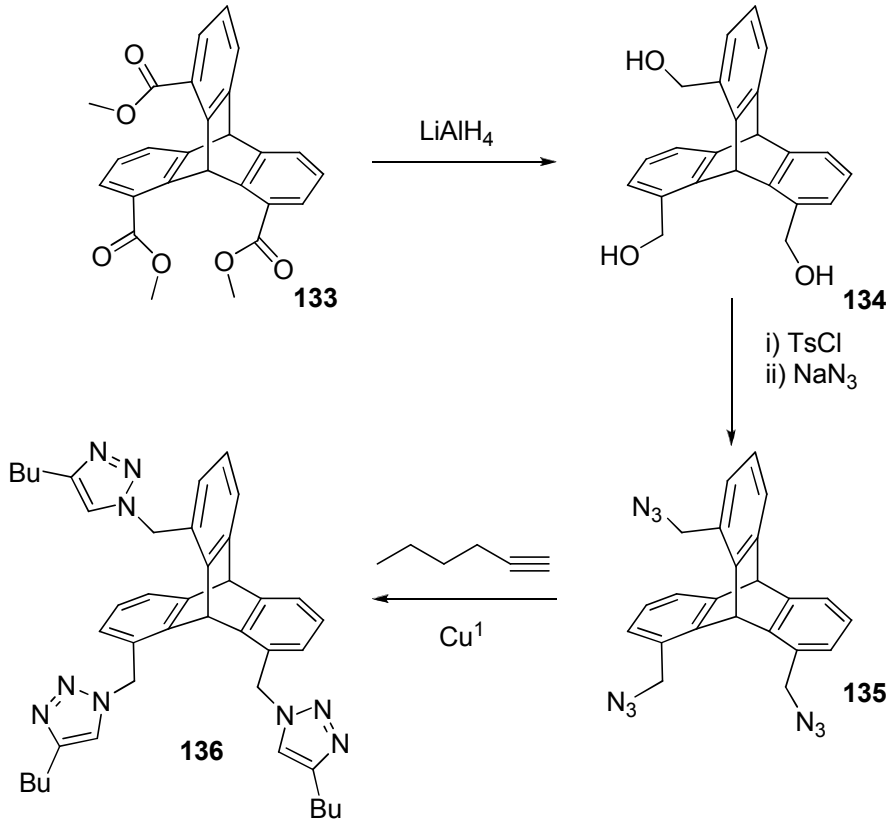

Scheme 4.3 - Proposed synthesis of 'clicked'-triptycene 136.

It was proposed that if compound **136** did not function well as an anion receptor then it could easily be converted into the tris-triazolium version by treatment with methyliodide.[131] It was also possible that intermediate **133** could be used to synthesise a tris-amide based anion receptor.

4.4.2 Synthesis

The synthesis for this section was carried out with assistance from an undergraduate project student (Becky Leithall). In general, the synthesis of triptycenes is achieved by an interesting type of Diels-Alder cycloaddition between corresponding benzyne and anthracene precursors (*fig*. 4.18).

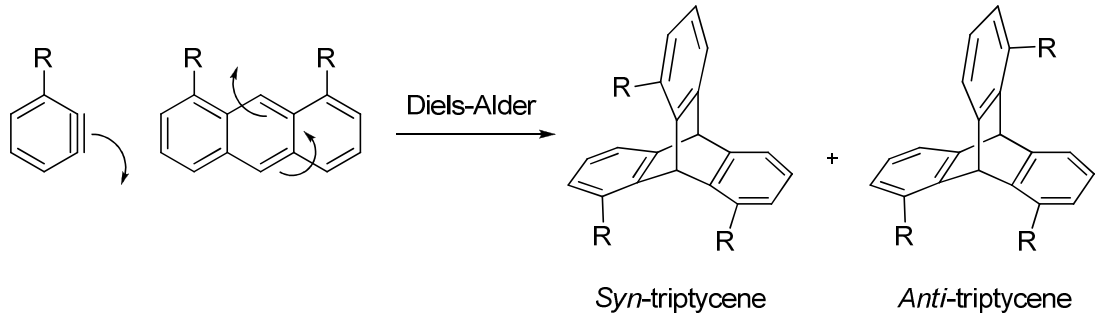

Figure 4.18 – Synthesis of triptycenes.

Just as with standard Diels-Alder reactions, the ability of the reaction to proceed or the ratio of isomers (*syn:anti*) obtained, is greatly affected by the nature of the R groups on the precursors.

For the synthesis of intermediate **133**, the anthracene precursor was first prepared *via* literature procedures (*sch.* 4.4).[149, 150] The benzyne for the reaction is generated *in-situ* from the corresponding amino acid and amyl nitrite.

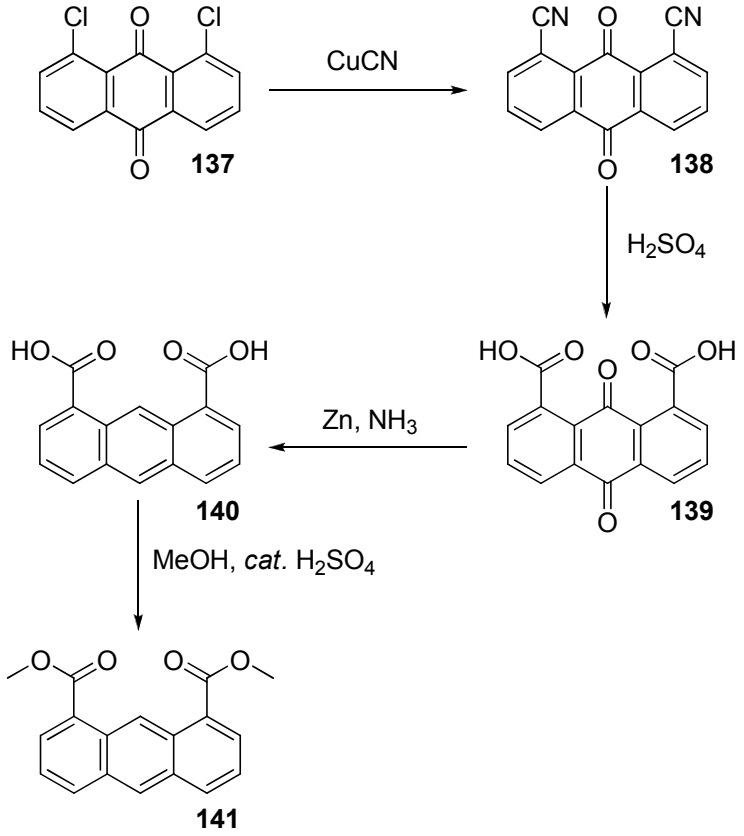

Scheme 4.4 – Synthesis of anthracene precursor.

The amino acid **144** was also synthesised according to Rogers and Averill (*sch.* 4.5).[149] However, given the complexity of the synthesis of **144** and its instability, exploratory reactions were done with the model compound anthranillic acid (*sch*. 4.6).

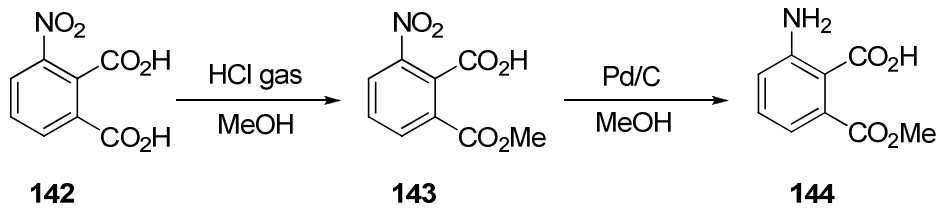

Scheme 4.5 – Synthesis of the amino acid for generation of the benzyne.[149]

The synthesis[149] (*sch.* 4.6) of this test compound (**145**) proved unsuccessful and changing the solvent/reaction conditions did not solve the problem. It was later discovered that this could have been due to an impure batch of the commercially available amyl nitrite.

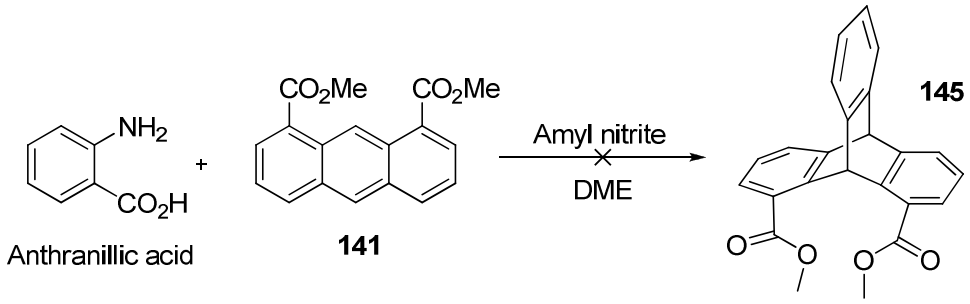

Scheme 4.6 – Attempted synthesis of test compound 145.

Success was achieved by changing to a more recent procedure[147] which involved isolating the reactive diazonium salt (**146**);[151] in older procedures[149, 152] the diazonium salt (**146**) is generated *in-situ* (*sch.* 4.7).

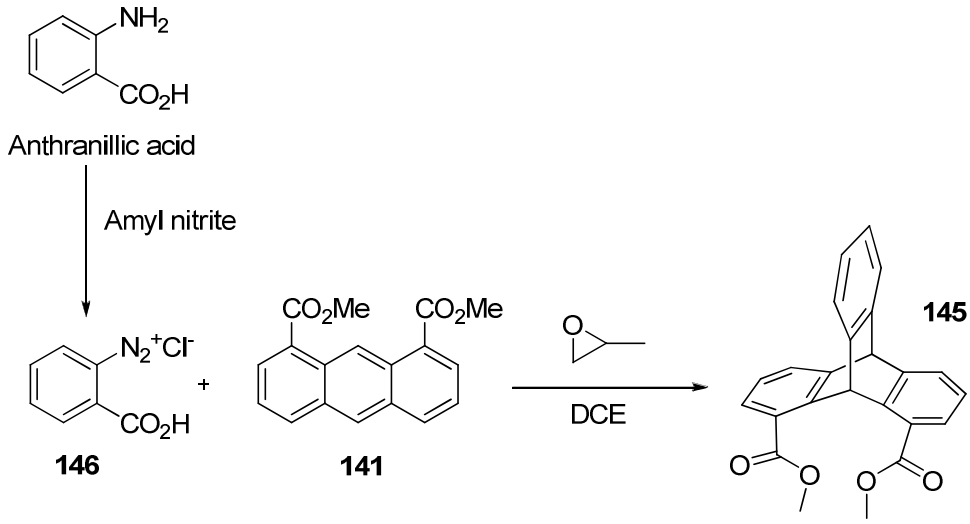

Scheme 4.7 – Synthesis of test compound 145.

Isolating this intermediate salt and purifying it for the next step resulted in a good yield for the reaction (82%), so this method was extended to the synthesis of **133** by first preparing the diazonium salt of **138** (*sch.* 4.8).

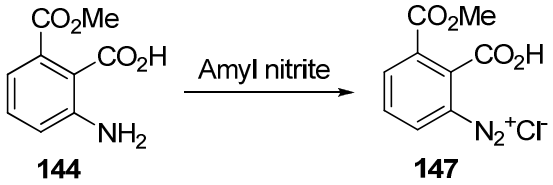

Scheme 4.8 – Synthesis of the diazonium salt of 144.

Subsequent reaction with the anthracene **141** only proceeded in 15% overall yield and resulted in both the *syn*- and *anti*- products with the undesired *anti*-product as the

major isomer. These isomers were difficult to separate by column chromatography as they had similar R_f values. The low yield and preference for the *anti*-isomer was thought due the steric hinderance of the cycloaddition by the bulky ester groups. Nonetheless, *syn*-**133** and *anti*-**133** were isolated in 3 and 12% yields respectively and both recrystallised from DCM:ethyl acetate (1:1 v/v).

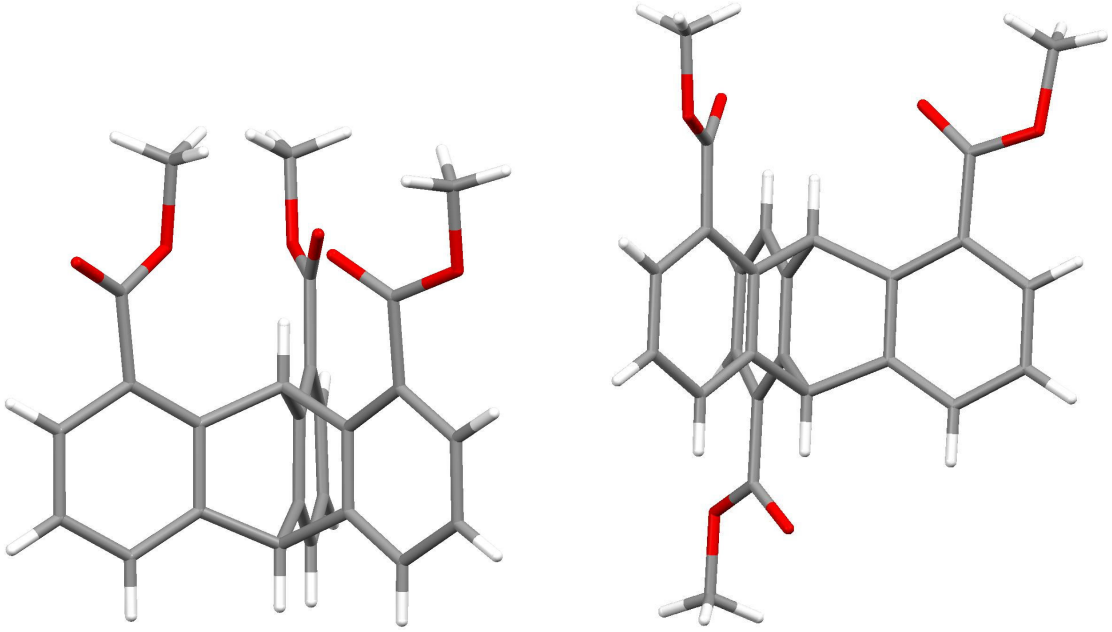

Figure 4.19 – X-ray crystal structures of *syn*-133 (left) and *anti*-133.

The structures (*fig.* 4.19) reveal the rigid triptycene framework with two of the carbonyl groups on each triptycene hydrogen bonding to the central CH. From these structures, we reasoned that if amide groups were appended, they would preorganise in the same way (in solution and the solid state) and not form a desired cavity for binding anions. However, the tris-triazole version (**136**) would not have this problem so proceeding with the synthesis; the next step was to reduce the tris-ester to the tris-alcohol (**134**) for conversion to the tris-azide (**135**). Sodium borohydride was tried first but resulted in incomplete reduction of all three esters so lithium aluminium hydride was found to be the reagent of choice. However the reaction only proceeded in moderate yield (45%) which limited this synthesis.

At this stage it was decided to stop work with triptycenes for the following reasons:

1. The synthesis of the anthracene (**141**) and diazonium (**147**) intermediates was not as straightforward as first perceived.

2. The reaction to form the triptycene was too low yielding and the preference for the *anti*-isomer was a major drawback in the synthesis. The synthesis of the tris(methoxycarbonyl)triptycene was also too low yielding.

3. A potential solution was to simply append amide groups to the triptycene. However it was reasoned that this would not result in an efficient anion receptor since the carbonyl groups would hydrogen bond to the central triptycene CH. With all the amide NH groups pointing outwards, a desired cavity for binding anions would not be formed (*fig.* 4.20).

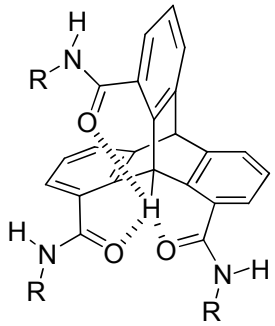

Figure 4.20 – Predicted preorganisation by intramolecular hydrogen bonding in a tris-amide triptycene.

4. In retrospect, the synthesis of 'clicked'-triptycene **136** would involve 11 steps which was not economically viable for the synthesis of an anion receptor, especially considering the low yields encountered.

4.5 Conclusions

Building on very recent investigations by other groups,[124-128] this chapter has documented an innovative exploration into the further application of triazoles in anion recognition chemistry. Their ease of synthesis by Sharpless/Meldal[121, 122] 'click' chemistry,[119] versatility and interesting properties has made them attractive candidates to exploit as hydrogen bond donors for anion binding.

In particular, we have united 'click' chemistry with the already established chemistry of 'strapped'-calix[4]pyrroles. This resulted in 'clicked'-calix[4]pyrrole **125** which functions as a highly efficient chloride transporter in POPC vesicles. We proposed it did this by two mechanisms depending on the nature of the counter cation; *viz.* with larger cations such as caesium, a co-transport mechanism operated. Whereas with smaller cations such as sodium, a chloride/nitrate antiport mechanism operated. This is in contrast to the parent calix[4]pyrrole **23** which functions as caesium chloride co-transporter only.

Proton-NMR titrations with compound **125** in acetonitrile-d_3 with a selection of anions revealed that, in addition to the pyrrole NH groups, the triazole CH was involved in hydrogen bonding to the guest anion in all cases.

Isothermal calorimetry titrations with **125** in acetonitrile revealed that the compound had an affinity for chloride that was a degree of magnitude greater than that of the parent calixpyrrole **23**. They also showed that compound **125** has a high affinity for bicarbonate which allows scope for using this receptor as a membrane transporter for bicarbonate and indeed, this should be a feature of future studies with this compound.

Other future work with 'clicked'-calixpyrroles should also include synthesising a version with two triazoles in the strap (**148**) and forming the triazolium version (**149**) of **125** (*fig.* 4.21). Both these receptors should have significantly enhanced affinities and selectivities for anions compared to compound **125**.

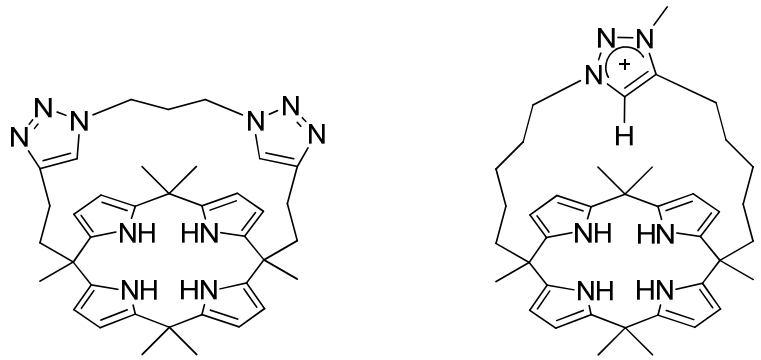

Figure 4.21 – Proposed future work with 'clicked'-calixpyrroles.

The potential use of the rigid C_3-symmetric triptycene framework for appending hydrogen bond donor groups for anion recognition has also been investigated in this chapter. With click chemistry in mind, we envisaged synthesising a tris-triazole tripodal receptor. However, after preliminary investigations, the synthesis of 1,8,13-substituted triptycenes proved too long, complicated and low yielding to be viable in the design of an anion receptor.

Click chemistry has only had a short period of existence but it is already having a diverse impact in many areas of chemistry and the versatility of it can only lead to exponential growth in this area.

Chapter 5 – Experimental Methods

5.1 General

Where necessary solvents were dried and purified prior to use. DCM and acetonitrile were distilled over calcium hydride. Anhydrous DMF and DMA on molecular sieves were purchased from Fluka. Triethylamine was distilled over KOH and stored under argon on KOH pellets. Thionyl chloride was distilled from 10% (w/w) triphenyl phosphate and stored under argon. Commercial grade chemicals were purchased from either, Aldrich Ltd., Alfa Aesar or Fluka and used without further purification unless otherwise stated. Reagents prepared in accordance with the literature have been referenced accordingly. *Trans*-dichlorobis(pyridine)platinum(II) was prepared by Roberto Quesada according to a literature procedure[86] at the University of Southampton. All syntheses have been carried out under an inert atmosphere of either argon or nitrogen. Tetrabutylammonium salts of the anions used for ^{1}H-NMR titration experiments were thoroughly dried overnight on a high vacuum. Pyrrole from Aldrich Ltd. was distilled under argon prior to use.

5.2 Instrumental Methods

NMR data were recorded on Bruker AM300, AC300 and DPX400 spectrometers. The data were referenced internally using the residual protio-solvent (^{1}H) or the signals of the solvent (^{13}C) with the chemical shifts reported in ppm. Low resolution mass spectra were recorded on a Micromass Platform II Single Quadrupole spectrometer or a Waters ZMD Single Quadrupole mass spectrometer. High resolution mass spectra were recorded on a VG 70-250-SE normal geometry double focusing mass spectrometer by the mass spectrometry service at the University of Soutampton. Melting points were carried

out using an Electrothermal 9100 melting point apparatus. Elemental analyses were performed in duplicate by Medac Ltd.

5.3 Titration Methods

^{1}H-NMR titrations were carried out by two methods:

1. **Old Method (used for Chapter 2)**

   This involves preparation of 500 µl of a 0.01 M solution of host in an NMR tube and 1 ml of a 0.1 M solution of guest. The guest is titrated in suitable aliquots into the host solution and the NMR taken after each addition. This results in an increasing guest concentration and decreasing host concentration in the NMR tube. The NMR spectra are referenced to residual protio-solvent peaks and the shifts of the relevant peaks recorded at each titrant. The data is input into the WIN-EQNMR computer program[69] to solve the association constant(s).

2. **Updated Method (Other Chapters)**

   This involves preparation of 1.5 ml of a 0.01 M solution of host. From this solution, 500 µl is added to the NMR tube. The rest of the solution (1 ml) is used to make a 0.15 M solution of guest. The host/guest solution is titrated in suitable aliquots into the host solution and the NMR taken after each addition. This results in a *constant* host concentration with increasing guest concentration in the NMR tube. The NMR spectra are referenced to residual protio-solvent peaks and the shifts of the relevant peaks recorded at each titrant. The data is input into the WIN-EQNMR computer program[69] to solve the association constant(s).

5.4 Synthetic Procedures

5.4.1 From Synthetic Schemes in Chapter 2

3-(*n*-Butylureamethyl)pyridine (60): 3-(Aminomethyl)pyridine (1 ml, 9.25 mmol) was dissolved in degassed chloroform (~30 ml) under N_2. *n*-Butylisocyanate (2 ml, 19.54 mmol) was added and the solution stirred for ~2 days. The solvent was then evaporated and the crude product washed with hexanes to give a fine white powder (1.71 g, 89%). M.p. 140-144 ^{o}C. ^{1}H-NMR (300 MHz, $CDCl_3$) δ0.84 (t, 3H), δ1.27 (m, 2H), δ1.39 (m, 2H), δ3.09 (br q, 2H), δ4.33 (d, 2H), δ4.52 (br t, 1H), δ4.88 (br t, 1H), δ7.17 (dd, 1H), δ7.59 (d, 1H), δ8.41 (dd, 1H), δ8.45 (d, 1H). ^{13}C{^{1}H}-NMR (75 MHz, $CDCl_3$) δ13.7 (CH_3), δ20.0 (CH_2), δ32.3 (CH_2), δ40.1 (CH_2), δ41.6 (CH_2), δ123.6 (CH), δ135.4 (CH), δ135.6 (C), δ148.2 (CH), δ148.5 (CH), δ158.7 (C). LR-MS (ESI-) m/z Calcd: 207.2 Found: 206.3 $(M-H)^+$. Anal. Calcd. for "$C_{11}H_{17}N_3O$": C=63.7%, H=8.9%, N=20.3% Found: C=63.6%, H=8.4%, N=19.9%. IR (cm^{-1}) 3323, 2951, 2928, 1626, 1558, 1251.

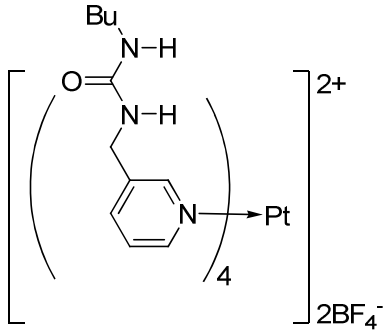

[Tetrakis(3-(*n*-butylureamethyl)pyridine)platinum(II)] ditetrafluoroborate (59): $Pt(EtCN)_2Cl_2$[70] (0.1 g, 0.27 mmol) was refluxed with compound **60** (0.224 g, 1.08 mmol) and $AgBF_4$ (0.116 g, 0.594 mmol) in acetonitrile (~30 ml) for 24 hrs at 100 ^{o}C in darkness. The resulting mixture was filtered through a glass fibre filter pad and the solvent slowly evaporated off to leave a partly crystalline grey powder (114.53 mg, 35%). M.p. decomp. ~256 ^{o}C. ^{1}H-NMR (300 MHz, DMSO-d_6) δ0.86 (t, J_1=$J_2$7.32, 3H, CH_3), δ1.28 (m, 4H, 2xCH_2), δ2.97 (m, 2H, CH_2), δ4.21 (d, *J*5.5, 2H, CH_2), δ6.10 (t, J_1=$J_2$5.5, 1H, NH), δ6.42 (t, J_1=$J_2$5.5, 1H, NH), δ7.57 (dd, J_1=$J_2$5.5, 1H, pyridine CH), δ7.84 (d, *J*8.0, 1H, pyridine CH), δ8.94 (d, *J*5.1, 1H, α-pyridine CH), δ9.06 (s, 1H, α-pyridine CH). ^{13}C{^{1}H}-NMR (75 MHz, DMSO-d_6) δ13.6 (CH_3), δ19.5 (CH_2), δ32.0 (CH_2), δ39.1 (CH_2), δ40.3 (CH_2), δ126.9 (CH), δ139.5 (CH), δ140.9 (C), δ149.7 (CH),

δ150.6 (CH), δ158.0 (C). LR-MS (ESI+) m/z Calcd: 1197.79 Found: 511.9 $(M\text{-}2BF_4)^{2+}$. Anal. Calcd. for "$PtC_{44}H_{68}N_{12}O_4B_2F_8$": C=44.1%, H=5.7%, N=14.0% Found: C=44.8%, H=5.9%, N=13.9%. IR (cm^{-1}) 3381, 1661, 1633, 1545, 1434, 1325, 1048.

***N*-(Isoquinolin-8-yl)-pyrrole-2-carboxamide (65):** Pyrrole-2-carboxylic acid (1.1 g, 9.91 mmol) was dissolved in thionyl chloride (~50 ml) and refluxed at 90 ^oC for ~3 hrs until no further gas evolved from the reaction. The thionyl chloride was removed and the crude product re-dissolved in dry DCM (~20 ml) under $N_{2(g)}$. This solution was slowly added to a solution of 8-aminoisoquinoline (1 g, 6.94 mmol) and triethylamine (4.14 ml, 4 eqv.) in dry DCM (~40 ml) and the resulting mixture was then stirred overnight at RT. A salt had precipitated which was filtered off. The excess triethylamine was removed by washes with 5% $NaHCO_{3(aq)}$ (50 ml) and water (4x50 ml). The DCM solution was dried over $MgSO_4$ and the crude product absorbed onto a minimum amount of silica and flash columned with ethyl acetate to yield a yellowish sludge. This was slowly columned with Hexane:Ethyl acetate (3:7) to yield a pale yellow powder (748.5 mg, 41%). M.p. 184-187 ^oC. ^1H-NMR (300 MHz, DMSO-d_6) δ6.23 (s, 1H), δ7.01 (s, 1H), δ7.2 (s, 1H), δ7.80 (m, 4H), δ8.53 (d, 1H), δ9.38 (s, 1H), δ10.18 (s, 1H), δ11.73 (br s, 1H). $^{13}C\{^1H\}$-NMR (75 MHz, DMSO-d_6) δ109.0 (CH), δ111.9 (CH), δ120.2 (CH), δ122.7 (C), δ123.5 (CH), δ123.9 (CH), δ125.6 (CH), δ130.4 (C), δ134.6 (CH), δ135.9 (C), δ142.7 (C), δ148.5 (CH), δ159.9 (C). LR-MS (ESI-) m/z Calcd: 237.26 Found: 236.2 $(M\text{-}H)^+$. Anal. Calcd. for "$C_{14}H_{11}N_3O$": C=70.9%, H=4.7%, N=17.7% Found: C=70.7%, H=4.7%, N=17.7%. IR (cm^{-1}) 3271, 1668, 1550, 1322, 1277, 1136.

***N*-(Pyridin-3-ylmethyl)-pyrrole-2-carboxamide (66):** Pyrrole-2-carboxylic acid (1.7 g, 15.3 mmol) was dissolved in thionyl chloride (~25 ml) and refluxed at 90 ^oC for ~3 hrs until no further gas evolved from the reaction. The thionyl chloride was removed and the crude product re-dissolved in dry DCM (~20 ml) under $N_{2(g)}$. This solution was slowly added to a solution of 3-aminomethylpyridine (1.16 g, 10.71 mmol) and triethylamine (4.5 ml, 4 eqv.) in dry DCM (~25 ml) and the resulting mixture was then stirred for 3 hrs at RT. The triethylamine was removed by washes with 5% $NaHCO_{3(aq)}$ (50 ml) and water (4x50 ml). The DCM solution was dried over $MgSO_4$ and the crude product absorbed onto a minimum amount of silica and flash columned with ethyl acetate to yield an off-yellow powder (548 mg, 25%). M.p. 131-134 ^oC. ^1H-NMR (300 MHz, DMSO-d_6) δ4.50 (d, 2H), δ6.14 (d, 1H), δ6.86 (s, 1H.), δ6.92 (s, 1H), δ7.40 (dd, 1H), δ7.75 (d, 1H), δ8.51 (d, 1H), δ8.59 (m, 2H), δ11.50 (br s, 1H). $^{13}C\{^1H\}$-NMR (75 MHz, DMSO-d_6) δ40.4

(CH_2), δ108.5 (CH), δ110.0 (CH), δ121.4 (CH), δ123.3 (CH), δ125.8 (C), δ134.9 (CH), δ135.3 (C), δ147.9 (CH), δ148.7 (CH), δ160.6 (C). LR-MS (ESI-) m/z Calcd: 201.22 Found: 200.2 $(M-H)^+$. Anal. Calcd. for "$C_{11}H_{11}N_3O$": C=65.7%, H=5.5%, N=20.9% Found: C=65.1%, H=5.5%, N=20.8%. IR (cm^{-1}) 3317, 1688, 1489, 1312, 1250, 1134.

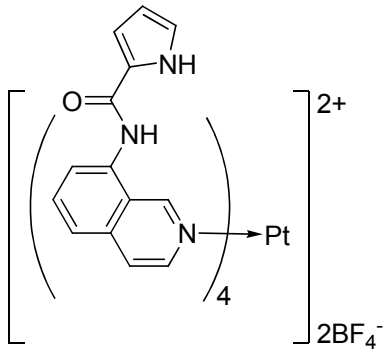

[Tetrakis(*N*-(isoquinolin-8-yl)-pyrrole-2-carboxamide)platinum(II)] ditetrafluoroborate (60): $Pt(EtCN)_2Cl_2$[70] (39.63 mg, 0.11 mmol) was dissolved in dry $MeNO_2$ (~10 ml). $AgBF_4$ (45.13 mg, 0.23 mmol) was added under darkness and the mixture refluxed for 3 hrs in the dark. The mixture was allowed to cool slightly and filtered through a microfibre filter while still hot. This filtrate was refluxed with compound **65** (100 mg, 0.42 mmol) for a further 3 hrs. The reaction mixture was again filtered through a microfibre filter and allowed to cool before being saturated with diethyl ether. This solution was left to stand in the freezer overnight to yield a pale yellow precipitate which was collected by filtration (85 mg, 61%). M.p. decomp. ~228 ^oC. ^1H-NMR (300 MHz, DMSO-d_6) δ6.32 (m, 1H, pyrrole CH), δ7.17 (m, 2H, β-pyrrole CH), δ7.80 (d, *J*7.3, 1H, isoquin. CH), δ7.88 (d, *J*8.0, 1H, isoquin. CH), δ7.97 (dd, $J_1$7.3/ $J_2$8.0, 1H, isoquin. CH), δ8.14 (d, *J*6.5, 1H, isoquin. CH), δ9.13 (d, *J*6.5, 1H, α-isoquin. CH), δ9.83 (s, 1H, α-isoquin. CH), δ10.27 (s, 1H, amide NH), δ11.59 (s, 1H, pyrrole NH). $^{13}C\{^1H\}$-NMR (75 MHz, DMSO-d_6) δ109.5 (CH), δ112.8 (CH), δ120.3 (CH), δ122.7 (C), δ123.3 (CH), δ123.9 (CH), δ124.5 (CH), δ125.2 (C), δ134.2 (CH), δ135.8 (C), δ136.2 (C), δ142.5 (CH), δ153.4 (CH), δ159.8 (C). LR-MS (ESI+) m/z Calcd: 1317.71 Found: 571.3 $(M-2BF_4)^{2+}$, 1230.3 $(M-BF_4)^+$. Anal. calcd. for "$C_{56}H_{44}B_2F_8N_{12}O_4Pt+1MeNO_2$": C=49.7%, H=3.5%, N=13.2% Found: C=49.8%, H=3.3%, N=13.4%. IR (cm^{-1}) 3285, 1633, 1491, 1397, 1049.

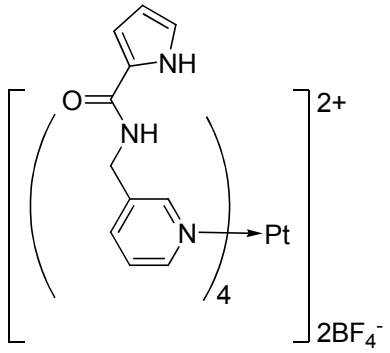

[Tetrakis(*N*-(pyridin-3-ylmethyl)-pyrrole-2-carboxamide)platinum(II)] ditetrafluoroborate (61): $Pt(EtCN)_2Cl_2$[70] (93.47 mg, 0.25 mmol) was dissolved in dry $MeNO_2$ (~20 ml). $AgBF_4$ (106.42 mg, 0.55 mmol) was added under darkness and the mixture refluxed for 3 hrs in the dark. The mixture was allowed to cool slightly and filtered through a microfibre filter while still hot. This filtrate was refluxed with compound **66** (200 mg, 0.99 mmol) for a further 3hrs. The reaction mixture was again filtered through a microfibre filter and allowed to cool before being saturated with diethyl ether. This solution was left to stand in the freezer overnight to yield an off-yellow precipitate which was collected by filtration, redissolved in the absolute minimum amount of $MeNO_2$ and rapidly saturated with diethyl ether again. The precipitate was filtered and dried to yield a cream powder (141.6 mg, 48%). M.p. decomp. ~215 ^oC. ^1H-NMR (300 MHz, DMSO-d_6) δ4.41 (d, *J*5.8, 2H), δ6.12 (m, 1H, pyrrole CH), δ6.76 (m, 1H, β-pyrrole CH), δ6.93 (m, 1H, β-pyrrole CH), δ7.55 (dd, $J_1$8.3/ $J_2$5.5, 1H, pyridine CH), δ7.85 (d, *J*8.3, 1H, pyridine CH), δ8.55 (t, J_1=$J_2$5.8, 1H, α-pyridine CH), δ8.91 (d, *J*5.5, 1H, amide NH), δ9.0 (s, 1H, α-pyridine CH), δ11.41 (s, 1H, pyrrole NH). $^{13}C\{^1H\}$-NMR (100 MHz, DMSO-d_6) δ63.3 (CH_2), δ108.8 (CH), δ110.5 (CH), δ122.0 (CH), δ125.3 (CH), δ126.9 (C), δ139.6 (CH), δ149.9 (CH), δ160.4 (CH), δ160.9 (CH), δ180.6 (C). LR-MS (ESI+) m/z Calcd: 1173.59 Found: 499.5 $(M\text{-}2BF_4)^{2+}$. Anal. calcd. for "$PtC_{44}H_{44}N_{12}O_4B_2F_8$+1$MeNO_2$": C=43.8%, H=3.8%, N=14.8% Found: C=43.6%, H=3.9%, N=14.8%. IR (cm^{-1}) 3256, 1627, 1387, 1042.

8-(*n*-butylurea)isoquinoline (71):[68] 8-aminoisoquinoline[71, 72] (500 mg, 3.47 mmol) was dissolved in dry dichloromethane (~20 ml) under N_2. *n*-Butylisocyanate (1.94 ml, 17.34 mmol) was added and the solution stirred for 5 days. The solution was then filtered and the product recovered by allowing slow *n*-hexane diffusion through the dichloromethane solution. The precipitate was then filtered and dried to leave a fine pale yellow powder (458 mg, 58%). ^1H-NMR (300 MHz, DMSO-d_6) δ0.93 (t, 3H), δ1.30 (m,

2H), δ1.43 (m, 2H), δ3.18 (q, 2H,), δ6.60 (t, 1H), δ7.53 (d, 1H), δ7.66 (t, 1H), δ7.77 (d, 1H), δ8.15 (d, 1H), δ8.48 (d, 1H), δ8.87 (s, 1H), δ9.49 (s, 1H). LR-MS (ESI+) m/z Calcd: 243.2 Found: 244.2 $(M+H)^+$, 509.3 $(2M+Na)^+$, 752.4 $(3M+Na)^+$, 995.6 $(4M+Na)^+$. Spectra agrees with the literature.[68]

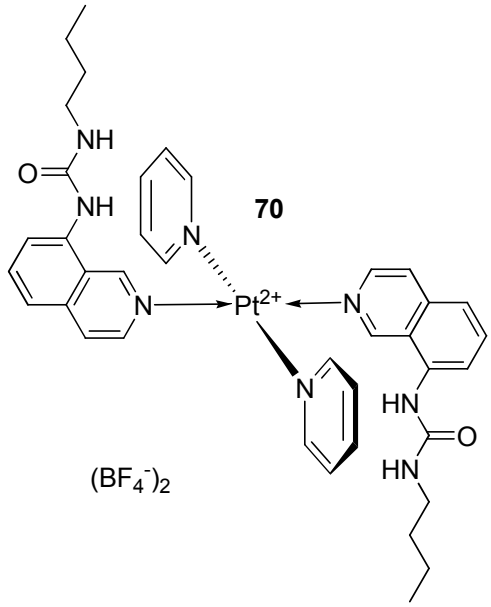

***Trans*-[bis(8-(*n*-butylurea)isoquinoline)bispyridineplatinum(II)] ditetrafluoroborate (70):** *Trans*-dichlorobis(pyridine)platinum(II)[86] (106.5 mg, 0.25 mmol) was dissolved in nitromethane (~20 ml) with silver tetrafluoroborate (107.07 mg, 0.55 mmol). The solution was refluxed in darkness for 2.5 hrs at 111 °C. The refluxing solution was then exposed to light for 0.5 hrs and hot filtered through microfibre paper into a solution of compound **71** (114.64 mg, 0.5 mmol) in nitromethane (~20 ml). The solution was refluxed for a further 3hrs in the light at 111 °C. The resulting solution was microfibre filtered while hot, reduced to minimum volume, precipitated with diethyl ether and the crude product collected by filtration. This was partially dissolved in acetonitrile and decanted twice, then boiled in diethyl ether/DCM (1:1) overnight and filtered yielding a green powder (121 mg, 48 %). M.p. decomp. ~250 °C. ^{1}H-NMR (300 MHz, DMSO-d_6) δ0.95 (t, $J_1$7.29/$J_2$6.96, 6H, CH_3), δ1.40 (m, 4H, CH_2), δ1.50 (m, 4H, CH_2), δ3.16 (m, 4H, CH_2), δ6.57 (t, J_1=$J_2$5.49, 2H, NH), δ7.6 (t, $J_1$6.6/$J_2$7.68, 4H, pyridine CH), δ7.76 (t, $J_1$8.4/$J_2$8.04, 4H, isoquin. CH), δ7.91 (t, $J_1$8.04/$J_2$7.68, 1H, pyridine CH), δ8.01 (br t, 2H, isoquin. CH), δ8.05 (d, *J*6.75, 2H, isoquin. CH), δ8.79 (d, *J*6.6, 2H, α-isoquin. CH), δ8.88 (s, 2H, NH), δ9.03 (d, *J*5.13, 4H, α-pyridine CH), δ9.73 (s, 2H, α-isoquin. CH). ^{13}C{^{1}H}-NMR (75 MHz, DMSO-d_6) δ13.7 (CH_3), δ19.6 (CH_2), δ31.8 (CH_2), δ39.3

(CH_2), δ121.9 (CH), δ123.5 (CH), δ124.4 (CH), δ127.5 (CH), δ134.7 (CH), δ136.2 (CH), δ137.8 (C), δ141.0 (C), δ141.7 (CH), δ151.9 (CH), δ153.8 (CH), δ155.5 (C). LR-MS (ESI+) m/z Calcd: 1013.5 Found: 420.4 $(M-2BF_4)^{2+}$, 926.8 $(M-BF_4)^{+}$. Anal. Calcd. for "$C_{38}H_{44}B_2F_8N_8O_2Pt$+1DCM": C=42.6%, H=4.2%, N=10.2% Found: C=42.7%, H=4.1%, N=10.5%.

5.4.2 From Synthetic Schemes in Chapter 3

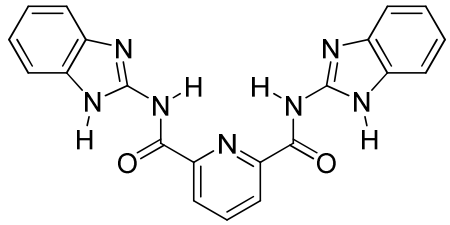

2,6-Bis(2-carboxamidobenzimidazolyl)pyridine (88): 2-Aminobenzimidazole (1 g, 7.51 mmol) was dissolved in dry DMA (~50 ml) with DMAP (1 microspatula) and TEA (1 ml) and stirred for 15 mins. Meanwhile, 2,6-pyridinedicarbonyldichloride (766.1 mg, 3.76 mmol) was dissolved in dry DMA (~50 ml) and slowly added under N_2 to the prepared solution and stirred for 3 days. A salt was filtered off and the DMA removed *in-vacuo*. The oily residue was triturated with MeOH to precipitate a yellow powder which was filtered, resuspended in MeOH and boiled for a few mins. The suspension was cooled slightly, filtered and dried to leave a fine yellow powder (1.21 g, 81%). M.p. 303-306 ^{o}C. ^{1}H-NMR (300 MHz, DMSO-d_6) δ7.17 (d, *J*7.89, 4H, benzene CH), δ7.56 (br m, 4H, benzene CH), δ8.40 (dd, $J_1$7.14/$J_2$6.78, 1H, pyridine CH), δ8.50 (d, *J*7.53, 2H, pyridine CH), δ12.42 (s, 2H, amide NH), δ12.87 (s, 2H, imidazole NH). ^{13}C-NMR (75 MHz, DMSO-d_6) δ111.8 (CH), δ117.3 (CH), δ121.4 (CH), δ126.4 (CH), δ140.3 (C), δ146.2 (C), δ147.9 (C), δ162.9 (C). LR-MS (ESI+) m/z Calcd: 397.4 Found: 398.2 $(M+H)^{+}$. Anal. Calcd. for "$C_{21}H_{15}N_7O_2$+H_2O": C=60.72%, H=4.12%, N=23.6% Found: C=60.54%, H=3.89%, N=23.28%. IR (cm^{-1}) 3342, 3231, 1681, 1628, 1557, 1453, 1417, 1270.

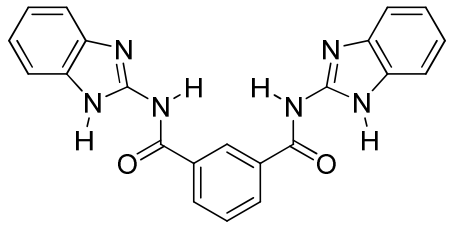

2,6-Bis(benzimidazol-2-yl)isophthalamide (89): 2-Aminobenzimidazole (500 mg, 3.76 mmol) was dissolved in MeCN (~70 ml) with DMAP (1 microspatula) and TEA (500 µl) and heated to 60 ^{o}C to dissolve the amine. Isophthaloyl dichloride (381.2 mg, 1.88 mmol) in MeCN (~70 ml) was slowly added under N_2 to the prepared solution and stirred overnight at 55 ^{o}C. The precipitate was filtered, washed with water (3x30 ml) and diethyl ether (2x20 ml) before being dried in-vacuo to leave a pale yellow powder (642 mg, 86%). M.p. decomp. >340 ^{o}C. ^{1}H-NMR (300 MHz, DMSO-d_6) δ6.20 (s, 1H, imidazole NH), δ6.23 (s, 1H, imidazole NH), δ6.74 (t, $J_1$7.32/$J_2$6.96, 4H, benzene CH), δ7.07 (t, $J_1$7.68/$J_2$6.57, 4H, benzene CH), δ7.22 (m, 2H, pyridine CH), δ7.80 (t, $J_1$7.68/$J_2$8.04, 2H, pyridine CH), δ8.03 (s, 1H, amide NH), δ8.04 (s, 1H, amide NH), δ8.12 (s, 1H, pyridine CH). ^{13}C-NMR (75 MHz, DMSO-d_6) δ112.5 (CH), δ115.9 (CH), δ119.3 (CH), δ124.1 (CH), δ128.4 (CH), δ129.7 (CH), δ130.8 (C), δ132.3 (CH), δ134.8 (C), δ143.3 (C), δ154.4 (C), δ168.3 (C). LR-MS (ESI+) m/z Calcd: 396.4 Found: 397.2 $(M+H)^+$, 398.3 $(M+2H)^+$. HR-MS (ES+) Calcd: 397.1413 $(M+H)^+$ Found: 397.1406 $(M+H)^+$. IR (cm^{-1}) 3446, 3419, 3082, 1692, 1651, 1461, 1321.

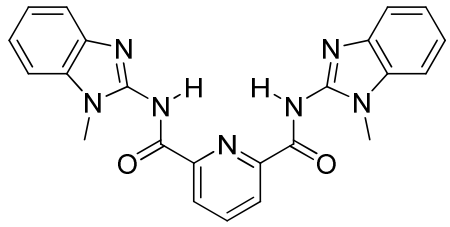

2,6-Bis(2-carboxamido-1-methylbenzimidazolyl)pyridine (90): 2-Amino-1-methylbenzimidazole (460 mg, 3.13mmol) was dissolved in dry DMA (~20 ml) with TEA (~600 µl) and DMAP (1 microspatula). Meanwhile, 2,6-pyridinedicarbonyl dichloride (318.81 mg, 1.56 mmol) was dissolved in dry DMA (~25 ml) and slowly added to the amine solution under N_2. The resulting solution was stirred at RT for 3 days, after which a salt was removed by filtration. The DMA was removed in-vacuo and the residue precipitated with methanol (~70 ml). The precipitate was filtered off and recrystallised twice from DMF/MeOH in the freezer to leave fine off-white needles

which were filtered, washed with MeOH and diethyl ether. The crystals were then suspended in MeOH (100 ml), boiled for 5 mins, cooled slightly and filtered to leave a fine white powder (359.6 mg, 54%). M.p. 260-264 ^{o}C. ^{1}H-NMR (300 MHz, DMSO-d_6) δ3.74 (s, 6H, imidazole CH_3), δ7.28 (m, 4H, benzene CH), δ7.62 (m, 4H, benzene CH), δ8.37 (br t, 1H, pyridine CH), δ8.47 (br d, 2H, pyridine CH), δ11.89 (br s, 2H, amide NH). ^{13}C-NMR (75 MHz, DMSO-d_6) δ30.3 (CH_3), δ110.2 (CH), δ118.6 (CH), δ122.3 (CH), δ126.2 (CH), δ134.9 (C), δ140.3 (C), δ145.1 (C), δ147.6 (C), δ163.5 (C). LR-MS (ESI+) m/z Calcd: 425.4 Found: 426.2 $(M+H)^+$, 448.2 $(M+Na)^+$. Anal. Calcd. for "$C_{23}H_{19}N_7O_2$": C=64.93%, H=4.5%, N=23.03% Found: C=64.83%, H=4.45%, N=22.82%. IR (cm^{-1}) 3232, 1558, 1484, 1379, 1350, 1301, 1258, 1162.

6-(4-Butylphenylcarbamoyl)-pyridine-2-carboxylic acid (95): Compound **94**[107] (1.5 g, 8.28 mmol) was dissolved in thionyl chloride (~80 ml) and refluxed for 2 hrs at 90 ^{o}C. The thionyl chloride was removed *in-vacuo* and the crude material redissolved in dry DCM (100 ml). This solution was slowly added to a dry DCM (100 ml) solution of 4-butylaniline (1.19 ml, 7.53 mmol), triethylamine (1.5 ml) and DMAP (cat.) under nitrogen. The resulting mixture was stirred overnight at room temperature under nitrogen. The solution was washed with a saturated aqueous sodium hydrogencarbonate solution (~50 ml), dried over $MgSO_4$, absorbed onto silica and flash columned on silica gel eluted with hexanes:ethyl acetate (3:2). This afforded a white powder (2.5 g, 8 mmol) which was dissolved in dioxane/25% water (100 ml) with KOH (1 g, 0.018 mol) and stirred overnight at room temperature. The solution was reduced to minimum volume, taken up with water and acidified with concentrated HCl. This aqueous phase was extracted with DCM, dried over $MgSO_4$, precipitated with petroleum ether and filtered to leave the title compound as a fine white powder (2.3 g, 97%). M.p. 145-148 ^{o}C. ^{1}H-NMR (300 MHz, DMSO-d_6) δ0.90 (t, 3H), δ1.30 (m, 2H), δ1.54 (m, 2H), δ2.58 (t, 2H), δ7.22 (d, 2H), δ7.70 (d, 2H), δ8.30 (m, 2H), δ8.37 (m, 1H), δ10.78 (s, 1H). ^{13}C-NMR (100 MHz, DMSO-d_6) δ13.8 (CH_3), δ21.7 (CH_2), δ33.1 (CH_2), δ34.3 (CH_2), δ120.7 (CH), δ125.8 (CH), δ126.9 (CH), δ128.6 (CH), δ135.6 (C), δ138.4 (C), δ140.2 (CH), δ146.1 (C), δ149.3 (C), δ161.2 (C), δ164.7 (C). LR-MS (ESI-) m/z Calcd: 298.3 Found: 297.1 (M-H). HR-MS (ES+) Calcd: 299.1396 $(M+H)^+$ Found: 299.1390 $(M+H)^+$. IR (cm^{-1}) 3080, 2848, 2541, 1722, 1694, 1428, 1247.

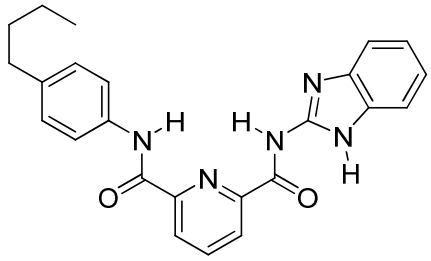

2-(Carboxamidobenzimidazolyl)-6-(4-butylphenylcarbamoyl)pyridine (91): 2-Aminobenzimidazole (89.3 mg, 0.67 mmol), EDCI (141.4 mg, 0.74 mmol), compound **95** (200 mg, 0.67 mmol) and DMAP (cat.) were dissolved in dry pyridine (~50 ml) and stirred under nitrogen for 3 days.

The pyridine was removed *in-vacuo* and the residue precipitated with DCM/diethyl ether. The precipitate was filtered, washed with water (~100 ml) followed by diethyl ether (~100 ml) and recrystallised by slow evaporation of a methanolic solution of the crude compound. This afforded off-white needles (149.6 mg, 54%). M.p. 248-252 ^{o}C. ^{1}H-NMR (300 MHz, DMSO-d_6) δ0.92 (br t, 3H, CH_3), δ1.34 (m, 2H, CH_2), δ1.58 (m, 2H, CH_2), δ4.07 (m, 2H, CH_2), δ7.15 (d, *J*6.03, 2H, benzene CH), δ7.26 (d, *J*6.03, 2H, benzene CH), δ7.55 (m, 2H, benzene CH), δ7.73 (d, *J*6.39, 2H, benzene CH), δ8.33 (m, 1H, pyridine CH), δ8.45 (m, 2H, pyridine CH), δ11.22 (s, 1H, amide NH), δ12.43 (s, 1H, benzimid. amide NH), δ12.52 (s, 1H, imidazole NH). ^{13}C-NMR (100 MHz, DMSO-d_6) δ13.8 (CH_3), δ21.7 (CH_2), δ33.1 (CH_2), δ34.3 (CH_2), δ121.9 (CH), δ125.7 (CH), δ125.9 (CH), δ128.5 (CH), δ135.5 (C), δ138.7 (C), δ140.0 (CH), δ146.0 (C), δ147.6 (C), δ149.4 (C), δ161.5 (C), δ163.0 (C). LR-MS (ESI+) m/z Calcd: 413.5 Found: 414.2 $(M+H)^+$. HR-MS (ES+) Calcd: 414.1930 $(M+H)^+$ Found: 414.1926 $(M+H)^+$. IR (cm^{-1}) 3492, 3356, 3291, 2927, 1625, 1558, 1454.

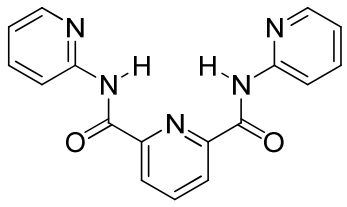

N, N'-Bis(2-pyridyl)pyridine-2,6-dicarboxamide (92): 2-Aminopyridine (706.8 mg, 7.51 mmol) was dissolved in dry DCM (~25 ml) with TEA (~1 ml) and DMAP (1 microspatula). Meanwhile, 2,6-pyridinedicarbonyl dichloride (766.1 mg, 3.76 mmol) was dissolved in dry DCM (~30 ml) and slowly added to the amine solution under N_2. The resulting solution was stirred at RT for 3 days and the DCM reduced in-vacuo and the

crude product precipitated with addition of hexanes (~40 ml). The crude product was redissolved in the minimum amount of DCM and crystallised by slow evaporation of the solvent to leave large white needles of pure title compound (723.2 mg, 60%). ^{1}H-NMR (300 MHz, DMSO-d_6) δ7.25 (m, 2H, pyridine CH), δ7.91 (m, 2H, pyridine CH), δ8.31 (m, 3H, pyridine CH), δ8.41 (d, *J*8.04, 2H, pyridine CH), δ8.49 (m, 2H, pyridine CH), δ11.81 (s, 2H, amide NH). ^{13}C-NMR (75 MHz, DMSO-d_6) δ114.8 (2xCH), δ120.3 (2xCH), δ125.8 (2xCH), δ138.4 (2xCH), δ139.8 (CH), δ148.0 (2xCH), δ148.9 (2xC), δ151.6 (2xC), δ162.7 (2xC). LR-MS (ESI+) m/z Calcd: 319.3 Found: 320.2 $(M+H)^+$, 342.1 $(M+Na)^+$. Agrees with literature.[108]

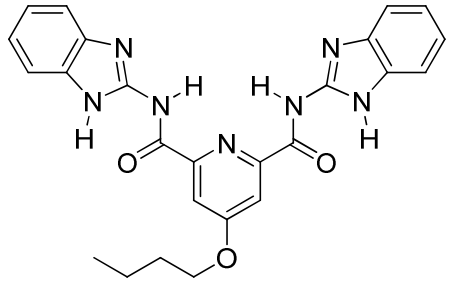

2,6-Bis(2-carboxamidobenzimidazolyl)-4-butoxypyridine (96): Compound **99** (250 mg, 1.05 mmol) was refluxed in thionyl chloride (30 ml) for 3 hrs until no further gas evolved. The thionyl chloride was removed *in-vacuo* and the crude residue taken up in dry DMA (~40 ml). To this solution was added 2-aminobenzimidazole (278 mg, 2.09 mmol), triethylamine (0.5 ml) and DMAP (cat.) and the resulting mixture stirred for 3 days at room temperature under argon. The solvent was reduced *in-vacuo* and precipitated with cold methanol. The precipitate was filtered, washed with methanol and diethylether and dried to leave the title compound as white powder (415 mg, 84%). M.p. 320-324 ^{o}C. ^{1}H-NMR (400 MHz, DMSO-d_6) δ0.95 (t, $J_1$7.52/$J_2$7.04, 3H, CH_3), δ1.49 (m, 2H, CH_2), δ1.78 (m, 2H, CH_2), δ4.30 (t, J_1= $J_2$6.52, 2H, CH_2), δ7.16 (d, *J*6.04, 4H, benzene CH), δ7.56 (s, 4H, benzene CH), δ7.90 (s, 2H, pyridine CH), δ12.38 (s, 2H, amide NH), δ12.80 (s, 2H, imidazole NH). ^{13}C-NMR (100 MHz, DMSO-d_6) δ13.6 (CH_3), δ18.6 (CH_2), δ30.2 (CH_2), δ68.6 (CH_2), δ111.7 (CH), δ112.1 (4xCH), δ117.2 (CH), δ121.4 (4xCH), δ132.7 (C), δ140.7 (C), δ146.1 (2xC), δ149.9 (2xC), δ162.7 (2xC), δ167.5 (2xC), δ181.0 (C). LR-MS (ESI+) m/z Calcd: 469.5 Found: 470.2 $(M+H)^+$. HR-MS (ES+) Calcd: 470.1941 $(M+H)^+$ Found: 470.1936 $(M+H)^+$. IR (cm^{-1}) 3392, 3295, 2956, 1686, 1568, 1451.

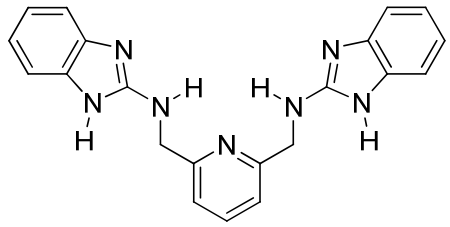

2,6-Bis((benzimidazol-2-ylamino)methyl)pyridine (100): Compound **102** (507.4 mg, 3.76 mmol) and 2-aminobenzimidazole (1 g, 7.51 mmol) were stirred in ethanol/acetonitrile 1:1 (20 ml) overnight at room temperature under argon. The solvent was removed *in-vacuo* and the crude solid thoroughly dried under high vacuum. The solid was taken up in absolute ethanol (50 ml) and a mixture of $NaBH_4$ (1.44 g, 38 mmol) and $NaCNBH_3$ (2.39 g, 38 mmol) was carefully added in portions. The resulting solution was left to stir for 48 hrs under argon at room temperature. The solvent was removed and the residue taken up in water and basified with aqueous $NaHCO_3$ which resulted in a precipitate which was filtered. This precipitate was extracted on the filter funnel with hot acetonitrile (150 ml). The solvent was removed and the white sludge repeatedly azeotroped with toluene/methanol to precipitate a white powder which was filtered and washed with toluene to leave the pure title compound (894.7 mg, 64%). M.p. 220-224 ^{o}C. ^{1}H-NMR (300 MHz, DMSO-d_6) δ4.61 (d, *J*5.64, 4H, CH_2), δ6.86 (m, 4H, benzene CH), δ7.14 (m, 4H, benzene CH), δ7.25 (d, *J*6.03, 2H, pyridine CH), δ7.69 (t, $J_1$7.92/$J_2$7.17, 1H, pyridine CH), δ10.89 (s, 2H, imdazole NH). ^{13}C-NMR (100 MHz, DMSO-d_6) δ47.3 (CH_2), δ111.3 (4xCH), δ120.4 (2xCH), δ123.2 (4xCH), δ129.7 (4xC), δ138.3 (CH), δ150.5 (2xC), δ155.7 (2xC). LR-MS (ESI+) m/z Calcd: 369.4 Found: 370.3 $(M+H)^+$. HR-MS (ES+) Calcd: 370.1780 $(M+H)^+$ Found: 370.1773 $(M+H)^+$. IR (cm^{-1}) 3052, 1630, 1567, 1460, 1264.

2-(2-(2-(4-Amino-3-nitrophenoxy)ethoxy)ethoxy)ethanol (111): 4-amino-3-nitrophenol (500 mg, 3.24 mmol), 2-[2-(2-chlorethoxy)-ethoxy]-ethanol (656.4 mg, 3.89 mmol) and caesium carbonate (1.59 g, 4.87 mmol) were stirred in dry DMF (40 ml) at 80 ^{o}C for 12 hrs under nitrogen. The DMF was removed *in-vacuo* and the residue extracted with DCM, absorbed onto silica and flash columned on silica gel eluted with ethyl acetate to afford the product as a dark orange oil (797.2 mg, 86%). ^{1}H-NMR (300 MHz, DMSO-d_6) δ3.42 (m, 8H), δ3.71 (t, 2H), δ4.04 (t, 2H), δ4.56 (t, 1H), δ7.01 (d, 1H), δ7.17 (dd, 1H), δ7.24 (s, 2H), δ7.39 (d, 1H). ^{13}C-NMR (75 MHz, DMSO-d_6) δ60.2 (CH_2), δ67.8 (CH_2), δ68.8 (CH_2), δ69.7 (CH_2), δ69.9 (CH_2), δ72.4 (CH_2), δ106.1 (CH),

δ120.7 (CH), δ127.5 (CH). LR-MS (ESI-) m/z Calcd: 286.3 Found: 285.5 (M-H). IR (cm^{-1}) 3220, 3049, 1690, 1544, 1460, 1164.

4-(2-(2-(2-(Allyloxy)ethoxy)ethoxy)ethoxy)-2-nitrobenzenamine (112): Compound **111** (740 mg, 2.58 mmol), allyl bromide (0.3 ml, 3.36 mmol), sodium hydroxide (144.8 mg, 3.62 mmol) and $TBA^+HSO_4^-$ (15 mg, cat.) were heated in toluene (60 ml) at 80 ^oC under nitrogen for 1 day. The toluene was removed *in-vacuo* and the product extracted with DCM and flash columned on silica gel eluted with DCM/methanol (2%) to yield the product as an orange oil (97 mg, 12%). ^{1}H-NMR (300 MHz, DMSO-d_6) δ3.55 (m, 8H), δ3.71 (t, 2H), δ3.92 (d, 2H), δ4.04 (t, 2H), δ5.20 (m, 2H), δ5.90 (m, 1H), δ6.98 (d, 1H), δ7.16 (m, 1H), δ7.24 (s, 2H), δ7.38 (d, 1H). ^{13}C-NMR (100 MHz, CD_2Cl_2) δ69.1 (CH_2), δ70.2 (CH_2), δ70.3 (CH_2), δ71.3 (CH_2), δ71.4 (CH_2), δ71.5 (CH_2), δ72.8 (CH_2), δ108.2 (CH), δ117.1 (CH_2), δ120.9 (CH), δ127.7 (CH), δ132.2 (C), δ135.8 (CH), δ140.9 (C), δ150.6 (C). IR (cm^{-1}) 3220, 2964, 1630, 1576, 1454, 1238.

Carbonyl diisocyanate (116): This was prepared according to a modified literature procedure[116] as follows; under an inert atmosphere, trichloroisocyanuric acid (3.67 g, 0.016 mmol) and *N*-chlorocarbonyl isocyanate (5 g, 0.05 mol) were introduced consecutively to a micro-distillation setup with a 2-neck receiving flask at 0 ^oC. The reaction was warmed with stirring to 50 ^oC for 1 hr during which time Cl_2 gas was liberated which was periodically evacuated with N_2 gas. The temperature was gradually raised to 90 ^oC for 1 hr and then 130 ^oC to begin distillation of the product which was eventually completed with the aid of a vacuum. This yielded an off-white oil which was stored under nitrogen on dry ice and used in the next step as soon as possible without purification or analysis.

Carbonylbis(carbamoylchloride) (117): This was prepared according to a modified literature procedure[115] as follows; crude carbonyl diisocyanate was taken up in dry DCM (40 ml) and cooled to -88 ^oC. Dry HCl gas was bubbled through this solution for 2 hrs and then left to stir for a further 4 hrs at -88 ^oC. This resulted in a white precipitate which was kept suspended in the DCM under nitrogen on dry ice ready for use in the next step without purification or analysis.

Spirobarbiturate (103): The DCM solution of **117** was slowly allowed to reach -2 ^oC during which time the DCM and any residual HCl gas were removed *in-vacuo*. The resulting white precipitate was then dissolved in dry THF (50 ml) at -2 ^oC.

Meanwhile barbituric acid (6.07 g, 0.047 mol) was partially dissolved in dry THF (125 ml) under nitrogen and cooled to -88 ^{o}C. To this slurry was added drop-wise, a solution of ^{t}butyl-lithium (2.5 M solution in hexanes, 37.6 ml, 0.094 mol) in dry THF (~25 ml). This resulted in a slurry which was slowly allowed to reach -2 ^{o}C. The THF solution of **117** was slowly introduced to the slurry *via* cannula and the resulting slurry allowed to reach room temperature before being stirred overnight.

The slurry was quenched with water (~70 ml) which resulted in two phases with a precipitate which was filtered and washed with copious THF, water and DCM. The precipitate was purified by suspension in DMF and refluxing for a few hours, followed by hot filtration of the precipitate. This process was repeated except with a DMF/THF solution (75/25 ml) followed by drying *in-vacuo* to leave a yellow powder (410 mg, 4% overall yield). Mp. decomp. >350 ^{o}C. ^{1}H-NMR (300 MHz, DMSO-d_6) δ10.09 (s, 4H). ^{13}C-NMR (75 MHz, DMSO-d_6) δ84.3 (C), δ149.9 (C), δ166.7 (C). LR-MS (ESI+) m/z Calcd: 240.1 Found: 241.4 $(M+H)^{+}$. IR (cm^{-1}) 3041, 1685, 1567, 1382.

5.4.3 From Synthetic Schemes in Chapter 4

7-Bromoheptan-2-one (127):- To a solution of 1-methylcyclohexanol (6.85 g, 0.06 mol) in chloroform (200 ml) was added potassium carbonate (49.75 g, 0.36 mol). The reaction mixture was stirred at 0 ^{o}C for 10 min and bromine (47.93 g, 0.3 mol) was then added. After stirring at 0 ^{o}C for 5 hrs the reaction was quenched with a saturated aqueous sodium thiosulfate solution and filtered. The organic layer was separated, washed with water, dried over sodium sulfate and concentrated *in-vacuo*. The concentrate was filtered through a short plug of silica, eluted with ethyl acetate which was then reduced *in-vacuo* to leave an off yellow oil. ^{1}H-NMR ($CDCl_3$, 300 MHz) δ1.42 (m, 2H), δ1.56 (m, 2H), δ1.83 (m, 2H), δ2.10 (s, 3H), δ2.42 (t, 2H), δ3.35 (t, 2H). Agrees with literature.[138]

2-(5-Bromopentyl)-2-methyl-1,3-dioxolane (128):- Compound **127** (7.5 g, 0.04 mol), ethylene glycol (4.35 g, 0.07 mol) and *para*-toluenesulfonic acid (900 mg, cat.) were refluxed in benzene (~200 ml) with azeotropic water removal by a Dean-Stark trap overnight. The reaction mixture was cooled and neutralised with a 5% aqueous sodium hydrogencarbonate solution (50 ml). The organic layer was separated, dried over magnesium sulfate, concentrated *in-vacuo* and flash columned on silica gel, eluted with hexanes:ethyl acetate (4:1). This yielded an off yellow oil (9 g, 99%). ^{1}H-NMR ($CDCl_3$,

300 MHz) δ1.27 (s, 3H), δ1.39 (m, 4H), δ1.60 (m, 2H), δ1.81 (m, 2H), δ3.37 (t, 2H), δ3.89 (m, 4H). Agrees with literature.[139]

2-(Hept-6-ynyl)-2-methyl-1,3-dioxolane (129a):- Compound **128** (4 g, 0.017 mol) was taken up in dry DMF (~15 ml) and cooled to 0 ˚C under argon. To this solution was added a slurry of 18 wt. % sodium acetylide in xylene/light mineral oil (6.8 ml). The resulting slurry was allowed to reach room temperature and stirred overnight. The reaction mixture was diluted with diethyl ether and quenched with water. The organic layer was then washed with 1 M HCl, brine and water, dried over sodium sulfate and concentrated *in-vacuo*. The crude material was flash columned on silica gel eluted with hexanes:ethyl acetate (4:1) to leave a colourless oil (2.82 g, 92%). ^{1}H-NMR ($CDCl_3$, 300 MHz) δ1.18 (s, 3H), δ1.29 (m, 4H), δ1.44 (m, 2H), δ1.52 (m, 2H), δ1.84 (t, 1H), δ2.06 (m, 2H), δ3.80 (m, 4H). ^{13}C{^{1}H}-NMR ($CDCl_3$, 75 MHz) δ19.8 (CH_2), δ25.1 (CH_2), δ25.2 (CH_2), δ30.0 (CH_2), δ30.4 (CH_2), δ40.6 (CH_2), δ66.1 (2xCH_2), δ69.8 (CH), δ86.0 (C), δ111.5 (C). LR-MS (CI) m/z Calcd: 182.3 Found: 183.2 $(M+H)^+$. HR-MS (EI+) m/z Calcd: 167.1072 $(M-CH_3)^+$ Found: 167.1076 $(M-CH_3)^+$. IR (cm^{-1}) 3309, 2929, 2865, 1376, 1252, 1218.

1,4-Bis(6-(2-methyl-1,3-dioxolan-2-yl)hexyl)-1*H*-1,2,3-triazole (130):- Compound **128** (3.8 g, 0.016 mol) and sodium azide (3.12 g, 0.048 mol) were stirred in DMF (15 ml) overnight at 60 ^{o}C. The reaction was cooled to room temperature and compound **4** (2.75 g, 0.015 mol) added in DMF (5 ml). Copper sulfate pentahydrate (400 mg, 10 mol %) and sodium ascorbate (634 mg, 20 mol %) were dissolved in water (5 ml) and added to the reaction and the resulting mixture stirred overnight at room temperature. Water was added and the mixture extracted with ethyl acetate. The organic layer was washed with 5% aqueous sodium hydrogencarbonate and brine, dried over magnesium sulfate, concentrated and columned on silica gel eluted with 2% methanol/DCM. This yielded a colourless oil (2.94 g, 50%). ^{1}H-NMR ($CDCl_3$, 300 MHz) δ1.17 (s, 6H), δ1.30 (m, 8H), δ1.56 (m, 6H), δ1.78 (m, 2H), δ2.58 (t, 2H), δ3.78 (m, 8H), δ4.17 (t, 2H), δ7.19 (s, 1H). ^{13}C{^{1}H}-NMR ($CDCl_3$, 100 MHz) δ22.7 (CH_2), δ22.9 (2xCH_3), δ23.0 (CH_2), δ24.8 (CH_2), δ25.9 (CH_2), δ28.6 (CH_2), δ28.7 (CH_2), δ29.5 (CH_2), δ38.1 (CH_2), δ38.3 (CH_2), δ49.4 (CH_2), δ63.8 (4xCH_2), δ109.1 (C), δ109.3 (C), δ119.7 (CH), δ147.3 (C). LR-MS (ESI+) m/z Calcd: 381.5 Found: 382.4 $(M+H)^+$, 404.4 $(M+Na)^+$. HR-MS (ES+) m/z Calcd: 382.2706 $(M+H)^+$, 404.2525 $(M+Na)^+$ Found: 382.2694 $(M+H)^+$, 404.2515 $(M+Na)^+$. IR (cm^{-1}) 3398, 2936, 2862, 1709, 1360.

1,4-Bis(6,6-di(pyrrol-2-yl)heptyl)-1*H*-1,2,3-triazole (131):- Compound **130** (1.43 g, 3.74 mmol) was stirred in 10% water/acetone (50 ml) with *para*-toluenesulfonic acid (700 mg, ~1 eqv.) for 20hrs at room temperature. The reaction mixture was concentrated, taken up with a little 5% aqueous sodium hydrogencarbonate solution, extracted with DCM, dried over sodium sulfate and concentrated to leave an off-yellow oil in quantitative yield which was used in the next step without further purification or analysis.

The oil (1 g, 3.4 mmol) was taken up in pyrrole (9.46 ml, 0.14 mol) and TFA (141 µl, 1.67 mmol) was added with stirring. The resulting mixture was then stirred at 60 ^{o}C for 0.5 hrs. The reaction was quenched with 0.1 M NaOH and the solution extracted with DCM and dried over sodium sulfate. The crude material was gradient columned on silica gel, starting with hexanes:ethyl acetate (4:1) to remove pyrrole and two by-products and increasing to hexanes:ethyl acetate (1:1) to remove the product as an off-white foam (812 mg, 45%). ^{1}H-NMR ($CDCl_3$, 300 MHz) δ1.22 (m, 8H), δ1.55 (s, 6H), δ1.62 (m, 2H), δ1.82 (m, 2H), δ1.92 (m, 4H), δ2.64 (t, 2H), δ4.22 (t, 2H), δ6.04 (s, 4H), δ6.11 (s, 4H), δ6.57 (s, 4H), δ7.17 (s, 1H), δ7.74 (s, 2H), δ7.78 (s, 2H). ^{13}C{^{1}H}-NMR (CD_2Cl_2, 75 MHz) δ24.2 (CH_2), δ24.5 (CH_2), δ25.8 (CH_2), δ26.2 (CH_3), δ27.2 (CH_2), δ29.7 (CH_2), δ29.9 (CH_2), δ30.6 (CH_2), 39.3 (C), 41.3 (CH_2), 50.3 (CH_2), 104.7 (CH), 108.0 (CH), 117.1 (CH), 120.9 (CH), 138.4 (C), 138.6 (C), 148.4 (C). LR-MS (ESI+) m/z Calcd: 525.7 Found: 548.6 $(M+Na)^+$. HR-MS (ES+) m/z Calcd: 548.3478 $(M+Na)^+$ Found: 548.3466 $(M+Na)^+$. IR (cm^{-1}) 3304, 2938, 1648, 1554, 1241.

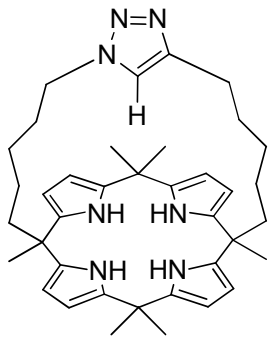

Clicked-calix[4]pyrrole (125):- Compound **131** (808 mg, 1.54 mmol) was dissolved in acetone (150 ml) under argon and $BF_3.OEt_2$ (289 µl, 1.5 eqv.) was added. The resulting solution was stirred at room temperature for 3 hrs and quenched with 0.1 M NaOH. The solution was extracted with DCM exhaustively, dried over sodium sulfate and flash columned on silica gel eluted with hexanes:ethyl acetate (1:1) to leave a pink oil. This oil was triturated with methanol which produced fine white crystals which were collected

and washed with ice-cold methanol to yield the pure title compound (41 mg, 5%). M.p. decomp. ~222 ^{o}C. ^{1}H-NMR (CD_3CN, 300 MHz) δ1.05 (m, 5H, CH_2), δ1.30 (m, 5H, CH_2), δ1.36 (s, 6H, 2xCH_3), δ1.45 (s, 12H, 4xCH_3), δ1.57 (m, 3H, CH_2), δ1.76 (m, 3H, CH_2), δ2.61 (t, $J_1$5.28/$J_2$4.89, 2H, CH_2), δ4.26 (t, $J_1$4.53/$J_2$4.50, 2H, CH_2), δ5.83 (s, 8H, β-pyrrole CH), δ7.53 (s, 1H, triazole CH), δ7.95 (s, 4H, pyrrole NH). ^{13}C{^{1}H}-NMR (CD_3CN, 75 MHz) δ24.4 (CH_2), δ24.7 (CH_2), δ26.1 (CH_2), δ26.2 (CH_2), δ27.0 (CH_2), δ28.2 (2xCH_3), δ28.8 (CH_2), δ30.2 (4xCH_3), 30.9 (CH_2), 31.6 (CH_2), 35.6 (CH_2), 41.4 (2xC), 41.5 (2xC), 50.7 (CH_2), 103.9 (4xCH), 105.1 (4xCH), 122.5 (CH), 138.3 (2xC), 138.4 (2xC), 138.7 (2xC), 138.8 (2xC), 149.1 (C). LR-MS (ESI+) m/z Calcd: 605.9 Found: 606.6 $(M+H)^+$, 628.6 $(M+Na)^+$. HR-MS (ES+) m/z Calcd: 606.4284 $(M+H)^+$ Found: 606.4271 $(M+H)^+$. IR (cm^{-1}) 3294, 2935, 1708, 1363.

1,8-Bis(methoxycarbonyl)triptycene (145): 1,8-Bis(methoxycarbonyl)anthracene (500 mg, 1.7 mmol) was dissolved in DCE (50 mL) and benzenediazonium-2-carboxylate hydrochloride[151] (1.4 g, 7.5 mmol) was added. 1,2-Epoxypropane (12 mL) was added to the reaction vessel and the resulting solution allowed to reflux overnight. Solvents were removed from the brown solution under reduced pressure. The resulting brown oil was purified by column chromatography (Silica gel, 100% DCM, R_f: 0.53), to give white powder of pure title compound (0.52g, 82%). ^{1}H-NMR ($CDCl_3$, 300 MHz) δ7.93 (s, 1H), δ7.60 (m, 4H), δ7.39 (m, 1H), 7.03 (m, 4H), δ5.50 (s, 1H), δ4.02 (s, 6H). Spectrum agrees with literature.[152]

1-Methyl-2-hydrogen-3-diazoniumphthalate hydrochloride (147): (14.14 g, 0.063 mol) was dissolved in a minimum quantity of methanol followed by addition of palladium/carbon 10 wt. % (1 g, cat.). The reaction vessel was evacuated and back-filled with hydrogen gas. The reaction mixture was stirred vigorously at room temperature overnight. The Pd/C was removed by filtration and the methanol removed under reduced pressure, leaving an off-white oil. This oil was taken up in ethanol and acidified with concentrated HCl. Isoamyl nitrite was added slowly at 0 ^{o}C and stirred for 15 min. Ether was added and reaction stirred for a further 15 min. The resulting precipitate was collected by filtration and dried on a high vacuum line (12.55 g, 82%). ^{1}H-NMR (300 MHz, MeOD) δ7.40 (d *J*8.28 1H), δ6.87 (d *J*7.92 1H) δ6.65 (dt *J*8.29, 7.90 1H), δ2.38 (s 3H). ^{13}C-NMR (100 MHz, MeOD) δ53.6 (CH_3), δ118.1 (C), δ118.6 (C), δ121.7 (CH), δ122.4 (CH), δ135.6 (CH), δ135.9 (CH), 161.3 (C), 165.9 (C). IR (cm^{-1}) 3053, 2279, 1745, 1716, 1290, 1101.

***Syn-* and *anti*-tris(methoxycarbonyl)triptycene (133):** Compound **141** (2 g, 6.8 mmol) was dissolved in DCE (50 mL) and compound **147** (7.3 g, 0.03 mol) added. 1,2-epoxypropane (45 mL) was added to the reaction vessel and the resulting mixture allowed to reflux overnight. Solvents were removed from the brown solution under reduced pressure. The resulting brown oil was purified and the isomers separated by column chromatography (silica gel, ethyl acetate : hexane, 1:4 (v/v), *anti*-isomer R_f: 0.19, *syn*-isomer R_f: 0.13). The fractions for each isomer were each recrystallised from DCM:ethyl acetate, 1:1 (v/v) to give colourless crystals. Yields: ***Anti*-127** (0.084 g, 3%), ***Syn*-127** (0.35 g, 12%). ***Anti*-127**: ^{1}H-NMR (300 MHz, DMSO-d_6) δ7.60 (m, 6H), δ7.18 (m, 3H), δ6.84 (s, 1H), δ5.75 (s, 1H), δ3.97 (s, 6H), δ3.31 (s, 3H). ***Syn*-127**: ^{1}H-NMR (300 MHz, DMSO-d_6) δ8.12 (s, 1H), δ7.67 (m, 3H), δ7.40 (m, 3H), δ7.14 (m, 3H), δ5.94 (s, 1H), δ3.94 (s, 9H). LR-MS (ESI+) m/z. Calcd: 428. Found: 451.2 (M + Na^+), 879.4 (2M + Na^+). Spectra agrees with literature.[149]

1,8,13-tris(methanol)triptycene (134): 1,8,13-tris(methoxycarbonyl)triptycene (100 mg, 0.230 mmol) was dissolved in dry THF (10 mL) and slowly injected into a mixture of lithium aluminium hydride (26.57 mg, 0.7 mmol) suspended in dry THF under an inert atmosphere. The mixture was stirred at room temperature overnight. The reaction was quenched by addition of methanol until no more effervescence was observed. A solid was filtered from the reaction mixture, and the solvents removed under reduced pressure, affording a white solid. The solid was washed in methanol before being boiled in acetonitrile and filtered to give pure title compound (35.6 mg, 45%). M.p. decomp. >300 ^{o}C. ^{1}H-NMR (400 MHz, DMSO-d_6) δ7.33 (d, *J*6.52, 3H), δ6.95 (m, 6H), δ6.57 (s, 1H), δ5.61 (s, 1H), δ5.20 (t, 3H), δ4.80 (d, *J*4.52, 6H). ^{13}C-NMR (100 MHz, DMSO-d_6) 146.2 (C), 142.9 (C), 136.5 (C), 124.4 (CH), 124.3 (CH), 122.5 (CH), 61.2 (CH_2), 53.0 (CH), 48.6 (CH). LR-MS (ESI+) m/z. Calcd: 344.4. Found: 367.2 (M + $Na)^+$. IR (cm^{-1}) 3236, 2951, 1732, 1432, 1238.

References

[1] J.-M. Lehn, *Angew. Chem. Int. Ed.,* **1988**, *27*, 89-112.
[2] J.-M. Lehn, *Nobel Prize Lecture* **1987**.
[3] G. R. Desiraju, *Acc. Chem. Res.,* **2002**, *35*, 565-573.
[4] E. V. Anslyn and D. A. Dougherty, *Modern Physical Organic Chemistry*, Sausalito, California, **2006**, p. *op. cit.*
[5] J. W. Steed and J. L. Atwood, *Supramolecular Chemistry*, John Wiley & Sons Ltd, Chichester, **2000**, p. *op. cit.*
[6] J. L. Sessler, P. A. Gale and W.-S. Cho, *Anion Receptor Chemistry*, The Royal Society of Chemistry, Dorchester, **2006**, p. *op. cit.*
[7] P. D. Beer and P. A. Gale, *Angew. Chem. Int. Ed.,* **2001**, *40*, 486-516.
[8] R. A. Pascal Jr, J. Spergel and D. Van Engen, *Tetrahedron Lett.,* **1986**, *27*, 4099-4102.
[9] S. Valiyaveetil, J. F. J. Engbersen, W. Verboom and D. N. Reinhoudt, *Angew. Chem. Int. Ed.,* **1993**, *32*, 900-901.
[10] K. Kavallieratos, S. Gala, D. Austin and R. H. Crabtree, *J. Am. Chem. Soc.,* **1997**, *119*, 2325-2326.
[11] K. Kavallieratos, C. M. Bertao and R. H. Crabtree, *J. Org. Chem.,* **1999**, *64*, 1675-1683.
[12] C. A. Hunter and D. H. Purvis, *Angew. Chem. Int. Ed.,* **1992**, *31*, 792-795.
[13] S. J. Brooks, S. E. Garcia-Garrido, M. E. Light, P. A. Cole and P. A. Gale, *Chem. Eur. J.,* **2007**, *13*, 3320-3329.
[14] M. J. Chmielewski and J. Jurczak, *Chem. Eur. J.,* **2006**, *12*, 7652-7667.
[15] P. V. Santacroce, J. T. Davis, M. E. Light, P. A. Gale, J. C. Iglesias-Sanchez, P. Prados and R. Quesada, *J. Am. Chem. Soc.,* **2007**, *129*, 1886-1887.
[16] K. Choi and A. D. Hamilton, *J. Am. Chem. Soc.,* **2001**, *123*, 2456-2457.
[17] K. Choi and A. D. Hamilton, *J. Am. Chem. Soc.,* **2003**, *125*, 10241.
[18] M. Boiocchi, L. D. Boca, D. Esteban-Gomez, L. Fabbrizzi, M. Licchelli and E. Monzani, *J. Am. Chem. Soc.,* **2004**, *126*, 16507.
[19] T. Gunnlaugsson, P. E. Kruger, T. Clive Lee, R. Parkesh, F. M. Pfeffer and G. M. Hussey, *Tetrahedron Lett.,* **2003**, *44*, 6575-6578.
[20] P. S. Lakshminarayanan, I. Ravikumar, E. Suresh and P. Ghosh, *Chem. Commun.,* **2007**, 5214-5216.
[21] C. Caltagirone and P. A. Gale, *Chem. Soc. Rev.,* **2009**, *38*, 520-563.
[22] D. Meshcheryakov, F. Arnaud-Neu, V. Bohmer, M. Bolte, V. Hubscher-Bruder, E. Jobin, I. Thondorf and S. Werner, *Org. Biomol. Chem.,* **2008**, *6*, 1004-1014.
[23] J. L. Sessler, S. Camiolo and P. A. Gale, *Coord. Chem. Rev.,* **2003**, *240*, 17-55.
[24] J. L. Sessler, M. J. Cyr, V. Lynch, E. McGhee and J. A. Ibers, *J. Am. Chem. Soc.,* **1990**, *112*, 2810.
[25] J. L. Sessler and D. Seidel, *Angew. Chem. Int. Ed.,* **2003**, *42*, 5134-5175.
[26] J. L. Sessler and J. Seidel, *Angew. Chem.,* **2003**, *115*, 5292-5333.
[27] S. J. Coles, P. A. Gale and M. B. Hursthouse, *CrystEngComm.,* **2001**, *3*, 259-261.
[28] A. Baeyer, *Dtsch. Chem. Ges.,* **1886**, *19*, 2184.
[29] P. A. Gale, J. L. Sessler, V. Kral and V. Lynch, *J. Am. Chem. Soc.,* **1996**, *118*, 5140-5141.
[30] J. L. Sessler, D. E. Gross, W.-S. Cho, V. Lynch, F. P. Schmidtchen, G. W. Bates, M. E. Light and P. A. Gale, *J. Am. Chem. Soc.,* **2006**, *128*, 12281-12288.

[31] R. Custelcean, L. H. Delmau, B. A. Moyer, J. L. Sessler, W.-S. Cho, D. E. Gross, G. W. Bates, S. J. Brooks, M. E. Light and P. A. Gale, *Angew. Chem. Int. Ed.,* **2005**, *44*, 2537-2542.
[32] F. P. Schmidtchen, *Org. Lett.,* **2002**, *4*, 431-434.
[33] G. W. Bates, P. A. Gale and M. E. Light, *CrystEngComm.,* **2006**, *8*, 300.
[34] C. C. Tong, R. Quesada, J. L. Sessler and P. A. Gale, *Chem. Commun.,* **2008**, 6321-6323.
[35] C. N. Warriner, P. A. Gale, M. E. Light and M. B. Hursthouse, *Chem. Commun.,* **2003**, *15*, 1810-1811.
[36] P. A. Gale, *Chem. Commun.,* **2005**, *30*, 3761-3772.
[37] X. Liu, C. A. Kilner and M. A. Halcrow, *Chem. Commun.,* **2002**, 704.
[38] S. L. Renard, C. A. Kilner, J. Fisher and M. A. Halcrow, *J. Chem. Soc. Dalt. Trans.,* **2002**, 4206-4212.
[39] S. Nieto, J. Perez, L. Riera, V. Riera, D. Miguel, J. A. Golen and A. L. Rheingold, *Inorg. Chem.,* **2007**, *46*, 3407-3418.
[40] J. Perez and L. Riera, *Chem. Commun.,* **2008**, 533-543.
[41] P. D. Beer, *Acc. Chem. Res.,* **1998**, *31*, 71-80.
[42] F. Szemes, D. Hesek, Z. Chen, S. W. Dent, M. G. B. Drew, A. J. Goulden, A. R. Graydon, A. Grieve, R. J. Mortimer, T. Wear, J. S. Weightman and P. D. Beer, *Inorg. Chem.,* **1996**, *35*, 5868-5879.
[43] P. D. Beer, F. Szemes, V. Balzani, C. M. Sala, M. G. B. Drew, S. W. Dent and M. Maestri, *J. Am. Chem. Soc.,* **1997**, *119*, 11864-11875.
[44] G. V. Oshovsky, D. N. Reinhoudt and W. Verboom, *Angew. Chem. Int. Ed.,* **2007**, *46*, 2366-2393.
[45] S. L. Tobey, B. D. Jones and E. V. Anslyn, *J. Am. Chem. Soc.,* **2003**, *125*, 4026-4027.
[46] R. Custelcean, B. A. Moyer and B. P. Hay, *Chem. Commun.,* **2005**, *48*, 5971-5973.
[47] R. Custelcean, P. Remy, P. V. Bonnesen, D. Jiang and B. A. Moyer, *Angew. Chem. Int. Ed.,* **2008**, *47*, 1866-1870.
[48] J. A. Tovilla, R. Vilar and A. J. P. White, *Chem. Commun.,* **2005**, *2005*, 4839-4841.
[49] R. Vilar, *Eur. J. Inorg. Chem.,* **2008**, 357-367.
[50] P. Diaz, J. A. Tovilla, P. Ballester, J. Benet-Buchholz and R. Vilar, *J. Chem. Soc. Dalt. Trans.,* **2007**, 3516-3525.
[51] A. D. Hamilton and D. Van Engen, *J. Am. Chem. Soc.,* **1987**, *109*, 5035-5036.
[52] C. A. Hunter, *J. Chem. Soc. Chem. Commun.,* **1991**, *11*, 749-751.
[53] C. A. Hunter, *J. Am. Chem. Soc.,* **1992**, *114*, 5303-5311.
[54] F. J. Carver, C. A. Hunter and R. J. Shannon, *J. Chem. Soc. Chem. Commun.,* **1994**, *10*, 1277-1280.
[55] P. D. Beer, P. A. Gale and D. K. Smith, *Supramolecular Chemistry*, Oxford University Press, Oxford, **1999**, p. *op. cit.*
[56] P. S. Corbin and S. C. Zimmerman, *J. Am. Chem. Soc.,* **2000**, *122*, 3779.
[57] P. S. Corbin, S. C. Zimmerman, P. A. Thiessen, N. A. Hawryluk and T. J. Murray, *J. Am. Chem. Soc.,* **2001**, *123*, 10475-10488.
[58] M. F. Mayer, S. Nakashima and S. C. Zimmerman, *Org. Lett.,* **2005**, *7*, 3005-3008.
[59] A. M. McGhee, C. Kilner and A. J. Wilson, *Chem. Commun.,* **2008**, 344-346.
[60] C. Frassineti, S. Ghelli, P. Gans, A. Sabatini, M. S. Moruzzi and A. Vacca, *Anal. Biochem.,* **1995**, *231*, 374.
[61] R. P. Sijbesma and E. W. Meijer, *Chem. Commun.,* **2003**, *1*, 5.
[62] J. H. K. K. Hirschberg, L. Brunsveld, A. Ramzi, J. A. J. M. Vekemans, R. P. Sijbesma and E. W. Meijer, *Nature,* **2000**, *407*, 167.
[63] B. R. Cameron and S. J. Loeb, *Chem. Commun.,* **1997**, 573-574.
[64] C. R. Bondy, P. A. Gale and S. J. Loeb, *Chem. Commun.,* **2001**, 729-730.

[65] J. March, *Advanced Organic Chemistry, Reactions, Mechanisms and Structures*, Wiley-Interscience, New York, **1992**, p. 421.
[66] C. R. Bondy, P. A. Gale and S. J. Loeb, *J. Supramol. Chem.,* **2002**, *2*, 93-96.
[67] C. H. Hunter and R. J. Shannon, *Chem. Commun.,* **1996**, 1361-1362.
[68] C. R. Bondy, P. A. Gale and S. J. Loeb, *J. Am. Chem. Soc.,* **2004**, *126*, 5030-5031.
[69] M. J. Hynes, *J. Chem. Soc. Dalt. Trans.,* **1993**, 311-312.
[70] V. Y. Kukushkin, A. Oskarsson and L. I. Elding, *Inorg. Synth.,* **1997**, *31*, 279-284.
[71] R. H. F. Manske and M. Kulka, *Canad. J. Res.,* **1949**, *27B*, 161-167.
[72] Y. Ahmad and D. H. Hey, *J. Chem. Soc.,* **1961**, 3882-3885.
[73] R. Custelcean, V. Sellin and B. A. Moyer, *Chem. Commun.,* **2007**, 1541-1543.
[74] D. A. Jose, D. K. Kumar, B. Ganguly and A. Das, *Inorg. Chem.,* **2007**, *46*, 5817-5819.
[75] S. O. Kang, M. A. Hossain, D. Powell and K. Bowman-James, *Chem. Commun.,* **2005**, *3*, 328-330.
[76] S. Kubik, R. Kirchner, D. Nolting and J. Seidel, *J. Am. Chem. Soc.,* **2002**, *124*, 12752-12760.
[77] C. Reyheller and S. Kubik, *Org. Lett.,* **2007**, *9*, 5271-5274.
[78] P. W. Pflugrath and F. A. Quiocho, *Nature,* **1985**, *314*, 257-260.
[79] B. L. Jacobson and F. A. Quiocho, *J. Mol. Biol.,* **1988**, *204*, 783-787.
[80] S. O. Kang, R. A. Begum and K. Bowman-James, *Angew. Chem. Int. Ed.,* **2006**, *45*, 7882-7894.
[81] L. R. Eller, M. Stepien, C. J. Fowler, J. T. Lee, J. L. Sessler and B. A. Moyer, *J. Am. Chem. Soc.,* **2007**, *129*, 11020-11021.
[82] B. P. Hay, T. K. Firman and B. A. Moyer, *J. Am. Chem. Soc.,* **2005**, *127*, 1810-1819.
[83] I. El Drubi Vega, P. A. Gale, M. E. Light and S. J. Loeb, *Chem. Commun.,* **2005**, 4913-4915.
[84] V. S. Bryantsev and B. P. Hay, *Chem. Commun.,* **2008**, 2417-2428.
[85] V. S. Bryantsev and B. P. Hay, *J. Am. Chem. Soc.,* **2005**, *127*, 8282-8283.
[86] P. C. Kong and F. D. Rochon, *Can. J. Chem.,* **1978**, *56*, 441-445.
[87] M. J. Chmielewski, L. Zhao, A. Brown, D. Curiel, M. R. Sambrook, A. L. Thompson, S. M. Santos, V. Felix, J. J. Davis and P. D. Beer, *Chem. Commun.,* **2008**, 3154-3156.
[88] S.-K. Chang and A. D. Hamilton, *J. Am. Chem. Soc.,* **1988**, *110*, 1318-1319.
[89] S.-K. Chang, D. Van Engen, E. Fan and A. D. Hamilton, *J. Am. Chem. Soc.,* **1991**, *113*, 7640-7645.
[90] P. Tecilla and A. D. Hamilton, *J. Chem. Soc. Chem. Commun.,* **1990**, 1232.
[91] P. Tecilla, R. P. Dixon, G. Slobodkin, D. S. Alavi, D. H. Waldeck and A. D. Hamilton, *J. Am. Chem. Soc.,* **1990**, *112*, 9408.
[92] J. P. Mathias, E. E. Simanek and G. M. Whitesides, *J. Am. Chem. Soc.,* **1994**, *116*, 4326-4340.
[93] J. A. Zerkowski, J. P. Mathias and G. M. Whitesides, *J. Am. Chem. Soc.,* **1994**, *116*, 4305-4315.
[94] A. Bielejewska, C. E. Marjo, L. J. Prins, P. Timmerman, F. de Jong and D. N. Reinhoudt, *J. Am. Chem. Soc.,* **2001**, *123*, 7518-7533.
[95] P. Lipkowski, A. Bielejewska, H. Kooijman, A. L. Spek, P. Timmerman and D. N. Reinhoudt, *Chem. Commun.,* **1999**, 1311-1312.
[96] P. V. Mason, N. R. Champness, S. R. Collinson, M. G. Fisher and G. Goretzki, *Eur. J. Org. Chem.,* **2006**, *6*, 1444-1449.
[97] S.-I. Kondo, T. Hayashi, Y. Sakuno, Y. Takezawa, T. Yokoyama, M. Unno and Y. Yano, *Org. Biomol. Chem.,* **2007**, *5*, 907-916.
[98] J. D. Carr, L. Lambert, D. E. Hibbs, M. B. Hursthouse, K. M. A. Malik and J. H. R. Tucker, *Chem. Commun.,* **1997**, 1649.

[99] J. D. Carr, S. J. Coles, M. B. Hursthouse, M. E. Light, J. H. R. Tucker and J. Westwood, *Angew. Chem. Int. Ed.,* **2000**, *39*, 3296.
[100] S. R. Collinson, T. Gelbrich, M. B. Hursthouse and J. H. R. Tucker, *Chem. Commun.,* **2001**, 555-556.
[101] J. Westwood, S. J. Coles, S. R. Collinson, G. Gasser, S. J. Green, M. B. Hursthouse, M. E. Light and J. H. R. Tucker, *Organometallics,* **2004**, *23*, 946-951.
[102] B. S. Rasmussen, U. Elezcano and T. Skrydstrup, *J. Chem. Soc. Perkin Trans. 1,* **2002**, 1723.
[103] C.-Y. Hung, T. Hopfner and R. P. Thummel, *J. Am. Chem. Soc.,* **1993**, *115*, 12601-12602.
[104] J. Larsen, B. S. Rasmussen, R. G. Hazell and T. Skrydstrup, *Chem. Commun.,* **2004**, 202.
[105] S. J. Brooks, P. A. Gale and M. E. Light, *Chem. Commun.,* **2006**, 4344.
[106] P. A. Gale, J. Garric, M. E. Light, B. A. McNally and B. D. Smith, *Chem. Commun.,* **2007**, 1736.
[107] K. G. Hull, M. Visnick, W. Tautz and A. Sheffron, *Tetrahedron,* **1997**, *53*, 12405.
[108] H. Hou, Y. Wei, Y. Song, L. Mi, M. Tang, L. Li and Y. Fan, *Angew. Chem. Int. Ed.,* **2005**, *44*, 6067-6074.
[109] R. M. Izatt, J. S. Bradshaw, M. L. Colter, Y. Nakatsuji, N. O. Spencer, M. F. Brown, G. Arena, P. K. Tse, B. E. Wilson, J. D. Lamb and N. Kent Dalley, *J. Org. Chem.,* **1985**, *50*, 4865-4872.
[110] J. Garric in Thesis entitled Conception, Synthesis and Study of New Helicoidal Capsules: Molecular Apple Peels, University of Bordeaux I, Bordeaux, **2005**.
[111] N. W. Alcock, R. G. Kingston, P. Moore and C. Pierpoint, *J. Chem. Soc. Dalt. Trans.,* **1984**, 1937.
[112] L. Fielding, *Tetrahedron,* **2000**, *56*, 6151-6170.
[113] R. H. Grubbs, *Handbook of Metathesis*, Wiley VCH, Germany, **2003**, p. *op. cit.*
[114] J. P. Powers, S. Li, J. C. Jaen, J. Liu, N. P. C. Walker, Z. Wang and H. Wesche, *Biorg. Med. Chem. Lett.,* **2006**, *16*, 2842-2845.
[115] B. Akteries and J. C. Jochims, *Chem. Ber.,* **1986**, *119*, 669-682.
[116] B. Akteries and J. C. Jochims, *Chem. Ber.,* **1986**, *119*, 83-95.
[117] R. Huisgen, *Angew. Chem. Int. Ed.,* **1963**, *2*, 565-632.
[118] A. Michael, *J. Prakt. Chem.,* **1893**, *48*, 94.
[119] H. C. Kolb, M. G. Finn and K. B. Sharpless, *Angew. Chem. Int. Ed.,* **2001**, *40*, 2004-2021.
[120] J. E. Moses and A. D. Moorhouse, *Chem. Soc. Rev.,* **2007**, *36*, 1249-1262.
[121] V. V. Rostovtsev, L. G. Green, V. V. Fokin and K. B. Sharpless, *Angew. Chem. Int. Ed.,* **2002**, *41*, 2596-2599.
[122] C. W. Tornoe, C. Christensen and M. Meldal, *J. Org. Chem.,* **2002**, *67*, 3057.
[123] D. Fournier, R. Hoogenboom and U. S. Schubert, *Chem. Soc. Rev.,* **2007**, *36*, 1369-1380.
[124] Y. Li and A. H. Flood, *J. Am. Chem. Soc.,* **2008**, *130*, 12111-12122.
[125] Y. Li and A. H. Flood, *Angew. Chem. Int. Ed.,* **2008**, *47*, 2649-2652.
[126] Y. Li, M. Pink, J. A. Karty and A. H. Flood, *J. Am. Chem. Soc.,* **2008**, *130*, 17293-17295.
[127] R. M. Meudtner and S. Hecht, *Angew. Chem. Int. Ed.,* **2008**, *47*, 4926-4930.
[128] H. Juwarker, J. M. Lenhardt, D. M. Pham and S. L. Craig, *Angew. Chem. Int. Ed.,* **2008**, *47*, 3740-3743.
[129] A. P. Davis, J. J. Perry and R. P. Williams, *J. Am. Chem. Soc.,* **1997**, *119*, 1793.
[130] A. J. Ayling, M. Nieves Perez-Payan and A. P. Davis, *J. Am. Chem. Soc.,* **2001**, *123*, 12716-12717.

[131] A. Kumar and P. S. Pandey, *Org. Lett.,* **2008**, *10*, 165-168.
[132] C. H. Lee, H. Miyaji, D. W. Yoon and J. L. Sessler, *Chem. Commun.,* **2008**, 24-34.
[133] D. W. Yoon, H. Hwang and C. H. Lee, *Angew. Chem. Int. Ed.,* **2002**, *41*, 1757-1759.
[134] D. W. Yoon, D. E. Gross, V. Lynch, J. L. Sessler, B. P. Hay and C. H. Lee, *Angew. Chem.,* **2008**, *120*, 5116-5120.
[135] C. H. Lee, H. K. Na, D. W. Yoon, D. H. Won, W.-S. Cho, V. Lynch, S. V. Shevchuk and J. L. Sessler, *J. Am. Chem. Soc.,* **2003**, *125*, 7301-7306.
[136] J. Yoo, M. S. Kim, S. J. Hong, J. L. Sessler and C. H. Lee, *J. Org. Chem.,* **2009**, *74*, 1065-1069.
[137] H. Miyaji, H. K. Kim, E. K. Sim, C. H. Lee, W.-S. Cho, J. L. Sessler and C. K. Lee, *J. Am. Chem. Soc.,* **2005**, *127*, 12510.
[138] W.-C. Zhang and C.-J. Li, *J. Org. Chem.,* **2000**, *65*, 5831-5833.
[139] H. Rudler and T. Durand-Reville, *J. Organometallic Chem.,* **2001**, *617*, 571-587.
[140] P. Wu and V. V. Fokin, *Aldrichimica Acta,* **2007**, *40*, 7-17.
[141] P. A. Gale, M. E. Light, B. A. McNally, K. Navakhun, K. E. Sliwinski and B. D. Smith, *Chem. Commun.,* **2005**, 3773-3775.
[142] A. P. Davis, D. N. Sheppard and B. D. Smith, *Chem. Soc. Rev.,* **2007**, *36*, 348-357.
[143] A. V. Koulov, T. N. Lambert, R. Shukla, M. Jain, J. M. Boon, B. D. Smith, H. Y. Li, D. N. Sheppard, J. B. Joos, J. P. Clare and A. P. Davis, *Angew. Chem. Int. Ed.,* **2003**, *42*, 4931-4933.
[144] M. P. Wintergerst, T. G. Levitskaia, B. A. Moyer, J. L. Sessler and L. H. Delmau, *J. Am. Chem. Soc.,* **2008**, *130*, 4129-4139.
[145] P. V. Santacroce, O. A. Okunola, P. Y. Zavalij and J. T. Davis, *Chem. Commun.,* **2006**, 3246-3248.
[146] X. X. Peng, H. Y. Lu, T. Han and C. F. Chen, *Org. Lett.,* **2007**, *9*, 895-898.
[147] X. Z. Zhu and C. F. Chen, *J. Am. Chem. Soc.,* **2005**, *127*, 13158-13159.
[148] T. Ross Kelly, X. Cai, F. Damkaci, S. B. Panicker, B. Tu, S. M. Bushell, I. Cornella, M. J. Piggott, R. Salives, M. Cavero, Y. Zhao and S. Jasmin, *J. Am. Chem. Soc.,* **2007**, *129*, 376-386.
[149] M. E. Rogers and B. A. Averill, *J. Org. Chem.,* **1986**, *51*, 3308-3314.
[150] S. Akiyama, S. Misumi and M. Nakagawa, *Bull. Chem. Soc. Jpn.,* **1962**, *35*, 1829.
[151] H. Duerr, H. Nickels, L. A. Pacala and M. Jones Jr., *J. Org. Chem.,* **1980**, *45*, 973-980.
[152] M. Kuritani, Y. Sakata, F. Ogura and M. Nakagawa, *Bull. Chem. Soc. Jpn.,* **1973**, *46*, 605-610.

Appendix 1 – X-Ray Crystal Structure Data

The crystal structures reported in Chapters 2, 3 and 4 were solved by the EPSRC National Crystallography Service based at the University of Southampton by Dr Mark E. Light. The refinement of the structures and the fractional coordinates are reported for the sake of completeness and so that the structures can be rendered from this text if necessary.

Structures from Chapter 2

Hydrogen sulfate complex of receptor 59:

Table 1. Crystal data and structure refinement details.

Identification code	**2006sot0749**
Empirical formula	$C_{44}H_{70}N_{12}O_{12}PtS_2$
	$C_{44}H_{68}N_{12}O_4Pt^{2+} \cdot 2(HSO_4)^-$
Formula weight	1218.33
Temperature	120(2) K
Wavelength	0.71069 Å
Crystal system	Monoclinic
Space group	$P2_1/c$
Unit cell dimensions	a = 16.685(4) Å
	b = 8.9880(14) Å β = 92.453(7)°
	c = 17.319(3) Å
Volume	2594.9(9) Å^3
Z	2
Density (calculated)	1.559 Mg / m^3
Absorption coefficient	2.855 mm^{-1}
F(000)	1248
Crystal	Slab; Colourless
Crystal size $0.3 \times 0.1 \times 0.04$ mm^3	
θ range for data collection	3.27 – 25.88°
Index ranges	$-20 \le h \le 20$, $-10 \le k \le 10$, $-21 \le l \le 21$
Reflections collected	26222
Independent reflections	4914 [R_{int} = 0.1792]
Completeness to θ = 25.88°	97.8 %
Absorption correction	Semi–empirical from equivalents
Max. and min. transmission	0.8944 and 0.4713
Refinement method	Full-matrix least-squares on F^2
Data / restraints / parameters	4914 / 172 / 338
Goodness-of-fit on F^2	0.999
Final R indices [$F^2 > 2\sigma(F^2)$]	$R1$ = 0.0739, $wR2$ = 0.1395
R indices (all data)	$R1$ = 0.1927, $wR2$ = 0.1769
Largest diff. peak and hole	1.113 and −1.845 e Å^{-3}

Diffractometer: *Nonius KappaCCD* area detector (ϕ scans and ω scans to fill *asymmetric unit*). **Cell determination:** DirAx (Duisenberg, A.J.M.(1992). J. Appl. Cryst. 25, 92-96.) **Data collection:** Collect (Collect: Data collection software, R. Hooft, Nonius B.V., 1998). **Data reduction and cell refinement**: *Denzo* (Z. Otwinowski & W. Minor, *Methods in Enzymology* (1997) Vol. **276**: *Macromolecular Crystallography*, part A, pp. 307–326; C. W. Carter, Jr. & R. M. Sweet, Eds., Academic Press). **Absorption correction**: Sheldrick, G. M. SADABS - Bruker Nonius area detector scaling and absorption correction - V2.10 **Structure solution**: *SHELXS97* (G. M. Sheldrick, Acta Cryst. (1990) A**46** 467–473). **Structure refinement**: *SHELXL97* (G. M. Sheldrick (1997), University of Göttingen, Germany). **Graphics:** Cameron - A Molecular Graphics Package. (D. M. Watkin, L. Pearce and C. K. Prout, Chemical Crystallography Laboratory, University of Oxford, 1993).

Special details: All hydrogen atoms were placed in idealised positions and refined using a riding model.

Table 2. Atomic coordinates [× 10^4], equivalent isotropic displacement parameters [$Å^2$ × 10^3] and site occupancy factors. U_{eq} is defined as one third of the trace of the orthogonalized U^{ij} tensor.

Atom	*x*	*y*	*z*	U_{eq}	*S.o.f.*
Pt1	5000	0	5000	51(1)	1
C1A	8260(30)	2920(30)	9600(30)	198(14)	0.50
C2A	8799(17)	1750(40)	9240(20)	149(8)	0.50
C3A	8351(19)	290(30)	9054(17)	111(8)	0.50
C4A	7700(20)	490(40)	8400(9)	116(10)	0.50
C1B	8760(20)	730(50)	9770(30)	198(14)	0.50
C2B	8668(16)	2020(40)	9180(20)	149(8)	0.50
C3B	7794(17)	2230(30)	8887(16)	111(8)	0.50
C4B	7506(19)	940(40)	8356(11)	116(10)	0.50
C5	7945(7)	−196(16)	7134(8)	65(3)	1
C6	8171(7)	−873(15)	5790(7)	69(4)	1
C7	7496(7)	−996(13)	5179(6)	55(3)	1
C8	7646(7)	−1582(12)	4458(6)	60(3)	1
C9	7014(7)	−1743(13)	3900(7)	70(4)	1
C10	6273(6)	−1279(12)	4070(6)	55(3)	1
C11	6720(7)	−588(12)	5303(7)	55(3)	1
C12	4273(6)	−2574(12)	4183(6)	50(3)	1
C13	4468(7)	−2966(13)	5495(7)	58(3)	1
C14	4122(7)	−4361(14)	5432(8)	62(3)	1
C15	3824(7)	−4821(13)	4720(8)	63(3)	1
C16	3908(7)	−3935(12)	4073(7)	57(3)	1
C17	3633(7)	−4387(14)	3260(7)	72(4)	1
C18	2174(8)	−4695(13)	3281(9)	80(4)	1
C19	740(7)	−5258(18)	3157(12)	133(7)	1
C20	270(11)	−5940(30)	2463(14)	228(13)	1
C21	450(15)	−5340(30)	1667(16)	214(13)	1
C22	128(13)	−6500(30)	1086(17)	225(13)	1
N1	7898(6)	938(12)	7647(6)	82(3)	1
N2	8024(5)	192(9)	6384(5)	52(2)	1
N3	6118(5)	−714(10)	4773(5)	53(2)	1
N4	4555(5)	−2081(10)	4875(5)	53(2)	1
N5	2915(6)	−5329(9)	3223(6)	67(3)	1
N6	1560(6)	−5685(13)	3179(9)	117(5)	1
O1	7923(5)	−1538(9)	7335(4)	73(2)	1
O2	2084(6)	−3381(9)	3421(6)	101(3)	1
O3	5601(4)	8636(8)	8033(4)	66(2)	1
O4	4878(5)	9314(11)	6894(4)	84(3)	1
O5	6016(4)	7794(8)	6835(4)	64(2)	1
O6	6158(5)	10237(7)	7172(6)	77(2)	1
S1	5583(2)	8955(4)	7200(2)	71(1)	1

Bromide complex of receptor 70:

Table 1. Crystal data and structure refinement.

Identification code	**2007sot1536**	
Empirical formula	$C_{38}H_{44}Br_2N_8O_2Pt$	
Formula weight	999.72	
Temperature	120(2) K	
Wavelength	0.71073 Å	
Crystal system	Monoclinic	
Space group	*P*21/*n*	
Unit cell dimensions	a = **14.0597(5) Å**	α = **90**°
	b = **9.3584(2) Å**	β = **95.3300(10)**°
	c = **14.9751(4) Å**	γ = **90**°
Volume	1961.85(10) Å^3	
Z	2	
Density (calculated)	1.692 Mg / m^3	
Absorption coefficient	5.657 mm^{-1}	
F(000)	984	
Crystal Blade;	Colourless	
Crystal size	0.16 × 0.05 × 0.01 mm^3	
θ range for data collection	3.02 − 27.48°	
Index ranges	$-18 \le h \le 18$, $-12 \le k \le 12$, $-19 \le l \le 19$	
Reflections collected	20717	
Independent reflections	4480 [R_{int} = 0.0427]	
Completeness to θ = 27.48°	99.8 %	
Absorption correction	Semi−empirical from equivalents	
Max. and min. transmission	0.9456 and 0.4647	
Refinement method	Full-matrix least-squares on F^2	
Data / restraints / parameters	4480 / 0 / 233	
Goodness-of-fit on F^2	1.115	
Final R indices [$F^2 > 2\sigma(F^2)$]	*R1* = 0.0318, *wR2* = 0.0620	
R indices (all data)	*R1* = 0.0435, *wR2* = 0.0678	
Largest diff. peak and hole	1.770 and −0.798 e Å^{-3}	

Diffractometer: *Nonius KappaCCD* area detector (ϕ scans and ω scans to fill *asymmetric unit* sphere). **Cell determination:** DirAx (Duisenberg, A.J.M.(1992). J. Appl. Cryst. 25, 92-96.) **Data collection:** Collect (Collect: Data collection software, R. Hooft, Nonius B.V., 1998). **Data reduction and cell refinement**: *Denzo* (Z. Otwinowski & W. Minor, *Methods in Enzymology* (1997) Vol. **276**: *Macromolecular Crystallography*, part A, pp. 307−326; C. W. Carter, Jr. & R. M. Sweet, Eds., Academic Press). **Absorption correction**: *SORTAV* (R. H. Blessing, Acta Cryst. A**51** (1995) 33−37; R. H. Blessing, J. Appl. Cryst. **30** (1997) 421−426). S**tructure solution**: *SHELXS97* (G. M. Sheldrick, Acta Cryst. (1990) A**46** 467−473). S**tructure refinement**: *SHELXL97* (G. M. Sheldrick (1997), University of Göttingen, Germany). **Graphics:** Cameron - A Molecular Graphics Package. (D. M. Watkin, L. Pearce and C. K. Prout, Chemical Crystallography Laboratory, University of Oxford, 1993).

Table 2. Atomic coordinates [× 10^4], equivalent isotropic displacement parameters [$Å^2$ × 10^3] and site occupancy factors. U_{eq} is defined as one third of the trace of the orthogonalized U^{ij} tensor.

Atom	*x*	*y*	*z*	U_{eq}	*S.o.f.*
Pt1	5000	0	0	17(1)	1
O1	2492(2)	4345(3)	3183(2)	31(1)	1
N1	5557(2)	1901(4)	–319(2)	23(1)	1
N2	3709(2)	961(3)	–65(2)	19(1)	1
N3	2789(3)	2382(4)	2337(2)	25(1)	1
N4	3714(3)	2852(4)	3638(2)	35(1)	1
C1	5864(3)	2829(5)	325(3)	35(1)	1
C2	6220(4)	4149(6)	110(4)	56(2)	1
C3	6254(5)	4507(6)	–769(5)	62(2)	1
C4	5939(4)	3556(5)	–1432(4)	47(1)	1
C5	5593(3)	2256(5)	–1186(3)	30(1)	1
C6	3194(3)	1260(4)	–875(3)	23(1)	1
C7	2390(3)	2061(4)	–910(3)	23(1)	1
C8	2043(3)	2585(4)	–114(3)	20(1)	1
C9	1231(3)	3470(4)	–115(3)	26(1)	1
C10	956(3)	3953(5)	686(3)	27(1)	1
C11	1444(3)	3588(4)	1508(3)	24(1)	1
C12	2245(3)	2736(4)	1542(3)	19(1)	1
C13	2550(3)	2212(4)	715(3)	17(1)	1
C14	3396(3)	1408(4)	693(3)	17(1)	1
C15	2969(3)	3280(4)	3068(3)	24(1)	1
C16	4001(3)	3634(5)	4467(3)	33(1)	1
C17	3537(4)	3076(6)	5263(3)	37(1)	1
C18	3959(4)	3733(6)	6145(3)	42(1)	1
C19	3464(5)	3211(7)	6951(4)	60(2)	1
Br21	4660(1)	–991(1)	–2469(1)	27(1)	1

Sulfate complex of receptor 70 from nitromethane:

Table 1. Crystal data and structure refinement details.

Identification code	**2008sot0774 (mgf101SO4)**	
Empirical formula	$C_{120}H_{150}B_2F_8N_{30}O_{26}Pt_3S_2$ $3(C_{38}H_{44}N_8O_2Pt)^{2+}.6(CH_3NO_2).2(O_4S)^{2-}$ $.2(BF_4)^-$	
Formula weight	3251.71	
Temperature	120(2) K	
Wavelength	0.71073 Å	
Crystal system	Triclinic	
Space group	*P*–1	
Unit cell dimensions	a = 12.6995(4) Å	α = 76.749(2)°
	b = 13.8948(4) Å	β = 89.381(2)°
	c = 20.3426(5) Å	γ = 73.750(2)°
Volume	3348.97(16) Å^3	
Z	1	
Density (calculated)	1.612 Mg / m^3	
Absorption coefficient	3.249 mm^{-1}	
F(000)	1636	
Crystal	Block; Yellow	
Crystal size	0.2 × 0.2 × 0.1 mm^3	
θ range for data collection	3.02 – 25.03°	
Index ranges	$-15 \le h \le 15$, $-16 \le k \le 16$, $-24 \le l \le 24$	
Reflections collected	49439	
Independent reflections	11804 [R_{int} = 0.0820]	
Completeness to θ = 25.03°	99.8 %	
Absorption correction	Semi–empirical from equivalents	
Max. and min. transmission	0.7371 and 0.5527	
Refinement method	Full-matrix least-squares on F^2	
Data / restraints / parameters	11804 / 506 / 882	
Goodness-of-fit on F^2	1.031	
Final R indices [$F^2 > 2\sigma(F^2)$]	$R1$ = 0.0439, $wR2$ = 0.0929	
R indices (all data)	$R1$ = 0.0747, $wR2$ = 0.1050	
Largest diff. peak and hole	2.312 and –0.977 e Å^{-3}	

Diffractometer: *Nonius KappaCCD* area detector (ϕ scans and ω scans to fill *asymmetric unit*). **Cell determination:** DirAx (Duisenberg, A.J.M.(1992). J. Appl. Cryst. 25, 92-96.) **Data collection:** Collect (Collect: Data collection software, R. Hooft, Nonius B.V., 1998). **Data reduction and cell refinement**: *Denzo* (Z. Otwinowski & W. Minor, *Methods in Enzymology* (1997) Vol. **276**: *Macromolecular Crystallography*, part A, pp. 307–326; C. W. Carter, Jr. & R. M. Sweet, Eds., Academic Press). **Absorption correction**: Sheldrick, G. M. SADABS - Bruker Nonius area detector scaling and absorption correction - V2.10 **Structure solution**: *SHELXS97* (G. M. Sheldrick, Acta Cryst. (1990) A**46** 467–473). **Structure refinement**: *SHELXL97* (G. M. Sheldrick (1997), University of Göttingen, Germany). **Graphics:** Cameron - A Molecular Graphics Package. (D. M. Watkin, L. Pearce and C. K. Prout, Chemical Crystallography Laboratory, University of Oxford, 1993).

Special details: All hydrogen atoms were identified in the difference map and then placed in idealised positions and refined using a riding model.

Table 2. Atomic coordinates [× 10⁴], equivalent isotropic displacement parameters [Å² × 10³] and site occupancy factors. U_{eq} is defined as one third of the trace of the orthogonalized U^{ij} tensor.

Atom	*x*	*y*	*z*	U_{eq}	*S.o.f.*
Pt1	1455(1)	1823(1)	3459(1)	24(1)	1
O1	–4208(3)	3884(3)	1500(2)	38(1)	1
O2	1722(3)	7374(3)	2891(2)	48(1)	1
N1	350(3)	1986(3)	4172(2)	29(1)	1
N2	2623(3)	1626(3)	2772(2)	26(1)	1
N3	496(3)	1211(3)	2980(2)	24(1)	1
N4	–2467(4)	3215(3)	2010(2)	35(1)	1
N5	–3404(4)	4905(3)	1924(2)	33(1)	1
N6	2305(3)	2533(3)	3916(2)	24(1)	1
N7	1579(4)	5724(3)	3133(2)	32(1)	1
N8	740(4)	6883(3)	2168(2)	44(1)	1
C1	–518(5)	2846(5)	4092(3)	42(2)	1
C2	–1255(6)	2956(6)	4580(3)	59(2)	1
C3	–1126(6)	2188(6)	5159(4)	72(2)	1
C4	–233(7)	1317(6)	5253(4)	74(2)	1
C5	484(5)	1239(4)	4738(3)	45(2)	1
C6	3368(4)	706(4)	2845(3)	35(2)	1
C7	4179(5)	543(4)	2397(3)	39(2)	1
C8	4228(5)	1330(4)	1865(3)	38(2)	1
C9	3473(5)	2276(5)	1799(3)	52(2)	1
C10	2669(5)	2400(4)	2261(3)	38(2)	1
C11	746(4)	171(4)	3024(3)	29(1)	1
C12	48(4)	–226(4)	2764(3)	31(1)	1
C13	–977(4)	407(4)	2430(3)	30(1)	1
C14	–1756(5)	14(4)	2186(3)	42(2)	1
C15	–2723(5)	668(4)	1884(3)	45(2)	1
C16	–2971(5)	1740(4)	1820(3)	36(2)	1
C17	–2235(4)	2164(4)	2056(3)	30(1)	1
C18	–1209(4)	1491(4)	2370(2)	23(1)	1
C19	–432(4)	1829(4)	2669(2)	25(1)	1
C20	–3426(4)	3998(4)	1790(3)	29(1)	1
C21	–4246(4)	5874(4)	1631(3)	33(1)	1
C22	–4153(4)	6250(4)	874(3)	33(1)	1
C23	–4983(5)	7249(4)	558(2)	32(1)	1
C24	–4884(5)	7562(4)	–201(3)	40(2)	1
C25	3047(4)	2054(4)	4452(3)	36(2)	1
C26	3522(5)	2595(4)	4769(3)	37(2)	1
C27	3289(4)	3680(4)	4554(3)	33(2)	1
C28	3759(4)	4281(4)	4868(3)	35(2)	1
C29	3492(5)	5319(5)	4612(3)	42(2)	1
C30	2764(4)	5819(4)	4039(3)	37(2)	1
C31	2281(4)	5276(4)	3715(3)	30(1)	1
C32	2526(4)	4176(4)	3976(2)	28(1)	1

C33	2070(4)	3545(4)	3700(2)	26(1)	1
C34	1373(5)	6713(4)	2740(3)	38(2)	1
C35	498(5)	7836(4)	1647(3)	40(2)	1
C36	983(5)	7694(4)	988(3)	37(2)	1
C37	741(5)	8695(4)	440(3)	45(2)	1
C38	1326(6)	8559(5)	−204(3)	61(2)	1
Pt2	10000	5000	0	22(1)	1
O3	6131(3)	8715(3)	1928(2)	46(1)	1
N9	11403(3)	5216(3)	299(2)	23(1)	1
N10	9218(3)	6523(3)	−158(2)	26(1)	1
N11	7425(4)	7705(3)	1379(2)	34(1)	1
C39	11733(4)	4950(4)	957(3)	29(1)	1
C40	12716(5)	5014(4)	1183(3)	35(2)	1
C41	13393(5)	5385(4)	720(3)	40(2)	1
C42	13036(4)	5716(4)	37(3)	35(2)	1
C43	12047(4)	5604(4)	−150(2)	25(1)	1
C44	9232(4)	7163(4)	−772(3)	34(2)	1
C45	8617(5)	8172(4)	−923(3)	40(2)	1
C46	7928(4)	8580(4)	−443(3)	32(1)	1
C47	7222(5)	9593(4)	−594(3)	46(2)	1
C48	6548(5)	9904(4)	−118(3)	50(2)	1
C49	6584(5)	9288(4)	537(3)	49(2)	1
C50	7311(4)	8325(4)	727(3)	33(1)	1
C51	7965(4)	7923(4)	213(3)	25(1)	1
C52	8633(4)	6885(4)	311(3)	27(1)	1
C53	6913(5)	7934(4)	1942(3)	37(2)	1
N12A	7338(4)	7229(4)	2518(2)	52(2)	0.399(8)
C54A	6953(12)	7282(15)	3235(10)	59(2)	0.399(8)
C55A	7723(11)	7799(14)	3499(10)	87(4)	0.399(8)
C56A	8891(12)	7222(16)	3612(8)	84(4)	0.399(8)
C57A	9260(20)	6460(20)	4240(11)	146(6)	0.399(8)
N12B	7338(4)	7229(4)	2518(2)	52(2)	0.601(8)
C54B	7003(10)	7420(12)	3156(7)	59(2)	0.601(8)
C55B	7983(11)	7162(10)	3663(7)	87(4)	0.601(8)
C56B	8701(10)	6117(10)	3860(6)	84(4)	0.601(8)
C57B	9595(14)	5957(10)	4338(6)	146(6)	0.601(8)
O8	3249(5)	7905(4)	1665(3)	79(2)	1
O9	2686(4)	9101(4)	2206(3)	71(2)	1
N13	3260(5)	8248(5)	2171(3)	57(2)	1
C58	4035(6)	7618(6)	2738(3)	66(2)	1
O10	4281(5)	4836(5)	2809(3)	117(3)	1
O11	4476(6)	3166(6)	2994(4)	129(3)	1
N14	4748(7)	3953(8)	3055(4)	106(3)	1
C59	5765(7)	3780(9)	3484(4)	114(4)	1
O12	7596(6)	1234(7)	3750(3)	127(3)	1
O13	7757(8)	−369(7)	4048(4)	174(4)	1
N15	7211(7)	550(8)	3836(4)	113(3)	1
C60	6054(9)	723(8)	3733(5)	114(4)	1
F1	7189(4)	1189(5)	5969(3)	143(2)	1
F2	5456(3)	1276(4)	5939(2)	94(2)	1

F3	6160(3)	2212(3)	5084(2)	78(1)	1
F4	6609(8)	542(5)	5275(3)	188(3)	1
B1	6336(6)	1336(6)	5556(4)	45(2)	1
S1	9432(1)	4787(1)	2147(1)	27(1)	1
O4	8706(3)	4470(4)	2669(2)	56(1)	1
O5	9339(3)	4315(3)	1584(2)	44(1)	1
O6	9089(3)	5919(3)	1910(2)	47(1)	1
O7	10581(3)	4468(3)	2418(2)	35(1)	1

Sulfate complex of 70 from DMSO:

Table 1. Crystal data and structure refinement details.

Identification code	**2008sot0775 (mgf101SO4(ii))**	
Empirical formula	$C_{38}H_{48}N_8O_8PtS$	
Formula weight	971.99	
Temperature	120(2) K	
Wavelength	0.71069 Å	
Crystal system	Triclinic	
Space group	*P*–1	
Unit cell dimensions	a = 12.0709(11) Å	α = 69.502(6)°
	b = 12.2392(13) Å	β = 72.956(6)°
	c = 15.3701(15) Å	γ = 76.034(7)°
Volume	2009.0(3) Å^3	
Z	2	
Density (calculated)	1.607 Mg / m^3	
Absorption coefficient	3.605 mm^{-1}	
F(000)	980	
Crystal	Lath; Pale Green	
Crystal size	0.12 × 0.07 × 0.01 mm^3	
θ range for data collection	2.92 – 25.02°	
Index ranges	$-14 \le h \le 14$, $-14 \le k \le 12$, $-18 \le l \le 17$	
Reflections collected	17653	
Independent reflections	6960 [R_{int} = 0.0811]	
Completeness to θ = 25.02°	97.9 %	
Absorption correction	Semi–empirical from equivalents	
Max. and min. transmission	0.9648 and 0.6615	
Refinement method	Full-matrix least-squares on F^2	
Data / restraints / parameters	6960 / 6 / 522	
Goodness-of-fit on F^2	1.199	
Final *R* indices [$F^2 > 2\sigma(F^2)$]	*R1* = 0.0934, *wR2* = 0.1732	
R indices (all data)	*R1* = 0.1572, *wR2* = 0.2002	
Largest diff. peak and hole	2.042 and –0.991 e Å^{-3}	

Diffractometer: *Nonius KappaCCD* area detector (ϕ scans and ω scans to fill *asymmetric unit*). **Cell determination:** DirAx (Duisenberg, A.J.M.(1992). J. Appl. Cryst. 25, 92-96.) **Data collection:** Collect (Collect: Data collection software, R. Hooft, Nonius B.V., 1998). **Data reduction and cell refinement**: *Denzo* (Z. Otwinowski & W. Minor, *Methods in Enzymology* (1997) Vol. **276**: *Macromolecular Crystallography*, part A, pp. 307–326; C. W. Carter, Jr. & R. M. Sweet, Eds., Academic Press). **Absorption correction**: Sheldrick, G. M. SADABS - Bruker Nonius area detector scaling and absorption correction - V2.10 S**tructure solution**: *SHELXS97* (G. M. Sheldrick, Acta Cryst. (1990) A**46** 467–473). S**tructure refinement**: *SHELXL97* (G. M. Sheldrick (1997), University of Göttingen, Germany). **Graphics:** Cameron - A Molecular Graphics Package. (D. M. Watkin, L. Pearce and C. K. Prout, Chemical Crystallography Laboratory, University of Oxford, 1993).

Special details: All hydrogen atoms were placed in idealised positions and refined using a riding model. Except those of the water that were included in restrained positions.

Table 2. Atomic coordinates [× 10^4], equivalent isotropic displacement parameters [$Å^2 \times 10^3$] and site occupancy factors. U_{eq} is defined as one third of the trace of the orthogonalized U^{ij} tensor.

Atom	*x*	*y*	*z*	U_{eq}	*S.o.f.*
Pt1	0	0	0	28(1)	1
O1	3797(12)	−893(12)	3553(9)	50(3)	1
N1	−1431(10)	−532(11)	1025(9)	26(3)	1
N2	216(12)	882(12)	825(10)	36(3)	1
N3	2945(11)	−474(13)	2294(10)	36(3)	1
N4	4046(13)	−2250(13)	2813(10)	42(4)	1
C1	−2516(12)	−42(15)	939(12)	31(4)	1
C2	−3485(16)	−302(14)	1636(12)	36(4)	1
C3	−3337(15)	−1188(15)	2492(13)	37(4)	1
C4	−2226(16)	−1708(18)	2581(13)	50(5)	1
C5	−1259(16)	−1371(17)	1832(12)	42(5)	1
C6	−476(15)	1941(15)	862(12)	37(4)	1
C7	−311(14)	2562(14)	1368(14)	38(4)	1
C8	611(17)	2190(15)	1850(12)	38(4)	1
C9	855(17)	2855(18)	2352(13)	45(5)	1
C10	1747(18)	2426(17)	2770(14)	48(5)	1
C11	2477(17)	1334(19)	2754(14)	51(5)	1
C12	2277(15)	630(15)	2321(12)	37(4)	1
C13	1338(15)	1067(15)	1817(11)	35(4)	1
C14	1074(13)	442(14)	1304(11)	27(4)	1
C15	3615(15)	−1198(17)	2932(12)	36(4)	1
C16	4588(16)	−3222(16)	3501(12)	42(5)	1
C17	5597(16)	−3987(16)	3046(13)	41(5)	1
C18	6139(17)	−5058(17)	3709(13)	46(5)	1
Pt2	5000	5000	0	29(1)	1
O2	1913(10)	4202(12)	5296(9)	47(3)	1
N5	3945(12)	4082(12)	−139(10)	33(3)	1
N6	5178(11)	3819(11)	1275(9)	27(3)	1
N7	2883(12)	4409(13)	3729(10)	38(4)	1
N8	1619(13)	5944(14)	4158(10)	45(4)	1
C19	7200(17)	−5750(20)	3218(18)	68(7)	1
C20	4339(15)	3045(15)	−306(11)	33(4)	1
C21	3658(15)	2412(17)	−473(12)	38(4)	1
C22	2475(17)	2865(17)	−435(12)	42(5)	1
C23	2027(16)	3906(17)	−213(12)	41(5)	1
C24	2790(14)	4493(14)	−73(11)	30(4)	1
C25	6124(15)	2908(14)	1343(12)	36(4)	1
C26	6259(17)	2155(17)	2211(14)	37(5)	1
C27	5476(15)	2243(16)	3054(12)	36(4)	1
C28	5625(16)	1461(15)	3943(12)	35(4)	1
C29	4824(16)	1632(17)	4736(12)	40(4)	1
C30	3884(15)	2587(15)	4711(12)	38(4)	1
C31	3746(14)	3390(15)	3834(12)	34(4)	1

C32	4542(13)	3183(15)	2982(11)	28(4)	1
C33	4404(14)	3919(14)	2076(12)	32(4)	1
C34	2081(15)	4840(17)	4451(13)	39(4)	1
C35	710(20)	6552(19)	4777(14)	60(6)	1
C36	390(20)	7840(20)	4226(15)	67(7)	1
C37	−660(20)	8480(20)	4787(16)	69(7)	1
C38	−970(20)	9750(20)	4190(20)	78(8)	1
S1	2361(4)	7172(4)	1478(3)	30(1)	1
O3	2202(11)	6764(11)	741(8)	46(3)	1
O4	3143(11)	6281(11)	2042(8)	43(3)	1
O5	1223(11)	7410(12)	2107(9)	44(4)	1
O6	2903(11)	8253(10)	1027(8)	39(3)	1
O7	268(13)	4398(14)	7014(9)	58(4)	1
O8	70(13)	5945(15)	1070(10)	60(4)	1

Structures from Chapter 3

DMSO solvate of compound 88:

Table 1. Crystal data and structure refinement details.

Identification code	**2007sot0175 (mgf134(xiii))**
Empirical formula	$C_{23}H_{21}N_7O_3S$
Formula weight	475.53
Temperature	120(2) K
Wavelength	0.71073 Å
Crystal system	Monoclinic
Space group	$P2_1/n$
Unit cell dimensions	a = 19.3932(4) Å b = 5.87740(10) Å β = 102.8420(10)° c = 19.4872(4) Å
Volume	2165.62(7) Å^3
Z	4
Density (calculated)	1.458 Mg / m^3
Absorption coefficient	0.193 mm^{-1}
F(000)	992
Crystal	Slab; Pale Yellow
Crystal size	0.35 × 0.2 × 0.04 mm^3
θ range for data collection	3.16 – 27.48°
Index ranges	$-25 \le h \le 25$, $-7 \le k \le 7$, $-25 \le l \le 22$
Reflections collected	29058
Independent reflections	4975 [R_{int} = 0.0594]
Completeness to θ = 27.48°	99.8 %
Absorption correction	Semi–empirical from equivalents
Max. and min. transmission	0.9923 and 0.9256
Refinement method	Full-matrix least-squares on F^2
Data / restraints / parameters	4975 / 0 / 326
Goodness-of-fit on F^2	1.082
Final R indices [$F^2 > 2\sigma(F^2)$]	$R1$ = 0.0505, $wR2$ = 0.1252
R indices (all data)	$R1$ = 0.0681, $wR2$ = 0.1377
Extinction coefficient	0.030(2)
Largest diff. peak and hole	0.490 and –0.612 e Å^{-3}

Diffractometer: *Nonius KappaCCD* area detector (ϕ scans and ω scans to fill *asymmetric unit*). **Cell determination:** DirAx (Duisenberg, A.J.M.(1992). J. Appl. Cryst. 25, 92-96.) **Data collection:** Collect (Collect: Data collection software, R. Hooft, Nonius B.V., 1998). **Data reduction and cell refinement**: *Denzo* (Z. Otwinowski & W. Minor, *Methods in Enzymology* (1997) Vol. **276**: *Macromolecular Crystallography*, part A, pp. 307–326; C. W. Carter, Jr. & R. M. Sweet, Eds., Academic Press). **Absorption correction**: Sheldrick, G. M. SADABS - Bruker Nonius area detector scaling and absorption correction - V2.10 S**tructure solution**: *SHELXS97* (G. M. Sheldrick, Acta Cryst. (1990) A**46** 467–473). S**tructure refinement**: *SHELXL97* (G. M. Sheldrick (1997), University of Göttingen, Germany). **Graphics:** Cameron - A Molecular Graphics Package. (D. M. Watkin, L. Pearce and C. K. Prout, Chemical Crystallography Laboratory, University of Oxford, 1993).

Special details: All hydrogen atoms were placed in idealised positions and refined using a riding model, those of the NH were freely refined.

Table 2. Atomic coordinates [$\times 10^4$], equivalent isotropic displacement parameters [$Å^2 \times 10^3$] and site occupancy factors. U_{eq} is defined as one third of the trace of the orthogonalized U^{ij} tensor.

Atom	*x*	*y*	*z*	U_{eq}	*S.o.f.*
C1	7816(1)	694(3)	4222(1)	21(1)	1
C2	8451(1)	1610(3)	4121(1)	25(1)	1
C3	9063(1)	337(4)	4340(1)	28(1)	1
C4	9050(1)	−1780(4)	4668(1)	29(1)	1
C5	8430(1)	−2704(3)	4788(1)	26(1)	1
C6	7816(1)	−1438(3)	4548(1)	23(1)	1
C7	6741(1)	−23(3)	4230(1)	22(1)	1
C8	5595(1)	−1466(3)	4335(1)	24(1)	1
C9	4814(1)	−1028(3)	4129(1)	22(1)	1
C10	4356(1)	−2452(3)	4389(1)	26(1)	1
C11	3641(1)	−1977(3)	4214(1)	27(1)	1
C12	3403(1)	−142(3)	3775(1)	25(1)	1
C13	3900(1)	1154(3)	3533(1)	20(1)	1
C14	3658(1)	3156(3)	3058(1)	20(1)	1
C15	4095(1)	6148(3)	2402(1)	19(1)	1
C16	3606(1)	9087(3)	1783(1)	20(1)	1
C17	3184(1)	10842(3)	1445(1)	23(1)	1
C18	3502(1)	12416(3)	1088(1)	25(1)	1
C19	4216(1)	12223(3)	1063(1)	25(1)	1
C20	4634(1)	10471(3)	1400(1)	24(1)	1
C21	4325(1)	8893(3)	1777(1)	20(1)	1
C22	6639(1)	2200(4)	2273(1)	30(1)	1
C23	6406(1)	6259(4)	2805(1)	33(1)	1
N1	7113(1)	−1846(3)	4554(1)	24(1)	1
N2	7129(1)	1571(3)	4031(1)	23(1)	1
N3	6008(1)	84(3)	4096(1)	24(1)	1
N4	4593(1)	751(3)	3709(1)	21(1)	1
N5	4180(1)	4234(3)	2828(1)	21(1)	1
N6	4625(1)	7033(3)	2175(1)	22(1)	1
N7	3468(1)	7273(3)	2190(1)	20(1)	1
O1	5835(1)	−3101(2)	4707(1)	32(1)	1
O2	3031(1)	3732(2)	2904(1)	25(1)	1
O3	5577(1)	2817(2)	2896(1)	28(1)	1
S1	5904(1)	3961(1)	2352(1)	21(1)	1

DMF/H_2O solvate of compound 90:

Table 1. Crystal data and structure refinement details.

Identification code	**2007sot0568**	
Empirical formula	$C_{49}H_{49.67}N_{15}O_{7.34}$	
Formula weight	966.06	
Temperature	120(2) K	
Wavelength	0.71073 Å	
Crystal system	Triclinic	
Space group	*P*–1	
Unit cell dimensions	a = 10.5481(3) Å	α = 87.777(2)°
	b = 13.6951(4) Å	β = 80.974(2)°
	c = 16.4507(6) Å	γ = 77.225(2)°
Volume	2288.88(13) $Å^3$	
Z	2	
Density (calculated)	1.402 Mg / m^3	
Absorption coefficient	0.098 mm^{-1}	
F(000)	1015	
Crystal	Shard; Colourless	
Crystal size	0.3 × 0.2 × 0.2 mm^3	
θ range for data collection	2.91 – 27.48°	
Index ranges	$-13 \le h \le 13$, $-17 \le k \le 17$, $-21 \le l \le 21$	
Reflections collected	50681	
Independent reflections	10471 [R_{int} = 0.0708]	
Completeness to θ = 27.48°	99.7 %	
Absorption correction	Semi–empirical from equivalents	
Max. and min. transmission	0.9806 and 0.9611	
Refinement method	Full-matrix least-squares on F^2	
Data / restraints / parameters	10471 / 36 / 662	
Goodness-of-fit on F^2	1.064	
Final R indices [$F^2 > 2\sigma(F^2)$]	*R1* = 0.0970, *wR2* = 0.2437	
R indices (all data)	*R1* = 0.1353, *wR2* = 0.2727	
Extinction coefficient	0.0753(19)	
Largest diff. peak and hole	1.865 and −1.038 e $Å^{-3}$	

Diffractometer: *Nonius KappaCCD* area detector (ϕ scans and ω scans to fill *asymmetric unit*). **Cell determination:** DirAx (Duisenberg, A.J.M.(1992). J. Appl. Cryst. 25, 92-96.) **Data collection:** Collect (Collect: Data collection software, R. Hooft, Nonius B.V., 1998). **Data reduction and cell refinement**: *Denzo* (Z. Otwinowski & W. Minor, *Methods in Enzymology* (1997) Vol. **276**: *Macromolecular Crystallography*, part A, pp. 307–326; C. W. Carter, Jr. & R. M. Sweet, Eds., Academic Press). **Absorption correction**: Sheldrick, G. M. SADABS - Bruker Nonius area detector scaling and absorption correction - V2.10 **Structure solution**: *SHELXS97* (G. M. Sheldrick, Acta Cryst. (1990) A**46** 467–473). **Structure refinement**: *SHELXL97* (G. M. Sheldrick (1997), University of Göttingen, Germany). **Graphics:** Cameron - A Molecular Graphics Package. (D. M. Watkin, L. Pearce and C. K. Prout, Chemical Crystallography Laboratory, University of Oxford, 1993).

Special details: All hydrogen atoms were placed in idealised positions and refined using a riding model, except those of the waters which were refined under contraints.

Table 2. Atomic coordinates [$\times 10^4$], equivalent isotropic displacement parameters [$Å^2 \times 10^3$] and site occupancy factors. U_{eq} is defined as one third of the trace of the orthogonalized U^{ij} tensor.

Atom	*x*	*y*	*z*	U_{eq}	*S.o.f.*
O1	4568(1)	705(1)	1606(1)	30(1)	1
O2	7420(1)	2719(1)	2136(1)	32(1)	1
N1	2461(1)	−140(1)	−45(1)	25(1)	1
N2	3195(1)	−566(1)	1132(1)	24(1)	1
N3	3741(1)	883(1)	373(1)	24(1)	1
N4	5678(1)	2317(1)	1218(1)	23(1)	1
N5	7272(1)	4297(1)	1540(1)	26(1)	1
N6	8599(1)	4043(1)	2652(1)	30(1)	1
N7	8161(1)	5528(1)	2068(1)	27(1)	1
C1	2434(1)	−1237(1)	1000(1)	25(1)	1
C2	2099(1)	−2033(1)	1469(1)	28(1)	1
C3	1284(1)	−2552(1)	1163(1)	31(1)	1
C4	831(1)	−2288(1)	415(1)	32(1)	1
C5	1163(1)	−1492(1)	−61(1)	31(1)	1
C6	1960(1)	−965(1)	251(1)	25(1)	1
C7	2273(1)	377(1)	−827(1)	31(1)	1
C8	3199(1)	101(1)	499(1)	23(1)	1
C9	4396(1)	1139(1)	939(1)	24(1)	1
C10	4936(1)	2064(1)	705(1)	23(1)	1
C11	4660(1)	2614(1)	−5(1)	25(1)	1
C12	5126(1)	3480(1)	−159(1)	29(1)	1
C13	5864(1)	3759(1)	374(1)	27(1)	1
C14	6148(1)	3148(1)	1047(1)	23(1)	1
C15	7017(1)	3370(1)	1630(1)	26(1)	1
C16	7971(1)	4575(1)	2059(1)	26(1)	1
C17	7654(1)	6342(1)	1529(1)	34(1)	1
C18	8914(1)	5607(1)	2674(1)	30(1)	1
C19	9332(1)	6417(1)	2934(1)	38(1)	1
C20	10095(2)	6240(1)	3562(1)	46(1)	1
C21	10416(2)	5288(2)	3916(1)	49(1)	1
C22	9985(1)	4478(1)	3663(1)	41(1)	1
C23	9215(1)	4662(1)	3032(1)	31(1)	1
O3	4427(1)	6450(1)	2298(1)	30(1)	1
O4	6292(1)	8865(1)	3367(1)	31(1)	1
N8	3324(1)	3764(1)	2518(1)	23(1)	1
N9	3155(1)	5177(1)	1819(1)	25(1)	1
N10	4430(1)	4915(1)	2949(1)	23(1)	1
N11	5718(1)	7002(1)	3442(1)	22(1)	1
N12	6530(1)	8720(1)	4745(1)	24(1)	1
N13	6645(1)	10401(1)	4216(1)	23(1)	1
N14	6737(1)	10058(1)	5530(1)	24(1)	1
C24	2416(1)	4609(1)	1482(1)	24(1)	1
C25	1670(1)	4792(1)	843(1)	29(1)	1
C26	1029(1)	4049(1)	690(1)	32(1)	1

C27	1135(1)	3154(1)	1146(1)	31(1)	1
C28	1887(1)	2972(1)	1775(1)	27(1)	1
C29	2528(1)	3716(1)	1929(1)	24(1)	1
C30	3727(1)	2969(1)	3094(1)	30(1)	1
C31	3697(1)	4655(1)	2449(1)	22(1)	1
C32	4749(1)	5823(1)	2838(1)	23(1)	1
C33	5519(1)	6067(1)	3475(1)	21(1)	1
C34	5914(1)	5377(1)	4078(1)	24(1)	1
C35	6525(1)	5674(1)	4685(1)	25(1)	1
C36	6685(1)	6654(1)	4678(1)	24(1)	1
C37	6269(1)	7291(1)	4048(1)	21(1)	1
C38	6371(1)	8376(1)	4016(1)	23(1)	1
C39	6617(1)	9671(1)	4796(1)	22(1)	1
C40	6837(1)	11252(1)	4568(1)	23(1)	1
C41	7004(1)	12169(1)	4229(1)	27(1)	1
C42	7268(1)	12845(1)	4752(1)	30(1)	1
C43	7334(1)	12628(1)	5583(1)	29(1)	1
C44	7138(1)	11717(1)	5927(1)	28(1)	1
C45	6903(1)	11034(1)	5403(1)	23(1)	1
C46	6658(1)	9530(1)	6314(1)	30(1)	1
O5	6490(1)	925(1)	2591(1)	38(1)	1
O6	4872(1)	8468(1)	2148(1)	38(1)	1
O8	894(3)	2337(2)	4643(2)	38(1)	0.33
O7	36(2)	2053(1)	3269(1)	86(1)	1
N15	−150(2)	462(2)	3072(1)	105(1)	1
C48	−342(3)	−517(2)	3235(2)	164(1)	1
C49	−42(2)	1157(3)	3524(2)	112(1)	1
C47	−82(3)	704(3)	2179(2)	110(1)	1

Water solvate of compound 91:

Table 1. Crystal data and structure refinement details.

Identification code	**2007sot0569 (mgf170)**
Empirical formula	$C_{24}H_{25}N_5O_3$
Formula weight	431.49
Temperature	120(2) K
Wavelength	0.71073 Å
Crystal system	Monoclinic
Space group	$P2_1/c$
Unit cell dimensions	a = 16.9981(5) Å
	b = 6.2221(2) Å β = 103.902(2)°
	c = 20.6979(6) Å
Volume	2124.97(11) Å^3
Z	4
Density (calculated)	1.349 Mg / m^3
Absorption coefficient	0.092 mm^{-1}
F(000)	912
Crystal	Needle; Colourless
Crystal size	0.32 × 0.02 × 0.02 mm^3
θ range for data collection	3.43 – 27.48°
Index ranges	$-22 \le h \le 22$, $-8 \le k \le 7$, $-24 \le l \le 26$
Reflections collected	21026
Independent reflections	4844 [R_{int} = 0.0780]
Completeness to θ = 27.48°	99.5 %
Absorption correction	Semi–empirical from equivalents
Max. and min. transmission	0.9982 and 0.9613
Refinement method	Full-matrix least-squares on F^2
Data / restraints / parameters	4844 / 3 / 299
Goodness-of-fit on F^2	1.123
Final R indices [$F^2 > 2\sigma(F^2)$]	$R1$ = 0.0874, $wR2$ = 0.1437
R indices (all data)	$R1$ = 0.1447, $wR2$ = 0.1671
Extinction coefficient	0.0015(4)
Largest diff. peak and hole	0.355 and –0.309 e Å^{-3}

Diffractometer: *Nonius KappaCCD* area detector (ϕ scans and ω scans to fill *asymmetric unit*). **Cell determination:** DirAx (Duisenberg, A.J.M.(1992). J. Appl. Cryst. 25, 92-96.) **Data collection:** Collect (Collect: Data collection software, R. Hooft, Nonius B.V., 1998). **Data reduction and cell refinement**: *Denzo* (Z. Otwinowski & W. Minor, *Methods in Enzymology* (1997) Vol. **276**: *Macromolecular Crystallography*, part A, pp. 307–326; C. W. Carter, Jr. & R. M. Sweet, Eds., Academic Press). **Absorption correction**: Sheldrick, G. M. SADABS - Bruker Nonius area detector scaling and absorption correction - V2.10 S**tructure solution**: *SHELXS97* (G. M. Sheldrick, Acta Cryst. (1990) A**46** 467–473). S**tructure refinement**: *SHELXL97* (G. M. Sheldrick (1997), University of Göttingen, Germany). **Graphics:** Cameron - A Molecular Graphics Package. (D. M. Watkin, L. Pearce and C. K. Prout, Chemical Crystallography Laboratory, University of Oxford, 1993).

Special details: All hydrogen atoms were located in the difference map and then refined using a riding model, except those of the water which were freely refined.

Table 2. Atomic coordinates [$\times 10^4$], equivalent isotropic displacement parameters [$Å^2 \times 10^3$] and site occupancy factors. U_{eq} is defined as one third of the trace of the orthogonalized U^{ij} tensor.

Atom	*x*	*y*	*z*	U_{eq}	*S.o.f.*
C1	−740(2)	6291(7)	1533(2)	47(1)	1
C2	−375(2)	4066(7)	1570(2)	35(1)	1
C3	202(2)	3809(6)	1112(2)	29(1)	1
C4	614(2)	1606(6)	1186(2)	31(1)	1
C5	1250(2)	1370(6)	787(2)	26(1)	1
C6	1914(2)	2744(6)	906(2)	27(1)	1
C7	2518(2)	2577(6)	562(2)	26(1)	1
C8	2461(2)	993(6)	75(2)	22(1)	1
C9	1803(2)	−405(6)	−51(2)	29(1)	1
C10	1208(2)	−204(6)	308(2)	32(1)	1
C11	3700(2)	1974(6)	−289(2)	20(1)	1
C12	4312(2)	1136(6)	−649(2)	20(1)	1
C13	5021(2)	2301(6)	−604(2)	21(1)	1
C14	5593(2)	1506(6)	−915(2)	22(1)	1
C15	5433(2)	−387(6)	−1278(2)	22(1)	1
C16	4702(2)	−1416(5)	−1304(1)	19(1)	1
C17	4494(2)	−3437(5)	−1699(2)	19(1)	1
C18	3456(2)	−6238(5)	−1935(1)	19(1)	1
C19	3275(2)	−9182(5)	−2532(2)	20(1)	1
C20	3306(2)	−10962(6)	−2933(2)	23(1)	1
C21	2665(2)	−12398(6)	−3030(2)	25(1)	1
C22	2017(2)	−12069(6)	−2728(2)	28(1)	1
C23	1991(2)	−10307(6)	−2325(2)	25(1)	1
C24	2627(2)	−8844(6)	−2231(2)	22(1)	1
N1	3064(2)	675(5)	−289(1)	21(1)	1
N2	4151(2)	−699(4)	−990(1)	19(1)	1
N3	3804(2)	−4388(4)	−1626(1)	19(1)	1
N4	3798(2)	−7476(4)	−2333(1)	20(1)	1
N5	2759(2)	−6951(5)	−1855(1)	21(1)	1
O1	3817(1)	3733(4)	−13(1)	27(1)	1
O2	4919(1)	−4145(4)	−2058(1)	23(1)	1
O3	2578(2)	−3774(4)	−875(1)	29(1)	1

Barbital complex of receptor 88:

Table 1. Crystal data and structure refinement details.

Identification code	**2007sot0234 (mgf134xiv)**	
Empirical formula	$C_{33}H_{39}N_9O_7S_2$	
Formula weight	737.85	
Temperature	120(2) K	
Wavelength	0.71073 Å	
Crystal system	Triclinic	
Space group	*P*−1	
Unit cell dimensions	a = 9.9882(4) Å	α = 64.158(2)°
	b = 14.1537(5) Å	β = 86.751(3)°
	c = 14.7208(8) Å	γ = 70.732(3)°
Volume	1758.73(13) Å^3	
Z	2	
Density (calculated)	1.393 Mg / m^3	
Absorption coefficient	0.213 mm^{-1}	
F(000)	776	
Crystal	Block; Colourless	
Crystal size	0.4 × 0.12 × 0.07 mm^3	
θ range for data collection	3.08 − 27.48°	
Index ranges	$-12 \le h \le 12$, $-18 \le k \le 17$, $-16 \le l \le 19$	
Reflections collected	20558	
Independent reflections	7607 [R_{int} = 0.0609]	
Completeness to θ = 27.48°	94.4 %	
Absorption correction	Semi−empirical from equivalents	
Max. and min. transmission	0.9853 and 0.9297	
Refinement method	Full-matrix least-squares on F^2	
Data / restraints / parameters	7607 / 0 / 499	
Goodness-of-fit on F^2	1.023	
Final *R* indices [$F^2 > 2\sigma(F^2)$]	*R1* = 0.0561, *wR2* = 0.1274	
R indices (all data)	*R1* = 0.0976, *wR2* = 0.1467	
Largest diff. peak and hole	0.898 and −0.489 e Å^{-3}	

Diffractometer: *Nonius KappaCCD* area detector (ϕ scans and ω scans to fill *asymmetric unit*). **Cell determination:** DirAx (Duisenberg, A.J.M.(1992). J. Appl. Cryst. 25, 92-96.) **Data collection:** Collect (Collect: Data collection software, R. Hooft, Nonius B.V., 1998). **Data reduction and cell refinement**: *Denzo* (Z. Otwinowski & W. Minor, *Methods in Enzymology* (1997) Vol. **276**: *Macromolecular Crystallography*, part A, pp. 307−326; C. W. Carter, Jr. & R. M. Sweet, Eds., Academic Press). **Absorption correction**: Sheldrick, G. M. SADABS - Bruker Nonius area detector scaling and absorption correction - V2.10 S**tructure solution**: *SHELXS97* (G. M. Sheldrick, Acta Cryst. (1990) A**46** 467−473). S**tructure refinement**: *SHELXL97* (G. M. Sheldrick (1997), University of Göttingen, Germany). **Graphics:** Cameron - A Molecular Graphics Package. (D. M. Watkin, L. Pearce and C. K. Prout, Chemical Crystallography Laboratory, University of Oxford, 1993).

Special details: All hydrogen atoms were placed in idealised positions and refined using a riding model, except those of the NH which were freely refined.

Table 2. Atomic coordinates [$\times 10^4$], equivalent isotropic displacement parameters [$Å^2 \times 10^3$] and site occupancy factors. U_{eq} is defined as one third of the trace of the orthogonalized U^{ij} tensor.

Atom	*x*	*y*	*z*	U_{eq}	*S.o.f.*
O1	3534(1)	1411(1)	989(1)	29(1)	1
O2	10602(1)	−2299(1)	2144(1)	26(1)	1
N1	2580(1)	2800(1)	−973(1)	22(1)	1
N2	4222(1)	2612(1)	−2041(1)	22(1)	1
N3	4937(1)	1428(1)	−292(1)	21(1)	1
N4	7117(1)	−302(1)	1125(1)	19(1)	1
N5	9647(1)	−1250(1)	491(1)	21(1)	1
N6	10896(1)	−1200(1)	−931(1)	21(1)	1
N7	11984(1)	−2562(1)	579(1)	25(1)	1
C1	1910(1)	3552(1)	−1937(1)	22(1)	1
C2	518(1)	4280(1)	−2279(1)	25(1)	1
C3	204(1)	4905(1)	−3319(1)	27(1)	1
C4	1228(1)	4801(1)	−3993(1)	28(1)	1
C5	2608(1)	4055(1)	−3646(1)	26(1)	1
C6	2943(1)	3425(1)	−2598(1)	22(1)	1
C7	3935(1)	2271(1)	−1083(1)	20(1)	1
C8	4684(1)	1036(1)	706(1)	21(1)	1
C9	5890(1)	118(1)	1458(1)	20(1)	1
C10	5676(1)	−261(1)	2484(1)	25(1)	1
C11	6763(1)	−1112(1)	3201(1)	28(1)	1
C12	8047(1)	−1545(1)	2871(1)	25(1)	1
C13	8181(1)	−1116(1)	1839(1)	20(1)	1
C14	9596(1)	−1607(1)	1511(1)	22(1)	1
C15	10828(1)	−1660(1)	55(1)	20(1)	1
C16	12194(1)	−1857(1)	−1072(1)	21(1)	1
C17	12831(1)	−1764(1)	−1963(1)	26(1)	1
C18	14158(1)	−2547(1)	−1870(1)	28(1)	1
C19	14832(1)	−3411(1)	−931(1)	29(1)	1
C20	14206(1)	−3516(1)	−39(1)	29(1)	1
C21	12885(1)	−2721(1)	−135(1)	23(1)	1
O3	7505(1)	638(1)	−1245(1)	24(1)	1
O4	9820(1)	−316(1)	−3600(1)	36(1)	1
O5	5548(1)	2771(1)	−4501(1)	36(1)	1
N8	8727(1)	237(1)	−2452(1)	24(1)	1
N9	6535(1)	1689(1)	−2882(1)	22(1)	1
C22	7592(1)	850(1)	−2146(1)	20(1)	1
C23	8872(1)	376(1)	−3432(1)	24(1)	1
C24	7896(1)	1439(1)	−4274(1)	23(1)	1
C25	6557(1)	2010(1)	−3907(1)	25(1)	1
C26	7500(1)	1213(1)	−5136(1)	29(1)	1
C27	6603(1)	454(1)	−4824(1)	44(1)	1
C28	8716(1)	2293(1)	−4653(1)	26(1)	1

C29	10081(1)	1959(1)	−5132(1)	34(1)	1
S1A	3815(1)	4548(1)	3138(1)	27(1)	0.8807(2)
O6A	2982(1)	5179(1)	2111(1)	29(1)	0.8807(2)
C30A	3386(1)	5502(1)	3673(1)	33(1)	0.8807(2)
C31A	5617(1)	4490(1)	2911(1)	33(1)	0.8807(2)
S1B	3843(1)	5308(1)	2578(1)	27(1)	0.1193(2)
O6B	3084(2)	4566(2)	2509(2)	29(1)	0.1193(2)
C30B	3816(3)	5542(2)	3735(2)	33(1)	0.1193(2)
C31B	5573(3)	4492(2)	3081(2)	33(1)	0.1193(2)
S2	323(1)	2970(1)	1285(1)	31(1)	1
O7	493(1)	3359(1)	171(1)	35(1)	1
C32	−1254(1)	4017(1)	1335(1)	43(1)	1
C33	1594(1)	3314(1)	1778(1)	54(1)	1

Barbital complex of receptor 96:

Table 1. Crystal data and structure refinement details.

Identification code	**2008sot0641 (mgf250BARB)**
Empirical formula	$C_{35}H_{41}N_9O_7S$
Formula weight	731.83
Temperature	120(2) K
Wavelength	0.71073 Å
Crystal system	Monoclinic
Space group	$P2_1/c$
Unit cell dimensions	a = 9.9352(2) Å
	b = 13.9203(2) Å β = 91.5240(10)°
	c = 25.7967(4) Å
Volume	3566.45(10) Å^3
Z	4
Density (calculated)	1.363 Mg / m^3
Absorption coefficient	0.153 mm^{-1}
F(000)	1544
Crystal	Rod; Colourless
Crystal size	0.3 × 0.04 × 0.03 mm^3
θ range for data collection	2.93 – 25.03°
Index ranges	$-9 \le h \le 11$, $-16 \le k \le 16$, $-30 \le l \le 30$
Reflections collected	34448
Independent reflections	6287 [R_{int} = 0.0685]
Completeness to θ = 25.03°	99.7 %
Absorption correction	Semi–empirical from equivalents
Max. and min. transmission	0.9954 and 0.9555
Refinement method	Full-matrix least-squares on F^2
Data / restraints / parameters	6287 / 0 / 498
Goodness-of-fit on F^2	1.072
Final R indices [$F^2 > 2\sigma(F^2)$]	$R1$ = 0.0680, $wR2$ = 0.1210
R indices (all data)	$R1$ = 0.0975, $wR2$ = 0.1366
Largest diff. peak and hole	0.334 and –0.320 e Å^{-3}

Diffractometer: *Nonius KappaCCD* area detector (ϕ scans and ω scans to fill *asymmetric unit*). **Cell determination:** DirAx (Duisenberg, A.J.M.(1992). J. Appl. Cryst. 25, 92-96.) **Data collection:** Collect (Collect: Data collection software, R. Hooft, Nonius B.V., 1998). **Data reduction and cell refinement**: *Denzo* (Z. Otwinowski & W. Minor, *Methods in Enzymology* (1997) Vol. **276**: *Macromolecular Crystallography*, part A, pp. 307–326; C. W. Carter, Jr. & R. M. Sweet, Eds., Academic Press). **Absorption correction**: Sheldrick, G. M. SADABS - Bruker Nonius area detector scaling and absorption correction - V2.10 S**tructure solution**: *SHELXS97* (G. M. Sheldrick, Acta Cryst. (1990) A**46** 467–473). S**tructure refinement**: *SHELXL97* (G. M. Sheldrick (1997), University of Göttingen, Germany). **Graphics:** Cameron - A Molecular Graphics Package. (D. M. Watkin, L. Pearce and C. K. Prout, Chemical Crystallography Laboratory, University of Oxford, 1993).

Special details: All hydrogen atoms were placed in idealised positions and refined using a riding model, except for the NH's which were freely refined.

Table 2. Atomic coordinates [$\times 10^4$], equivalent isotropic displacement parameters [$Å^2 \times 10^3$] and site occupancy factors. U_{eq} is defined as one third of the trace of the orthogonalized U^{ij} tensor.

Atom	*x*	*y*	*z*	U_{eq}	*S.o.f.*
O1	7850(2)	9564(2)	5804(1)	22(1)	1
O2	4891(2)	9681(2)	3305(1)	28(1)	1
O3	4033(2)	7764(2)	4876(1)	23(1)	1
N1	9899(3)	10754(2)	5994(1)	19(1)	1
N2	10356(3)	11739(2)	5336(1)	20(1)	1
N3	8660(3)	10565(2)	5186(1)	18(1)	1
N4	6801(3)	9872(2)	4485(1)	17(1)	1
N5	6811(3)	10525(2)	3482(1)	19(1)	1
N6	8169(3)	11237(2)	2845(1)	22(1)	1
N7	6089(3)	10774(2)	2594(1)	20(1)	1
C1	11157(3)	11984(2)	5770(1)	20(1)	1
C2	12071(3)	12741(3)	5830(1)	25(1)	1
C3	12679(4)	12851(3)	6316(1)	30(1)	1
C4	12418(3)	12224(3)	6726(1)	27(1)	1
C5	11517(3)	11470(2)	6670(1)	22(1)	1
C6	10889(3)	11377(2)	6183(1)	19(1)	1
C7	9626(3)	11016(2)	5496(1)	18(1)	1
C8	7813(3)	9870(2)	5355(1)	18(1)	1
C9	6802(3)	9500(2)	4962(1)	17(1)	1
C10	5919(3)	8789(2)	5129(1)	17(1)	1
C11	4964(3)	8442(2)	4774(1)	20(1)	1
C12	4937(3)	8819(2)	4273(1)	19(1)	1
C13	5858(3)	9518(2)	4151(1)	17(1)	1
C14	5796(3)	9911(2)	3610(1)	21(1)	1
C15	7021(3)	10842(2)	2983(1)	18(1)	1
C16	7971(3)	11451(2)	2318(1)	21(1)	1
C17	8814(4)	11890(3)	1968(1)	28(1)	1
C18	8310(4)	12031(2)	1466(1)	28(1)	1
C19	7015(4)	11748(2)	1314(1)	24(1)	1
C20	6176(4)	11308(2)	1659(1)	23(1)	1
C21	6672(3)	11174(2)	2159(1)	19(1)	1
C22	3927(4)	7449(2)	5410(1)	23(1)	1
C23	2754(3)	6755(2)	5424(1)	26(1)	1
C24	3028(4)	5762(3)	5203(1)	31(1)	1
C25	3965(4)	5154(3)	5550(2)	39(1)	1
O4	9080(2)	11380(2)	4132(1)	23(1)	1
O5	12631(2)	13279(2)	4532(1)	27(1)	1
O6	10520(3)	13304(2)	2857(1)	33(1)	1
N8	10762(3)	12422(2)	4340(1)	19(1)	1
N9	9901(3)	12295(2)	3490(1)	21(1)	1
C26	11774(3)	13043(2)	4210(1)	21(1)	1
C27	9874(3)	11999(2)	3997(1)	20(1)	1
C28	10671(3)	13029(2)	3304(1)	22(1)	1
C29	10101(4)	14763(3)	4016(1)	31(1)	1

C30	11399(4)	14557(2)	3732(1)	26(1)	1
C31	11729(3)	13476(2)	3668(1)	22(1)	1
C32	13116(3)	13366(2)	3422(1)	25(1)	1
C33	13512(4)	12324(3)	3312(2)	34(1)	1
S1	2401(1)	9814(1)	2208(1)	33(1)	1
O7	3488(3)	10566(2)	2245(1)	37(1)	1
C34	1648(4)	9773(4)	2828(2)	48(1)	1
C35	3251(5)	8685(3)	2247(2)	54(1)	1

DMSO solvate of reaction intermediate for compound 106:

Table 1. Crystal data and structure refinement.

Identification code	**2007sot1162**	
Empirical formula	$C_{25}H_{25}N_9O_8S_2$	
Formula weight	643.66	
Temperature	120(2) K	
Wavelength	0.71073 Å	
Crystal system	Monoclinic	
Space group	$P2_1/n$	
Unit cell dimensions	a = **15.6119(5) Å**	α = **90**°
	b = **8.1998(2) Å**	β = **99.7100(10)**°
	c = **22.5696(7) Å**	γ = **90**°
Volume	2847.84(14) Å^3	
Z	4	
Density (calculated)	1.501 Mg / m^3	
Absorption coefficient	0.253 mm^{-1}	
F(000)	1336	
Crystal	Needle; Yellow	
Crystal size	0.35 × 0.03 × 0.02 mm^3	
θ range for data collection	2.95 – 27.48°	
Index ranges	$-20 \le h \le 20$, $-10 \le k \le 10$, $-29 \le l \le 29$	
Reflections collected	27933	
Independent reflections	6508 [R_{int} = 0.0747]	
Completeness to θ = 27.48°	99.5 %	
Absorption correction	Semi–empirical from equivalents	
Max. and min. transmission	0.9950 and 0.9166	
Refinement method	Full-matrix least-squares on F^2	
Data / restraints / parameters	6508 / 0 / 401	
Goodness-of-fit on F^2	1.119	
Final R indices [$F^2 > 2\sigma(F^2)$]	$R1$ = 0.0935, $wR2$ = 0.1641	
R indices (all data)	$R1$ = 0.1375, $wR2$ = 0.1859	
Largest diff. peak and hole	0.907 and –0.487 e Å^{-3}	

Diffractometer: *Nonius KappaCCD* area detector (ϕ scans and ω scans to fill *asymmetric unit* sphere). **Cell determination:** DirAx (Duisenberg, A.J.M.(1992). J. Appl. Cryst. 25, 92-96.) **Data collection:** Collect (Collect: Data collection software, R. Hooft, Nonius B.V., 1998). **Data reduction and cell refinement**: *Denzo* (Z. Otwinowski & W. Minor, *Methods in Enzymology* (1997) Vol. **276**: *Macromolecular Crystallography*, part A, pp. 307–326; C. W. Carter, Jr. & R. M. Sweet, Eds., Academic Press). **Absorption correction**: *SORTAV* (R. H. Blessing, Acta Cryst. A**51** (1995) 33–37; R. H. Blessing, J. Appl. Cryst. **30** (1997) 421–426). S**tructure solution**: *SHELXS97* (G. M. Sheldrick, Acta Cryst. (1990) A**46** 467–473). S**tructure refinement**: *SHELXL97* (G. M. Sheldrick (1997), University of Göttingen, Germany). **Graphics:** Cameron - A Molecular Graphics Package. (D. M. Watkin, L. Pearce and C. K. Prout, Chemical Crystallography Laboratory, University of Oxford, 1993).

Special details: All hydrogen atoms were placed in idealised positions and refined using a riding model.

Table 2. Atomic coordinates [$\times 10^4$], equivalent isotropic displacement parameters [$Å^2 \times 10^3$] and site occupancy factors. U_{eq} is defined as one third of the trace of the orthogonalized U^{ij} tensor.

Atom	*x*	*y*	*z*	U_{eq}	*S.o.f.*
O1	7086(2)	7794(4)	3299(1)	28(1)	1
O2	3145(2)	5826(4)	4229(1)	23(1)	1
O3	9506(2)	9733(5)	3438(2)	40(1)	1
O4	10601(2)	11350(5)	3698(2)	46(1)	1
O5	1713(2)	4437(5)	5581(2)	38(1)	1
O6	1112(3)	4754(6)	6373(2)	56(1)	1
N1	5249(2)	6880(4)	3971(2)	18(1)	1
N2	6783(2)	8465(4)	4224(2)	21(1)	1
N3	4347(2)	6674(4)	4876(2)	20(1)	1
N4	7616(2)	10313(5)	4900(2)	25(1)	1
N5	8164(2)	9562(5)	4080(2)	23(1)	1
N6	4320(2)	7632(5)	5859(2)	24(1)	1
N7	3211(2)	6041(5)	5440(2)	24(1)	1
N8	9910(3)	10751(6)	3781(2)	31(1)	1
N9	1708(3)	5031(6)	6082(2)	36(1)	1
C1	5721(3)	6961(5)	3527(2)	21(1)	1
C2	5428(3)	6425(6)	2952(2)	27(1)	1
C3	4590(3)	5819(6)	2813(2)	31(1)	1
C4	4081(3)	5740(6)	3260(2)	23(1)	1
C5	4451(3)	6255(5)	3833(2)	17(1)	1
C6	3911(3)	6213(5)	4328(2)	19(1)	1
C7	3968(3)	6798(5)	5382(2)	21(1)	1
C8	3056(3)	6440(6)	6006(2)	25(1)	1
C9	2404(3)	6073(6)	6336(2)	30(1)	1
C10	2457(3)	6720(6)	6913(2)	32(1)	1
C11	3140(3)	7684(7)	7157(2)	37(1)	1
C12	3802(3)	8080(7)	6847(2)	35(1)	1
C13	3751(3)	7434(6)	6264(2)	27(1)	1
C14	6603(3)	7754(5)	3673(2)	21(1)	1
C15	7508(3)	9444(5)	4408(2)	22(1)	1
C16	8405(3)	11083(6)	4904(2)	23(1)	1
C17	8847(3)	12175(6)	5316(2)	26(1)	1
C18	9643(3)	12786(6)	5217(2)	30(1)	1
C19	9995(3)	12324(6)	4717(2)	30(1)	1
C20	9550(3)	11239(6)	4301(2)	26(1)	1
C21	8754(3)	10623(5)	4391(2)	22(1)	1
S101	1325(1)	7185(1)	922(1)	21(1)	1
O101	1095(2)	7523(4)	252(1)	23(1)	1
C101	2481(3)	7138(6)	1089(2)	30(1)	1
C102	1144(3)	5059(6)	997(2)	31(1)	1
S201	1280(1)	6410(2)	2635(1)	35(1)	1
O201	1964(3)	5245(6)	2506(2)	55(1)	1
C201	1819(3)	7909(7)	3132(2)	34(1)	1
C202	717(4)	5413(8)	3154(3)	49(2)	1

HCl complex of compound 91:

Table 1. Crystal data and structure refinement details.

Identification code	**2007sot0800 (mgf170(ii))**
Empirical formula	$C_{25}H_{28}ClN_5O_3$
Formula weight	481.97
Temperature	120(2) K
Wavelength	0.71073 Å
Crystal system	Monoclinic
Space group	$P2_1/n$
Unit cell dimensions	a = 7.6178(2) Å
	b = 18.3484(6) Å β = 90.894(2)°
	c = 16.8855(5) Å
Volume	2359.87(12) Å^3
Z	4
Density (calculated)	1.357 Mg / m^3
Absorption coefficient	0.200 mm^{-1}
F(000)	1016
Crystal	Fragment; Colourless
Crystal size	0.15 × 0.1 × 0.07 mm^3
θ range for data collection	2.92 – 27.48°
Index ranges	$-9 \le h \le 9$, $-23 \le k \le 23$, $-21 \le l \le 21$
Reflections collected	33754
Independent reflections	5391 [R_{int} = 0.0946]
Completeness to θ = 27.48°	99.8 %
Absorption correction	Semi–empirical from equivalents
Max. and min. transmission	0.9862 and 0.9607
Refinement method	Full-matrix least-squares on F^2
Data / restraints / parameters	5391 / 0 / 309
Goodness-of-fit on F^2	1.012
Final R indices [$F^2 > 2\sigma(F^2)$]	*R1* = 0.0564, *wR2* = 0.1283
R indices (all data)	*R1* = 0.0933, *wR2* = 0.1455
Largest diff. peak and hole	0.775 and –0.391 e Å^{-3}

Diffractometer: *Nonius KappaCCD* area detector (ϕ scans and ω scans to fill *asymmetric unit*). **Cell determination:** DirAx (Duisenberg, A.J.M.(1992). J. Appl. Cryst. 25, 92-96.) **Data collection:** Collect (Collect: Data collection software, R. Hooft, Nonius B.V., 1998). **Data reduction and cell refinement**: *Denzo* (Z. Otwinowski & W. Minor, *Methods in Enzymology* (1997) Vol. **276**: *Macromolecular Crystallography*, part A, pp. 307–326; C. W. Carter, Jr. & R. M. Sweet, Eds., Academic Press). **Absorption correction**: Sheldrick, G. M. SADABS - Bruker Nonius area detector scaling and absorption correction - V2.10 **Structure solution**: *SHELXS97* (G. M. Sheldrick, Acta Cryst. (1990) A**46** 467–473). **Structure refinement**: *SHELXL97* (G. M. Sheldrick (1997), University of Göttingen, Germany). **Graphics:** Cameron - A Molecular Graphics Package. (D. M. Watkin, L. Pearce and C. K. Prout, Chemical Crystallography Laboratory, University of Oxford, 1993).

Special details: All hydrogen atoms were placed in idealised positions and refined using a riding model.

Table 2. Atomic coordinates [$\times 10^4$], equivalent isotropic displacement parameters [$Å^2 \times 10^3$] and site occupancy factors. U_{eq} is defined as one third of the trace of the orthogonalized U^{ij} tensor.

Atom	*x*	*y*	*z*	U_{eq}	*S.o.f.*
O1	767(3)	1496(1)	7348(1)	33(1)	1
O2	732(2)	5186(1)	6239(1)	30(1)	1
N1	1429(3)	1836(1)	6088(1)	23(1)	1
N2	941(3)	3270(1)	6509(1)	22(1)	1
N3	1929(3)	4294(1)	5480(1)	24(1)	1
N4	3354(3)	4471(1)	4267(1)	22(1)	1
N5	2561(3)	5465(1)	4886(1)	23(1)	1
C1	3838(4)	−1585(1)	2469(2)	34(1)	1
C2	3659(3)	−1634(1)	3368(1)	25(1)	1
C3	3059(3)	−913(1)	3723(1)	23(1)	1
C4	3036(3)	−915(1)	4624(1)	23(1)	1
C5	2566(3)	−195(1)	5002(1)	22(1)	1
C6	1953(3)	403(1)	4568(1)	22(1)	1
C7	1577(3)	1062(1)	4934(1)	22(1)	1
C8	1788(3)	1140(1)	5750(1)	22(1)	1
C9	2372(3)	546(1)	6199(1)	24(1)	1
C10	2751(3)	−107(1)	5821(1)	24(1)	1
C11	940(3)	1966(1)	6835(1)	23(1)	1
C12	535(3)	2752(1)	7033(1)	22(1)	1
C13	−247(3)	2899(1)	7759(1)	25(1)	1
C14	−634(3)	3614(1)	7948(1)	26(1)	1
C15	−223(3)	4159(1)	7413(1)	25(1)	1
C16	571(3)	3959(1)	6712(1)	21(1)	1
C17	1066(3)	4543(1)	6138(1)	23(1)	1
C18	2572(3)	4734(1)	4905(1)	22(1)	1
C19	3888(3)	5054(1)	3795(1)	22(1)	1
C20	4747(3)	5075(1)	3073(1)	24(1)	1
C21	5096(3)	5763(1)	2776(1)	27(1)	1
C22	4622(3)	6400(1)	3187(2)	27(1)	1
C23	3768(3)	6373(1)	3901(2)	26(1)	1
C24	3395(3)	5687(1)	4193(1)	23(1)	1
O3	8824(3)	3246(1)	4592(1)	40(1)	1
C25	7836(4)	2804(2)	4069(2)	41(1)	1
Cl1	2871(1)	2850(1)	4570(1)	26(1)	1

Structures from Chapter 4

Methanol complex of compound 125:

Table 1. Crystal data and structure refinement details.

Identification code	**2008sot1075**	
Empirical formula	$C_{40}H_{59}N_7O_2$	
Formula weight	669.94	
Temperature	120(2) K	
Wavelength	0.71073 Å	
Crystal system	Orthorhombic	
Space group	*Pbca*	
Unit cell dimensions	a = 10.2826(2) Å	α = **90**°
	b = **20.5801(6) Å**	β = **90**°
	c **35.6410(10) Å**	γ = **90**°
Volume	**7542.2(3) Å^3**	
Z	8	
Density (calculated)	1.180 Mg / m^3	
Absorption coefficient	0.074 mm^{-1}	
F(000)	2912	
Crystal	Block; Colourless	
Crystal size	0.3 × 0.2 × 0.05 mm^3	
θ range for data collection	3.02 − 25.01°	
Index ranges	$-12 \le h \le 8$, $-15 \le k \le 24$, $-42 \le l \le 42$	
Reflections collected	43094	
Independent reflections	6648 [R_{int} = 0.1269]	
Completeness to θ = 25.01°	99.8 %	
Absorption correction	Semi−empirical from equivalents	
Max. and min. transmission	0.9963 and 0.9781	
Refinement method	Full-matrix least-squares on F^2	
Data / restraints / parameters	6648 / 0 / 475	
Goodness-of-fit on F^2	1.030	
Final R indices [$F^2 > 2\sigma(F^2)$]	$R1$ = 0.0656, $wR2$ = 0.1445	
R indices (all data)	$R1$ = 0.1318, $wR2$ = 0.1737	
Extinction coefficient	0.0027(4)	
Largest diff. peak and hole	0.275 and −0.251 e Å^{-3}	

Diffractometer: *Nonius KappaCCD* area detector (ϕ scans and ω scans to fill *asymmetric unit*). **Cell determination:** DirAx (Duisenberg, A.J.M.(1992). J. Appl. Cryst. 25, 92-96.) **Data collection:** Collect (Collect: Data collection software, R. Hooft, Nonius B.V., 1998). **Data reduction and cell refinement**: *Denzo* (Z. Otwinowski & W. Minor, *Methods in Enzymology* (1997) Vol. **276**: *Macromolecular Crystallography*, part A, pp. 307−326; C. W. Carter, Jr. & R. M. Sweet, Eds., Academic Press). **Absorption correction**: Sheldrick, G. M. SADABS - Bruker Nonius area detector scaling and absorption correction - V2.10 **Structure solution**: *SHELXS97* (G. M. Sheldrick, Acta Cryst. (1990) A**46** 467−473). **Structure refinement**: *SHELXL97* (G. M. Sheldrick (1997), University of Göttingen, Germany). **Graphics:** Cameron - A Molecular Graphics Package. (D. M. Watkin, L. Pearce and C. K. Prout, Chemical Crystallography Laboratory, University of Oxford, 1993).

Special details: All hydrogen atoms were placed in idealised positions and refined using a riding model.

Table 2. Atomic coordinates [$\times 10^4$], equivalent isotropic displacement parameters [$Å^2 \times 10^3$] and site occupancy factors. U_{eq} is defined as one third of the trace of the orthogonalized U^{ij} tensor.

Atom	*x*	*y*	*z*	U_{eq}	*S.o.f.*
C39	1766(3)	1254(2)	3595(1)	48(1)	1
C40	2849(3)	1218(2)	126(1)	50(1)	1
O1	3611(2)	1056(1)	450(1)	38(1)	1
O2	656(2)	1382(1)	3365(1)	39(1)	1
C1	6492(2)	2354(2)	676(1)	29(1)	1
C2	7820(3)	2416(2)	640(1)	34(1)	1
C3	8301(3)	1838(2)	481(1)	34(1)	1
C4	7277(3)	1420(2)	424(1)	31(1)	1
C5	7253(3)	725(2)	287(1)	35(1)	1
C6	6277(3)	646(2)	−34(1)	42(1)	1
C7	8605(3)	555(2)	129(1)	45(1)	1
C8	6966(3)	265(2)	609(1)	33(1)	1
C9	7802(3)	−73(2)	830(1)	42(1)	1
C10	7075(3)	−385(2)	1114(1)	42(1)	1
C11	5793(3)	−234(2)	1064(1)	34(1)	1
C12	4605(3)	−467(2)	1279(1)	35(1)	1
C13	4305(3)	−1169(2)	1161(1)	43(1)	1
C14	3443(3)	−43(2)	1202(1)	33(1)	1
C15	2268(3)	−174(2)	1034(1)	39(1)	1
C16	1474(3)	385(2)	1069(1)	40(1)	1
C17	2153(3)	851(2)	1257(1)	32(1)	1
C18	1804(3)	1540(2)	1363(1)	34(1)	1
C19	2186(3)	1678(2)	1772(1)	37(1)	1
C20	324(3)	1624(2)	1330(1)	43(1)	1
C21	2466(3)	2009(2)	1099(1)	31(1)	1
C22	1999(3)	2357(2)	800(1)	34(1)	1
C23	3049(3)	2706(2)	641(1)	34(1)	1
C24	4150(2)	2567(1)	842(1)	31(1)	1
C25	5512(3)	2841(2)	823(1)	32(1)	1
C26	5516(3)	3428(2)	557(1)	38(1)	1
C27	5924(3)	3059(2)	1222(1)	33(1)	1
C28	5042(3)	3579(2)	1398(1)	36(1)	1
C29	5091(3)	3600(2)	1823(1)	38(1)	1
C30	4401(3)	3026(2)	2004(1)	39(1)	1
C31	4379(3)	3029(2)	2430(1)	42(1)	1
C32	4416(3)	1832(2)	2586(1)	39(1)	1
C33	3507(3)	1412(2)	2710(1)	33(1)	1
C34	3576(3)	693(2)	2741(1)	49(1)	1
C35	3572(3)	365(2)	2354(1)	54(1)	1
C36	3841(3)	−357(2)	2354(1)	54(1)	1
C37	3774(3)	−647(2)	1960(1)	47(1)	1
C38	4907(3)	−445(2)	1706(1)	40(1)	1
N1	6177(3)	1750(1)	539(1)	32(1)	1
N2	5737(2)	160(1)	755(1)	33(1)	1

N3	3367(2)	584(1)	1335(1)	32(1)	1
N4	3785(2)	2138(1)	1121(1)	31(1)	1
N5	3840(2)	2415(1)	2580(1)	39(1)	1
N6	2595(2)	2369(2)	2691(1)	43(1)	1
N7	2391(2)	1752(1)	2773(1)	42(1)	1

Compound 125.$(DMSO)_3$:

Table 1. Crystal data and structure refinement details.

Identification code	**2009sot0155 (CTIV22 JAN31,09)**
Empirical formula	$C_{44}H_{69}N_7O_3S_3$
	$C_{38}H_{51}N_7$, $3(C_2H_6OS)$
Formula weight	840.24
Temperature	120(2) K
Wavelength	0.71073 Å
Crystal system	Monoclinic
Space group	$P2_1/n$
Unit cell dimensions	a = 10.4348(2) Å
	b = 22.9357(3) Å β = 100.8400(10)°
	c = 19.7522(3) Å
Volume	4642.93(13) $Å^3$
Z	4
Density (calculated)	1.202 Mg / m^3
Absorption coefficient	0.205 mm^{-1}
F(000)	1816
Crystal	Block; Colourless
Crystal size	$0.2 \times 0.2 \times 0.2$ mm^3
θ range for data collection	3.00 – 25.03°
Index ranges	$-12 \le h \le 12$, $-27 \le k \le 27$, $-23 \le l \le 23$
Reflections collected	44419
Independent reflections	8189 [R_{int} = 0.0721]
Completeness to θ = 25.03°	99.7 %
Absorption correction	Semi–empirical from equivalents
Max. and min. transmission	0.9798 and 0.9501
Refinement method	Full-matrix least-squares on F^2
Data / restraints / parameters	8189 / 0 / 542
Goodness-of-fit on F^2	1.560
Final R indices [$F^2 > 2\sigma(F^2)$]	$R1$ = 0.0658, $wR2$ = 0.1078
R indices (all data)	$R1$ = 0.0950, $wR2$ = 0.1159
Largest diff. peak and hole	0.383 and –0.432 e $Å^{-3}$

Diffractometer: *Nonius KappaCCD* area detector (ϕ scans and ω scans to fill *asymmetric unit*). **Cell determination:** DirAx (Duisenberg, A.J.M.(1992). J. Appl. Cryst. 25, 92-96.) **Data collection:** Collect (Collect: Data collection software, R. Hooft, Nonius B.V., 1998). **Data reduction and cell refinement**: *Denzo* (Z. Otwinowski & W. Minor, *Methods in Enzymology* (1997) Vol. **276**: *Macromolecular Crystallography*, part A, pp. 307–326; C. W. Carter, Jr. & R. M. Sweet, Eds., Academic Press). **Absorption correction**: Sheldrick, G. M. SADABS - Bruker Nonius area detector scaling and absorption correction - V2.10 S**tructure solution**: *SHELXS97* (G. M. Sheldrick, Acta Cryst. (1990) A**46** 467–473). S**tructure refinement**: *SHELXL97* (G. M. Sheldrick (1997), University of Göttingen, Germany). **Graphics:** Cameron - A Molecular Graphics Package. (D. M. Watkin, L. Pearce and C. K. Prout, Chemical Crystallography Laboratory, University of Oxford, 1993).

Special details: All hydrogen atoms were located form the difference map and then placed in geometric positions and refined using a riding model, except those attached to nitrogen which were freely refined.

Table 2. Atomic coordinates [× 10^4], equivalent isotropic displacement parameters [Å^2 × 10^3] and site occupancy factors. U_{eq} is defined as one third of the trace of the orthogonalized U^{ij} tensor.

Atom	*x*	*y*	*z*	U_{eq}	*S.o.f.*
N1	1173(2)	2138(1)	4810(1)	19(1)	1
N2	−1043(2)	1147(1)	4321(1)	20(1)	1
N3	−477(2)	1231(1)	2718(1)	19(1)	1
N4	1748(2)	2210(1)	3207(1)	18(1)	1
N5	896(2)	4396(1)	4606(1)	27(1)	1
N6	2183(2)	4518(1)	4670(1)	30(1)	1
N7	2448(2)	4551(1)	4046(1)	30(1)	1
C1	2505(3)	2115(1)	4850(1)	17(1)	1
C2	2987(3)	1761(1)	5395(1)	22(1)	1
C3	1934(3)	1561(1)	5692(1)	22(1)	1
C4	811(3)	1800(1)	5318(1)	19(1)	1
C5	−585(3)	1765(1)	5425(1)	21(1)	1
C6	−617(3)	1465(1)	6121(1)	27(1)	1
C7	−1463(3)	1419(1)	4861(1)	19(1)	1
C8	−2767(3)	1307(1)	4788(2)	23(1)	1
C9	−3150(3)	968(1)	4189(2)	23(1)	1
C10	−2074(3)	867(1)	3901(1)	20(1)	1
C11	−1937(3)	541(1)	3252(1)	22(1)	1
C12	−876(3)	71(1)	3407(2)	28(1)	1
C13	−3234(3)	227(1)	2973(2)	31(1)	1
C14	−1659(3)	957(1)	2698(1)	22(1)	1
C15	−2469(3)	1153(1)	2114(2)	29(1)	1
C16	−1761(3)	1555(1)	1785(2)	29(1)	1
C17	−532(3)	1597(1)	2166(1)	20(1)	1
C18	630(3)	1937(1)	2012(1)	19(1)	1
C19	1036(3)	1666(1)	1369(1)	26(1)	1
C20	202(3)	2579(1)	1866(1)	22(1)	1
C21	1779(3)	1921(1)	2603(1)	17(1)	1
C22	3009(3)	1697(1)	2653(1)	22(1)	1
C23	3734(3)	1853(1)	3313(1)	21(1)	1
C24	2938(3)	2174(1)	3644(1)	19(1)	1
C25	3193(3)	2449(1)	4357(1)	19(1)	1
C26	4666(3)	2428(1)	4636(2)	25(1)	1
C27	2764(3)	3090(1)	4320(2)	23(1)	1
C28	−1152(3)	2392(1)	5434(1)	21(1)	1
C29	−450(3)	2783(1)	6017(2)	25(1)	1
C30	−567(3)	3436(1)	5846(2)	24(1)	1
C31	231(3)	3611(1)	5310(2)	24(1)	1
C32	293(3)	4266(1)	5200(2)	29(1)	1
C33	349(3)	4350(1)	3931(2)	26(1)	1
C34	1331(3)	4445(1)	3581(1)	21(1)	1
C35	1314(3)	4379(1)	2829(2)	27(1)	1
C36	1418(3)	3740(1)	2625(1)	26(1)	1

C37	1071(3)	3624(1)	1853(1)	25(1)	1
C38	1248(3)	2983(1)	1671(2)	24(1)	1
S1	2841(1)	762(1)	4206(1)	23(1)	1
O1	1502(2)	1000(1)	3949(1)	23(1)	1
C39	2667(3)	232(1)	4845(2)	40(1)	1
C40	3126(3)	265(1)	3553(2)	34(1)	1
S2	3059(1)	2050(1)	8534(1)	23(1)	1
O2	4490(2)	2204(1)	8639(1)	26(1)	1
C41	2200(3)	2707(1)	8277(2)	37(1)	1
C42	2658(3)	1683(1)	7725(2)	32(1)	1
S3	933(1)	581(1)	8704(1)	40(1)	1
O3	2338(2)	568(1)	8650(2)	64(1)	1
C43	861(3)	775(2)	9569(2)	43(1)	1
C44	435(3)	−157(1)	8747(2)	37(1)	1

Compound 125.$(DMSO)_2$:

Table 1. Crystal data and structure refinement details.

Identification code	**2009sot0158**
Empirical formula	$C_{42}H_{63}N_7O_2S_2$ $C_{38}H_{51}N_7$, $2(C_2H_6OS)$
Formula weight	762.11
Temperature	120(2) K
Wavelength	0.71073 Å
Crystal system	Triclinic
Space group	*P*–1
Unit cell dimensions	a = 10.5958(3) Å α = 84.7310(10)° b = 11.3296(3) Å β = 89.8080(10)° c = 17.7452(4) Å γ = 76.5870(10)°
Volume	2063.03(9) $Å^3$
Z	2
Density (calculated)	1.227 Mg / m^3
Absorption coefficient	0.173 mm^{-1}
F(000)	824
Crystal	Fragment; Colourless
Crystal size	0.3 × 0.2 × 0.04 mm^3
θ range for data collection	3.01 – 27.48°
Index ranges	$-13 \le h \le 13$, $-14 \le k \le 14$, $-22 \le l \le 23$
Reflections collected	36159
Independent reflections	9378 [R_{int} = 0.0691]
Completeness to θ = 27.48°	99.2 %
Absorption correction	Semi–empirical from equivalents
Max. and min. transmission	0.9931 and 0.9498
Refinement method	Full-matrix least-squares on F^2
Data / restraints / parameters	9378 / 15 / 462
Goodness-of-fit on F^2	2.012
Final R indices [$F^2 > 2\sigma(F^2)$]	$R1$ = 0.1338, $wR2$ = 0.3323
R indices (all data)	$R1$ = 0.1744, $wR2$ = 0.3578
Largest diff. peak and hole	4.558 and −1.762 e $Å^{-3}$

Diffractometer: *Nonius KappaCCD* area detector (ϕ scans and ω scans to fill *asymmetric unit*). **Cell determination:** DirAx (Duisenberg, A.J.M.(1992). J. Appl. Cryst. 25, 92-96.) **Data collection:** Collect (Collect: Data collection software, R. Hooft, Nonius B.V., 1998). **Data reduction and cell refinement**: *Denzo* (Z. Otwinowski & W. Minor, *Methods in Enzymology* (1997) Vol. **276**: *Macromolecular Crystallography*, part A, pp. 307–326; C. W. Carter, Jr. & R. M. Sweet, Eds., Academic Press). **Absorption correction**: Sheldrick, G. M. SADABS - Bruker Nonius area detector scaling and absorption correction - V2.10 S**tructure solution**: *SHELXS97* (G. M. Sheldrick, Acta Cryst. (1990) A**46** 467–473). S**tructure refinement**: *SHELXL97* (G. M. Sheldrick (1997), University of Göttingen, Germany). **Graphics:** Cameron - A Molecular Graphics Package. (D. M. Watkin, L. Pearce and C. K. Prout, Chemical Crystallography Laboratory, University of Oxford, 1993).

Special details: All hydrogen atoms were placed in idealised positions and refined using a riding model.
One of the DMSO molecules is disordered and is surrounded by various significant electron density peaks. Various attempts were made to refine a number of DMSO PARTS using rigid body restraints. However, even with 4 PARTS there were still residual peaks. It was decided to revert to the original model as adding extra parameters had not improved the fit.

The triazole ring is disordered over the two possible configurations

Table 2. Atomic coordinates [× 10^4], equivalent isotropic displacement parameters [Å^2 × 10^3] and site occupancy factors. U_{eq} is defined as one third of the trace of the orthogonalized U^{ij} tensor.

Atom	*x*	*y*	*z*	U_{eq}	*S.o.f.*
N7A	4045(10)	3650(9)	5253(6)	40(1)	0.348(5)
N6A	3607(10)	4204(9)	5922(4)	40(1)	0.348(5)
N5A	2549(9)	5208(9)	5721(5)	40(1)	0.348(5)
C32A	2332(11)	5276(10)	4927(5)	40(1)	0.348(5)
C33A	3256(12)	4313(11)	4638(4)	40(1)	0.348(5)
C32B	4037(5)	3595(6)	5277(4)	40(1)	0.652(5)
N6B	3038(6)	3535(5)	5804(3)	40(1)	0.652(5)
N5B	1963(5)	4520(5)	5596(3)	40(1)	0.652(5)
N7B	2298(6)	5189(5)	4939(3)	40(1)	0.652(5)
C33B	3580(6)	4617(6)	4742(3)	40(1)	0.652(5)
N1	2295(4)	3611(4)	824(2)	18(1)	1
N2	1073(4)	3342(3)	2491(2)	19(1)	1
N3	3511(4)	1001(3)	3007(2)	18(1)	1
N4	4752(4)	1227(3)	1322(2)	17(1)	1
C1	3257(4)	3603(4)	296(2)	17(1)	1
C2	3273(5)	4804(4)	101(3)	22(1)	1
C3	2313(5)	5543(4)	523(3)	22(1)	1
C4	1722(5)	4780(4)	972(3)	20(1)	1
C5	553(5)	5104(4)	1483(3)	22(1)	1
C6	−620(5)	5765(5)	973(3)	30(1)	1
C7	264(5)	4004(4)	1916(3)	20(1)	1
C8	−820(5)	3539(5)	1922(3)	27(1)	1
C9	−655(5)	2571(4)	2507(3)	24(1)	1
C10	539(4)	2449(4)	2851(3)	22(1)	1
C11	1216(5)	1580(5)	3500(3)	23(1)	1
C12	1645(6)	2309(5)	4105(3)	31(1)	1
C13	249(5)	880(5)	3858(3)	35(1)	1
C14	2370(4)	685(4)	3227(3)	20(1)	1
C15	2551(5)	−532(5)	3135(3)	25(1)	1
C16	3824(5)	−953(4)	2848(3)	21(1)	1
C17	4411(4)	13(4)	2776(3)	18(1)	1
C18	5773(4)	76(4)	2562(3)	19(1)	1
C19	6596(5)	−1221(5)	2507(3)	25(1)	1
C20	5809(4)	805(4)	1799(3)	19(1)	1
C21	6844(4)	1143(5)	1452(3)	23(1)	1
C22	6390(4)	1791(5)	743(3)	22(1)	1
C23	5086(4)	1822(4)	670(3)	17(1)	1
C24	4109(4)	2439(4)	41(2)	18(1)	1
C25	4845(5)	2764(5)	−667(3)	24(1)	1
C26	3308(5)	1542(4)	−178(3)	21(1)	1
C27	829(5)	5969(5)	2048(3)	28(1)	1
C28	−269(6)	6388(5)	2599(3)	36(1)	1
C29	144(6)	6888(6)	3304(3)	38(1)	1
C30	998(7)	5858(7)	3804(4)	53(2)	1

C31	1376(6)	6190(6)	4553(3)	45(2)	1
C34	5190(6)	2688(5)	5290(3)	33(1)	1
C35	5180(5)	1861(5)	4659(3)	26(1)	1
C36	6450(5)	937(5)	4591(3)	26(1)	1
C37	6401(5)	73(5)	3985(3)	26(1)	1
C38	6351(5)	704(4)	3173(3)	22(1)	1
O1	1999(3)	1237(3)	1477(2)	21(1)	1
S1	970(1)	521(1)	1480(1)	22(1)	1
C39	1728(5)	−895(5)	1124(3)	29(1)	1
C40	−31(5)	1180(5)	665(3)	28(1)	1
S2	4550(2)	4534(2)	2703(1)	55(1)	1
O2	3754(3)	3637(3)	2919(2)	28(1)	1
C41	6086(12)	4043(11)	3019(5)	175(7)	1
C42	5198(7)	4173(7)	1806(3)	49(2)	1

Syn-isomer of compound 133:

Table 1. Crystal data and structure refinement details.

Identification code	**2008sot0125 (mgf246b)**
Empirical formula	$C_{26}H_{20}O_6$
Formula weight	428.42
Temperature	120(2) K
Wavelength	0.71073 Å
Crystal system	Orthorhombic
Space group	$Pna2_1$
Unit cell dimensions	a = 15.9180(5) Å
	b = 27.8591(8) Å
	c = 13.8758(2) Å
Volume	6153.4(3) Å^3
Z	12 (3 molecules)
Density (calculated)	1.387 Mg / m^3
Absorption coefficient	0.099 mm^{-1}
F(000)	2688
Crystal	Block; Colourless
Crystal size	0.2 × 0.12 × 0.09 mm^3
θ range for data collection	2.92 – 27.48°
Index ranges	$-20 \le h \le 20$, $-27 \le k \le 36$, $-17 \le l \le 16$
Reflections collected	42521
Independent reflections	7324 [R_{int} = 0.0753]
Completeness to θ = 27.48°	99.7 %
Absorption correction	Semi–empirical from equivalents
Max. and min. transmission	0.9912 and 0.9705
Refinement method	Full-matrix least-squares on F^2
Data / restraints / parameters	7324 / 155 / 904
Goodness-of-fit on F^2	1.052
Final R indices [$F^2 > 2\sigma(F^2)$]	$R1$ = 0.0679, $wR2$ = 0.1686
R indices (all data)	$R1$ = 0.1260, $wR2$ = 0.2055
Largest diff. peak and hole	0.643 and –0.531 e Å^{-3}

Diffractometer: *Nonius KappaCCD* area detector (ϕ scans and ω scans to fill *asymmetric unit*). **Cell determination:** DirAx (Duisenberg, A.J.M.(1992). J. Appl. Cryst. 25, 92-96.) **Data collection:** Collect (Collect: Data collection software, R. Hooft, Nonius B.V., 1998). **Data reduction and cell refinement**: *Denzo* (Z. Otwinowski & W. Minor, *Methods in Enzymology* (1997) Vol. **276**: *Macromolecular Crystallography*, part A, pp. 307–326; C. W. Carter, Jr. & R. M. Sweet, Eds., Academic Press). **Absorption correction**: Sheldrick, G. M. SADABS - Bruker Nonius area detector scaling and absorption correction - V2.10 S**tructure solution**: *SHELXS97* (G. M. Sheldrick, Acta Cryst. (1990) A**46** 467–473). S**tructure refinement**: *SHELXL97* (G. M. Sheldrick (1997), University of Göttingen, Germany). **Graphics:** Cameron - A Molecular Graphics Package. (D. M. Watkin, L. Pearce and C. K. Prout, Chemical Crystallography Laboratory, University of Oxford, 1993).

Special details: All hydrogen atoms were placed in idealised positions and refined using a riding model. Absolute structure not determined. The structure is pseudo centrosymmetric (Pnma) but refinement in this space-group proved unsatisfactory. One of the 3 molecules in the asymmetric unit shows disorder of its ester groups.

Table 2. Atomic coordinates [× 10⁴], equivalent isotropic displacement parameters [Å² × 10³] and site occupancy factors. U_{eq} is defined as one third of the trace of the orthogonalized U^{ij} tensor.

Atom	*x*	*y*	*z*	U_{eq}	*S.o.f.*
O101	−2879(2)	−210(2)	3211(3)	27(1)	1
O102	−2086(2)	314(2)	2401(3)	20(1)	1
O103	−829(3)	1089(2)	1699(3)	38(1)	1
O104	−524(3)	1095(2)	133(3)	30(1)	1
O105	−1224(2)	828(2)	4107(3)	28(1)	1
O106	−472(3)	1184(2)	5271(3)	27(1)	1
C101	−2719(4)	676(2)	2541(5)	30(1)	1
C102	−2217(4)	−101(3)	2820(4)	21(2)	1
C103	−1471(4)	−431(2)	2788(4)	21(2)	1
C104	−1671(5)	−923(3)	2796(5)	24(2)	1
C105	−1027(5)	−1271(3)	2779(5)	25(2)	1
C106	−201(5)	−1124(3)	2764(5)	28(2)	1
C107	−2(4)	−640(3)	2748(4)	18(2)	1
C108	−637(4)	−288(3)	2738(4)	18(2)	1
C109	861(4)	−431(2)	2750(4)	19(2)	1
C110	935(4)	−97(3)	1887(5)	21(2)	1
C111	1514(4)	−132(3)	1162(5)	20(2)	1
C112	1485(4)	185(3)	376(5)	24(2)	1
C113	835(4)	529(3)	335(5)	24(2)	1
C114	254(4)	575(2)	1099(5)	23(2)	1
C115	299(4)	260(3)	1885(5)	19(2)	1
C116	−279(4)	224(2)	2753(4)	16(1)	1
C117	−405(5)	950(3)	1037(5)	26(2)	1
C118	−1173(5)	1456(3)	27(6)	37(2)	1
C119	896(4)	−97(3)	3652(5)	21(2)	1
C120	1473(4)	−140(3)	4399(5)	23(2)	1
C121	1402(4)	173(2)	5180(5)	22(2)	1
C122	758(4)	506(3)	5211(5)	21(2)	1
C123	163(4)	542(2)	4462(4)	17(2)	1
C124	274(4)	239(3)	3665(5)	18(2)	1
C125	−577(4)	872(2)	4554(4)	21(2)	1
C126	−1181(4)	1480(2)	5476(5)	25(2)	1
O21A	3964(8)	711(6)	1816(9)	96(3)	0.50
C22A	4511(4)	779(2)	1205(3)	40(2)	0.50
O22A	4472(9)	538(6)	393(9)	32(3)	0.50
C21A	3802(12)	205(7)	227(18)	35(3)	0.50
O21B	3878(7)	762(6)	1700(10)	96(3)	0.50
C22B	4511(4)	779(2)	1205(3)	40(2)	0.50
O22B	4586(9)	471(6)	479(9)	32(3)	0.50
C21B	3910(13)	139(7)	322(17)	35(3)	0.50
O25A	2079(4)	1878(3)	3242(6)	29(2)	0.50
C25A	2778(4)	1758(2)	2962(4)	24(2)	0.50
O26A	2929(4)	1342(2)	3409(5)	21(1)	0.50

C26A	2297(7)	976(4)	3284(10)	32(2)	0.50
O25B	2120(4)	1896(3)	2582(6)	29(2)	0.50
C25B	2778(4)	1758(2)	2962(4)	24(2)	0.50
O26B	2926(4)	1330(2)	2536(6)	21(1)	0.50
C26B	2284(7)	970(4)	2639(10)	32(2)	0.50
O23A	4228(5)	546(3)	4059(5)	32(2)	0.50
C27A	4518(4)	766(2)	4739(4)	24(2)	0.50
O24A	4543(8)	492(4)	5525(7)	29(3)	0.50
C28A	3800(30)	214(19)	5730(30)	38(2)	0.50
O23B	3852(4)	800(3)	4261(5)	32(2)	0.50
C27B	4518(4)	766(2)	4739(4)	24(2)	0.50
O24B	4396(8)	604(5)	5631(6)	29(3)	0.50
C28B	3800(30)	219(18)	5730(30)	38(2)	0.50
C203	5221(4)	1115(2)	1315(4)	27(2)	1
C204	5782(4)	1163(3)	542(5)	27(2)	1
C205	6409(5)	1505(3)	551(5)	31(2)	1
C206	6484(4)	1817(3)	1330(5)	22(2)	1
C207	5917(4)	1777(3)	2107(5)	21(2)	1
C208	5271(4)	1422(3)	2103(5)	22(2)	1
C209	5873(4)	2105(3)	2958(5)	21(2)	1
C210	5923(4)	1770(3)	3848(4)	23(2)	1
C211	6517(4)	1808(3)	4585(5)	23(2)	1
C212	6442(4)	1491(3)	5356(5)	26(2)	1
C213	5817(4)	1152(3)	5397(5)	22(2)	1
C214	5221(4)	1124(2)	4655(4)	23(2)	1
C215	5301(4)	1429(3)	3868(5)	20(2)	1
C216	4713(4)	1448(3)	2982(5)	26(2)	1
C219	4982(4)	2307(3)	2989(5)	26(2)	1
C220	4792(4)	2798(3)	2988(5)	25(2)	1
C221	3964(5)	2936(3)	2969(5)	31(2)	1
C222	3337(4)	2590(3)	2960(5)	21(2)	1
C223	3510(4)	2102(3)	2999(5)	22(2)	1
C224	4362(4)	1957(3)	2983(5)	22(2)	1
O301	1172(3)	2449(2)	6697(4)	55(2)	1
O302	453(3)	2162(2)	5451(4)	42(2)	1
O303	754(4)	2212(2)	9016(4)	54(2)	1
O304	496(3)	2215(2)	10585(4)	39(1)	1
O305	2869(3)	3529(2)	7570(5)	47(1)	1
O306	2077(3)	3004(2)	8365(4)	51(1)	1
C301	1178(5)	1864(3)	5236(6)	40(2)	1
C302	543(5)	2455(3)	6198(4)	28(2)	1
C303	−200(4)	2774(3)	6303(5)	26(2)	1
C304	−778(4)	2811(3)	5554(5)	31(2)	1
C305	−1431(4)	3136(3)	5584(5)	29(2)	1
C306	−1497(4)	3453(3)	6374(5)	26(2)	1
C307	−929(4)	3432(2)	7106(5)	22(2)	1
C308	−265(4)	3083(3)	7105(5)	21(2)	1
C309	−889(4)	3752(3)	7971(5)	25(2)	1
C310	−924(4)	3433(3)	8865(5)	23(2)	1
C311	−1507(4)	3478(3)	9603(5)	33(2)	1

C312	−1443(4)	3163(3)	10363(5)	28(2)	1
C313	−839(4)	2817(3)	10405(5)	24(2)	1
C314	−251(4)	2771(3)	9657(4)	23(2)	1
C315	−311(4)	3085(3)	8878(5)	21(2)	1
C316	293(4)	3109(2)	7985(5)	21(1)	1
C317	404(4)	2390(3)	9684(5)	27(2)	1
C318	1153(5)	1860(3)	10682(6)	44(2)	1
C319	3(4)	3971(3)	7985(5)	22(2)	1
C320	186(4)	4454(3)	7981(5)	20(1)	1
C321	1044(4)	4596(3)	7951(5)	25(2)	1
C322	1657(4)	4265(3)	7927(5)	24(2)	1
C323	1482(4)	3762(3)	7977(4)	20(2)	1
C324	644(4)	3620(3)	7989(5)	21(1)	1
C325	2214(4)	3436(3)	7913(4)	19(2)	1
C326	2714(4)	2633(3)	8158(7)	54(2)	1

Anti-isomer of compound 133:

Table 1. Crystal data and structure refinement details.

Identification code	**2008sot0100 (mgf246)**	
Empirical formula	$C_{26}H_{20}O_6$	
Formula weight	428.42	
Temperature	120(2) K	
Wavelength	0.71073 Å	
Crystal system	Triclinic	
Space group	*P*–1	
Unit cell dimensions	a = 8.3873(3) Å	α = 93.812(2)°
	b = 9.5325(4) Å	β = 103.380(3)°
	c = 13.8215(6) Å	γ = 110.196(2)°
Volume	995.91(7) Å^3	
Z	2	
Density (calculated)	1.429 Mg / m^3	
Absorption coefficient	0.102 mm^{-1}	
F(000)	448	
Crystal	Fragment; Colourless	
Crystal size	0.18 × 0.1 × 0.03 mm^3	
θ range for data collection	2.97 – 27.48°	
Index ranges	$-10 \le h \le 10$, $-12 \le k \le 12$, $-17 \le l \le 17$	
Reflections collected	17844	
Independent reflections	4539 [R_{int} = 0.0692]	
Completeness to θ = 27.48°	99.3 %	
Absorption correction	Semi–empirical from equivalents	
Max. and min. transmission	0.9970 and 0.9719	
Refinement method	Full-matrix least-squares on F^2	
Data / restraints / parameters	4539 / 0 / 292	
Goodness-of-fit on F^2	1.002	
Final R indices [$F^2 > 2\sigma(F^2)$]	$R1$ = 0.0997, $wR2$ = 0.2076	
R indices (all data)	$R1$ = 0.1533, $wR2$ = 0.2428	
Largest diff. peak and hole	1.534 and –0.762 e Å^{-3}	

Diffractometer: *Nonius KappaCCD* area detector (ϕ scans and ω scans to fill *asymmetric unit*). **Cell determination:** DirAx (Duisenberg, A.J.M.(1992). J. Appl. Cryst. 25, 92-96.) **Data collection:** Collect (Collect: Data collection software, R. Hooft, Nonius B.V., 1998). **Data reduction and cell refinement**: *Denzo* (Z. Otwinowski & W. Minor, *Methods in Enzymology* (1997) Vol. **276**: *Macromolecular Crystallography*, part A, pp. 307–326; C. W. Carter, Jr. & R. M. Sweet, Eds., Academic Press). **Absorption correction**: Sheldrick, G. M. SADABS - Bruker Nonius area detector scaling and absorption correction - V2.10 S**tructure solution**: *SHELXS97* (G. M. Sheldrick, Acta Cryst. (1990) A**46** 467–473). S**tructure refinement**: *SHELXL97* (G. M. Sheldrick (1997), University of Göttingen, Germany). **Graphics:** Cameron - A Molecular Graphics Package. (D. M. Watkin, L. Pearce and C. K. Prout, Chemical Crystallography Laboratory, University of Oxford, 1993).

Special details: All hydrogen atoms were placed in idealised positions and refined using a riding model. An unidentified electron density peak exists ca 1.3Å from C11.

Table 2. Atomic coordinates [$\times 10^4$], equivalent isotropic displacement parameters [$Å^2 \times 10^3$] and site occupancy factors. U_{eq} is defined as one third of the trace of the orthogonalized U^{ij} tensor.

Atom	*x*	*y*	*z*	U_{eq}	*S.o.f.*
C1	2459(6)	3467(6)	–343(4)	42(1)	1
C2	3742(5)	2013(5)	659(3)	24(1)	1
C3	5331(5)	1604(4)	960(3)	24(1)	1
C4	6661(5)	2092(4)	467(3)	27(1)	1
C5	8157(5)	1748(5)	715(3)	28(1)	1
C6	8386(5)	896(5)	1491(3)	26(1)	1
C7	7080(5)	404(4)	1979(3)	22(1)	1
C8	5544(5)	740(4)	1723(3)	22(1)	1
C9	7177(5)	–476(4)	2860(3)	22(1)	1
C10	8233(6)	–5624(5)	3211(4)	35(1)	1
C11	7023(5)	–3778(4)	2822(3)	27(1)	1
C12	5407(5)	–3426(4)	2539(3)	24(1)	1
O3	6717(4)	–5193(3)	2961(3)	44(1)	1
O4	8492(5)	–2954(4)	2819(4)	60(1)	1
C13	3730(5)	–4585(5)	2257(3)	27(1)	1
C14	2218(5)	–4264(5)	1988(3)	29(1)	1
C15	2327(5)	–2772(5)	2006(3)	25(1)	1
C16	3975(5)	–1603(4)	2283(3)	21(1)	1
C17	5512(5)	–1926(4)	2544(3)	22(1)	1
C18	4283(5)	75(5)	2371(3)	24(1)	1
C19	2114(6)	3707(5)	4357(4)	41(1)	1
C20	3358(5)	1954(5)	3942(3)	26(1)	1
C21	4988(5)	1600(4)	4177(3)	22(1)	1
C22	6157(5)	2101(4)	5145(3)	24(1)	1
C23	7668(5)	1757(4)	5397(3)	24(1)	1
C24	8049(5)	924(4)	4681(3)	23(1)	1
C25	6905(5)	433(4)	3717(3)	21(1)	1
C26	5361(5)	745(4)	3459(3)	21(1)	1
O1	3979(4)	3065(4)	50(2)	38(1)	1
O2	2410(4)	1506(4)	913(2)	38(1)	1
O5	3616(4)	3253(3)	4509(3)	37(1)	1
O6	1975(4)	1187(4)	3347(2)	39(1)	1

Appendix 2 – Proton-NMR Titration Curves

Where reported, anion stability constants have been elucidated through ^{1}H-NMR titration experiments with anions in the form of their tetrabutylammonium salts at 298K in an appropriate deuterated solvent.

Data from these titration experiments has been fitted to the appropriate binding model with the resulting binding profile reported here for completeness.

^{1}H-NMR Titrations in Chapter 2

Receptor 59 with tetrabutylammonium bromide in DMSO-d_6.

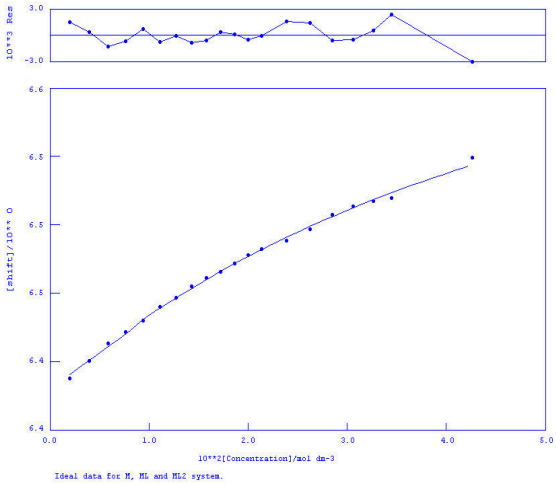

NO.	A	PARAMETER	DELTA	ERROR	CONDITION	DESCRIPTION
1	1	1.36708E+02	1.000E-01	3.185E+00	1.844E+00	BETA1
2	1	1.87754E+03	2.000E+00	1.018E+03	9.842E+02	BETA2
3	1	6.41751E+00	1.000E+00	1.659E-03	6.138E+00	M SHIFT
4	1	6.47611E+00	1.000E-01	4.686E-03	6.341E+01	ML SHIFT
5	1	6.63639E+00	5.000E-01	5.838E-02	6.708E+02	ML2 SHIFT

0RMS ERROR = 1.36E-03 MAX ERROR = 3.11E-03 AT OBS.NO. 20
RESIDUALS SQUARED = 2.76E-05
RFACTOR = 0.0181 PERCENT

Receptor 59 with tetrabutylammonium dihydrogen phosphate in DMSO-d_6.

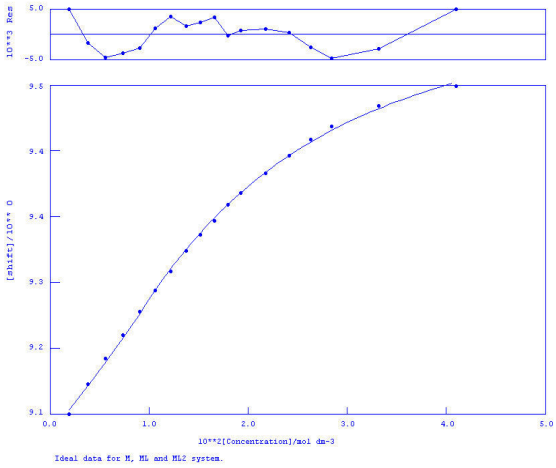

NO.	A	PARAMETER	DELTA	ERROR	CONDITION	DESCRIPTION
1	1	1.00587E+04	1.000E-01	2.802E+02	5.511E+00	BETA1
2	1	6.20300E+05	2.000E+00	7.861E+03	2.439E+00	BETA2
3	1	9.08337E+00	1.000E+00	3.698E-03	1.310E+00	M SHIFT
4	1	9.23128E+00	1.000E-01	2.224E-03	2.768E+00	ML SHIFT
5	1	9.66752E+00	5.000E-01	5.535E-03	4.878E+00	ML2 SHIFT

0RMS ERROR = 3.60E-03 MAX ERROR = 4.90E-03 AT OBS.NO. 18
RESIDUALS SQUARED = 1.68E-04
RFACTOR = 0.0328 PERCENT

Recetpor 59 with tetrabutylammonium acetate in DMSO-d_6.

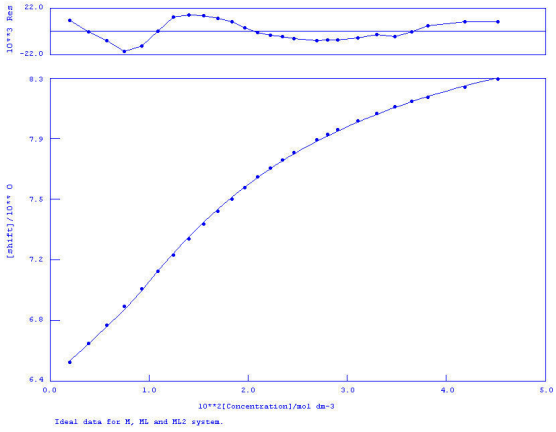

NO.	A	PARAMETER	DELTA	ERROR	CONDITION	DESCRIPTION
1	1	5.32935E+04	1.000E-01	9.876E+02	8.955E+00	BETA1
2	1	2.85559E+06	2.000E+00	2.770E+04	2.202E+00	BETA2
3	1	6.42031E+00	1.000E+00	1.069E-02	1.279E+00	M SHIFT
4	1	6.93949E+00	1.000E-01	5.612E-03	3.007E+00	ML SHIFT
5	1	9.00524E+00	5.000E-01	1.209E-02	5.805E+00	ML2 SHIFT

0RMS ERROR = 1.02E-02 MAX ERROR = 1.96E-02 AT OBS.NO. 4
 RESIDUALS SQUARED = 2.18E-03
 RFACTOR =   0.1205 PERCENT

Receptor 70 with tetrabutylammonium chloride in DMSO-d_6.

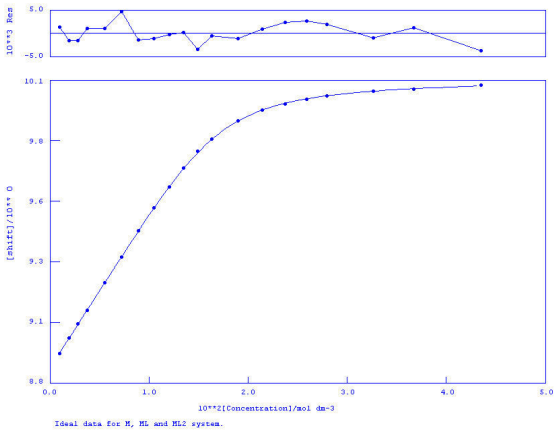

NO.	A	PARAMETER	DELTA	ERROR	CONDITION	DESCRIPTION
1	1	2.35114E+03	1.000E-01	1.239E+01	1.476E+00	BETA1
2	1	1.05903E+06	2.000E+00	4.407E+03	1.237E+00	BETA2
3	1	8.86569E+00	1.000E+00	1.712E-03	1.664E+00	M SHIFT
4	1	9.53818E+00	1.000E-01	2.604E-03	2.771E+00	ML SHIFT
5	1	1.01109E+01	5.000E-01	1.252E-03	1.980E+00	ML2 SHIFT

0RMS ERROR = 2.31E-03 MAX ERROR = 4.55E-03 AT OBS.NO. 6
 RESIDUALS SQUARED = 8.04E-05
 RFACTOR =   0.0208 PERCENT

Receptor 70 with tetrabutylammonium bromide in DMSO-d_6.

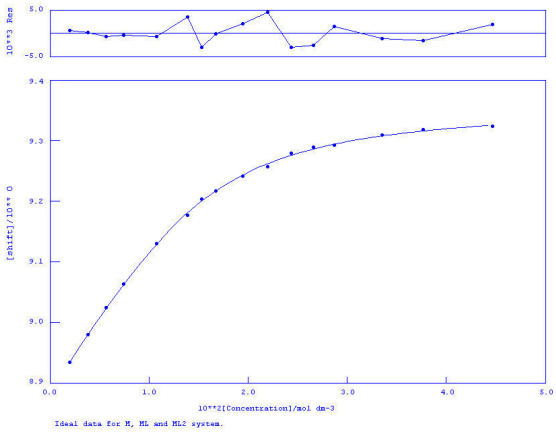

NO.	A	PARAMETER	DELTA	ERROR	CONDITION	DESCRIPTION
1	1	9.42176E+02	1.000E-01	9.415E+00	1.442E+00	BETA1
2	1	1.23308E+05	2.000E+00	6.041E+03	4.648E+00	BETA2
3	1	8.88545E+00	1.000E+00	2.740E-03	1.948E+00	M SHIFT
4	1	9.16721E+00	1.000E-01	3.303E-03	4.265E+00	ML SHIFT
5	1	9.36296E+00	5.000E-01	2.800E-03	4.576E+00	ML2 SHIFT

0RMS ERROR = 2.59E-03 MAX ERROR = 4.46E-03 AT OBS.NO. 10
RESIDUALS SQUARED = 7.36E-05
RFACTOR = 0.0233 PERCENT

Receptor 70 with tetrabutylammonium iodide in DMSO-d_6.

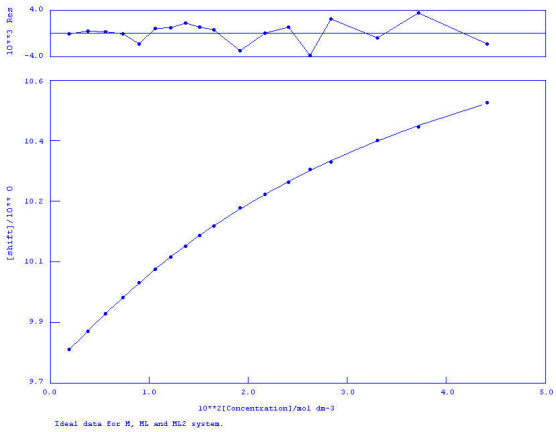

NO.	A	PARAMETER	DELTA	ERROR	CONDITION	DESCRIPTION
1	1	1.61269E+02	1.000E-01	2.428E+00	4.746E+00	BETA1
2	1	2.58997E+03	2.000E+00	2.685E+02	5.358E+02	BETA2
3	1	9.73874E+00	1.000E+00	2.370E-03	5.018E+00	M SHIFT
4	1	1.02654E+01	1.000E-01	6.556E-03	4.600E+01	ML SHIFT
5	1	1.12036E+01	5.000E-01	6.159E-02	3.606E+02	ML2 SHIFT

0RMS ERROR = 2.08E-03 MAX ERROR = 3.85E-03 AT OBS.NO. 14
RESIDUALS SQUARED = 5.61E-05
RFACTOR = 0.0174 PERCENT

Receptor 60 with tetrabutylammonium chloride in DMSO-d_6.

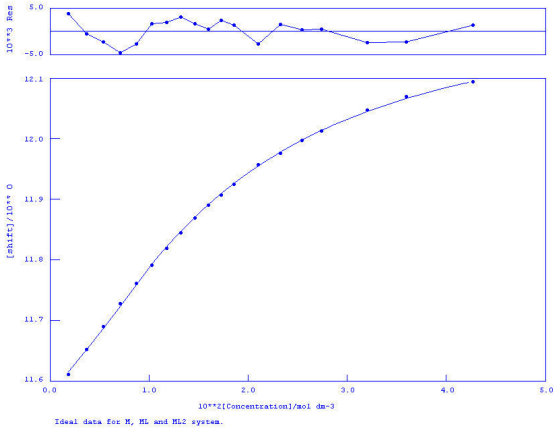

NO.	A	PARAMETER	DELTA	ERROR	CONDITION	DESCRIPTION
1	1	6.83854E+03	1.000E-01	1.859E+02	1.071E+01	BETA1
2	1	4.08534E+05	2.000E+00	4.428E+03	1.938E+00	BETA2
3	1	1.15802E+01	1.000E+00	2.517E-03	1.316E+00	M SHIFT
4	1	1.17644E+01	1.000E-01	1.593E-03	2.725E+00	ML SHIFT
5	1	1.22017E+01	5.000E-01	6.028E-03	1.157E+01	ML2 SHIFT

0RMS ERROR = 2.63E-03 MAX ERROR = 4.72E-03 AT OBS.NO. 4
 RESIDUALS SQUARED = 9.66E-05
 RFACTOR =   0.0190 PERCENT

Receptor 60 with tetrabutylammonium dihydrogen phosphate in DMSO-d_6.

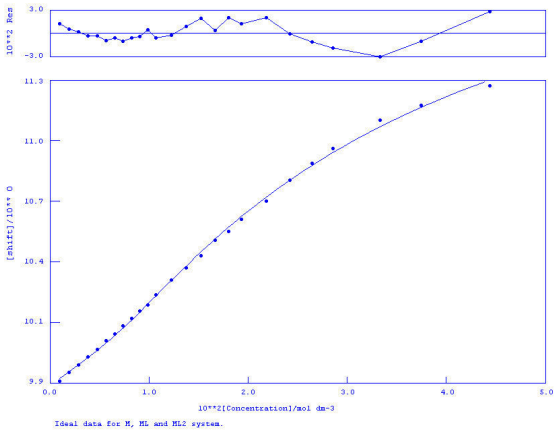

NO.	A	PARAMETER	DELTA	ERROR	CONDITION	DESCRIPTION
1	1	1.92162E+03	1.000E-01	5.729E+01	8.663E+00	BETA1
2	1	5.68065E+04	2.000E+00	5.961E+03	9.843E+01	BETA2
3	1	9.84794E+00	1.000E+00	1.069E-02	1.814E+00	M SHIFT
4	1	1.01842E+01	1.000E-01	1.209E-02	6.923E+00	ML SHIFT
5	1	1.23239E+01	5.000E-01	1.158E-01	7.534E+01	ML2 SHIFT

0RMS ERROR = 1.46E-02 MAX ERROR = 3.11E-02 AT OBS.NO. 23
 RESIDUALS SQUARED = 4.24E-03
 RFACTOR =   0.1248 PERCENT

Receptor 60 with tetrabutylammonium benzoate in DMSO-d_6.

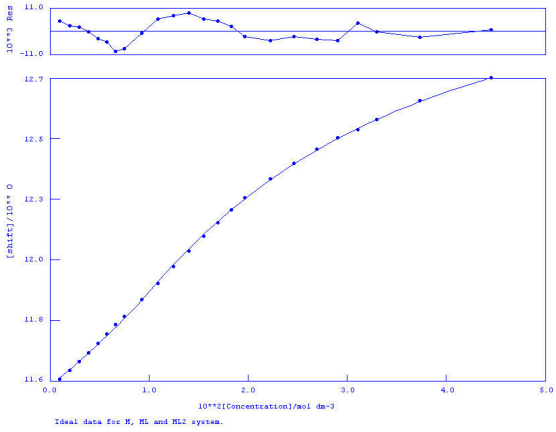

NO.	A	PARAMETER	DELTA	ERROR	CONDITION	DESCRIPTION
1	1	1.51898E+04	1.000E-01	2.865E+02	1.179E+01	BETA1
2	1	5.90432E+05	2.000E+00	8.479E+03	6.417E+00	BETA2
3	1	1.16017E+01	1.000E+00	3.683E-03	1.331E+00	M SHIFT
4	1	1.18883E+01	1.000E-01	2.801E-03	2.739E+00	ML SHIFT
5	1	1.32523E+01	5.000E-01	1.550E-02	1.556E+01	ML2 SHIFT

0RMS ERROR = 5.35E-03 MAX ERROR = 9.60E-03 AT OBS.NO. 7
 RESIDUALS SQUARED = 5.45E-04
 RFACTOR =   0.0393 PERCENT

Receptor 60 with tetrabutylammonium acetate in DMSO-d_6.

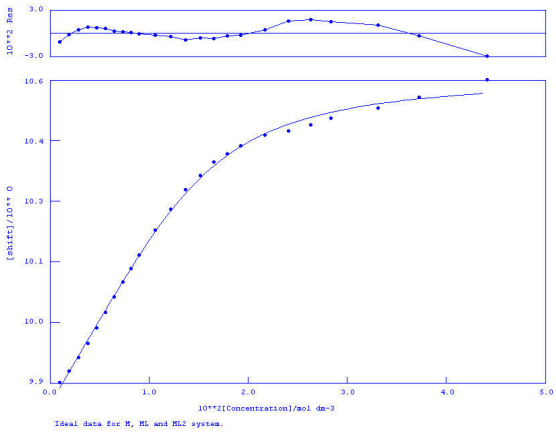

NO.	A	PARAMETER	DELTA	ERROR	CONDITION	DESCRIPTION
1	1	1.66148E+03	1.000E-01	3.703E+01	1.023E+00	BETA1
2	1	3.27237E+05	2.000E+00	1.330E+04	1.488E+00	BETA2
3	1	9.80378E+00	1.000E+00	8.065E-03	1.904E+00	M SHIFT
4	1	1.02012E+01	1.000E-01	9.344E-03	2.877E+00	ML SHIFT
5	1	1.05736E+01	5.000E-01	7.160E-03	2.267E+00	ML2 SHIFT

0RMS ERROR = 1.10E-02 MAX ERROR = 3.04E-02 AT OBS.NO. 24
 RESIDUALS SQUARED = 2.31E-03
 RFACTOR =   0.0959 PERCENT

Receptor 61 with tetrabutylammonium benzoate in DMSO-d_6.

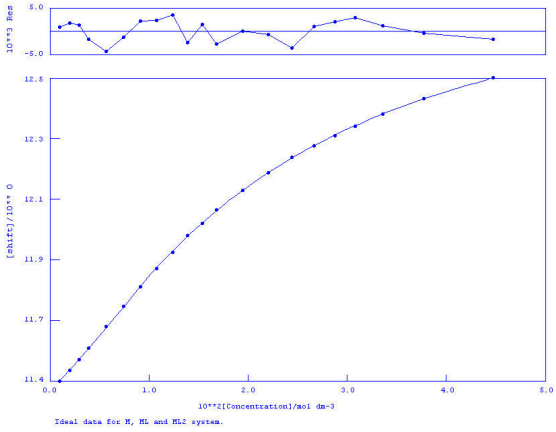

NO.	A	PARAMETER	DELTA	ERROR	CONDITION	DESCRIPTION
1	1	7.79475E+03	1.000E-01	1.181E+02	2.692E+01	BETA1
2	1	3.18645E+05	2.000E+00	3.235E+03	1.236E+01	BETA2
3	1	1.14080E+01	1.000E+00	1.706E-03	1.189E+00	M SHIFT
4	1	1.17737E+01	1.000E-01	1.453E-03	2.837E+00	ML SHIFT
5	1	1.29994E+01	5.000E-01	1.078E-02	3.575E+01	ML2 SHIFT

0RMS ERROR = 2.48E-03 MAX ERROR = 4.35E-03 AT OBS.NO. 5
 RESIDUALS SQUARED = 9.86E-05
 RFACTOR =   0.0181 PERCENT

Receptor 61 with tetrabutylammonium acetate in DMSO-d_6.

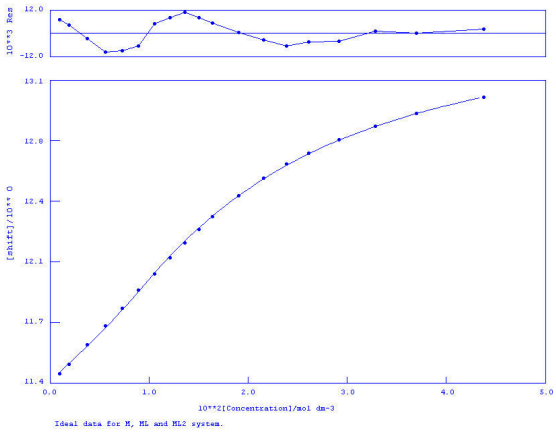

NO.	A	PARAMETER	DELTA	ERROR	CONDITION	DESCRIPTION
1	1	1.80856E+02	1.000E-01	4.867E+00	1.805E+01	BETA1
2	1	8.27326E+03	2.000E+00	4.619E+02	1.524E+02	BETA2
3	1	9.00195E+00	1.000E+00	1.302E-03	6.048E+00	M SHIFT
4	1	9.09162E+00	1.000E-01	3.297E-03	2.878E+01	ML SHIFT
5	1	9.45015E+00	5.000E-01	9.257E-03	1.118E+02	ML2 SHIFT

0RMS ERROR = 1.09E-03 MAX ERROR = 1.60E-03 AT OBS.NO. 13
 RESIDUALS SQUARED = 1.67E-05
 RFACTOR =   0.0103 PERCENT

^{1}H-NMR Titrations in Chapter 3

Receptor 88 with urea in 20%DMSO-d_6/MeNO$_2$-d_3.

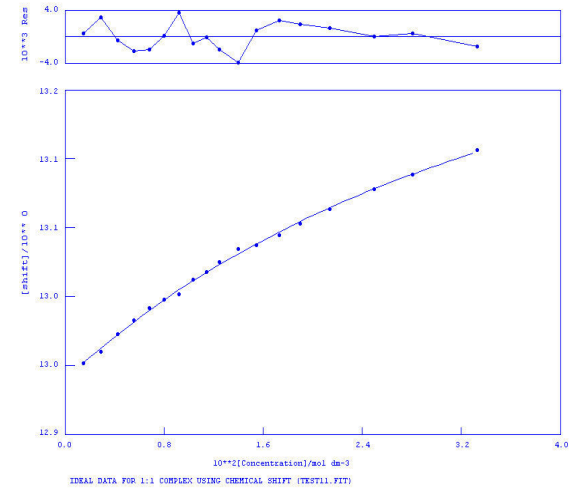

NO.	A	PARAMETER	DELTA	ERROR	CONDITION	DESCRIPTION
1	1	2.74745E+01	2.000E-01	1.658E+00	6.961E+01	K1
2	1	1.29487E+01	2.000E-01	1.399E-03	4.865E+00	SHIFT M
3	1	1.33741E+01	1.000E+00	1.381E-02	5.321E+01	SHIFT ML

0RMS ERROR = 2.09E-03 MAX ERROR = 3.95E-03 AT OBS.NO. 11
RESIDUALS SQUARED = 6.58E-05
RFACTOR = 0.0146 PERCENT

Receptor 88 with imidizolidone in 20%DMSO-d_6/MeNO$_2$-d_3.

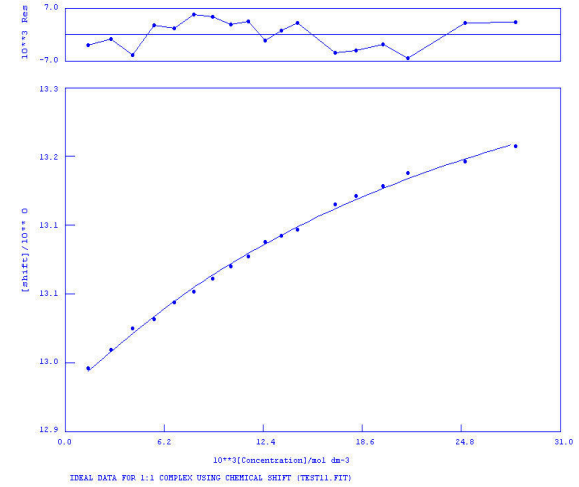

NO.	A	PARAMETER	DELTA	ERROR	CONDITION	DESCRIPTION
1	1	4.45422E+01	2.000E-01	3.339E+00	5.803E+01	K1
2	1	1.29449E+01	2.000E-01	2.946E-03	4.967E+00	SHIFT M
3	1	1.34874E+01	1.000E+00	1.857E-02	4.323E+01	SHIFT ML

0RMS ERROR = 3.99E-03 MAX ERROR = 6.39E-03 AT OBS.NO. 16
RESIDUALS SQUARED = 2.38E-04
RFACTOR = 0.0278 PERCENT

Receptor 88 with barbital in 30%DMSO-d_6/MeNO$_2$-d_3.

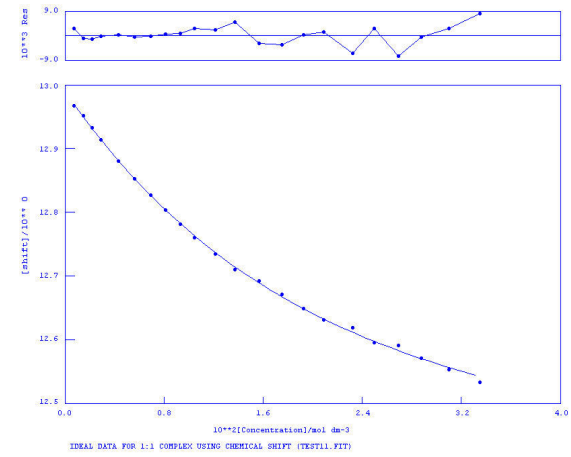

NO.	A	PARAMETER	DELTA	ERROR	CONDITION	DESCRIPTION
1	1	5.91465E+01	2.000E-01	2.068E+00	3.270E+01	K1
2	1	1.29615E+01	2.000E-01	2.093E-03	3.263E+00	SHIFT M
3	1	1.23051E+01	1.000E+00	9.290E-03	2.482E+01	SHIFT ML

0RMS ERROR = 3.61E-03 MAX ERROR = 7.98E-03 AT OBS.NO. 22
RESIDUALS SQUARED = 2.48E-04
RFACTOR = 0.0264 PERCENT

Receptor 88 with imidizolidone in 30%DMSO-d_6/MeNO$_2$-d_3.

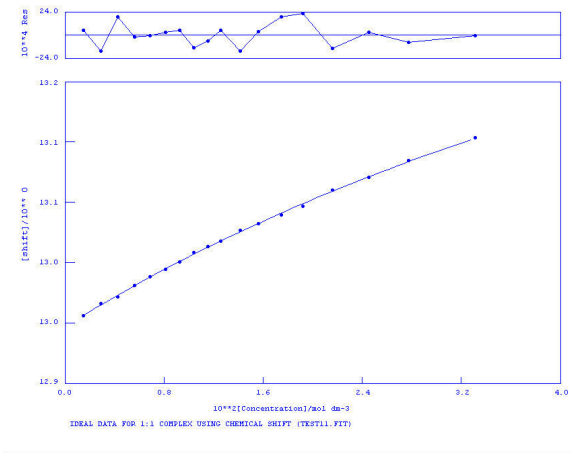

NO.	A	PARAMETER	DELTA	ERROR	CONDITION	DESCRIPTION
1	1	1.30281E+01	2.000E-01	9.027E-01	3.099E+02	K1
2	1	1.29563E+01	2.000E-01	8.627E-04	6.452E+00	SHIFT M
3	1	1.35920E+01	1.000E+00	3.024E-02	2.606E+02	SHIFT ML

0RMS ERROR = 1.25E-03 MAX ERROR = 2.20E-03 AT OBS.NO. 14
RESIDUALS SQUARED = 2.34E-05
RFACTOR = 0.0087 PERCENT

Receptor 88 with urea in 30% DMSO-d_6/$MeNO_2$-d_3.

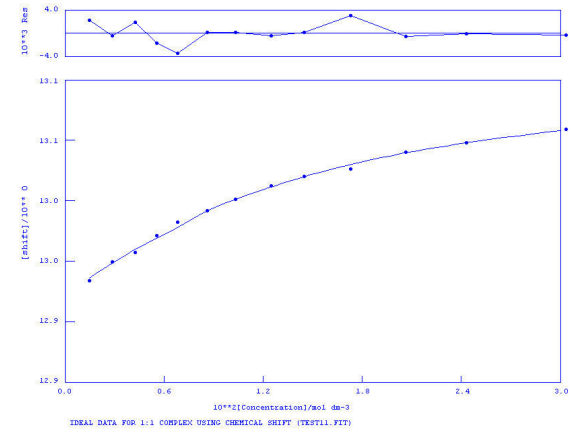

NO.	A	PARAMETER	DELTA	ERROR	CONDITION	DESCRIPTION
1	1	9.55761E+01	2.000E-01	1.067E+01	3.915E+01	K1
2	1	1.29582E+01	2.000E-01	1.380E-03	2.931E+00	SHIFT M
3	1	1.31076E+01	1.000E+00	6.377E-03	3.202E+01	SHIFT ML

0RMS ERROR = 1.82E-03 MAX ERROR = 3.51E-03 AT OBS.NO. 5
RESIDUALS SQUARED = 3.33E-05
RFACTOR = 0.0123 PERCENT

Receptor 96 with imidazolidone in 20% DMSO-d_6/$MeNO_2$-d_3.

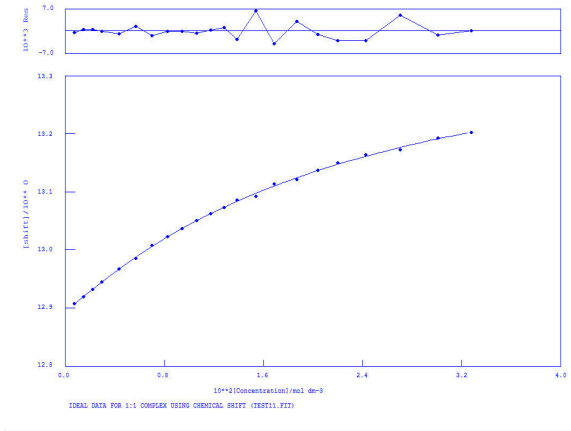

NO.	A	PARAMETER	DELTA	ERROR	CONDITION	DESCRIPTION
1	1	5.09494E+01	2.000E-01	1.659E+00	3.760E+01	K1
2	1	1.28517E+01	2.000E-01	1.474E-03	3.589E+00	SHIFT M
3	1	1.34124E+01	1.000E+00	7.733E-03	2.847E+01	SHIFT ML

0RMS ERROR = 2.53E-03 MAX ERROR = 6.23E-03 AT OBS.NO. 14
RESIDUALS SQUARED = 1.22E-04
RFACTOR = 0.0180 PERCENT

Receptor 96 with urea in 20% DMSO-d_6/$MeNO_2$-d_3.

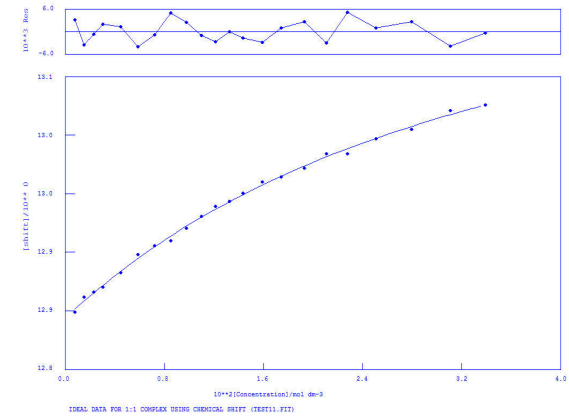

```
NO.   A    PARAMETER     DELTA      ERROR     CONDITION    DESCRIPTION
   1   1   3.30488E+01 2.000E-01 2.886E+00 1.113E+02     K1
   2   1   1.28532E+01 2.000E-01 1.758E-03 4.499E+00    SHIFT M
   3   1   1.32745E+01 1.000E+00 1.943E-02 8.983E+01     SHIFT ML

0RMS ERROR = 2.91E-03  MAX ERROR = 5.00E-03 AT OBS.NO. 18
 RESIDUALS SQUARED = 1.61E-04
 RFACTOR =     0.0209 PERCENT
```

Receptor 100 with TBA acetate in DMSO-d_6/0.5% water.

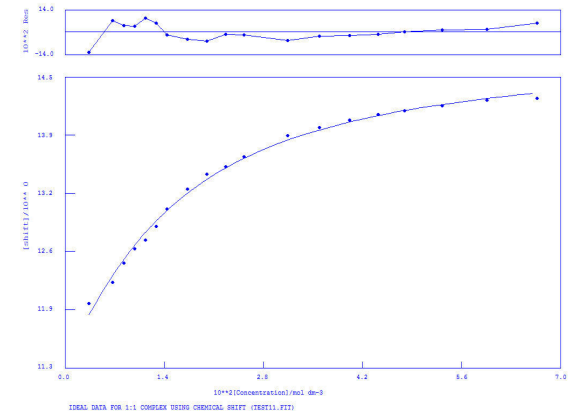

```
NO.   A    PARAMETER     DELTA      ERROR     CONDITION    DESCRIPTION
   1   1   9.40380E+01 2.000E-01 9.942E+00 2.586E+01     K1
   2   1   1.13401E+01 2.000E-01 6.931E-02 6.414E+00    SHIFT M
   3   1   1.48632E+01 1.000E+00 7.342E-02 1.271E+01     SHIFT ML

0RMS ERROR = 5.54E-02  MAX ERROR = 1.25E-01 AT OBS.NO.  1
 RESIDUALS SQUARED = 4.91E-02
 RFACTOR =     0.3788 PERCENT
```

Receptor 100 with TBA benzoate in DMSO-d_6/0.5% water.

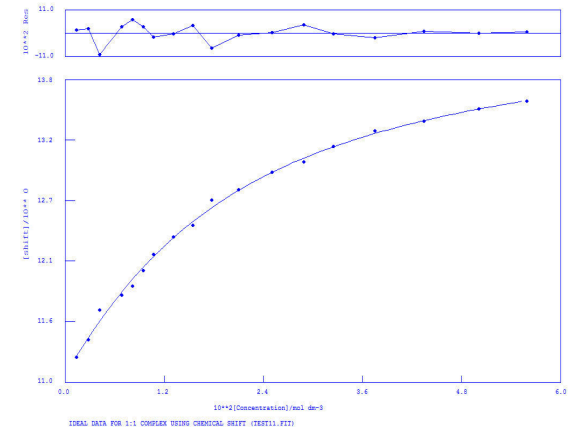

NO.	A	PARAMETER	DELTA	ERROR	CONDITION	DESCRIPTION
1	1	6.55206E+01	2.000E-01	5.988E+00	3.009E+01	K1
2	1	1.10575E+01	2.000E-01	3.298E-02	4.122E+00	SHIFT M
3	1	1.44031E+01	1.000E+00	8.913E-02	1.995E+01	SHIFT ML

0RMS ERROR = 4.15E-02 MAX ERROR = 1.04E-01 AT OBS.NO. 3
 RESIDUALS SQUARED = 2.58E-02
 RFACTOR =   0.3017 PERCENT

Appendix 3 – Proton-NMR Titration Stack Plots for Chapter 4

These ^{1}H-NMR titrations were conducted with compound **125** in acetonitrile-d_3 with a selections of anions as their tetrabutylammonium salts except for hydrogen carbonate (tetraethylammonium salt). Only the partial spectra of the regions of interest are shown.

Compound 125 with acetate:

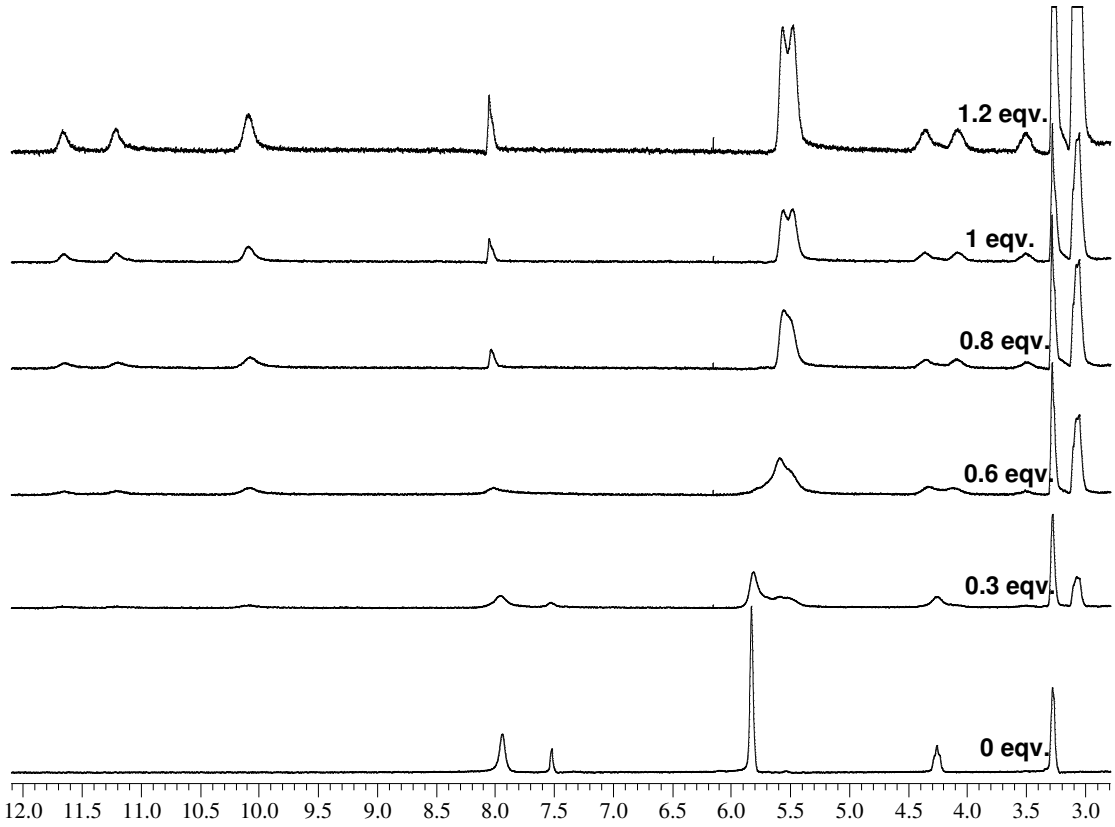

Compound 125 with hydrogen carbonate:

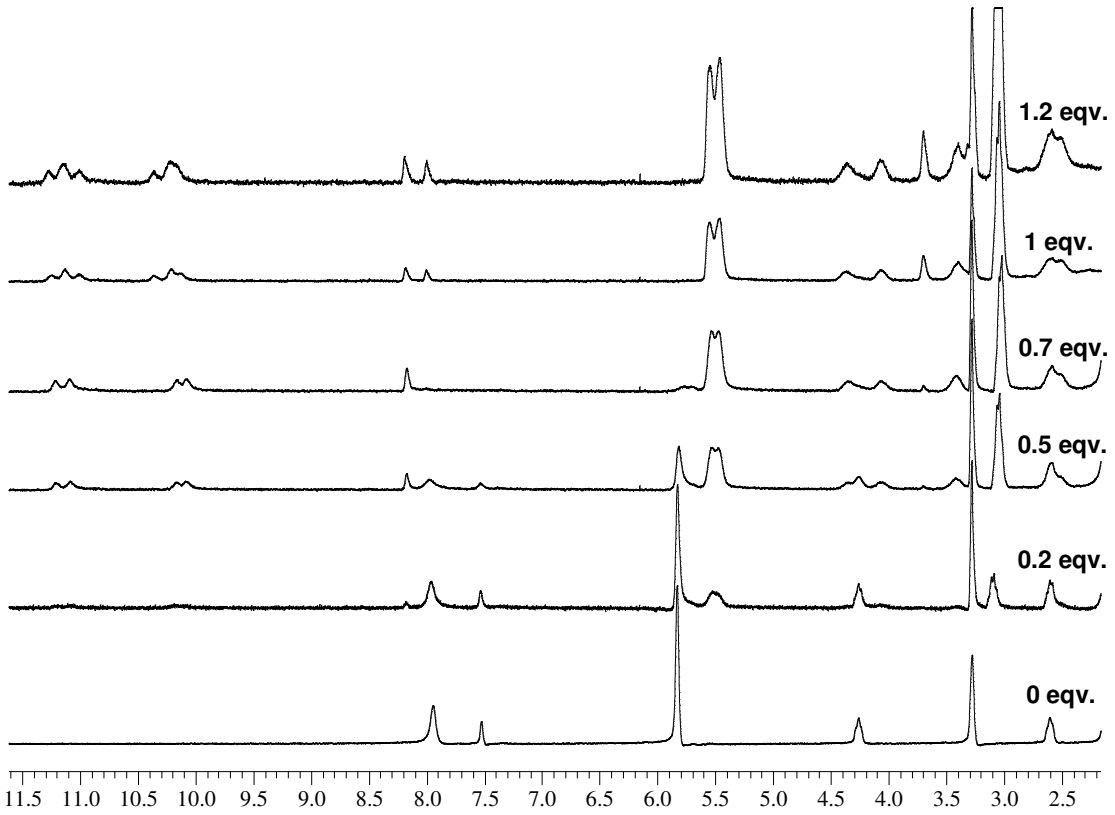

Compound 125 with bromide:

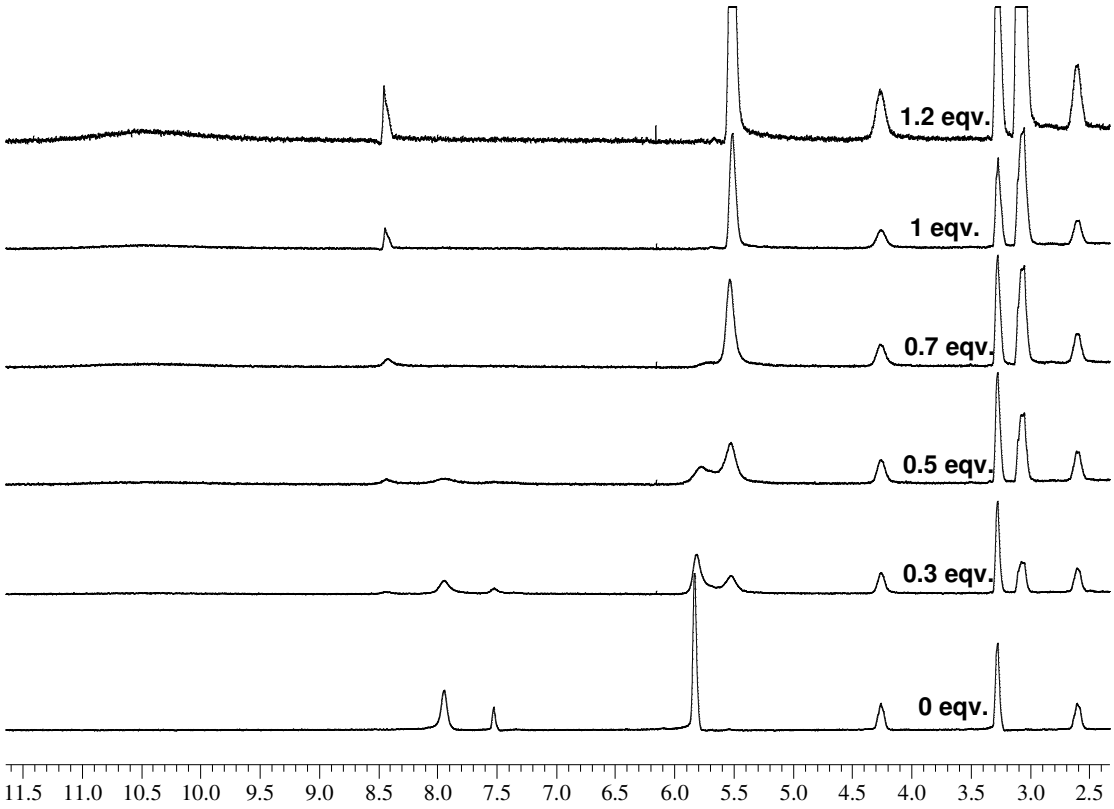

Compound 125 with dihydrogen phosphate:

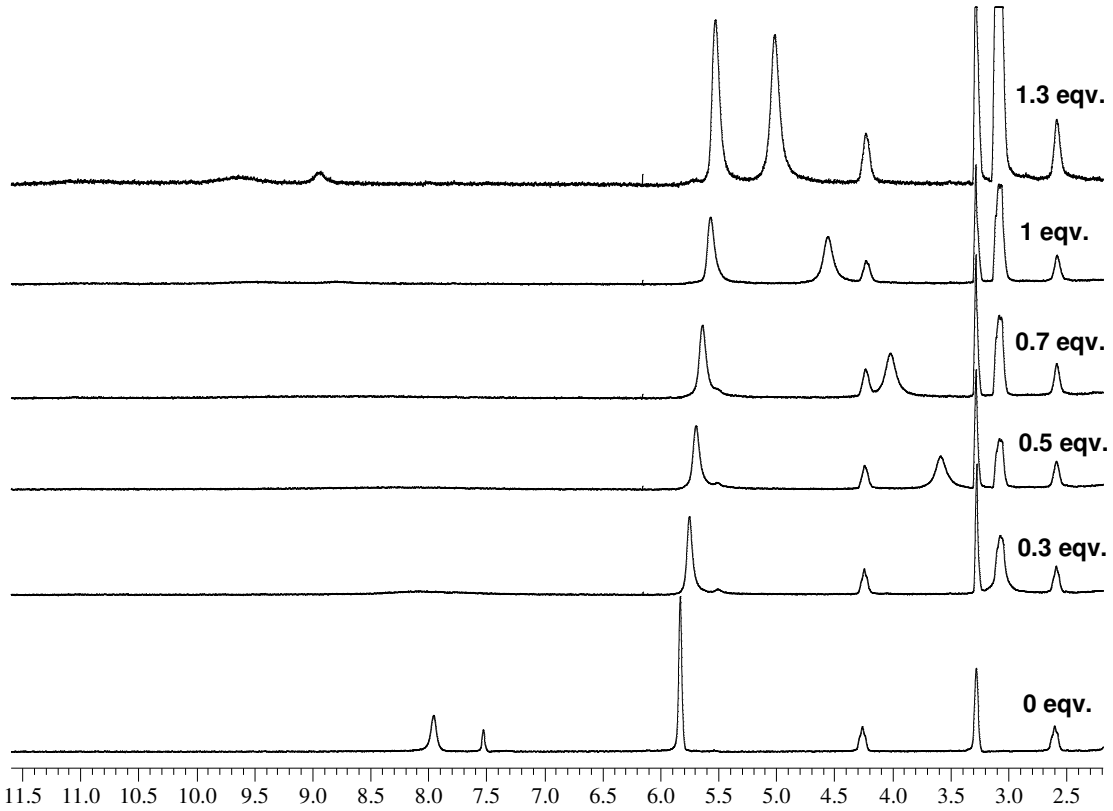

Appendix 4 – Isothermal Calorimetry Titration Curves for Chapter 4

The ITC titrations were conducted by Prof. Franz Schmidtchen of the Technical University of Munich, Germany. They were all carried out with compound **125** in dry solvents at 303K with a selection of anions as their tetraalkylammonium salts. The curves are reported here for completeness.

Compound 125 in acetonitrile:

Table 1: acetonitrile, 303 K; guest-into-host

entry	salt	conc. in cell	K_{ass} [M^{-1}]	ΔG^o [cal K^{-1} mol^{-1}]	ΔH^o [cal K^{-1} mol^{-1}]	ΔS^o [cal K^{-1} mol^{-1}]	remarks
1	TEA^+ $chloride^-$	0.94	1.3 e6	-8.47 e3	-12.0 e3	-11.6	n = 0.97
2	TEA^+ $benzoate^-$	0.94	6.0 e3	-5.23 e3	-9.90 e3	-15.4	n = 0.96
3	TBA^+ $dihydrogenphosphate^-$	0.94	8.2 e3	-5.42 e3	-4.61 e3	+2.7	n = 1.44
4	TBA^+ $dihydrogenphosphate^-$	0.96	7.77 e3	-5.39 e3	-5.14 e3	+0.8	n = 1.46
5	TEA^+ $isocyanate^-$	0.96	1.12 e6	-8.38 e3	-13.35 e3	-16.3	n = 0.95
6	TBA^+ $hydrogencarbonate^-$	0.96	2.03 e5	-7.36 e3	-11.40 e3	-13.3	n = 1.09

Table 2: acetonitrile, 303 K; host-into-guest;

entry	salt	conc. in cell	K_{ass} [M^{-1}]	ΔG^o [cal K^{-1} mol^{-1}]	ΔH^o [cal K^{-1} mol^{-1}]	ΔS^o [cal K^{-1} mol^{-1}]	remarks
7	TEA^+ $chloride^-$	0.327	2.6 e6	-8.89 e3	-11.88 e3	-9.8	n = 1.07
8	TBA^+ $fluoride^-$ × 3 H_2O	0.500	1.55 e5	-7.19 e3	-11.34 e3	-13.6	n = 0.90
9	TBA^+ $acetate^-$	0.574	1.64 e5	-7.23 e3	-13.12 e3	-19.4	n = 1.05
10	TBA^+ p-$nitrobenzoate^-$	0.522	1.30 e3	-4.32 e3	-8.54 e3	-13.9	n = 1.0

entry	1	2

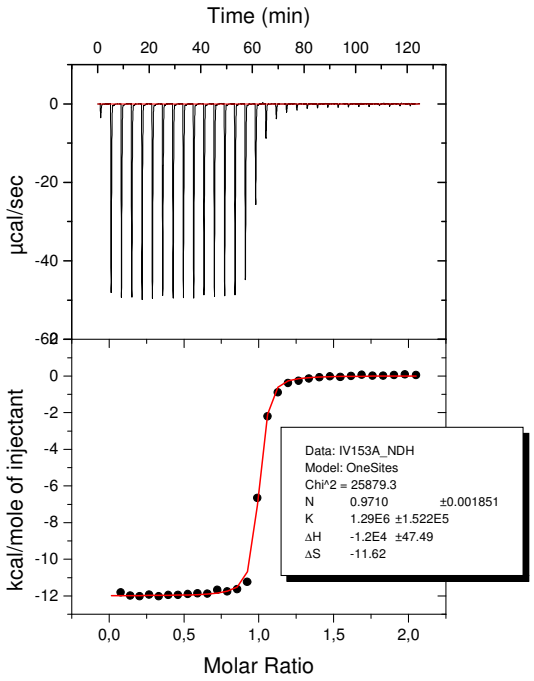

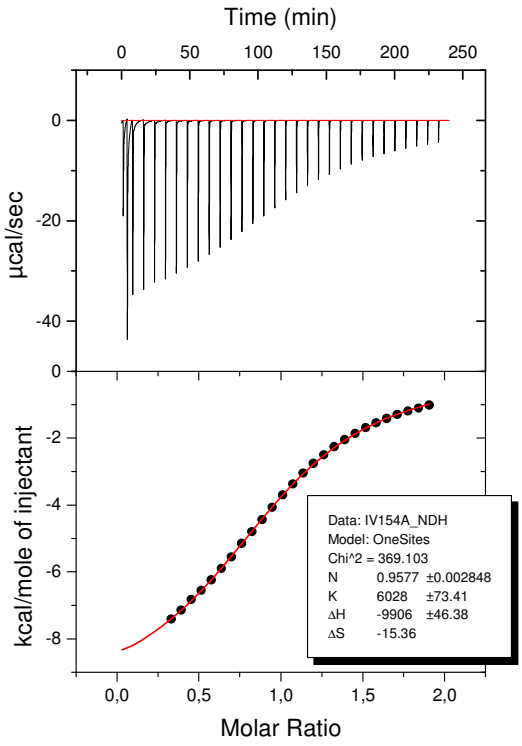

entry	3	4

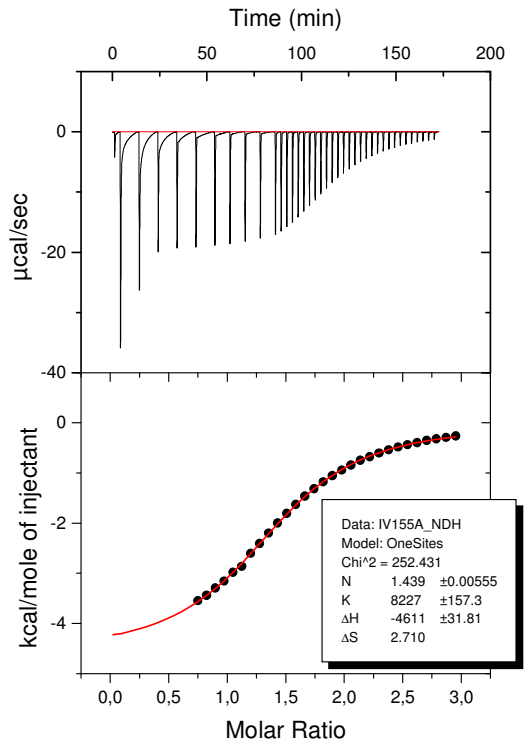

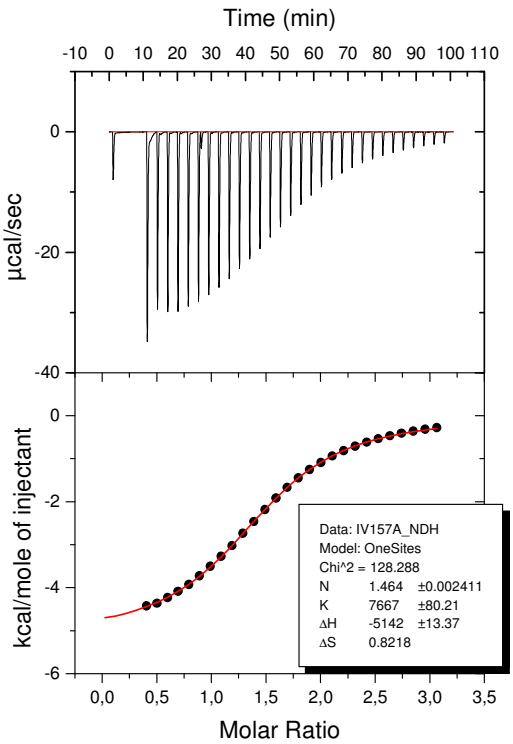

entry	5	6

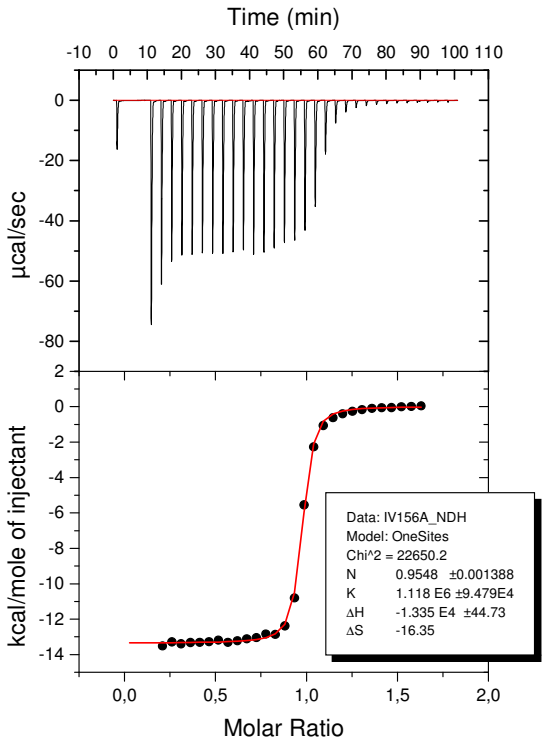

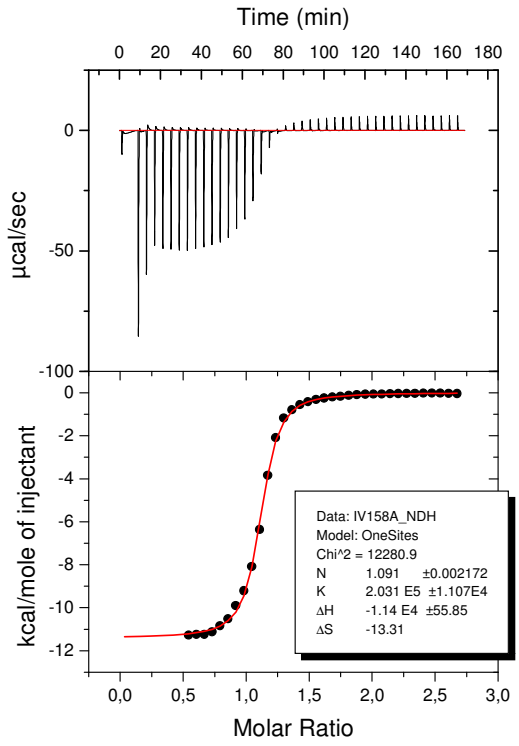

entry	7	8

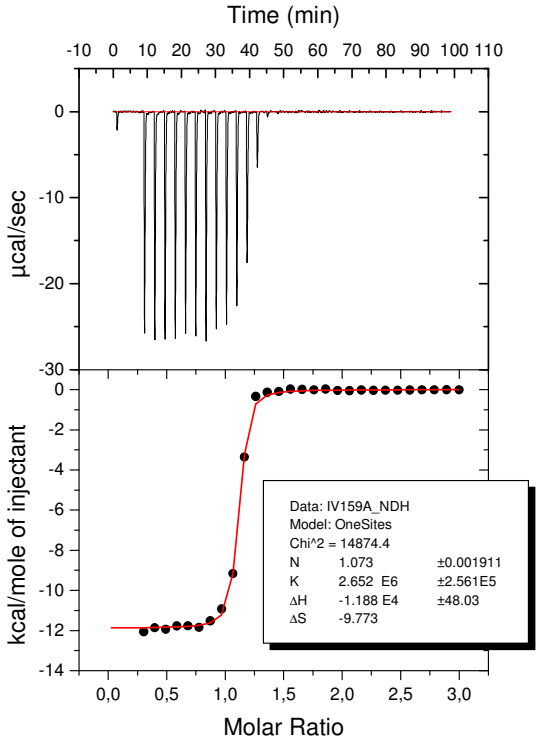

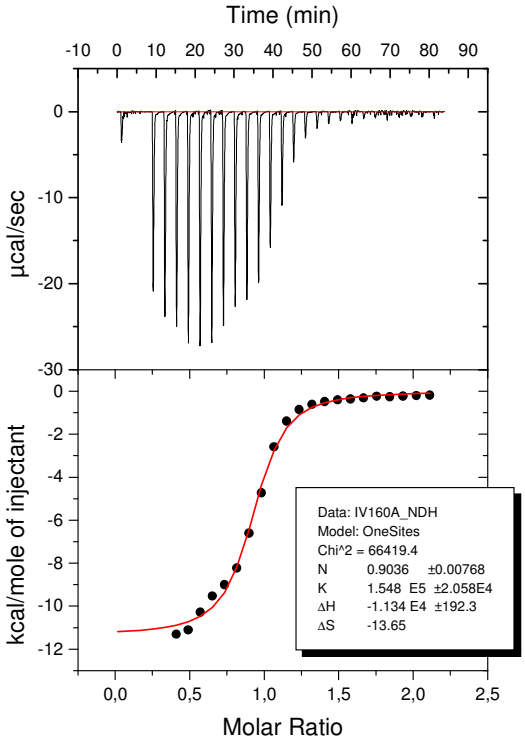

entry	9	10

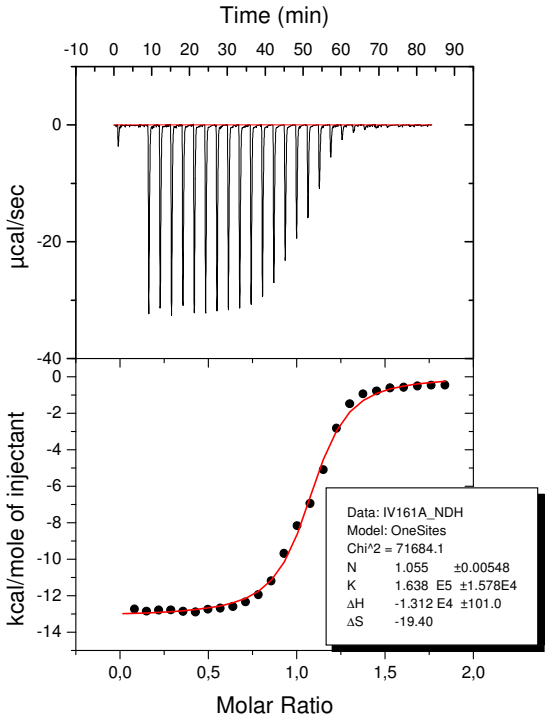
Time (min)
µcal/sec
kcal/mole of injectant
Molar Ratio
Data: IV161A_NDH
Model: OneSites
Chi^2 = 71684.1
N 1.055 ±0.00548
K 1.638 E5 ±1.578E4
ΔH -1.312 E4 ±101.0
ΔS -19.40

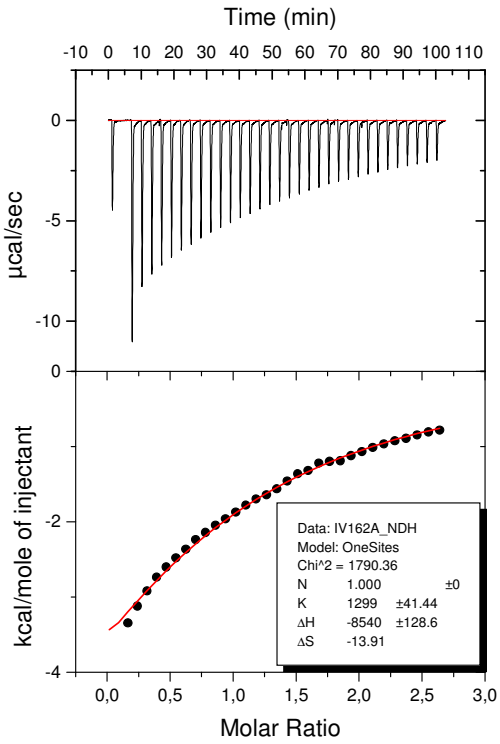
Time (min)
µcal/sec
kcal/mole of injectant
Molar Ratio
Data: IV162A_NDH
Model: OneSites
Chi^2 = 1790.36
N 1.000 ±0
K 1299 ±41.44
ΔH -8540 ±128.6
ΔS -13.91

Compound 125 in DCM:

Table 3: dichloromethane, 303 K; host into guest

entry	salt	conc. in cell	K_{ass} [M^{-1}]	ΔG^o [cal K^{-1} mol^{-1}]	ΔH^o [cal K^{-1} mol^{-1}]	ΔS^o [cal K^{-1} mol^{-1}]	remarks
11	TEA^+ $chloride^-$	0.294	2.68 e6	-8.91 e3	-13.2e3	-14.2	n = 1.2
12	TBA^+ $chloride^-$	0.655	4.7 e5	-7.86 e3	-11.8 e3	-13.0	n = 0.96
13	TEA^+ $nitrate^-$	0.598	6.07e3	-8.38 e3	-7.68 e3	-8.0	n = 0.99
14	TEA^+ $hydrogencarbonate^-$	0.62	1.77 e5	-7.27 e3	-9.93 e3	-8.7	n = 1.03

entry	**11**	**12**

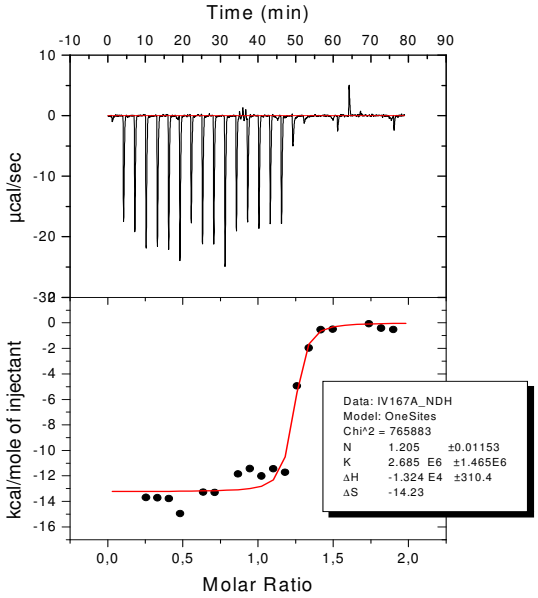

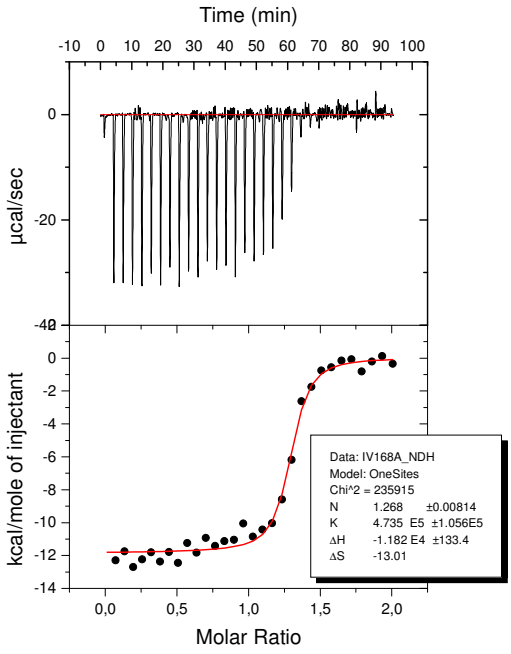

entry	**13**	**14**